Bulletin
of
The Geological Society of America

VOLUME 66 July 1955 NUMBER 7

CONTENTS

	Pages
Monoclines of the Colorado Plateau. By Vincent C. Kelley	789–804
Sub-Chattanooga residuum in Tennessee and Kentucky. By Charles Milton, Louis C. Conant, and Vernon E. Swanson	805–810
Deformation and igneous intrusion in southern British Columbia, Canada. By Alan R. Smith and John S. Stevenson	811–818
Cambrian contacts in eastern Pennsylvania. By Bradford Willard	819–834
Measurement of the deformation of the Sierra Nevada, California, since Middle Eocene. By F. S. Hudson	835–870
Catoctin formation near Luray, Virginia. By John C. Reed, Jr.	871–896
Transformation of indices in twin gliding. By A. Pabst	897–912
Crustal structure and surface-wave dispersion. Part IV: Atlantic and Pacific ocean basins. By Jack E. Oliver, Maurice Ewing, and Frank Press	913–946
Short Note: Growth phenomena in zircon of autochthonous granites. By Arie Poldervaart and F. Donald Eckelmann	947–948

Subscription $15.00 per year.

Printing Office: Mt. Royal & Guilford Aves., Baltimore 2, Md.

Communications for publications should be addressed to The Geological Society of America, Dr. H. R. Aldrich, Secretary, 419 West 117 Street, New York, N. Y.

Please give notice of change of address 4 weeks in advance. Claims for non-receipt of the Bulletin of a given month must be sent to the Secretary of the Society before the end of the second succeeding month.

Entered as second-class matter at the Post Office at Baltimore, Md.,
under the Act of Congress of July 16, 1894.
Accepted for mailing at special rate of postage provided for in Section 1103
Act of October 3, 1917, authorized on July 8, 1918.

PAPERS IN PRESS FOR FORTHCOMING ISSUES

Isotopic Composition and Distribution of Lead, Uranium, and Thorium in a Precambrian Granite. By George R. Tilton, Claire Patterson, H. Brown, M. Inghram, R. Hayden, D. Hess, and E. Larsen, Jr.

Geology of the Bridger Range, Montana. By William J. McMannis

Postglacial Volcanic Ash in the Rocky Mountains Piedmont, Montana and Alberta. By Leland Horberg and Richard Robie

Lake Chippewa, A Low Stage of Lake Michigan Indicated by Bottom Sediments. By J. L. Hough

Seismic Refraction Profiles in the Submerged Atlantic Coastal Plain near Ambrose Lightship. By R. O. Carlson and M. V. Brown

Evidence for No Cenozoic Isthmus of Tehuantepec Seaways. By J. Wyatt Durham, A. R. V. Arellano, and J. H. Peck, Jr.

Adamellite Intrusive North of Davis Inlet, Labrador. By E. P. Wheeler, 2nd

Engineering Geology Reference List. Compiled by Stafford C. Happ for Committee on Teaching Aids, Division on Engineering Geology, G.S.A.

Crustal Structure of the Arctic Regions from the L_G Phase. By Jack Oliver, Maurice Ewing, and Frank Press

Spilitic Intrusion near Ladron Peak, Socorro County, New Mexico. By Robert Duschatko and Arie Poldervaart

BULLETIN OF THE GEOLOGICAL SOCIETY OF AMERICA
VOL. 66, PP. 789-804, 10 FIGS. JULY 1955

MONOCLINES OF THE COLORADO PLATEAU

BY VINCENT C. KELLEY

ABSTRACT

Powell should be given the credit for the idea advanced in 1929 by Busk that a monocline is a double bend consisting of the anticlinal and synclinal bends. In the Colorado Plateau monoclines have an aggregate length of nearly 2500 miles, and the greatest nearly uninterrupted monocline is about 300 miles long. Every gradation from gentle open monoclines to overturned and thrust structures is present on the Plateau. Reversal of dip, either broad or locally abrupt, is common near the head or foot of the monoclines; however, the monoclinal designation should be retained on a regional basis. There is homology between monoclines and noses, anticlines, synclines, normal faults, and reverse faults.

The monoclines are thought to be tangentially compressive Laramide features, and in places they show pronounced coupling action. They are divided into a western group that may be genetically related to the Central Laramide Rockies and an eastern group related to the Eastern Laramide Rockies. Roughly dividing the two groups are the Uinta and San Juan basins and the Salt fold and fault belt of the Paradox basin.

CONTENTS

TEXT

	Page
Introduction	789
Derivation and definition of monocline	790
Structure	793
Age	797
Origin and regional relations	797
Summary and conclusions	799
References cited	802

ILLUSTRATIONS

Figure	Page
1. Index map of the western United States showing the location of the Colorado Plateau	790
2. First illustrations of monoclines (Powell, 1873, p. 184)	791
3. Suggested axial line symbols for mapping anticlinal bends (A) and synclinal bends (S)	792
4. Diagrammatic structural profiles of monoclines and terraces	793
5. Relationship of monoclines, noses, and chutes by structure contours	793
6. Diagrammatic variations of monoclines in cross section	795
7. Monoclines and the major tectonic divisions of the Colorado Plateau structural province	796
8. Deformation of a normal fault A into a thrust fault B by rotations of the fault plane	798
9. Kaibab uplift showing the relationships of the monoclines to the fold axes and faults; adapted from Strahler, 1948	800
10. Relationship of the Colorado Plateau monoclines to the Laramide structural trends of the adjacent Rockies	801

TABLE

Table	Page
1. Data on monoclines	794

INTRODUCTION

The Colorado Plateau is located in western North America and is a part of the grand cordillera. The Plateau is a segment of broad, general structural stability within the great mountain systems (Fig. 1). Altitudes range from about 2500 feet along the bottom of the Colorado River to about 13,000 feet in some of the isolated peaks or smaller plateaus that border or are scattered across the region. Altitudes between 6000 and 7000 feet are most common. In about one half of the Plateau the Colorado River and its tributaries have carved hundred of youthful canyons of unmatched grandeur. In the remainder of the area older and more mature erosion has given rise to a relief ranging from several hundreds to several thousands of feet between mountains, lesser plateaus, or mesas on the one hand, and broad valleys on the other.

The results of this paper are a part of a larger

study concerning the whole of the tectonics of the Plateau. The study was made possible by the Exploration Division of the U. S. Atomic Energy Commission.

—Applied to strata that dip for an indefinite or unknown length in one direction, and which do not apparently form sides of ascertained *anticlines* or *synclines*."

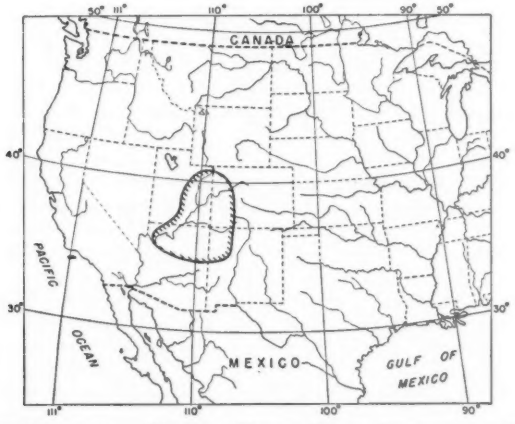

FIGURE 1.—INDEX MAP OF THE WESTERN UNITED STATES SHOWING THE LOCATION OF THE COLORADO PLATEAU

DERIVATION AND DEFINITION OF MONOCLINE

The term monocline was introduced in 1842 by the Rogers (Rogers and Rogers, 1843, p. 485) in place of the similar but hybrid term, unicline, used earlier by Darwin. They used "monoclinal" as a noun or an adjective, proposed apparently to express certain physiographic relations between ridges or valleys and the attitude of beds. A structural meaning was in part intimated, for H. D. Rogers referred to "monoclinal structure" in 1858 (v. 2, p. 10). However, as they explained in their original usage: "While the phrases, *anticlinal dip*, and *synclinal dip*, sufficiently express the directions of the beds, due to the concave and convex flexures, we propose the term *monoclinical*, to signify a sameness in the direction of the dip. . .". The Rogers made no mention of a special flexure in connection with monoclinal, and their features were always limbs of anticlines or synclines. Nevertheless, the term that many now consider the hallmark of Colorado Plateau structure had its beginnings in the studies of the classical Appalachian forms.

It is doubtful that Page (1865, p. 506) had the modern idea of a monocline when he gave the first formal handbook definition: "Monoclinal (Gr. *monos*, single, and *klino* I bend).

Powell may have gotten the term monoclinal from the works of the Rogers; when he encountered the steplike flexures along the Colorado River the word seemed admirably suited owing principally to the similar hogback development and partly to the apparent singleness of pronounced dip. Powell (1873, p. 459–461; 1875, p. 184–191) was probably the first with the modern idea of the monocline when he described the homology of "monoclinal folds" and faults and illustrated them in several excellent figures (Fig. 2). In 1876 Gilbert (p. 21), although without using the term monocline, defined the monoclinal fold as "a *double*[1] flexure, connecting strata at one level with the same strata at another level." The noun monocline rather than monoclinal was first used in 1882 by Dutton (1882a, p. 128; 1882b, p. 183–184) and Geikie (1882, p. 515).

In the years following the introduction of the term and the early descriptions of the magnificent occurrences in the Colorado Plateau by Powell (1875), Gilbert (1877, p. 11–13), and Dutton (1880, p. 25), there gradually developed a confusion in meaning. This confusion stemmed from usage of the term in physiography and from the misconception that monocline re-

[1] Italics are mine.

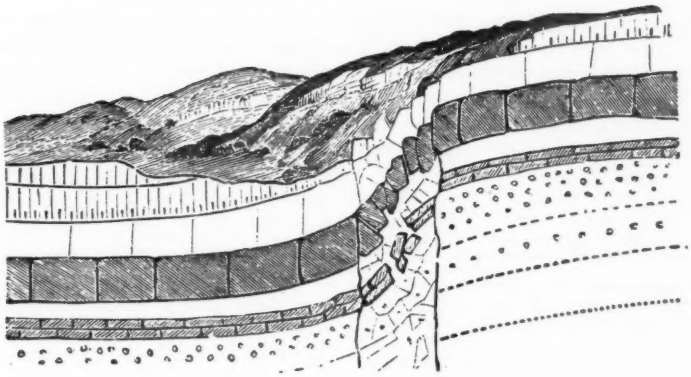

a

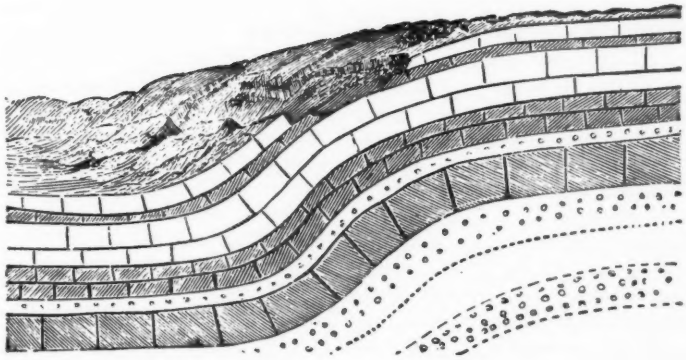

b

FIGURE 2.—FIRST ILLUSTRATIONS OF MONOCLINES (Powell, 1873, p. 184)

A. Section across a fault with walls widely separated, the intervening space filled with broken rock, still exhibiting the original stratification. B. A monoclinal fold

ferred only to the more steeply dipping limb or one slope of the fold.

In 1915 Daly (p. 53), as the result of observations in British Columbia, introduced the term homocline for any bedded sequence of rocks all dipping in the same direction; this, he pointed out, might be applied to limbs of anticlines or synclines, isoclines, tilted fault blocks, or monoclines. Daly (1916, p. 90) suggested that homocline would have been better for the cases cited by the Rogers, because they had similarity of dip rather than general form in mind. Daly believed that monocline should be restricted to the usages of Dutton and Geikie. One of Daly's principal proposals was that the noun monoclinal be dropped in favor of monocline.

The doubleness of the monocline often has been disregarded, but Busk (1929, p. 7) emphasized this aspect in dividing the monocline and similar structures into two parts, terming the upper part an anticlinal bend and the lower

part a synclinal bend.[2] This division is especially worthwhile, and on detailed or moderately detailed maps the apices or axes of both bends may be mapped separately to advantage (Fig. 3). Anticlinal and synclinal bends are also integral parts of structural terraces and certain overturns.

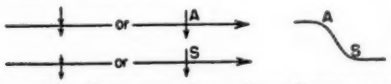

FIGURE 3.—SUGGESTED AXIAL LINE SYMBOLS FOR MAPPING ANTICLINAL BENDS (A) AND SYNCLINAL BENDS (S)

Most contemporary definitions of monoclines generally agree with the one by Lahee (1952, p. 174): a monocline "is a steplike bend in otherwise horizontal or gently dipping beds." The definitions in textbooks of Geikie, Willis, Nevin, Billings, Hills, and Forrester conform generally with this, but Willis (1929, p. 27) and Stočes and White (1935, p. 122) apparently consider only the steeper inclination to be the monocline. Stočes and White state that a monocline is "an inclination in one direction represented by the portion of a bed with a steeper dip connecting lower and higher segments of the same bed." This reflects the European nomenclature which refers to a monocline as a flexure and to a homocline as a monocline. Loomis (1937, p. 70) has presented a significant variation in his statement that "where strata are bent on one side of the median plane [axial surface] but not on the other, the fold is a monocline." From the old and prevailing point of view that a monocline is a double flexure, Loomis' definition might include only part of a normal monocline or a half monocline.

The principal features of a monocline which are brought out in definitions, explanations, or illustrations are:

(1) A single direction of dip in all limbs or parts, *i.e.* no reversal of direction
(2) Gentleness of associated regional dips, especially outside the head and foot (Lahee, 1952, p. 177) of the monocline
(3) Great ratio of length to width.

[2] Johnson and Huntley (1916, p. 64) first thought of dividing the monocline into two bends. However, their rather awkward terms "anti-homocline" for the upper bend and "syn-homocline" for the lower bend have never found general acceptance.

Billings (1954, p. 42) observes that dips range "from a few degrees to 90 degrees." Some writers illustrate the structure with a concentric type of bending; others with similar or semisimilar bending.

The relationship of monoclines to structural terraces is worthy of note. A terrace has been said to be the reverse of a monocline and to be a local flattening rather than a local steepening. Figure 4 shows that monoclines may be modified by terraces or that terraces and monoclines may alternate along regional and homoclinal structures. If the total length of flatter limbs is greater than that of steeper limbs, the structures are monoclines (A); if the situation is reversed the structures are terraces (B). The East Kaibab monocline of Arizona is modified or split by a terrace (Fig. 9).

The most common modification of monoclines is by anticlinal and synclinal bowing (Lahee, 1952, p. 179, 649). These take the form of either broad cross bendings or sharper noses[3] and structural chutes (Johnson and Huntley, 65–66; *see also* ravine, Clapp, 1929, p. 686). Clapp (1917, p. 568) used the term "monoclinal nose" for a structure simply called a nose by most geologists. Figure 5 shows that Clapp's modified phrase may be significant. The Defiance monocline of Arizona and New Mexico has many cross buckles in the form of noses and chutes (Fig. 7).

Hills (1953, p. 77) noted that petroleum geologists still use the term monocline for beds dipping uniformly in one direction. Although most writers use the term correctly, a perusal of volumes concerning structure of typical American oil fields (A.A.P.G., 1929) has revealed incorrect usages especially for regional dip; some were for homoclinal dip, and one for a terrace. Many U. S. Geological Survey geologists have used the term wrongly and several have done so on the Colorado Plateau. Recently Bock (1952) has termed certain wedge-shaped homoclines of the late Triassic basins of Pennsylvania "vertex monoclines". In view of the above, in view of the prevalent tendency to use the term as an adjective in "monoclinal dip", and in view of the fact that several of the

[3] Billings (1954, p. 62–63) uses the term nose for the place or the pattern of sharp bending, and a sharp synclinal bow or a chute is a nose also.

so-called classical monoclines on the Colorado Plateau are not precisely monoclines, it must be concluded that the standard or prevailing definition is not widely adhered to or acceptable. The original definitions of the Rogers (1842) and Page (1865) and the European usage are still followed by many in this country.

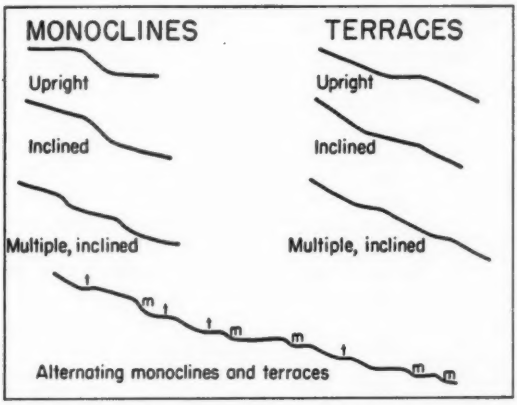

FIGURE 4.—DIAGRAMMATIC STRUCTURAL PROFILES OF MONOCLINES AND TERRACES

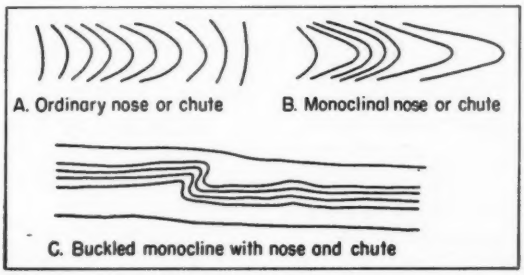

FIGURE 5.—RELATIONSHIP OF MONOCLINES, NOSES, AND CHUTES BY STRUCTURE CONTOURS
(All are plans)

STRUCTURE

In many respects the monoclines are the principal structural features of the Colorado Plateau. Most of the deformation has occurred along them. Their aggregate length is about 2500 miles, and the longest nearly uninterrupted monocline (Grand-Axial-Uinta) is about 300 miles.

Most of the monoclines are associated with uplifts and many form the demarcation between such uplifts and the adjoining basins. Some small monoclines are situated within the uplifts and basins or mark boundaries between uplifts or basins, on the ond hand, and platforms, benches, or saddles on the other. The uplifts and basins of the Plateau dominate its structure, and the basins alone constitute about one third of the area. Nevertheless, the principal magnitude of the deformation appears to lie in the monoclines. The structural relief in typical monoclines is commonly five times, and as much as ten times, that in the adjoining uplift above the head of the monocline or in the basin below the foot of the monocline. Regionally they represent lines of great vertical shift. Dutton in his earliest writings often referred to the monoclines as displacements even where there were no associated faults. The magnitude of the displacement or the

structural relief ranges from about 100 feet to as much as 14,000 feet along part of the Grand monocline.

TABLE 1.—DATA ON MONOCLINES*

Monocline	Length (miles)	Maximum height	Maximum dip
Balanced Rock	20	1000	30
Chinle	30	200	15
Comb	95	3000	45
Defiance	90	6000	60
East Kaibab	130	3500	85
Echo Cliffs	72	1500	40
Escalante	15	2500	40
Grand	150	14,000	80[a]
Gunnison	15	500	80
Hogback	120	8000	60
Lukachukai	10	500	25
Nacimiento	60	10,000+	60†
Nutria	30	2500	80
Organ Rock	40	1500	35
Rattlesnake	20	500	10
Red Lake	30	500	20
Redlands	25	500	70
San Rafael	60	3500	85
Uinta	120	30,000	70?
Upper Valley	35	1000	30
Waterpocket	70	7000	70

* Features such as the Uinta and parts of the Grand and Nacimiento are not strictly monoclines but owing to their homology with the monoclines they are included for comparative purposes.

† Overturned

Figure 6 illustrates the principal basic variations of monoclines in cross section. The uppermost sections *a*, *b*, and *c* illustrate an often-observed transition from gently dipping, broad, symmetrical bends to the more sharply flexed type in which the synclinal bend is sharper than the anticlinal bend. Several of the large monoclines of the Plateau have this type of bending at least locally.[4] Baker (1935, p. 1483) mentioned abrupt flattening at the bottom [foot] of some of the monoclines. The bottoms are more sharply bent than the heads locally on the Nutria, San Rafael, Waterpocket, and East Kaibab monoclines. Powell (Fig. 2) also showed the synclinal bend more sharply bent. In most places monoclines face with the regional dip, but locally they are opposed to the regional dip. Buckling on the monoclines is anomalous but occurs locally on the Grand and Gunnison monoclines. Monoclines show a homology and transition with high-angle normal faults and high-angle and low-angle thrust faults. Along many of the monoclines, at least locally, the direction of dip reverses near the top or bottom so that these monoclines are almost identical with anticlines or synclines.

One of the most characteristic aspects of the monoclines is that of having sinuous trends. Many courses of the monoclines are broad, smooth curves as along parts of the Grand, Comb, and East Kaibab structures. Others such as the San Rafael, Waterpocket, Nutria, and Hogback are marked by a series of short curves of similar length. The most contorted or wrinkled of all the monoclines is the Defiance with its many short, diagonal cross folds. The south end of the East Kaibab monocline at Coconino Point is the most sharply curved, and the direction in part changes by 180 degrees.

Other common features of the monoclines are their splits or branches, found especially along the East Kaibab monocline. There is also contrast of over-all form with reference to some of the adjacent uplifts. In the San Rafael, Monument, and White River uplifts the monoclines are convex away from the uplifts; along the Uinta, Kaibab and Echo Cliffs uplifts the monoclines are concave outward.

Regionally the monoclines can be grouped roughly according to the direction of facing (Luedke and Shoemaker, 1952). In Arizona and Utah all the large or first magnitude monoclines face generally eastward. These include principally the East Kaibab, San Rafael-Waterpocket, Echo Cliffs, Comb, and Defiance. The eastern front of this group, formed by the San Rafael, Comb, and Defiance, trends south-southeasterly, and the three are arranged in echelon to the front (Figs. 7, 10). The

[4] According to Stanley W. Lohman (Personal communication, May 7, 1954), the partly faulted Redlands and Ladder Creek monoclines, respectively west and south of Grand Junction, Colorado, locally display sharp "hinge" bends at the top and gentle bends at the bottom, the "hinge" bends being nearly 90 degrees. This form, which would be similar to that in *c* of Figure 6 if it were turned upside down, is anomalous on the Plateau.

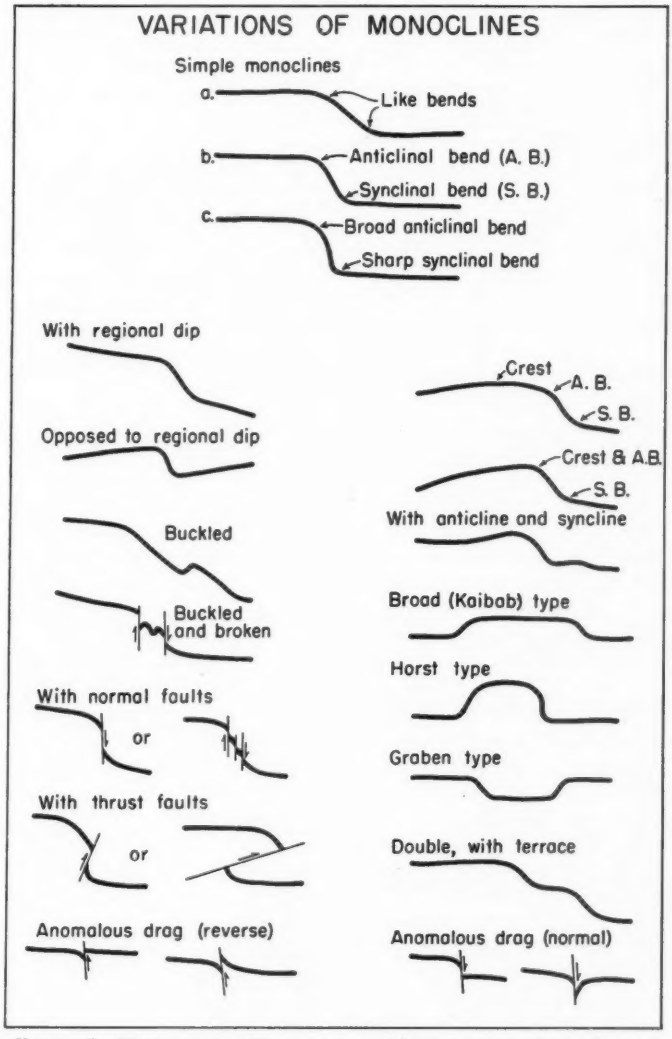

FIGURE 6.—DIAGRAMMATIC VARIATIONS OF MONOCLINES IN CROSS SECTION

associated uplifts trend generally northerly and are asymmetrical, with the steeper limb on the east. On the east and north a great group of uplifts and associated monoclines face west to south. These include principally the Uinta, Grand, Gunnison, Uncompahgre, Nacimiento, Nutria, and the northeastern part of the Hogback. Some of the minor monoclines in both groups face opposite to the facing of the major monoclines (Fig. 7). The average trend of the westerly group is northerly and the average trend of the easterly group is north-northwesterly, and hence they are not directly in opposition to each other. Lying generally between the two groups is the Uinta basin, the large Salt fold and fault belt, and part of the San Juan basin (Fig. 7).

In the western group a northeasterly trending cross alignment involves parts of several of the principal monoclines. This extends from the

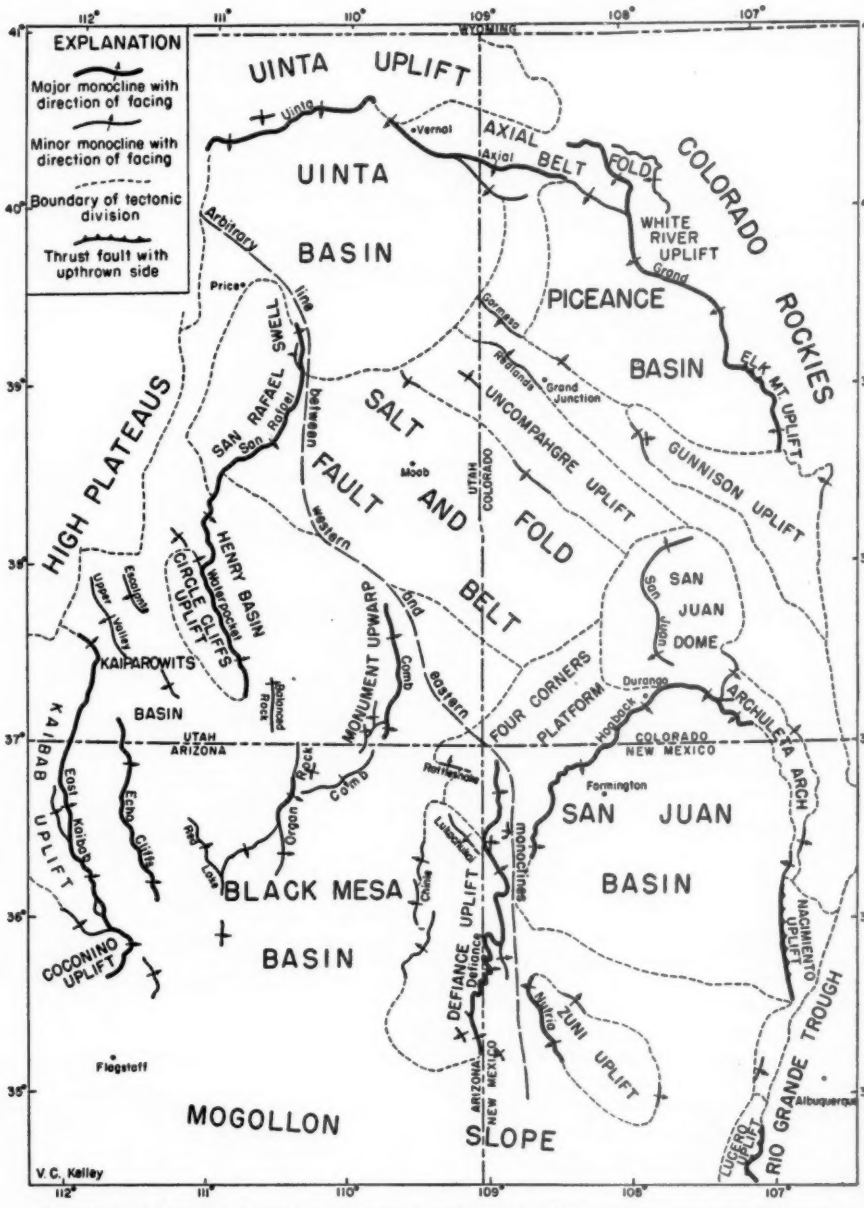

FIGURE 7.—MONOCLINES AND THE MAJOR TECTONIC DIVISIONS OF THE COLORADO PLATEAU STRUCTURAL PROVINCE

Some of the features are in whole or in part steep limbs of anticlines

southeast side of the Coconino uplift northeastward through the southwest fork of the Organ Rock monocline to the southern end of the Comb monocline. This Coconino lineament of monoclines may reflect a deep-seated tear that caused some right-lateral shift between

the northwestern (Kaibab-Monument) segment which has been moderately shortened by monoclines and folds, and the southeastern (Black Mesa basin) segment which has been only mildly shortened in the northeasterly direction.

In the eastern group of monoclines the Hogback monocline along the northwestern side of the San Juan basin faces southeastward in marked contrast to the others of the group. The Hogback monocline is backed by a platform rather than an upwarp as with the Defiance, Nutria, Monument, and other monoclines. This northeasterly trending structure, back of the Hogback monocline, has been termed the Four Corners platform (Kelley, 1950, p. 103). Although the Hogback monocline might be considered as a split from the Defiance, there is no continuity or connection between the two, and the Hogback might better be related to the mechanics of depression of the San Juan basin. It is difficult to connect this monocline genetically to the Eastern Rockies as is suggested for other monoclines of the group. Moreover, its northeasterly trend which parallels the Coconino lineament is not to be explained as a drape feature over a deep-seated tear. The Hogback monocline may have been initiated by tangential pressure transmitted from the San Rafael and Monument upthrusts through the flexured Salt fold and fault belt and Four Corners platform.

Age

The monoclines of the Colorado Plateau are considered to be Laramide in age. In most places no direct dating on the basis of strata involved or not involved in the deformation can be made. Gilbert (1880, pp. 10–11) early noted the Waterpocket monocline was formed at the close of Cretaceous time and prior to the deposition of the Eocene strata which lie undeformed across the plicated earlier strata. Gregory and Moore (1931, p. 131) assigned a similar age to the East Kaibab monocline on the basis of similar relations. The Grand monocline along the west side of the White River uplift in Colorado involves Eocene strata, and several of the monoclinal flexures along the Axial fold belt and the Uinta uplift involve the early Tertiary beds.

The Defiance monocline involves late Cretaceous strata but is truncated and overlain by beds that are probably Miocene (Chuska sandstone). Relationships near the north end of the Nacimiento uplift suggest some development of the early monoclinal flexure in pre-Wasatch (San José) time, but most of the deformation appears to have followed the lowermost beds of the Eocene formation. E. H. Baltz (1953, M. A. thesis, Univ. of N. M., p. 74–76) concluded that the Hogback monocline along the northwest side of the San Juan basin was initiated in latest Cretaceous time, continued to be deformed during Paleocene time, and was largely completed by early Eocene time. According to Childs (1950, p. 55–56) the Uinta basin began to be deformed at the rims in late Cretaceous time, and most of the monoclinal flexing was completed there by middle Eocene time.

Some monoclinal flexing is related to post-Eocene deformation along the great faults of the High Plateaus, but these structures are not considered here.

Despite the fact that many of the monoclines such as the San Rafael, Comb, Nutria, Echo Cliffs, and Organ Rock can not be directly dated, evidence is sufficient to enable general dating on the basis of similarity, and it appears that most of the monoclines are products of Laramide activity. The evidence suggests repeated or progressive growth and that their major deformations coincide closely with the major orogenic impulses of the adjacent Rockies. Furthermore, the stratigraphic relations along the monoclines that rim the San Juan and Uinta basins suggest that flexing along a single monocline was not everywhere simultaneous. Although the correlation of early Tertiary strata in widely separated areas is speculative, the present evidence suggests that the eastern monoclines began their growth before and continued their activity after the deformation of the western monoclines.

Origin and Regional Relations

The origin of the monoclines is of prime importance to any explanation of the formation of the Colorado Plateau. However, a discussion of the genesis of the Plateau tectonics would not ordinarily begin with an analysis of

the monoclines, for larger structural elements and their controlling forces are more fundamental. The structural origin of the Colorado Plateau is to be treated in a paper now in preparation (Kelley, 1955), and only the deformation of the monoclines is considered here; however, the monoclines are indicative as local linear modes of yielding to region-wide forces.

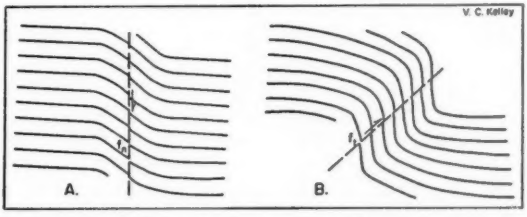

FIGURE 8.—DEFORMATION OF A NORMAL FAULT A INTO A THRUST FAULT B BY ROTATION OF THE FAULT PLANE

The earliest explanation of the monoclines called upon vertical forces and the creation of deep-seated vertical fractures over which the near-surface strata draped. Compression and shortening in the region were not considered. Even now it is perhaps most commonly held that vertical forces dominated the formation of the Plateau monoclines, uplifts, and basins. Nevin (1950, p. 59–60) has clearly presented this view.

About 20 years ago Baker (1935, p. 1500–1504) presented the idea of compression in the formation of the Colorado Plateau monoclines of Utah. He believed that they formed above deep-seated thrusts. It is not possible to determine from the surface form or structural profile of a monocline whether it formed above (1) a high-angle normal fault, (2) a vertical fault, (3) a high-angle reverse fault, or (4) a deep-seated buckle. Dutton (1880, p. 25) early made reference to the complete homology between monoclines and nearly vertical faults, and it is easy to imagine that simple vertical forces caused the faults as well as the monoclines. However, there are several features about the total form of the monoclines, their general relationship to one another, uplifts, and certain thrusts which point to a complex deforming action involving tangential compression in most if not all of the monoclines. It is not probable that the large monoclines if followed downward would everywhere pass into thrust faults. Rather it appears that the Precambrian basement may have buckled and that the buckles are broken by stretch thrusts only locally. The evidence which favors the hypothesis that compression was the dominating action in the formation of most of the large monoclines is as follows:

(1) Asymmetrical form of the uplifts
(2) Curving of the monoclines toward the uplifts at the terminations
(3) Small staggered and echelon folds along the crests of the uplifts
(4) Small staggered and echelon folds immediately above the heads or below the bottoms of the monoclines
(5) Sharper synclinal bends than anticlinal bends
(6) Small scission thrusts associated with the monoclines and uplifts
(7) Gradation on a regional scale between gentle monoclines and thrust faults.

Baker (1935, p. 1503) pointed out that, if the upwarps of the Plateau were formed by movement upward on reverse faults, the steep monoclinal limbs would be under tension, and normal faults parallel to the strike might form. Baker (1935, p. 1502) believed that if the monoclines were formed over normal faults of tensional origin the facing of the monoclines would be almost equally distributed west and east. In this he was considering only the predominantly east-facing western monoclines. Baker further believed that

"the low tensile strength of rock suggests the inference that fracturing under tension would result in the formation of numerous small, closely spaced, normal faults, instead of the few widely

spaced faults that would be expressed at the surface by the principal monoclines."

In the early stages of monocline formation little or no tilting may accompany the shift of the masses on both sides of the flex. As compression and deformation increase, high-angle fracturing (*f*) and some normal faulting may occur as in Figure 8 (A). With increased deformation, steepening of the monoclinal limb and general regional tilting in the uplift and basin adjacent to the monocline cause the early formed normal fault to rotate through the vertical to a moderately high-angle reverse fault. As the fault is flattened by the monoclinal steepening, relief of compression becomes easier and later deformation may succeed by thrusting on the fracture (*f*). Thus, in the early stages of monocline formation normal faults and possibly some tension on the flexing limb may accompany compression. As deformation proceeds the normal fracture is rotated into a position of a shear, and a thrust may result. Vanderwilt (1937, p. 88–89) described and illustrated this sort of development of monoclines into thrusts in his interpretation of the transition of the southern extension of the Grand monocline into the Elk Mountain thrusts near Snowmass Mountain. Similar relations are present elsewhere as along the Nacimiento and Lucero uplifts in New Mexico, along the White River uplift near Glenwood Springs, along the south side of the Uinta uplift in a minor way, near Crested Butte, and probably also along the Crookton thrust east of Gunnison, Colorado. If the forces which caused the monoclines were vertical and if there were horizontal tension, then normal faults, if formed, would persist, and very steep beds or overturned beds would not result.

If for some reason nearly vertical fractures were to form along a monocline at the time when the limb dipped only 20°, when the limb was rotated to vertical the fracture would be rotated into the position of a low-angle fault.

The wrinkling of the monoclinal trends by short, diagonal cross folds is strongly suggestive of a lateral component of shift during compression and upthrusting. This is strikingly illustrated in the Defiance monocline (Fig. 7). From the relations between the Defiance uplift and both the San Juan basin and the Zuni uplift it appears that a force-couple acting clockwise in the opposing Defiance and Zuni uplifts produced right-lateral shift and right-lateral buckling along the Defiance monocline. Inasmuch as this is along the dividing line between the east-facing and west-facing monoclines (Fig. 7), it may indicate regional right-lateral shift between the western and eastern parts of the Colorado Plateau.

Summary and Conclusions

Many if not most of the structures termed monoclines on the Colorado Plateau are by strict adherence to the simple definition not monoclines at all because the dip reverses its direction either side of the flexure. But to rule out such places on a regionally continuous flexure is to play on terminology and obscure the description and analysis of the principal lines of deformation. In the Colorado Plateau and in other broad structural provinces the monocline is the dominant feature, and the crestal and trough axes are not the critical or real structural features but rather only tangent lines determined by a horizon. Associated anticlines and synclines should be considered to be a part or an adjunct of the monocline rather than rule out the term monocline. Any monocline whose axes plunge has components of reversal; and most Plateau monoclines plunge. It is not meant to be implied, however, that all steep limbs of asymmetrical anticlines or synclines should be termed monoclines. The crux of the classification is in the regional relations. It may be significant to term some steep limbs of anticlines monoclines in a regional analysis, whereas in a local description it would not. The steep limb of a local anticline may be a part of a regional monocline.

In practice geologists probably will continue to refer to a narrow persistent downbend (or upbend) as a monocline. Relatively great length, narrowness of the steep limb, and dominance of the flexure in the deformation of the area should be the determining features of the designation. In regions where monoclines are prominent, a broad or even locally abrupt reversal of dip should not be cause for dropping the monoclinal designation. If this regional structural concept of a monocline is not ac-

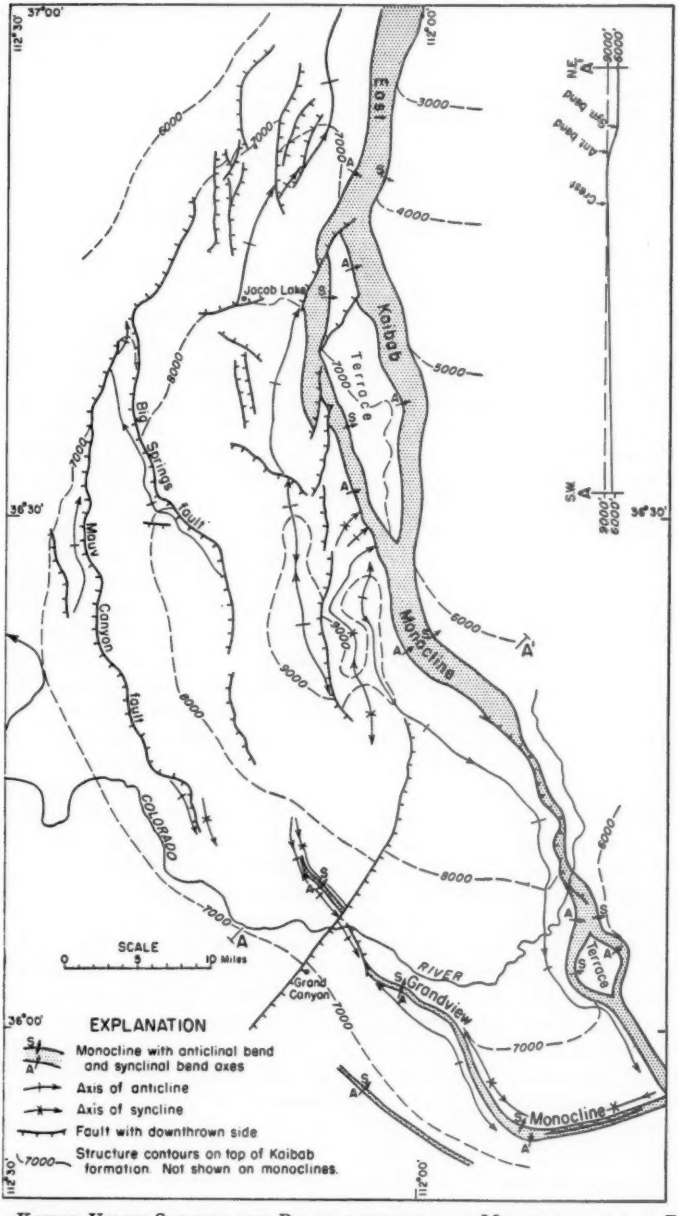

FIGURE 9.—KAIBAB UPLIFT SHOWING THE RELATIONSHIPS OF THE MONOCLINES TO THE FOLD AXES AND FAULTS; ADAPTED FROM STRAHLER, 1948

cepted, then the East Kaibab flexure, probably the original type, could not be termed a monocline (Fig. 9). For that matter most of the features on the Plateau currently termed bend because the beds above and below may not be horizontal. The layers involved may be sediment, flows, or foliation. Local steepening might involve some overturning. Monoclines

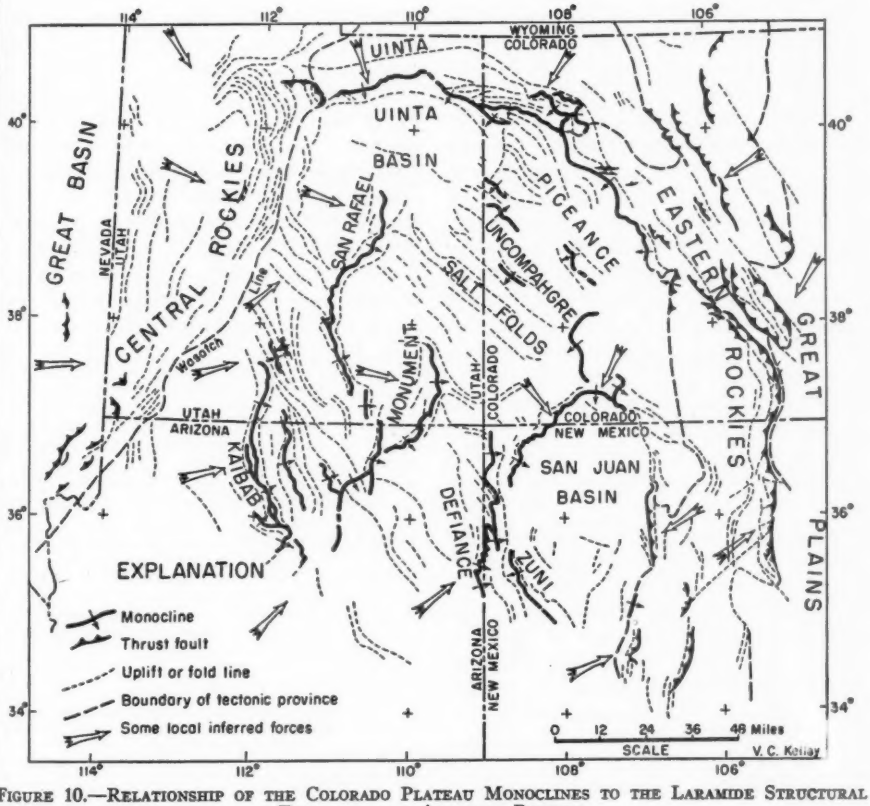

FIGURE 10.—RELATIONSHIP OF THE COLORADO PLATEAU MONOCLINES TO THE LARAMIDE STRUCTURAL TRENDS OF THE ADJACENT ROCKIES

monoclines are not so if the strict definition is followed.

Within the Plateau and elsewhere moderate dips are locally interrupted by steep dips, and such double flexures have been and may continue to be termed monoclines. Therefore, it is proposed that the definition of monocline not be restricted to "local steepening in otherwise gently dipping beds."

According to the proposal herein *a monocline is a double bend involving local steepening in otherwise less steeply inclined layers.* It is often, or ideally, a combination of anticlinal and synclinal bends. It is not always "a steplike" may be described as gentle or steep, narrow or broad, open or closed, level or plunging, overturned, buckled, broken, thrust, *etc.*

Almost every type of intensity of monocline is present on the Plateau from those of low to high dip, short to long steep limb, and straight to highly sinuous trend. They grade laterally into each other and laterally as well as vertically into high-angle normal or reverse faults. Also locally as along the Nacimiento, Lucero, and Elk Mountain uplifts former monoclines have been converted into pronounced thrust faults, and locally only the lower half or synclinal bend, often overturned, is still clearly revealed.

Where the uplifted side is stripped of its strata then the lower preserved part including the syncline or synclinal bend may be referred to as a half monocline.

The hypothesis that many of the monoclines are the result of vertical forces unaccompanied by compression cannot be refuted. Nevertheless, there is a considerable array of evidence favoring compression as the mode of their formation. Even so, it is not impossible that some of the monoclines were formed by vertical forces acting in a field or horizontal tension either before or after Laramide compression. It is, however, difficult to assign a tensional- and vertical-force origin to structures which appear to be so clearly Laramide in age in view of the compressive forces known to have been active in the orogenic belts of the Rockies to the east and west. In a sense the major monoclines are orogenic "lines" widely spaced across the Plateau, and in places along the east side of the province they are essentially a part of the Eastern Rockies. A structure such as the Nacimiento thrust, a part of the Eastern Rockies orogenic belt, was at an earlier stage a monocline similar to Nutria, Comb, or East Kaibab. The Nacimiento thrust at its north end passes into a typical Plateau monocline. The monoclines of the Plateau proper are merely weaker manifestations of the pronounced compressive deformations that took place in the Laramide Rockies to the east and to the west. The western monoclines may be related to and a manifestation of the compressive deformation of the Central Rockies belt, and the eastern monoclines are probably related in origin to the Eastern Rockies. Prongs of the Eastern Rockies do in a sense extend into the Plateau in the White River, Uinta, Gunnison, and Uncompahgre uplifts. Had time and compressive energy lasted the Plateau might have been completely converted to an orogenic province like the Rockies.

Nevertheless, it does not appear that a simple set of regional forces acting across the Plateau from the Central to the Eastern Rockies produced the monoclines of the Plateau; rather their distribution and form may be the result of the combined influence of (1) a mosaic of differing Precambrian subcrustal nuclei, (2) late Paleozoic deformational units, (3) Laramide compression and perhaps deep-seated thrusting from the west, and (4) Laramide compression and thrusting from the east. The deep-seated nuclei might be regular and irregular segments whose dispositions and shapes approximate those of the variously oriented tectonic divisions at the surface (Figs. 7, 10). The stress axes within adjacent nuclei might have been oriented quite differently, and the deformations in the form of monoclines and other folds would be obliquely oriented to correspond with adjoining segments or divisions. Something of this sort must have occurred to cause the contrasting structural trends that exist within the Plateau as shown in Figure 10 between the Monument uplift and the Four Corners platform or between the Circle Cliffs and San Rafael uplifts.

References Cited

American Association of Petroleum Geologists, 1929, Structure of Typical American Oil Fields, v. 1: Tulsa, 510 p.

Baker, A. A., 1935, Geologic structure of southeastern Utah: Am. Assoc. Petroleum Geologists Bull., v. 19, p. 1472–1507.

Billings, M. P., 1954, Structural geology: N. Y., Prentice-Hall, 514 p.

Busk, H. G., 1929, Earth flexures, their geometry and their representation and analysis in geological section with special reference to the problem of oil finding: Cambridge, England, The University Press, 106 p.

Childs, O. E., 1950, Geologic history of the Uinta basin, *in* Petroleum geology of the Uinta basin: Intermountain Assoc. Petroleum Geologists, Guidebook to the geology of Utah, No. 3, Salt Lake City, p. 49–59.

Clapp, F. G., 1917, Revision of the structural classification of petroleum and natural gas fields: Geol. Soc. America Bull., v. 28, p. 553–602.

—— 1929, Role of geologic structure in the accumulation of petroleum, *in* Structure of typical American oil fields, v. 2: Am. Assoc. Petroleum Geologists, Tulsa, p. 671, 684–686.

Daly, R. A., 1915, A geological reconnaissance between Golden and Kamloops, B. C., along the Canadian Pacific Railway: Geol. Survey Canada Mem. 68, 260 p.

—— 1916, Homocline and monocline: Geol. Soc. America Bull., v. 47, p. 89–92.

Dutton, C. E., 1880, Report on the geology of the High Plateaus of Utah with atlas: U. S. Geog. and Geol. Survey of the Rocky Mountain Region, Washington, 307 p.

—— 1882a, The physical geology of the Grand Canyon district: U. S. Geol. Survey, 2d Ann. Rept., p. 47–166.

—— 1882b, Tertiary history of the Grand Canyon district: U. S. Geol. Survey Mon. 2, 264 p.

Geikie, Archibald, 1882, Textbook of geology: London, MacMillan, 971 p.

Gilbert, G. K., 1876, The Colorado Plateau Province as a field for geological study: Am. Jour. Sci. 3rd ser., v. 12, p. 16–24, 85–103.

—— 1877, Report on the geology of the Henry Mountains: U. S. Geog. and Geol. Survey of the Rocky Mountain Region, Washington, 170 p.

Gregory, H. E., and Moore, R. C., 1931, The Kaiparowits region, a geographic and geologic reconnaissance of parts of Utah and Arizona: U. S. Geol. Survey Prof. Paper, 164, 161 p.

Hills, E. S., 1953, Outlines of structural geology: N. Y., Wiley, 182 p.

Johnson, R. H., and Huntley, L. G., 1916, Principles of oil and gas production: N. Y., Wiley, 371 p.

Kelley, V. C., 1950, Regional structure of the San Juan basin: N. M. Geol. Soc., San Juan basin, N. M. and Colo., First Field Conf. p. 101–108.

—— 1955, Regional tectonics of the Colorado Plateau and relationship to the origin and distribution of uranium: Univ. New Mexico Publications in Geology, no. 5, 1955. 120 p.

Lahee, F. H., 1952, Field geology: N. Y., McGraw-Hill, 883 p.

Luedke, R. G., and Shoemaker, E. M., 1952, Tectonic map of the Colorado Plateau: U. S. Geol. Survey Trace Elem. Memor. Rept. 301.

Loomis, F. B., 1937, Physiography of the United States: N. Y., Doubleday, 350 p.

Nevin, C. M., 1950, Principles of structural geology: N. Y., Wiley, 410 p.

Page, David, 1865, Handbook of geological terms: Edinburgh, Blackwood, 2d ed. 506 p.

Powell, J. W., 1873, Geological structure of a district of country lying to the north of the Grand Canyon of the Colorado: Am. Jour. Sci., 3rd ser., v. 5, p. 456–465.

—— 1875, Exploration of the Colorado River of the West and its tributaries: Washington, D. C., Govt. Print. Office, 291 p.

Rogers, H. D., 1858, The geology of Pennsylvania: Philadelphia, Geol. Survey Pa., v. 1, 586 p.; v. 2, 1045 p.

Rogers, W. B., and Rogers, H. D., 1843, On the physical structure of the Appalachian chain, as exemplifying the laws which regulated the elevation of great mountain chains generally: Assoc. Geographers and Naturalists, v. 1, Repts. 1st, 2d, and 3rd Mtg., 1840–1842, p. 474–531.

Stočes, Bohuslav, and White, C. H., 1935, Structural geology: N. Y., Van Nostrand, 460 p.

Strahler, A. N., 1948, Geomorphology and structure of the West Kaibab fault zone and Kaibab Plateau, Arizona: Geol. Soc. America Bull., v. 59, p. 513–540.

Vanderwilt, J. W., 1937, Geology and mineral deposits of the Snowmass Mountain area, Gunnison County, Colorado: U. S. Geol. Survey Bull. 884, 184 p.

Willis, Bailey, 1929, Geologic structures: N. Y., McGraw-Hill, 518 p.

University of New Mexico, Albuquerque, N. M.

Manuscript Received by the Secretary of the Society, July 2, 1954

Published with the Permission of the U. S. Atomic Energy Commission

BULLETIN OF THE GEOLOGICAL SOCIETY OF AMERICA
VOL. 66, PP. 805-810, 2 FIGS., 2 PLS. JULY 1955

SUB-CHATTANOOGA RESIDUUM IN TENNESSEE AND KENTUCKY

BY CHARLES MILTON, LOUIS C. CONANT, AND VERNON E. SWANSON

ABSTRACT

Between the Chattanooga shale and the underlying limestone in parts of Tennessee and Kentucky is a clayey gray to brown zone as much as several feet thick. This represents an interval of limestone that has been leached by sulfuric acid formed by oxidation of the abundant pyrite in the black shale. Alteration of the limestone decreases with distance from the base of the black shale; several stages of alteration are recognized and described. The acid also attacks the shale, as indicated by locally conspicuous efflorescences of copiapite, coquimbite, halotrichite, gypsum, and possibly other sulfates. Basaluminite, a hydrous aluminum sulfate previously reported only from England and France, was found in geodal cavities and thin seams in the residuum. The clayey zone has been previously interpreted as an ancient soil formed on the limestone surface during Devonian time.

Petrography and chemical composition of the leached zone are described and illustrated by photomicrographs. The nature of the shale-limestone contact where the leached clayey zone is absent is illustrated by a diamond-drill core from Tennessee. Many fresh outcrops and several dozen cores that penetrate the contact show no clayey material at this position.

The clayey zone does not represent an old soil.

CONTENTS

TEXT

	Page
Introduction	805
Pyritic content of the black shale	806
Limestone	807
Clayey residuum	808
Contact between unweathered shale and limestone	809
Conclusion	809
References cited	810

ILLUSTRATIONS

Figure	Page
1. Locations of outcrops	806
2. Schematic representation of formation of residuum	809

Plate	Facing page
1. Fresh and weathered contacts at base of Chattanooga shale and limestone	806
2. Photomicrographs of limestone—residuum sequence	807

TABLE

Table	Page
1. Analyses of soluble and insoluble constituents of unaltered limestone and residuum	808

INTRODUCTION

A gray to brown clayey zone as much as several feet thick underlies the Chattanooga shale and rests on Ordovician limestone in Tennessee and Kentucky. During recent studies of the Chattanooga shale Conant and Swanson investigated the stratigraphic relationship of this clay in the field, and Milton and others studied it in the laboratory. Specimens of the clayey rock and underlying limestone have been studied from five localities along the eastern and southern edge of the Nashville Basin (Fig. 1):

(1) West end of Cumberland River bridge, Burkesville, Cumberland County, Kentucky, (2) 8 miles southwest of Gainesboro, Jackson County, Tennessee, (3) 7 miles northwest of Manchester, Coffee County, Tennessee, (4) 0.9 mile west of Cornersville, Marshall County, Tennessee, (5) 3 miles northeast of Pulaski, Giles County, Tennessee.

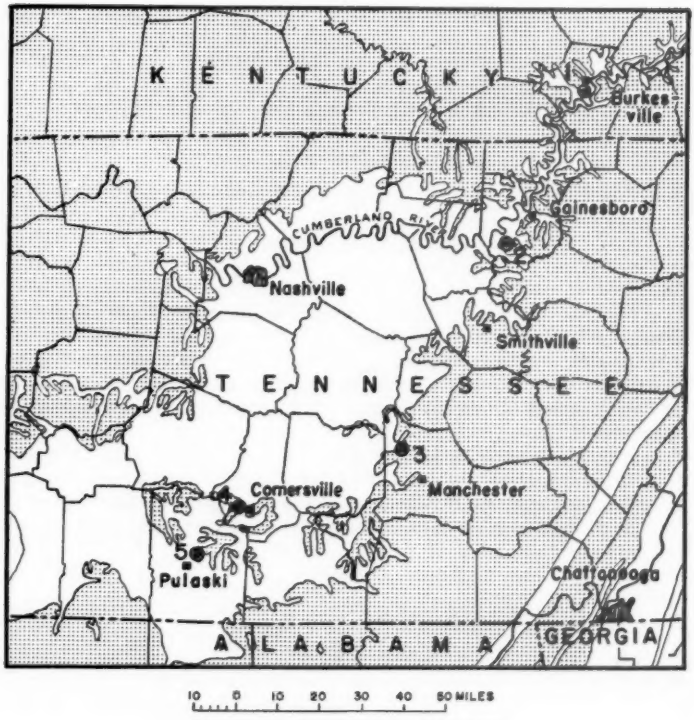

FIGURE 1.—LOCATIONS OF OUTCROPS

Shaded areas are underlain by Chattanooga shale. Central unshaded area is the Nashville Basin.

Good exposures of the residuum range in thickness from a few inches to at least 15 feet. Most exposures show an undulating lower boundary in places resting upon a pinnacled surface of limestone (Pl. 1, fig. 2). To understand the origin and history of this clayey zone, important features of the overlying black shale, the underlying unaltered limestone, and clayey zone are described.

PYRITIC CONTENT OF THE BLACK SHALE

The abundance of pyrite in the black shale is well established. Many hand specimens show masses of pyrite 1 cm or more across (Pl. 1, fig. 1), and most of the black shale specimens studied chemically and microscopically show pyrite to constitute about 10 per cent of the rock. Pyrite consists of half sulfur by weight,

PLATE 1.—FRESH AND WEATHERED CONTACTS AT BASE OF CHATTANOOGA SHALE

FIGURE 1.—UNWEATHERED CONTACT, AT 3 CM, BETWEEN CHATTANOOGA SHALE AND UNDERLYING LIMESTONE

The broad band in the limestone and the broken thin band in the shale are calcite. The gray lenses in the shale are pyrite, as is much of the material at top of the limestone. Core obtained by U. S. Bureau of Mines near Smithville, Tennessee.

FIGURE 2.—RESIDUUM BELOW CHATTANOOGA SHALE

Dashed ink line (above hammer) marks base of shale. The shovel stands against residuum that extends at least 5 feet down a widened joint. The hammer rests on a 1-inch layer of chert that extends through the residuum and the limestone pillars. Locality 5, near Pulaski, Tennessee.

FIGURE 1

FIGURE 2

FRESH AND WEATHERED CONTACTS AT BASE OF CHATTANOOGA SHALE

DETROIT PUBLIC LIBRARY

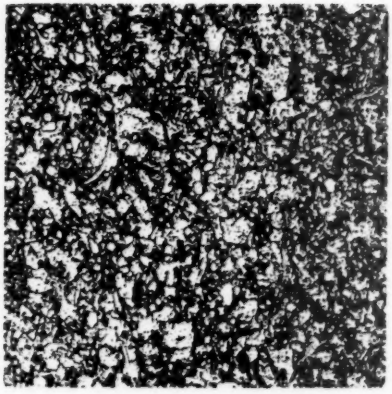

FIGURE 1

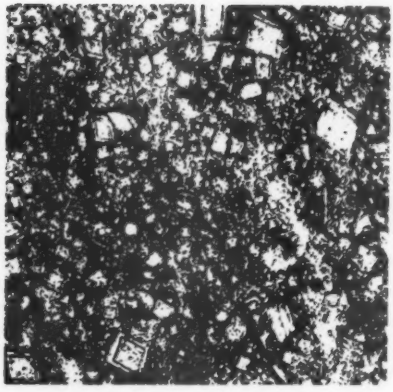

FIGURE 2

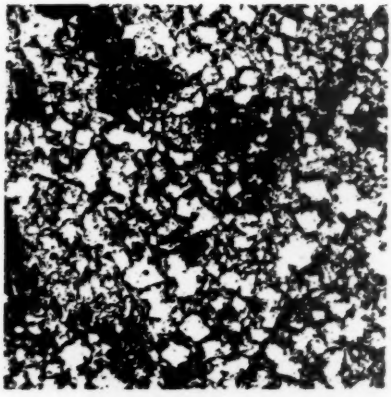

FIGURE 3

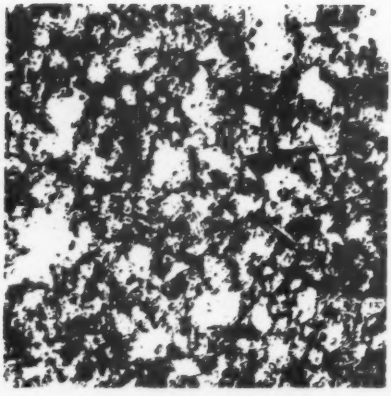

FIGURE 4

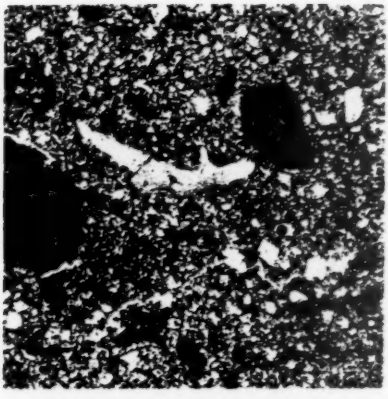

FIGURE 5

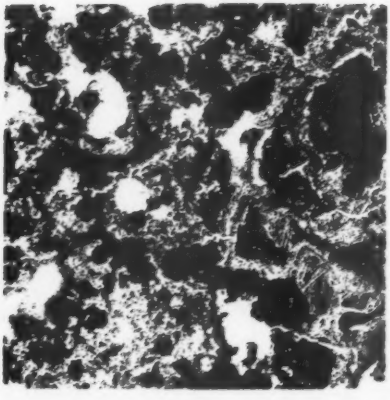

FIGURE 6

PHOTOMICROGRAPHS OF LIMESTONE — RESIDUUM SEQUENCE

which in turn constitutes about a third by weight of sulfuric acid; accordingly, a given weight of pyrite will oxidize to 1½ times that weight of sulfuric acid. This sulfuric acid, in turn, will react with and dissolve an equal weight of calcium carbonate. The shale in a column 1 foot square and 30 feet high—30 cubic feet—weighs approximately 4350 pounds. If 435 pounds of this is pyrite, it can produce 650 pounds of sulfuric acid, which can react with about 4½ cubic feet of limestone. Thus, the sulfuric acid originating from the weathering of this column of black shale could migrate downward and dissolve several cubic feet of the underlying limestone. Though the shale is normally impervious, weathering cracks permit the water to soak through it. A consideration of the concurrent disintegrative processes acting on the limestone, such as freezing and thawing of ground water, root action, and solution by carbonic acid, helps to explain the observed thicknesses of clayey material overlying the limestone.

All the sulfur in the black shale may not react immediately with underlying limestone, for much of it first reacts with the shale itself to form hydrous sulfates of aluminum, iron, and calcium—such as copiapite, coquimbite, halotrichite, and gypsum, all of which may be observed as conspicuous efflorescences in recently opened road cuts in the shale. These sulfur-bearing encrustations, however, are merely temporary, and eventually hydrolysis of the iron and aluminum sulfates will produce insoluble oxide compounds and free the sulfuric acid, which will react with the limestone just as if produced directly from pyrite. On the floor of an abandoned adit in the Chattanooga shale about 7 miles east of Smithville, DeKalb County, Tennessee, a white powdery sediment several inches thick was found in standing water. Tests showed it to be hydrous ferric sulfate, optically isotropic and "amorphous to X-rays."

Limestone

Thin sections of the unaltered gray limestone a few feet below the residuum show characteristic textual features (Pl. 2, fig. 1). The limestone has conspicuous small areas of coarsely crystallized calcite and consists of about three-quarters carbonate rhombohedra and one-quarter interstitial clayey and siliceous material. The upper part of the limestone, just below the residuum, is porous, and thin sections show numerous altered crystals and rhombohedral voids (Pl. 2, figs. 2–4).

Table 1 gives the chemical composition of the acid-soluble and insoluble constituents—corresponding roughly to the carbonate and clay content—of the fresh limestone at Burkesville and of the overlying residuum. The analyses indicate a virtually complete removal of calcium and magnesium carbonate, a con-

Plate 2.—PHOTOMICROGRAPHS OF LIMESTONE—RESIDUUM SEQUENCE

Figure 1.—Unaltered Limestone

Shows characteristic rhombohedra and a few microfossils in clayey goundmass. Locality 3, near Manchester, Tennessee; ×35.

Figure 2.—Partly Leached Limestone

Zoning in dolomite rhombs is probably caused by differential solution. Dark background is a clayey matrix. Locality 4, near Cornersville, Tennessee; ×100

Figure 3.—Leached Limestone

Rhombohedral voids and black areas of manganese oxide are conspicuous. Locality 1, near Burkesville, Kentucky; ×40

Figure 4.—Leached Limestone

Carbonate has been completely removed, but rhombohedral outlines are still present; clayey matrix appears black; ×100

Figure 5.—Microstructure of the Residuum

Just above Figure 2 of Plate 2; the carbonate has been completely dissolved and has left distinctive rhombohedral voids. The proportionately large amount of clay also has silicified fossils, dark phosphatic areas, and angular quartz particles; ×35

Figure 6.—Clayey Residuum Showing Basaluminite

Gray fibrous material is basaluminite; colloform matter is grayish-orange clay. Locality 5, near Pulaski, Tennessee; ×40

siderable addition of iron, alumina, and water, and a relative loss of silica. The quantities of alkalies remain about the same. Mineralogically, the material of the residuum is complex

TABLE 1.—ANALYSES OF SOLUBLE AND INSOLUBLE CONSTITUENTS OF UNALTERED LIMESTONE AND RESIDUUM

Locality 1, near Burkesville, Kentucky.

Analyst: S. M. Berthold

	Limestone Specimen 16N-1-2		Residuum Specimen 16N-1-1
	Acid soluble	Acid insoluble	
SiO_2	...	78.6	55.2
Al_2O_3	...	10.9	19.0
Fe_2O_3	1.7	1.4	5.8
FeO		0.34	0.32
MgO	12.6	0.62	0.86
CaO	24.4	0.12	0.08
Na_2O	0.10	0.71	0.66
K_2O	0.06	3.0	3.8
TiO_2	0.00	0.58	0.69
P_2O_5	0.17	0.05	0.54
MnO	0.10	0.06	0.42
Ignition	*	2.1	12.4
BaO	0.00	0.60	0.09
SO_3	0.17	1.2	0.50
		100.3	100.4

* Ignition loss on original limestone was 34.6%; added to acid soluble, makes 73.9% total soluble; *i.e.*, about one fourth of the limestone is clay, etc. (acid—$\frac{1}{10}$ HCl)

but, in general, the major constituents are probably potash-bearing clay minerals, possibly glauconite-celadonite, hydrous iron-bearing clays such as nontronite, also quartz and hydrous oxides of aluminum and iron.

CLAYEY RESIDUUM

After removal of carbonate from the limestone, the clayey residue undergoes further attack by sulfuric acid solutions, no longer neutralized by carbonate. The clayey residuum shows a characteristic zoning, each successive zone upward from the limestone corresponding to increased change by acid attack. Directly beneath the black shale are several inches of dominantly grayish-orange clay, often patchily interspersed with white, gray, and black areas. The grayish-orange (also yellow locally) clay is very fine-grained and has a microscopically banded structure suggestive of crystallization from a gel, rather than bedding. X-ray study indicates that quartz, illite, and other clayey material are major constituents. Carbonate and rhombohedral holes are absent. Relicts of the limestone, however, may still be found in the form of glauconite particles and organic aggregates that were once phosphatic and are now apparently chloritized. The white material, which shows colloform structure, is amorphous to X-rays and appears to be in part poorly crystallized clay, in part phosphatic material, possibly related to vashegyite. Figures 5 and 6 of Plate 2 show the microstructure of this upper zone in the residuum.

This severely altered upper layer commonly grades downward into "stratified" material, the bedded structure evidently inherited from the limestone. No evidence has been found of lithologic or chemical variations that would suggest inheritance from a soil profile. The textural variation in the "stratified" material is only such as might exist in uniform clayey limestone having slight variations in the clay-carbonate content or in grain size of the carbonate.

In many places the contact between the residuum and the underlying limestone is sharp, even where the limestone is somewhat leached, but in other places the contact between the residuum and the limestone is gradational. The general relations of all these phases are shown in Figure 2.

Locally the normal sequence of the residuum has been disturbed by slumping and by the freezing and thawing of ground water. Of interest in some of these disturbed zones is the rare mineral basaluminite, a hydrous aluminum sulfate, recently discovered in England and France, and, for the first time in North America, in Giles County, Tennessee. Basaluminite has the composition $2Al_2O_3 \cdot SO_3 \cdot 10H_2O$ or $3Al(OH)_3 \cdot Al(OH)SO_4 \cdot 5H_2O$ (Hollingsworth and Bannister, 1950, p. 9). In England it was found in fissures in the clayey matter that coats joint faces in "ironstone," and for a long time was erroneously called allophane. It lies

some 60 feet beneath a cover of impervious clays, and the possibility that it resulted from the weathering of soil in Jurassic time was considered and rejected by Hollingsworth and Bannister. They believe that alternate freezing and thawing during Pleistocene time shattered likewise show no sign of weathering at the contact.

Conclusion

In view of the unconformity between the Chattanooga shale and the underlying lime-

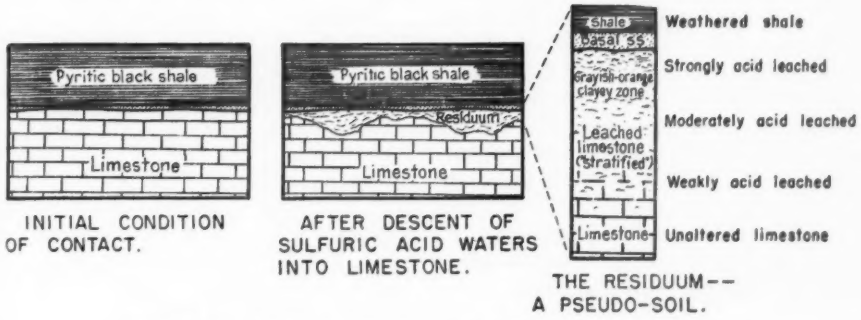

Figure 2.—Schematic Representation of Formation of Residuum

the ironstone, that these fissures trapped aluminum sulfate solutions formed from pyrite oxidizing at higher levels, and that these solutions reacted with the clay. These trapped solutions eventually evaporated, depositing the basaluminite.

Contact between Unweathered Shale and Limestone

If the residuum were merely the result of recent weathering, no residuum would be present at unweathered contacts. Recent deep highway cuts through the shale show no residuum except locally at the ends where the shale was at or close to the surface. Likewise, several dozen diamond-drill cores of the shale, obtained in the Smithville, Tennessee, area by the U. S. Bureau of Mines for the Atomic Energy Commission, show a sharp basal contact and no sign of residuum, even though the basal part may have a concentration of pyrite (Pl. 1, fig. 1). Mr. David H. Swann (Personal communication, May 13, 1953) reports that drill cores from southwestern Indiana and southern Illinois show a similar concentration of pyrite near the base of the New Albany shale (a correlative of the Chattanooga shale of Tennessee and Kentucky), but stone, and of the belief that the limestone surface was subjected to subaerial erosion prior to deposition of the black shale, it is not surprising that the clayey residuum has been interpreted as an ancient soil (paleosol). There is indeed a superficial but misleading resemblance to the A, B, and C horizons of the pedologists. Foerste (1901, p. 430–431) mentioned residual soil at the base of the Chattanooga shale in an area south of Nashville. Ulrich (1911, p. 454–459, 464–465) discussed the presence of residual soil along unconformities, and mentioned such material either just below or in the base of the Chattanooga but cited no convincing evidence. Kindle (1912, p. 122–123) described and illustrated residual clay below the black shale and considered it to be definitely a residuum on the pre-Chattanooga land surface. More recently Jillson (1951a, p. 5–6, 10; 1951b, p. 48) has mentioned the presence of an "old soil" below the Chattanooga shale in Cumberland County, Kentucky, but he did not describe it nor state evidence of its origin.

No evidence known to the writers favors the paleosol interpretation. Compaction of a pre-Chattanooga soil by the load of thousands of feet of subsequently deposited sediments certainly would have destroyed the rhombo-

hedral voids so conspicuous in the photomicrographs of the residuum; similarly, the empty casts of fossils that have been found in the clayey material at several places would have been squeezed beyond recognition. Evidence is lacking of life that was coexistent with the forming of the clayey residuum, such as plant roots or animal borings. Most convincing is the absence of the residuum in the subsurface, where cores consistently reveal a line-sharp contact between the shale and the limestone.

In summary, the clayey residuum observed at numerous outcrops is not the remnant of an ancient soil, but is the result of Recent weathering. The residuum is forming on the limestone today as a result of the continued attack by chemically active agents derived from weathering of the overlying pyritic black shale.

References Cited

Foerste, A. F., 1901, Silurian and Devonian limestone of Tennessee and Kentucky: Geol. Soc. America Bull., v. 12, p. 395–444.

Hollingsworth, S. E., and Bannister, F. A., 1950, Basaluminite and hydrobasaluminite, two new minerals from Northhamptonshire: Mineralog. Mag., v. 29, p. 1–17.

Jillson, W. R., 1951a, The Burkesville limestone: Frankfort, Ky., Roberts Printing Co., 15 p.

—— 1951b, The geology of Cumberland County, Kentucky: Frankfort, Ky., Roberts Printing Co., 124 p.

Kindle, E. M., 1912, The unconformity at the base of the Chattanooga shale in Kentucky. Am. Jour. Sci., 4th ser., v. 183, p. 120–136.

Ulrich, E. O., 1911, Revision of the Paleozoic systems: Geol. Soc. America Bull., v. 22, p. 281–680.

U. S. Geological Survey, Washington, D. C.
Manuscript Received by the Secretary of the Society, October 9, 1954
Publication Authorized by the Director, U. S. Geological Survey

52°
128°
126°
124°
COAST
RANGE
51°
Vancouver
Island
PACIFIC
OCEAN
49°
128°
126°
124°

STRUCTURAL MAP OF SOUTHERN BRITISH COLUMBIA

Showing batholiths, trend lines of intruded formations, and principal faults.
Formational boundaries adapted from Geological Survey of Canada Map 932, 1948

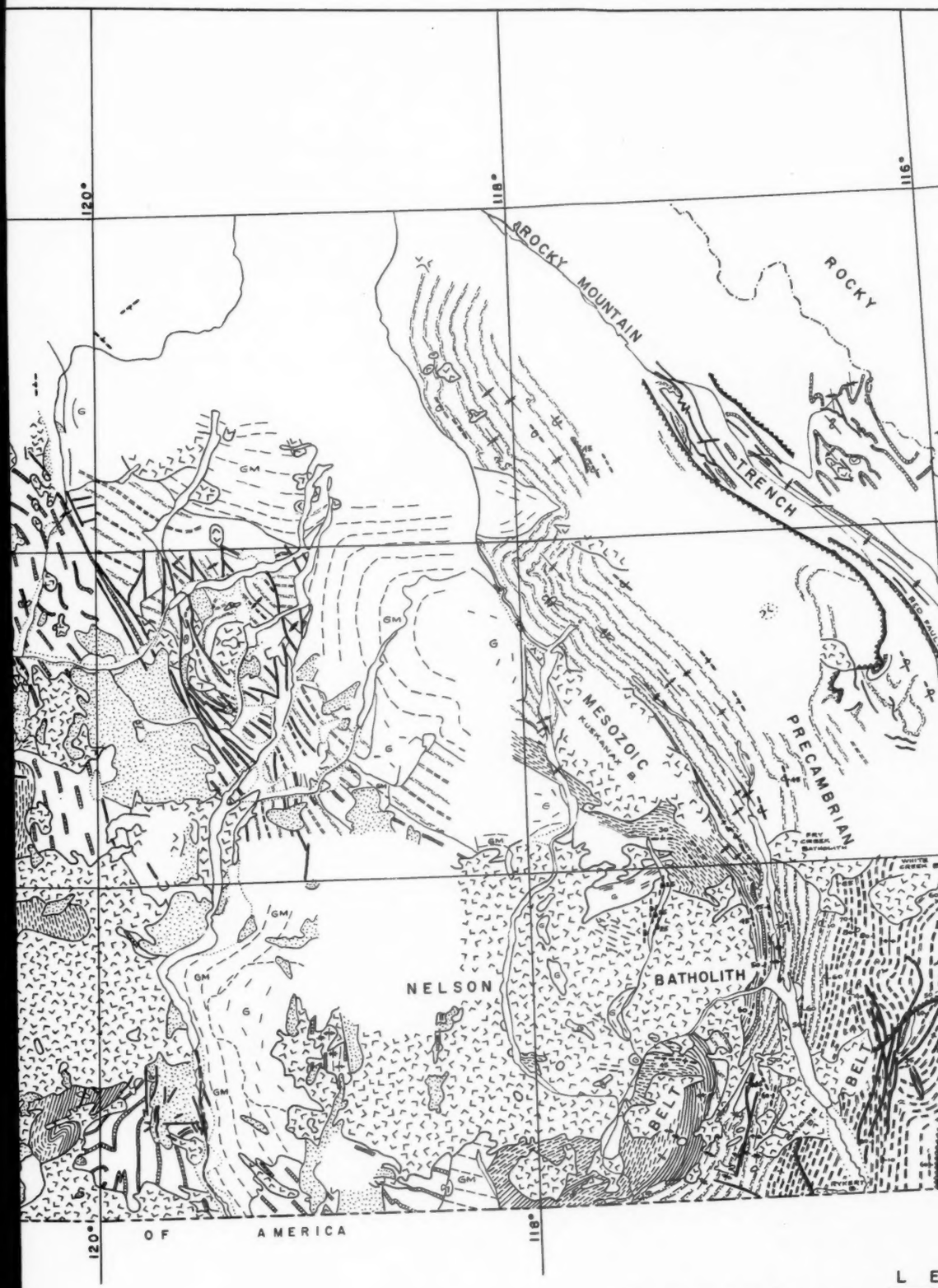

ERN BRITISH COLUMBIA
formations, and principal faults.
ical Survey of Canada Map 932, 1948

LEGEND

MESOZOIC

- Mesozoic undivided
- Lower Cretaceous
- Upper Cretaceous

TERTIARY

- Tertiary undivided

INTRUSIVE

- Granitic
- Basic

METAMORPHIC

- Granitic rocks of uncertain origin
- Granitic rocks and paragneisses

SYMBOLS

- Anticline & syncline
- Overturned anticline & isoclinal beds
- Plunging anticline
- Strike & dip of bedding
- Strike & dip overturned bedding
- Strike & dip of foliation

BULLETIN OF THE GEOLOGICAL SOCIETY OF AMERICA
VOL. 66, PP. 811-818, 2 PLS. JULY 1955

DEFORMATION AND IGNEOUS INTRUSION IN SOUTHERN BRITISH COLUMBIA, CANADA

BY ALAN R. SMITH AND JOHN S. STEVENSON

ABSTRACT

Regional deformation in southern British Columbia continued from Late Jurassic to Eocene, progressing from Vancouver Island and the Coast Range in the west eastward to the Rocky Mountains. The batholiths, reflecting this progression, are dioritic to granodioritic on Vancouver Island, predominantly granodioritic in the Coast Range, and principally granitic in central and eastern British Columbia. Regional linear elements–trends of formations, folds, and faults–tend to parallel the margins of the major intrusions. The pre-batholithic rocks were deformed approximately at the time of batholithic intrusion.

A detailed structural map of southern British Columbia illustrates these features.

CONTENTS

TEXT

	Page
Introduction	811
General geology	811
General structure	812
Coast Range batholith	812
Form	812
Western flank	813
Eastern flank	813
Nelson batholith	814
Rocky Mountain system	815
Emplacement of the batholiths	816
Thrust faults	817
Tertiary deformation	817
Conclusions	818
References cited	818

ILLUSTRATIONS

Plate	Facing page
1. Structural map of southern British Columbia	811
2. Index map of southern British Columbia	818

INTRODUCTION

Many reports and maps, especially those of the Geological Survey of Canada and the British Columbia Department of Mines, contain valuable information concerning igneous intrusion and deformation in southern British Columbia. However, no single publication has brought together this detailed material. In this paper the writers have compiled and studied the relevant information and supplemented it with field and laboratory experience to present a regional interpretation. Pleistocene and Recent deformation is not discussed.

The assistance of Professor James E. Gill of McGill University, who suggested the need for this study and contributed much helpful advice, is gratefully acknowledged.

GENERAL GEOLOGY

In southern British Columbia sediments, volcanics, and igneous intrusive masses are exposed. The pre-Cretaceous bedded rocks have been folded and faulted at various times and with different degrees of intensity. Some Cretaceous rocks are flat-lying and undisturbed; others are deformed, even intensely in some places. Tertiary volcanics and sediments, particularly prominent in the central part of the area, rest unconformably on the older rocks, and most are flat-lying or only midlly deformed. In general Mesozoic and Tertiary rocks are found in the western part of the area, Paleozoic, Mesozoic, and Tertiary rocks in the central part, and Precambrian, Paleozoic, Mesozoic, and Tertiary rocks in the eastern part (Pl. 1).

An index map (Pl. 2) is given which shows the locations of all maps used in the compilation of Plate 1.

The intrusive rocks, most of which are pre-Tertiary, underlie half of the area of southern British Columbia. These are divided into the Coast Range intrusive group and the Nelson intrusive group.

The Coast Range group includes the composite Coast Range batholith and smaller masses apparently closely related to it in origin. The main batholith is approximately 1250 miles long and 35–125 miles wide and is the largest exposure of batholithic rocks in the world. The larger part of this batholith extends northwest from the area under discussion. Its western boundary in southern British Columbia lies between Vancouver Island and the mainland; the eastern boundary extends northwest from Harrison Lake beyond Bridge River to Chilco Lake.

Groups of smaller batholiths and stocks parallel the southern margin of the main batholith. These batholiths found on Vancouver Island in the west and on the east side of Harrison Lake correspond with the Coast Range batholith in composition and probably in time of emplacement. These bodies are therefore considered as genetically related.

The Coast Range batholith in southern British Columbia is composed of quartz diorite and granodiorite. On Vancouver Island the satellitic bodies range from gabbro to granodiorite, while east of Harrison Lake they are composed chiefly of quartz diorite and granodiorite.

The Nelson intrusive group occupies the south-central part of the area. The main batholith (Pl. 1) is elliptical with the major axis extending approximately east-west from 117° to 119° W. Long. The southern boundary follows 49°15′ N. Lat., and the northern boundary is approximately at 50° N. Lat. Two well-marked satellitic belts extend around its eastern end and are apparently genetically related to the main batholith. In composition granite predominates, but granodiorites, local masses of syenite, and some alkaline bodies, perhaps not genetically related to the Nelson batholith, are also present.

Rocks adjacent to the Coast Range batholith show no intense metamorphism; however, large metamorphic aureoles adjoin the western and northern parts of the Nelson batholith. These zones consist largely of gneissic rocks and comprise the well-known Shuswap Complex. Pegmatites in sills or dykes are common within and around the Nelson batholith, especially in the northeast, but are not associated with the Coast Range batholith.

General Structure

Most pre-batholithic rocks of southern British Columbia show the effects of considerable deformation. Folds and faults generally extend directly to the igneous contacts where they are abruptly truncated. The magmas apparently advanced up to the present levels of batholithic rock, the main structural features of the roof rocks having already been established. Local features of contact zones resulted mainly from removal of material by magma. In a few places mapping of limited areas provided evidence of a pushing aside of wall rocks to make room for melts. Even some of the broader structural features associated with batholithic intrusion are distorted by powerful and extensive pushing aside.

A possible alternate explanation of the broad conformity of trend lines around batholiths is that the granitic intrusives conformed to pre-existing trend lines, in which case deviations from the regional trend would be difficult to explain. Folding of the bedded formations and intrusion of magmas may have occurred at different times in different parts of southern British Columbia, with the earliest deformation in the west and progressively later deformation toward the east. (*See* Pl. 1.)

Coast Range Batholith

Form

The crest line of the elongated Coast Range batholith rises irregularly from about 6000 feet just north of the city of Vancouver to approximately 11,000 feet near 52° N. Lat. The crest is near the east boundary of the batholith, from which point the surface of the batholith slopes gently westward and steeply eastward.

Western Flank

The western wall of the Coast Range batholith is a complex of intrusive masses of different ages, the oldest of which are basic. Bancroft (1913, p. 105), in his study of the Pacific coast and islands, states:

> "the shape of the individual batholith is very irregular, but as a rule its longest axis is approximately parallel to the structural trend of the region. Owing to this tendency on the part of batholiths to assume elongated elliptical outlines, the type of plutonic rock changes more frequently when crossing the Coast Range than when a traverse is made parallel to its general NW-SE direction."

On Vancouver Island two belts of satellitic intrusives cut through deformed Lower Jurassic formations and are parallel to the western margin of the Coast Range batholith.

The youngest formations involved in the main regional folding are Early Jurassic, found in the upper part of the Vancouver group, a thick series of Triassic volcanics and sediments. The lowest formations of the Vancouver group are conformably underlain by Permian limestones. These are underlain in turn by a series of nonfossiliferous sediments. Evidently from late Paleozoic to Early Jurassic time the western flank was relatively stable despite pronounced volcanic activity. Mountain building in the Coast Range started after the Late Triassic and by Early Cretaceous time erosion had exposed the batholithic intrusives in some localities as evidenced by granitic detritus in conglomerates of that age (Gunning, 1930, p. 62A). These sediments are flat-lying; any subsequent stresses must have deformed only local areas of the western flank.

Most folding west of the Coast Range probably occurred in Middle Jurassic time. It may have started in late Early Jurassic and could have continued through the Late Jurassic and, to a minor extent in local areas, into the Early Cretaceous. More probably deformation and igneous intrusion were completed in this area by late Middle Jurassic or early Late Jurassic.

Eastern Flank

The eastern wall of the Coast Range batholith is well exposed. Where the batholith cuts highly folded formations, it is steep-walled and slopes to the east. Eastward the main intrusive mass is in contact with a belt of folded Paleozoic rocks west of the Fraser River, and these, in turn, are in contact with a belt of deformed Mesozoic rocks east of the Fraser River. The Paleozoic belt is intruded by a line of small batholiths that extends from 49° N. Lat. northwest to the Bridge River area, a short distance beyond Lillooet (Pl. 1). Paleozoic formations are considerably more abundant than Mesozoic in this belt. The main Coast Range joins some of these smaller batholiths, and some of the intervening Paleozoic rocks may be roof-pendants of no great depth.

The Mesozoic belt includes an almost continuous mass of granodiorite which runs northwest from 120°30′ W. Long. at 49° N. Lat. to beyond Lytton at approximately 50°30′ N. Lat. (Pl. 1). The southern half of this mass separates Jurassic formations on the west from Triassic lavas on the east.

Both the Paleozoic and Mesozoic belts were deformed and intruded during the Late Jurassic. In the Paleozoic belt lower Upper Jurassic beds were deformed by late Late Jurassic time, and diorite, granodiorite, and granite were intruded toward the end of this folding. These intrusive bodies were eroded before Early Cretaceous, and detritus from them is found in basal conglomerates of the Early Cretaceous (Cairnes, 1942, descriptive notes, Map 737A). Similar evidence of deformation in the Late Jurassic is found in the Mesozoic belt (Cairnes, 1942, descriptive notes, Map 737A). Sediments and volcanics within the main batholith itself were probably also affected, but the evidence has been obliterated by an abundance of later intrusive material.

The Mesozoic rocks along the eastern flank of the batholith in the Bridge River and Chilco Lake districts were folded near the close of the Early Cretaceous. Lower Upper or upper Lower Cretaceous volcanics, which Dolmage (1929, p. 84A) describes as fresh-appearing, are only slightly folded with rather low dips and overlie strongly folded Lower Cretaceous (Eldorado) formations, in some places conformably. Since they are cut by the eastern wall of the Coast Range batholith, the upper Lower Cretaceous volcanics of these formations

may have been extruded during the close of the deformation of the Eldorado and older formations. The large masses of quartz diorite and granodiorite were intruded during this disturbance and were emplaced along the northwesterly trending lines of folding. Some of the intruded sediments are folded isoclinally adjacent to the wall of the batholith, which indicates later deformation at this place attributable to movements of the magma.

At Chilco Lake on the east side of the Coast Range batholith Lower Cretaceous beds containing the Knoxville fossil *Aucella crassicollis* Keyserling are folded and faulted. Beds containing this fossil on the west coast of Vancouver Island, however, are flat-lying and contain granodiorite detritus.

All Lower Cretaceous formations within the Paleozoic and Mesozoic belts immediately east of the Coast Range batholith are also deformed. The time at which this widespread deformation ceased in southern British Columbia is uncertain. No Upper Cretaceous rocks are definitely identified. The oldest undeformed rocks found along the east contact of the main batholith are Oligocene tuffs that rest on an eroded complex of pre-Upper Cretaceous rocks and granodioritic intrusives (McKenzie, 1921, p. 77A–78A). In the Paleozoic belt relatively undisturbed conglomerate, sandstone, and shale of the Paleocene Huntington formation rest unconformably on intrusives and deformed rocks.

In northern British Columbia near the Stikine River, Upper Cretaceous sediments containing granitic detritus are flat-lying, whereas Lower Cretaceous and older formations along the east contact are highly folded and intruded by batholiths of intermediate composition (Kerr, 1932, p. 306). Probably deformation and igneous intrusion were almost, if not entirely, completed in the center and eastern edge of the Coast Range batholith before Late Cretaceous time.

Nelson Batholith

The central part of southern British Columbia is largely occupied by the Nelson batholith, which is elliptical with the major axis extending east-west from 117° to 119° W. Long. The southern boundary follows 49°15' N. Lat., and the northern boundary is approximately along 50° N. Lat. (Pl. 1).

The western margin of the batholith contains abundant gneiss, the foliation of which conforms with that edge. This gneiss is chiefly granite and granodiorite in composition as is the batholith core and much of the near-by rock, some of which is porphyritic. The eastern part of the batholith as described by Cairnes (1934, p. 61), contains granite gneiss, porphyritic granite gneiss, porphyritic granite, granite, granodiorite, and pegmatitic granite. As the contacts between these granitic facies are gradational, the Nelson batholith is regarded as one large, composite mass.

The sedimentary formations along the eastern edge of the Nelson batholith are arranged in arcs. An inner arc, except where interrupted by a series of satellitic batholiths, is composed of Paleozoic and Mesozoic formations. The Windermere series lies east of this inner arc; this series was thought to be late Precambrian, but is now known to be in part Paleozoic (Park, 1938, p. 712–713; Little, 1949, descriptive notes, Map 49-22). The Precambrian Purcell series lies east of the Windermere series. A curving line of granitic batholiths trends northerly and north-westerly between the Windermere and the Purcell series and within the Wildermere; this line extends north into the Big Bend of the Columbia River and may continue farther northwest into the Precambrian Cariboo series of the Cariboo district.

The time of intrusion of the Nelson batholith is uncertain. Cairnes (1934, p. 73–75) has pointed out that intrusion of the various members probably took a long time, but was doubtlessly continuous since most contacts are gradational. The Triassic rocks of the Slocan series are the youngest formations cut, and it is evident that their folding was complete before the final advances and crystallization of the batholith. Because this mass is principally granite, whereas the Coast Range intrusives are mainly granodiorite and quartz diorite, Cairnes and others suggest that the Nelson batholith and its satellites are younger than the Coast Range intrusives, in view of the commonly observed sequence of intrusion and crystallization from "basic" to "acid" suites of

rocks. Thus the Nelson batholith would be Late Cretaceous or younger. (*See* Plate 2.)

Warren (1951, p. 8) has pointed out that certain coarse clastic sediments in the Lower Cretaceous Blairmore group, especially the Cadomin conglomerate at the base of the Blairmore, indicate a pronounced uplift west of the Rocky Mountain trench. Anderson (1951, M. S. thesis, McGill Univ.), from studies of the McDougall-Segur conglomerate in the upper part of the Blairmore, has shown that granite, granophyre, and various porphyritic igneous intrusive rocks were exposed when that conglomerate was deposited. The next pronounced uplift west of the Rockies is indicated by the pebble conglomerate and associated sandstones in the Upper Cretaceous Bighorn formation. Warren (1951, p. 9) notes that a great thickness of feldspathic sandstone deposited in the eastern Foothills region of the Rocky Mountains during late Late Cretaceous time, succeeded by quartzose sandstones of later Late Cretaceous and Paleocene age, which may indicate that the western front of the Rocky Mountain system was being uplifted and eroded. Warren states (1951, p. 10):

> "the evidence is quite definite that sediments from the Selkirk group of mountains (Purcell and Windermere series) were being deposited in the foothills area of the Rockies till very late in Cretaceous time."

If the source of the feldspathic sand and granophyric pebbles were granitic intrusions in the Selkirk system west of the Rocky Mountain trench, then the first intrusion in the Nelson area must have occurred in early Early Cretaceous. Before the end of the Early Cretaceous the terrain was uplifted, and the first batholiths were deroofed, which provided the source material for the Lower Cretaceous McDougall-Segur conglomerate. The feldspathic sands of late Cretaceous time would indicate a gradual or sudden but slight uplift, not so great as the earlier Early Cretaceous one. Therefore, the main period of mountain building and intrusion in the Nelson area would have occurred in early Early Cretaceous time.

An alternative view is that the clastic material of the Blairmore group came from the Coast mountains farther to the west before the main deformation and igneous intrusion of the present Nelson batholith region. All the materials might well have come from the Coast Range and intervening area.

The granite pebbles of the McDougall-Segur conglomerate contain abundant granophyre which is not common in either the Coast Range or Nelson intrusive groups, but is found in the sills of the Purcell series. Feldspar pebbles in the basal Windermere rocks suggest an Early Proterozoic or older granitic intrusion (Officers of the geological survey of Canada, 1947, p. 243). The writers believe that the source of the feldspathic material probably was in the Purcell series and was not related to the Nelson intrusive group.

Rocky Mountain System

The Rocky Mountain system lies between the Rocky Mountain trench to the west and the Alberta plains to the east (Pl. 2). The formations trend slightly west of north at the 49° parallel to more westerly at the 50°30′ parallel. Between 50°30′ and 52°00′ the formations strike about N.35°W. The system is about 64 miles wide near 49 N. Lat. and about 90 miles wide at the 52 N. Lat.

The Rocky Mountain trench is a pronounced topographic feature that extends along the western side of the Rocky Mountain system in southern British Columbia. The wide valleys of the north-flowing Columbia River follow it to the north and of the south-flowing Kootenay River to the south. In general the trench separates Precambrian formations on the west from Paleozoic formations on the east. Paleozoic strata do occur west of the trench in the Dogtooth Mountains near 51° N. Lat., and Precambrian formations are extensively developed east of the trench in the southern parts of the Rocky Mountain system between 49°00′ and 49°20′ N. Lat.

The Precambrian formations west of the trench and the Paleozoic formations on the east are in open folds. Close to the trench the strata on both sides are intensely deformed, commonly overturned, and extensively faulted. Evans (1933, Map 295A) has mapped underthrust faults on the east side north of 51° N. Lat. (Pl. 1).

The trench apparently marks a zone where

fault surfaces intersected during folding of the Rocky Mountains. Movement was localized by the resistant Precambrian rocks in the west against which the thinner Paleozoic formations were crumpled. Walker (1928, p. 40) noted a westward thinning of Paleozoic strata near the trench.

The eastern half of the Rocky Mountain system is a series of superimposed thrust sheets, which average about 2 miles thick. These faults dip steeply to the west but apparently, on the basis of oil-well data, flatten considerably with depth. Devonian to Upper Cretaceous strata are deformed in this section. The formations dip to the west at much flatter angles than do the surface thrust faults. With depth, however, the thrust faults are more nearly parallel to the bedding. On the surface the faults almost, if not exactly, parallel the strike of the formations for many miles. These thrust faults may have developed at depth as bedding-plane faults, and thrust younger beds over older beds to the east.

In the section of the Rocky Mountain system between 49° and 52° N. Lat., the Purcell formations have been thrust from the west over Upper Cretaceous Belly River formations, and here underly much of the Rocky Mountains.

The Rocky Mountain system is predominantly a large competent mass of Precambrian to Upper Paleozoic rock which has ridden over a Devonian to Upper Cretaceous basin, causing intense shearing.

The Upper Elk and Upper Highwood rivers map-sheet (Pub. No. 1980) shows flat-lying Willow Creek and Porcupine Hills formations turned up on edge along the most easterly thrust in the Rocky Mountain system. These Paleocene sediments lie conformably on flat-lying Upper Cretaceous St. Mary River beds which are also turned up along this thrust fault. Evidently thrusting and deformation continued at least to the close of the Paleocene.

The Ice River complex, an Eocene (?) laccolith of alkaline rocks, lies in the moderately folded Lower Paleozoic formations in the western half of the Rocky Mountain system 15 miles south of Field, British Columbia. Allan (1914, p. 191) has determined that folding antedates shearing, which, in turn, is older than the laccolithic intrusion. Thus intrusion follows deformation here as in the west of southern British Columbia.

Emplacement of the Batholiths

Two possible modes of emplacement of the Coast Range and Nelson batholiths and of the smaller satellitic batholiths are apparent. In many places truncation of structures and lack of unusual distortion near the batholiths suggest that fusion, assimilation, stoping or replacement, or some combination of these, provided space for the advancing magma. However, in some places much of the rock was pushed aside. Gunning (1932 p. 300) gives an excellent example of this mode of emplacement on a small scale. Trend lines around the southern end of the Coast Range batholith and around the east end of the Nelson batholith were probably formed by broad-scale and strong lateral pressures transmitted through the magma.

Pushing aside on a large scale is apparent around the Nelson batholith (Pl. 1). The dividing of trend lines north and south of the batholith, the almost semicircular, closely compressed belt of Mesozoic and Windermere rocks wrapped about its east side, and farther east the less intense folding in the northwest-trending Purcell rocks were probably caused by forces transmitted through the advancing magma. However, along the same eastern border the rock structures are cut off in most places without marked local disturbance.

Also, in places, linear structures in the walls of a batholith apparently governed the later introduction of granitic tongues from the main body. In the Salmo area granite tongues follow a north-striking zone of faulting the same age as fold structures to the north that were pushed aside by the main batholith. Thus a strong pushing aside accompanied the main upward advance followed by a prolonged period when material of the walls was incorporated by differential melting, solution, and stoping, all acting with different intensities in different places.

The Moyie and St. Mary faults southeast of the Nelson batholith were perhaps first formed when the batholith advanced, as indicated by the spatial relations of the batholith to the

faults, by the nature of the movements on the faults, and by the presence of westerly dipping, high-angle, reverse faults with large displacements (Rice 1941, p. 49–51). Rice concluded that the foliated Rykert batholith, which cuts across the St. Mary fault, was emplaced while the fault was still active, whereas the more massive and acidic Bayonne batholith, 10 miles farther north, appears to have risen after the movements were complete. The displacement on the St. Mary fault is at least 20,000 feet (Rice, 1941, p. 50) and on the Moyie fault (the Lenia fault in the United States), between 15,000 and 45,000 feet (Kirkham, 1930, p. 371). An active upward push caused by expansion owing to excessive heating and liquefaction of part of the crustal rocks in the vicinity of the Nelson batholith region, and the continuing effect of the horizontal compressive stresses, may have accelerated the advance of the Nelson batholith, thus causing extensive movement on thrust faults. North-striking faults found recently in Pilot Bay and at the head of Crawford Bay, both places north of the Bayonne batholith, suggest that the batholith generally followed two intersecting fault systems and did not deflect north-striking systems into northeast systems.

The St. Mary and Moyie thrust faults may be part of the Rocky Mountain system east of the trench and are probably late Late Cretaceous in age. This would again suggest that the Nelson batholith is Late Cretaceous in age.

Thrust Faults

Thrust faults have formed along the eastern flank of the Coast Range batholith, in the Purcell series east of the Nelson batholith, along the Rocky Mountain trench, and in multiplicity along the eastern part of the Rocky Mountain system, the deformation in which was largely the result of Paleocene thrust faulting.

Rice (1941, p. 49–52) believes that the St. Mary and Moyie thrust faults continue across the Rocky Mountain trench and become part of the Rocky Mountains, which would date them as late Late Cretaceous or Paleocene. The granitic apophyses of the Nelson batholith which cut these thrusts are also late Late Cretaceous.

Many faults along the eastern flank of the Coast Range batholith thrust Paleozoic rocks over Mesozoic formations. In the Hope area Paleozoic rocks on the west overlie Jurassic formations on the east. An ultrabasic intrusive later advanced along this thrust plane and is now exposed for 39 miles in the area of the Hope sheet (Map 737A).

Most of these thrust faults dip westward; some dip eastward. In the Rocky Mountain system adjacent to the trench, the eastward-dipping thrust planes are the result of underthrusting to the east. The Ferguson thrust fault in the Bridge River area dips eastward at a high angle and is vertical in places; this anomalous attitude may be attributed to folding of the fault plane subsequent to thrusting, perhaps caused by intrusion of the Bendor batholith, an outlier of the Coast Range batholith, just east of the fault.

Thrust faulting was important in deformation in southern British Columbia. The faults characteristically dip westward and therefore indicate that an easterly-directed shearing stress continued from at least the Early Cretaceous to the Paleocene. The Late Jurassic orogeny was probably also caused by easterly-directed stresses. These stresses developed first in the rocks on Vancouver Island, became concentrated farther to the east, and finally culminated in the Paleocene deformation of the Devonian to Late Cretaceous basin that produced the Rocky Mountain structures.

Tertiary Deformation

The Tertiary rocks in southern British Columbia are marked by local rather than general deformation.

The Upper Eocene Metchosin volcanics and the Upper Cretaceous Nanaimo sediments at the southern end of Vancouver Island are deformed into broad open folds. The Nanaimo sediments are cut by several westward-dipping thrust faults of minor displacement. Farther north on Vancouver Island, Gunning (1931, p. 63A–64A) refers to minor intrusive bodies of Early Oligocene age, against which the Upper Cretaceous formations are locally deformed. Upper Cretaceous and Upper Eocene formations are cut by small granitic bodies. These intrusions probably correlate in age with

the local gabbroic intrusions in the Upper Eocene volcanics of southern Vancouver Island. In the Beaverdell area of Central British Columbia Cairnes (1940, descriptive notes, Map 538A) describes Tertiary granite and syenite intrusives, one of which intrudes basal Tertiary sediments. The Ice River complex in the Rocky Mountains is probably Tertiary, as may be the minor block faulting in the Precambrian formations east of the Nelson batholith and in the Rocky Mountain system near 49° N. Lat.

Intrusion and deformation diminished during the Tertiary period. Volcanism, however, was extensive, and large areas of southern British Columbia, particularly the Interior Plateaux, were covered by lava flows and pyroclastic deposits.

Conclusions

Study of trend lines of formations and field relations between igneous and surficial rocks in southern British Columbia indicates that the bedded rocks were deformed by lateral compression and by broad-scale igneous intrusion. Contact zones show evidence of some pushing aside by intruded rocks. Many contact features, however, developed after emplacement of the batholiths. Structural, petrologic, and stratigraphic information concerning deformed and intruded formations shows that deformation generally spread across southern British Columbia from west to east, beginning in the Late Jurassic on Vancouver Island and culminating in the Eocene in the Rocky Mountains.

References Cited

Allan, J. A., 1914, Geology of Field map-area, B. C. and Alberta: Geol. Survey Canada Mem. 55, Map 142A.

Bancroft, J. A., 1913, Geology of the coast and islands between the strait of Georgia and Queen Charlotte sound: Geol. Survey Canada Mem. 23, Maps 272A, 273A.

Cairnes, C. E., 1934, Slocan mining camp, B. C.: Geol. Survey Canada Mem. 173.

—— 1940, Descriptive notes, Kettle River (west half): Geol. Survey Canada Map 538A.

—— 1942, Descriptive notes, Hope sheet: Geol. Survey Canada Map 737A.

Dolmage, V., 1929, Gun creek map-area: Geol. Survey Canada Summary Rept. 1928, pt. A, p. 78–93.

Evans, C. S., 1933, Brisco-Dogtooth map-area, B. C.: Geol. Survey Canada Summary Rept. 1932, pt. AII, p. 106–176.

Gunning, H. C., 1930, Geology and mineral deposits of Quatsino-Nimpkish area, Vancouver Island, B. C.: Geol. Survey Canada Summary Rept. 1929, pt. A., p. 94–143, Map 255A.

—— 1931, Buttle lake map-area, Vancouver Island, B. C.: Geol. Survey Canada Summary Rept. 1930, pt. A, p. 56–78.

—— 1932, Form and mechanics of intrusion of the Nimpkish "batholith": Royal Soc. Canada Trans., 3rd series, v. 26, sec. 4, p. 289–304.

Kerr, F. A., 1932, The character of the Coast Range composite batholith in northern British Columbia and southeastern Alaska: Royal Soc. Canada Trans., 3rd series, v. 26, sec. 4, p. 305–316.

Kirkham, Virgil R.D., 1930, The Moyie-Lenia overthrust fault: Jour. Geology, v. 38, p. 364–374.

Little, H. W., 1949, Preliminary map, Nelson (west half): Geol. Survey Canada Paper 49-22.

McKenzie, J. D., 1921, A reconnaissance between Taseko lake and Fraser River, B. C.: Geol. Survey Canada Summary Rept. 1920, pt. A, p. 70–81.

Officers of the geological survey of Canada, 1947, Geology and economic minerals of Canada, Geological Survey, 3rd ed., 357 p.

Park, C. F., Jr., 1938, Dolomite and jasperoid in the Metaline district, northeastern Washington: Econ. Geology, v. 33, no. 7, p. 709–724.

Rice, H. M. A., 1941, Nelson map-area, east half, British Columbia: Geol. Survey Canada Mem. 228, Map 603A.

Walker, J. F., 1928, Geology and mineral deposits of Windermere map-area, B. C.: Geol. Survey Canada Mem. 148, Map 2070.

Warren, P. S., 1951, The Rocky Mountain geosyncline in Canada: Royal Soc. Canada Trans., 3rd series, v. 45, sec. 4, p. 1–10.

Box 67, Mineral, Virginia: McGill University, Montreal, Quebec

Manuscript Received by the Secretary of the Society, October 2, 1953

52°
128°
126°
Hunter Island
Calvert Island
Owikeno Lake
51°
Quatsino
QUATSINO SOUND
Port Alice
255 A
Nimpkish L.
50°
KYUQUOT SOUND
50-37A
Zeballos
50-9A
Vancouver
Nootka Island
Nootka
NOOTKA SOUND
PACIFIC
CLAYOQUOT SOUND
49°
OCEAN
126°

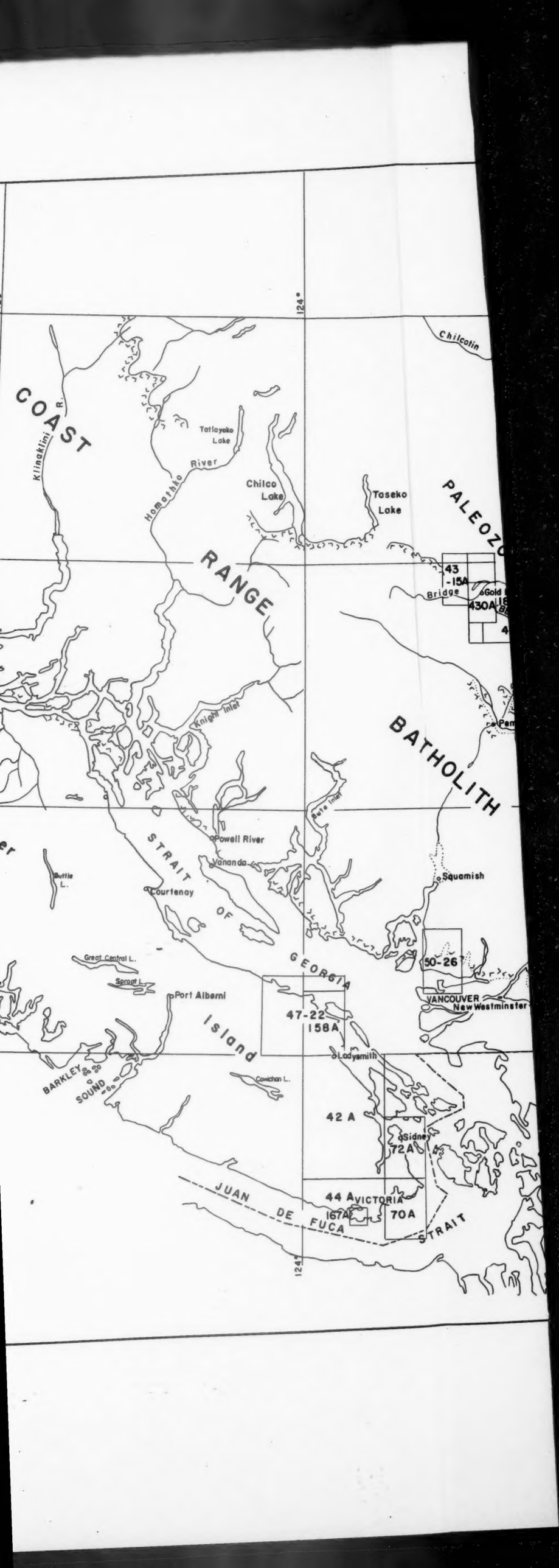
COAST
RANGE
PALEOZO
BATHOLITH
Chilcotin
Klinaklini R.
Tatlayoko Lake
Homathko River
Chilco Lake
Taseko Lake
Bridge
43-15A
430A
Knight Inlet
Bute Inlet
Powell River
Vananda
Courtenay
Squamish
Buttle L.
STRAIT OF GEORGIA
Great Central L.
Sproat L.
Port Alberni
50-26
VANCOUVER
New Westminster
47-22
158A
Island
Ladysmith
BARKLEY SOUND
Cowichan L.
42 A
Sidney
72A
44 A
167A
VICTORIA
70A
JUAN DE FUCA STRAIT
124°

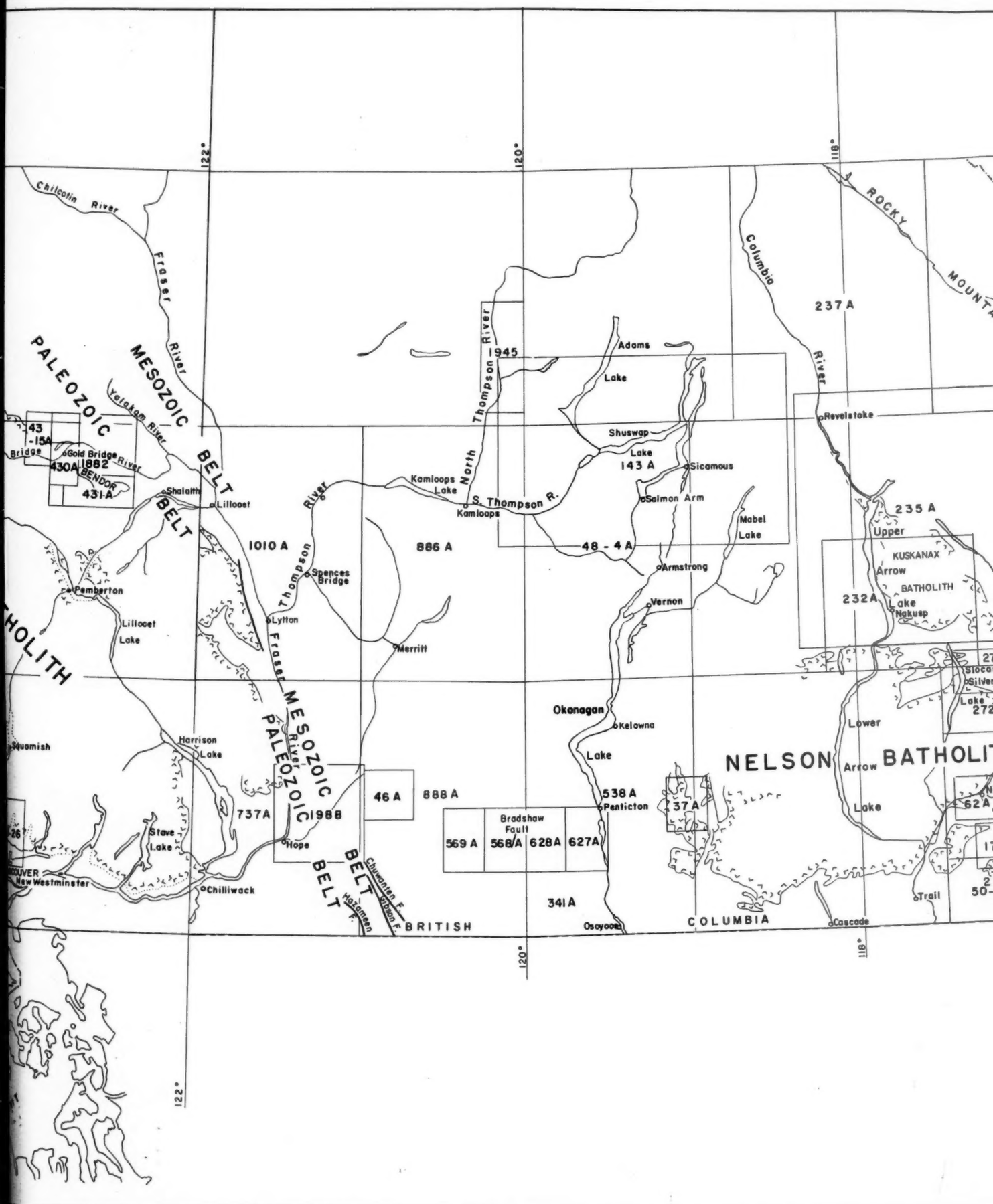

INDEX MAP OF SOUTHERN BRITISH COLUMBIA

Showing Geological Survey of Canada map-sheets used as source for data of structural map, Plate 1.
Geology adapted form Geological Survey of Canada Map 932, 1948

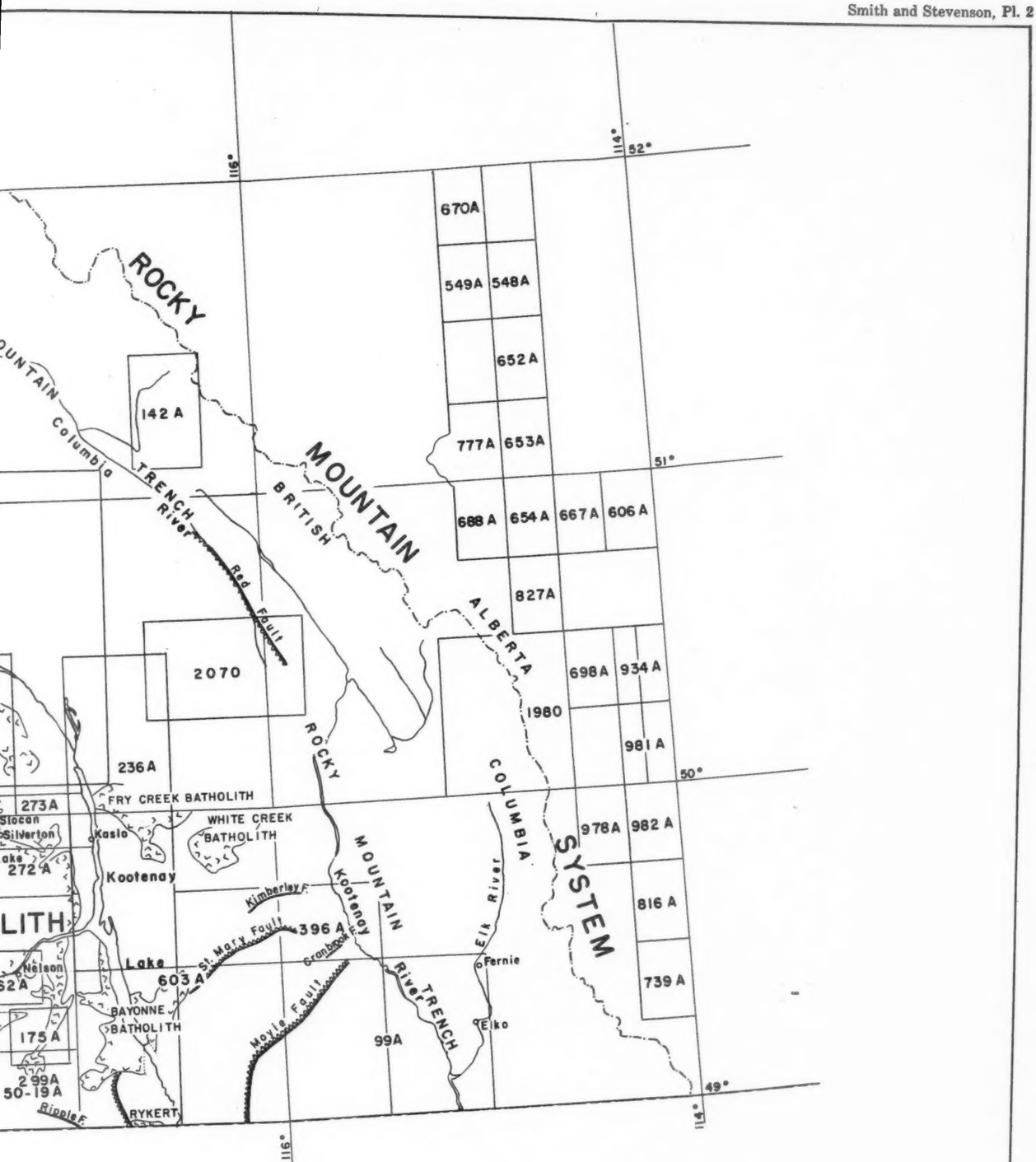

Scale in Miles
0 4 8 16 24 32

INTRUSIVE

Granitic

BULLETIN OF THE GEOLOGICAL SOCIETY OF AMERICA
VOL. 66, PP. 819-834, 4 FIGS., 4 PLS. JULY 1955

CAMBRIAN CONTACTS IN EASTERN PENNSYLVANIA

BY BRADFORD WILLARD

ABSTRACT

The Cambrian sequence in eastern Pennsylvania is:

Upper	Allentown limestone
	Limeport limestone
Middle (?)	Leithsville limestone
Lower	Hardyston quartzite

All ages, except the barren Leithsville, are paleontologically established. The Hardyston overlies Precambrian gnesisses; the Allentown is surmounted by the Ordovician Beekmantown limestone. Only the Cambrian-Precambrian and Allentown-Limeport contacts are defined in the literature. Because of lack of understanding of the Leithsville-Limeport relations, the age of the Leithsville has been questioned. Study of new and restudy of old exposures indicates that the Hardyston-Leithsville relations vary between transition and disconformity, the Leithsville-Limeport limestones are mutually transitional thereby implying a Middle Cambrian assignment to the Leithsville. The Beekmantown is ordinarily in conformity with the Allentown, but in at least one instance supposed Beekmantown overlies the Limeport in disconformity.

CONTENTS

TEXT

	Page
Introduction	819
Historical review	822
Contacts	824
Intrasystemic contacts	824
Intersystemic contacts	826
Summary and conclusions	831
References cited	832

ILLUSTRATIONS

Figure	Page
1. Sketch map of part of eastern Pennsylvania showing distribution of Cambrian and Ordovician limestones	820
2. Sketch map of eastern end of Buckingham Valley, Bucks County, Pennsylvania	821
3. Sketch map of vicinity of Carpentersville, New Jersey, and Raubsville, Pennsylvania	822
4. Sketch map of vicinity of Easton, Pennsylvania	825

Plate	Following page
1. Outcrops, Eastern Pennsylvania	828
2. Outcrops, Eastern Pennsylvania	
3. Outcrops, Eastern Pennsylvania and New Jersey	
4. Fullerton section along Lehigh Valley R. R., Lehigh County, Pennsylvania	

INTRODUCTION

Kittatinny Mountain, front range of the Appalachians, crosses Pennsylvania in a southwest-trending arc. The south face of the mountain, formed of Silurian quartzites and conglomerites, falls off sharply to a relatively high surface, the Slate Belt, which fills the northern half of the Lehigh Valley south of Kittatinny Mountain. The country rock here is Ordovician slate which is stream-dissected into rounded hills broken by a sprawling, median, east-west upland, the continuation from the west of Shochary Ridge. South of the Slate Belt, the surface again drops off, now to a flatter terrane underlain by Cambrian and Ordovician limestones. The southern boundary of the valley is marked by the Precambrian crystalline rocks of South-Mountain.

The areal geology is one of northeast-southwest-trending structures whose complexity reflects the late Ordovician Taconic disturbance, the Appalachian revolution and a third interval of tectonic activity, probably in late Triassic time. The limestones are a segment of the Great Valley which crosses New

Jersey and Pennsylvania and extends southward into the Shenandoah. South Mountain, unlike the single range of Kittatinny, ramifies into more or less discrete ridges interrupted by ham Valley, is larger and structurally quite unlike the rest. It is a north-tilted fault block of Paleozoic formations surrounded by Triassic continental strata. The limestones dip north-

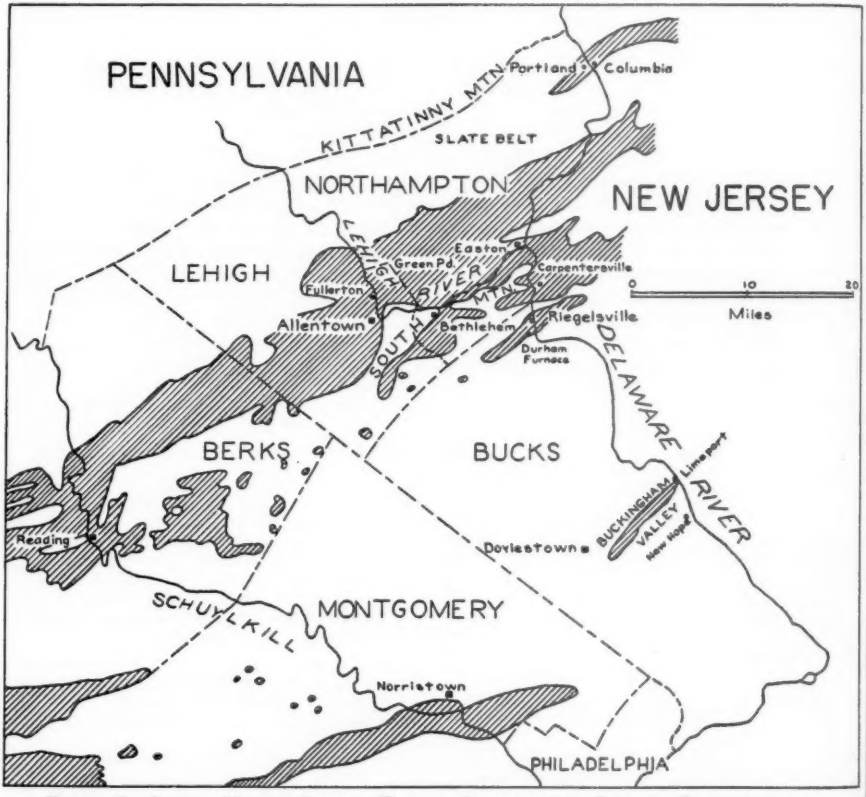

FIGURE 1.—SKETCH MAP OF PART OF EASTERN PENNSYLVANIA SHOWING DISTRIBUTION OF CAMBRIAN AND ORDOVICIAN LIMESTONES

Adapted from Pennsylvania Topographic and Geologic Survey Bull. M7, 1925, Pl. II

small, limestone-floored valleys whose structure is predominantly faulted, plunging synclines. Two such valleys in southeastern Northampton County open eastward onto the Delaware River Valley. The northern one is 4 miles down river from Easton; the second 1–2 miles farther south between Raubsville and Coffeetown (Fig. 3). The second extends eastward into New Jersey. Two additional limestone areas occupy parts of eastern Bucks County (Figs. 1, 2). The northern area, centered about Riegelsville, is structurally like those of Northampton County; the second, Buckingward under the Triassic Stockton. They terminate to the south either in fault contact with the Triassic Brunswick red beds, or against the Cambrian quartzite of Buckingham Mountain (Willard, *et al.*, 1950).

Current division (Howell, *et al.* 1950, p. 1358) separates the lowest Paleozoic of eastern Pennsylvania thus:

Ordovician: Lower, Beekmantown formation[1]

[1] Formation is used here according to Article 3 of "Classification and Nomenclature of Rock Units", Ashley, G. H., *et al.*, 1933, p. 423–459.

Cambrian:	Upper,	Allentown formation
		Limeport formation
	Middle (?),	Leithsville formation
	Lower,	Hardyston formation
Precambrian gneissic complex		

The lithology of the formations is:

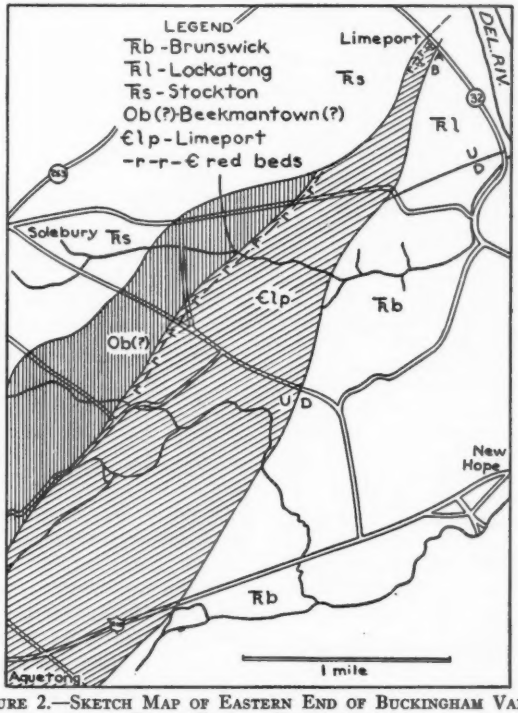

FIGURE 2.—SKETCH MAP OF EASTERN END OF BUCKINGHAM VALLEY, BUCKS COUNTY, PENNSYLVANIA

Showing distribution of Cambrian and Ordovician (?) limestones with relation to the Triassic

Hardyston: Variable, dominantly gray, brown-weathering, vitreous to massive quartzite, or arkosic sandstone, silicarenite, shale, conglomerate, jasper; limy beds reported in northern New Jersey. *Scolithus* is the only fossil recorded from the Lehigh Valley, but *Olenellus* and other Lower Cambrian fossils are known in New Jersey. In Bucks County, correlative of the Hardyston is the much thicker Chickies quartzite with the Hellam conglomerate at base. *Olenellus* has been reported from Buckingham Mountain in Bucks County. 25–300 ft.

Leithsville[2]: Dominated by dark-gray, buff-weathering, dolomitic limestone, and sericitic gray to brown shale sometimes verging upon phyllite; occasional silicarenite lenses. Bedding changes more or less rhythmically; shaly to platy to massive. No fossils identified. Ripple marks and mud cracks common. 800–900 ft.

Limeport: Gray to blue-gray dolomitic limestone, formerly included in lower part of Allentown. Bedding massive to submassive, regular; on exposure, weathers to alternate light and dark shades of blue-gray, blue and whitish. Oölite and quartz sand grains often common. Stromatolites ("cryptozoans") common and distinctive, including *Archaeozoön undulatum* and *Cryptozoön fieldii*. Dresbachian invertebrates occur in this formation in Buckingham Valley, Bucks County (Pl. 1, figs. 1, 2). 800–900 ft.

Allentown (*sensu stricto*): Lithology similar to the underlying Limeport, but oölite relatively scarce in higher beds. Stromatolites distinctive as *Anomalophycus compactus* and undescribed forms. Trempealeauian invertebrates occur in the restricted Allentown at Portland, Northampton County, Pennsylvania (Fig. 1). 400–500 ft.

Beekmantown: High magnesian limestone, massive-bedded, blue-gray, weathering whitish, chalky or buff. Many massive beds show laminations on weathered surfaces. Pseudofossils scarce. A sparce early Ordovician fauna is recognized in Lehigh and Northampton Counties. *N.B.* Beekmantown is here used provisionally until the age, stratigraphic relations, and position are better understood. 1000–1500 ft.

Most Cambrian contacts in eastern Pennsylvania are neither well-known nor adequately

[2] Pronounced as if spelled "Litesville".

described. Howell, Roberts, and Willard (1950, p. 1360) split Wherry's (1909, p. 416) original Allentown into overlying, restricted Allentown and underlying Limeport. They identified and

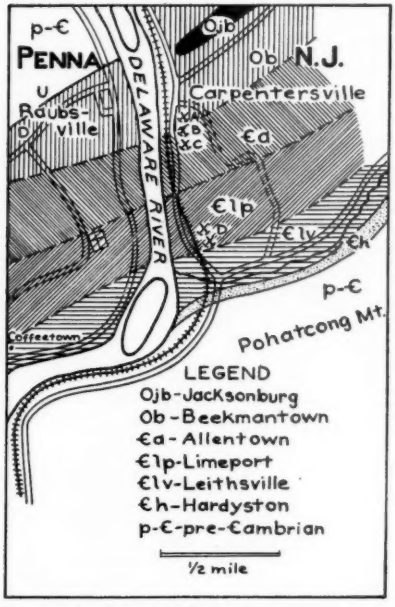

FIGURE 3.—SKETCH MAP OF THE VICINITY OF CARPENTERSVILLE, N. J., AND RAUBSVILLE, PENNSYLVANIA

Showing distribution of Cambrian and Lower Ordovician formations.

illustrated a disconformity between these two, and determined paleontologically the relative ages of the Allentown and Limeport as Trempealeauian and Dresbachian respectively. They recognized no median Upper Cambrian, the Franconian. The Leithsville was assigned to early or middle Cambrian age, since its contact with the overlying Limeport is transitional and it overlies the Hardyston of early Cambrian age. New data on the contacts substantiates the middle Cambrian age of the Leithsville. Mention of the Leithsville-Hardyston contact is found in the older literature and involved outmoded formational names. Though usually called conformable, at least one instance of disconformity has been described by Whitcomb (1948). There is a general agreement that the Cambrian-Precambrian contact is nonconformable. The Cambrian-Ordovician contact (Allentown-Beekmantown) was mentioned but not analyzed by B. L. Miller (1939a, p. 247; 1941, p. 197). New information now permits a more detailed description.

HISTORICAL REVIEW

In 1858, Henry D. Rogers recognized approximately the equivalents of the Precambrian crystallines, the Hardyston (and Chickies) and the limestones:

Auroral magnesian limestone	2,500–5,000 ft.
Primal sandstone	"about" 300 ft.
Gneissic system	

He did not divide his Auroral limestone, and mistakenly supposed the Primal sandstone to be the equivalent of the New York Potsdam. Rogers noted that the dark-blue Auroral grades down into micaceous slaty beds, in part our present-day Leithsville. He mentioned lithological varieties of the Primal. Rogers called the limestone-sandstone relations conformable, but described and figured the nonconformity between the sandstone and gneiss. Most of his observations seem to have been made in or near the Lehigh and Delaware valleys.

After a lapse of 25 or 30 years, the Second Pennsylvania Survey published findings by Frederick Prime, Jr. (1875; 1878; 1883) and others on the geology of Lehigh, Northampton, and Berks counties. *Maclurea* and *Euomphalus* were recorded from high in the present Beekmantown or low in the succeeding Jacksonburg (not included in this paper). Prime believed his fossiliferous Ordovician the equal of the New York Chazy, and retained the erroneous correlation of the basal Cambrian sandstone with the Potsdam. J. P. Lesley (1892, Chapter XVI, Formation No. 1) doubted the correctness of this Potsdam correlation and recognized the Cambrian and Ordovician ages of the magnesian limestones, although the Second Survey failed to subdivide them. Prime (1883, Chapter IV, p. 208) referred to a section on the Delaware River 1½ miles below Easton at Morgan Hill where coarse basal sandstone passes upward into limestones with quartz grains which in turn grades up into normal limestone. Elsewhere he noted "damourite slate" (*i.e.* sericitic

Leithsville) transitional between basal sandstone and lower Paleozoic limestone. Prime accepted the transitional relations between limestone and sandstone, but misunderstood the structure of the gneiss and called it and the overlying sandstone "conformable".

In New Jersey, Kümmel and Weller (1901, p. 149–150) named the Hardyston as a correction of "Hardystonville" of Wolff and Brooks (1898, p. 442–443, 454–456). Because of the presence of *Olenellus*, Weller (1903, p. 10–12) proved the Hardyston to be older than the Potsdam. Although he recognized the Cambrian and Ordovician ages of fossils from the overlying limestone, he did not subdivide it, and even today the New Jersey Survey refers to it in its entirety as the "Kittatinny". The United States Geological Survey's Trenton folio (Bascom, *et al.*, 1909a, p. 5) includes part of the limestone fault block in Bucks County. The name "Shenandoah" was used in this folio collectively for the Cambrian and Ordovician carbonate rocks. A like use is found in the contemporaneous Philadelphia folio (Bascom *et al.*, 1909b, p. 5).

In 1909, E. T. Wherry issued the first significant breakdown of the Lehigh Valley limestones. He named the Lower Ordovician the Coplay (today's Beekmantown), called the Upper Cambrian the Allentown, and proposed Leithsville for the limestone between Allentown and Hardyston. Because of the stratigraphic position between Upper and Lower Cambrian, the Leithsville was assigned to Middle or Lower Cambrian. Peck (1911, p. 25–26) was first to adopt Wherry's names, Leithsville and Allentown, along with Hardyston. He also used Coplay, but commented on the probability of its correlation with the Beekmantown. Wherry's terminology is not referred to in Bailey Willis's "Index to the Stratigraphy of North America" (1912). E. O. Ulrich (1911, Pl. 17) published the following sequence for northeastern Pennsylvania:

Ordovician:	Beekmantown (Coplay)
	Tribes Hill ls
Ozarkian:	Kittatinny (Allentown ls)
Cambrian:	Harding

"Harding" was evidently not a misprint for Hardyston because Ulrich repeated it in the text. His misapplication of the term Kittatinny which includes beds of Beekmantown age, and his unsubstantiated introduction of Tribes Hill are unaccountable misstatements by one whose grasp of North American stratigraphy was supposed to be encyclopaedic. His entire account of the Cambrian and Lower Ordovician succession in northeastern Pennsylvania and New Jersey is so erroneous as to be quite unreliable.

The name Coplay was dropped in favor of Beekmantown, because of supposed correlation with the New York type (Wilmarth, 1938, p. 516). Wherry's classification was further discarded by B. L. Miller (1934, p. 514) in his "Limestones of Pennsylvania":

Beekmantown
Conococheague (Allentown)
Tomstown
Hardyston

In describing the Cambrian and Ordovician of Northampton and Lehigh Counties, B. L. Miller (1939a, p. 233–249; 1941, p. 180–201) noted that certain Cambrian units of south-central Pennsylvania had not been identified in the east. He suggested that since Wherry's Leithsville is lithologically similar to the southern Tomstown of Stose (1909, p. 36–38), the name Tomstown should be applied in the Lehigh Valley. Conversely, he used the local name, Allentown, rather than Stose's Conococheague (1909, p. 43–47). John M. Hills (1935) through studies of the insoluble residues of the limestones in the Lehigh Valley confirmed the formational division of the Cambrian and used Wherry's terms.

Bascom, Wherry, Stose, and Jonas (1931, p. 17–23) separated the Cambrian of the Buckingham Valley into:

Conococheague
Elbrook
Tomstown
Hardyston

Except for the New Jersey name, Hardyston, they used the terminology of south-central Pennsylvania (Stose, 1909, p. 36–46). "Beekmantown (?)" was used for the barren, dolomitic limestone which overlies their Conococheague.

Howell, Roberts, and Willard (1950) further altered the nomenclature of the local Cambrian.

They preserved the term Allentown and revived Leithsville. They split the Allentown into the Limeport below, restricted Allentown to the remaining Upper Cambrian above. These two are separable paleontologically, although lithologically similar. The terminology was applied to Bucks County, the Lehigh Valley, and adjacent parts of New Jersey. They confined the use of Hardyston to the northern quartzite flanking South Mountain. In the Buckingham Mountain the more appropriate term, Chickies, was applied to the lowest Cambrian, because of the thick basal conglomerate, the Hellam, not present in the Hardyston to the north but characteristic of the Chickies in south-central Pennsylvania.

Contacts

Intrasystemic Contacts

Intrasystemic contacts, now recognized among the Cambrian formations, are:

Allentown-Limeport
Limeport-Leithsville
Leithsville-Hardyston

LEITHSVILLE-HARDYSTON CONTACT: Early studies of the Cambrian in eastern Pennsylvania mentioned the transitional relations between the "Potsdam" sandstone (*i.e.* Hardyston) and the overlying limestone (Rogers, 1858, p. 100; Prime, 1883, p. 1210). In New Jersey, 2 miles south of Carpentersville, Ludlum (1940, p. 9) reported such a transition between the Hardyston and "Kittatinny". In Bucks County the analogous Chickies-Leithsville contact is buried. On U. S. Highway 611, south of its intersection with Pennsylvania Route 212 at Durham Furnace, (Fig. 1) a Hardyston-Leithsville contact was formerly exposed in a section now slumped and overgrown. Here, slightly micaceous, sandy shale at the top of the Hardyston passes upward into the limy, lower shale of the Leithsville. Half a mile north of Raubsville on the Delaware River (Fig. 3) is an eastward-sloping gneissic hill, Elephant Rock. Hardyston wraps around its northern edge, Leithsville is exposed in the valley to the north. Contact as here seen between U. S. Highway 611 and the River is similar to that at Durham Furnace.

On the south bank of the Lehigh 5 miles east of Bethlehem at Redington, (Fig. 1) the Cambrian is well exposed in quarries wherein the Leithsville was formerly extensively worked. Immediately west of the village the Leithsville-Hardyston relations may be seen in an abandoned quarry. The relationship recalls that observed north of Raubsville, although the exposure is not so good and may be faulted. In marked contrast to these transitional contacts is a Leithsville ("Tomstown")-Hardyston disconformity in an abandoned quarry three-quarters of a mile east of Hellertown, Northampton County, described by Whitcomb (1948).

LEITHSVILLE-LIMEPORT CONTACT: Because the Cambrian portion of the valley limestones had not been subdivided prior to the investigations by Wherry and Miller, their predecessors said nothing about intra- or interformational, limestone contacts. Miller (1939a, p. 227) apparently believed the Leithsville-Limeport formations to be conformable when he wrote:

> "In few places have contacts of the Tomstown [Leithsville] and the overlying Allentown [old use] limestones been observed. They appear to be perfectly conformable, although the former is regarded as Lower and the latter as Upper Cambrian with no indication of a Middle Cambrian such as has been noted elsewhere in the Appalachian region."

Miller (1941, p. 184) reiterated this statement but did not cite a locality where the contact could be seen.

Extensive cuts have recently been made along the newly constructed U. S. Highway 22 which by-passes to the north of the cities of the Lehigh Valley (Figs. 1, 4). This route is hereinafter referred to as the By-pass. The cuts were studied by the writer during the summer of 1953 as part of his assignment with the Pennsylvania Topographic and Geologic Survey. The use in this account of the data collected has been authorized by Dr. R. W. Stone, at that time Acting Director of the Survey. During the fall of 1953, graduate students from Lehigh University worked with the author in further studies of the By-pass exposures.

In Easton, the By-pass follows the Bushkill Valley westward from the Delaware River (Fig. 4). Eight- to nine-tenths of a mile west of the River the grade runs almost east-west along

the south side of the Kill. Long cuts nearly parallel to the strike expose limestone. Identifiable stromatolites and the lithology assign it to the Limeport. The beds dip 40°–45° S.

Directly north of the cuts across the Kill, old quarries show south-tilted dip slopes of barren Leithsville limestone with sericitic shale interbeds. The Leithsville passes south under the Limeport. Examination of the limestone along both sides of the road shows here a mingling of stromatolite-bearing beds with barren limestone having sericitic shale interbeds. The stromatolites die out downward as the shale increases.

In East Allentown, a Limeport-Leithsville near-contact was found where the Lehigh County map (Miller, *et al.*, 1941, Pl. 1) shows a small patch of Allentown on a hill at the name "Eve". Railroad cuts and abandoned quarries along the east bank of the Lehigh River expose limestones. In a large quarry immediately west of the crest of the hill, the Leithsville exhibits characteristic sedimentation rhythms. At the top of this quarry along the north and northwest rim, 6–8 feet of light-gray to buff dolomitic limestone carries dubious stromatolites suggesting *Cryptozoön fieldii*. No oölite was found. The beds are conformable with the Leithsville. At a cut on a spur track of the Lehigh and New England R.R. two-tenths of a mile northeast, steeply north-dipping Leithsville is overlain by a light-gray bed similar to that in the quarry. However, here additional Leithsville-type beds overlie the light-gray stratum. Obviously, naming any part of these beds is equivocal. Yet, the sequence suggests the Limeport-Leithsville transition.

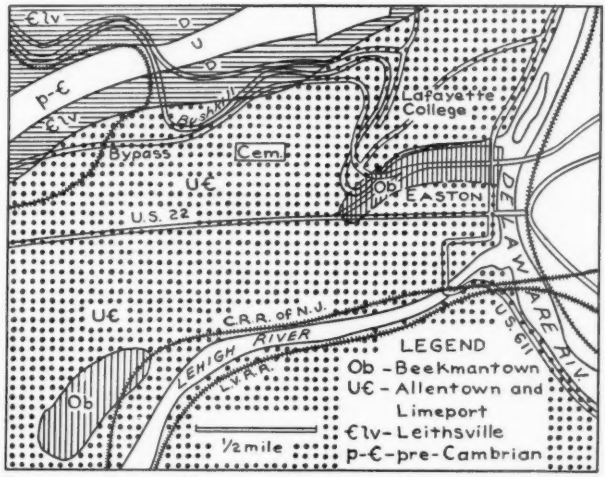

FIGURE 4.—SKETCH MAP OF THE VICINITY OF EASTON, PENNSYLVANIA
Showing distribution of Cambrian and Lower Ordovician stromatolites

There is a good exposure of the transition midway between Glendon and Island Park on the south bank of the Lehigh River 3 miles above its meeting with the Delaware (Fig. 1). Road and Lehigh Valley R.R. cuts show beds that rise in a crest-faulted anticline. The lowest beds of the Limeport are recognized by color alterations, oölite and stromatolites, probably *Cryptozoön fieldii*. These grade down into barren Leithsville consisting of sericitic shale alternating with platy to massive, dolomitic limestone. Stromatolites mingle with the highest, shaly beds. The thickness of the transition is 125–150 feet.

LIMEPORT-ALLENTOWN CONTACT: The description of the Limeport-Allentown contact by Howell, Roberts and Willard (1950, p. 1364) is based on a section 5½ miles west of the Delaware-Lehigh confluence in a railroad cut along the north bank of the Lehigh River (Fig. 1):

"East of Nancy Run in Northampton County, Pennsylvania, one of the best sections of stromatolitic Limeport beds in eastern Pennsylvania is exposed. At the eastern end of this section, at least ten biostromes may be seen. *Cryptozoön fieldii* is common in the lower beds of the section, while *Archaeozoön undulatum* and *Dolatophycus expansus* are numerous in the higher beds. Westward along this same section there is a distinct, disconformable erosional break (Pl. 1, figs. 1, 2) 15 feet above which occurs a biostrome of a new species of Trempealeauian *Cryptozoön*. Since below the break there are Dresbachian Limeport stromatolites, this disconformity may represent medial late Cambrian, or Franconian time."

Another contact has since been found in a long cut on the Delaware, Lackawanna and Western R.R. 1 mile north of Columbia, N. J., and west of the first underpass east of the Delaware River (Fig. 1). The beds dip southeast. From the underpass westward, the first strata encountered are medium-gray dolomitic limestone with little color variation, the beds 8–12 inches thick plus some platy and flaggy layers. The presence of well-preserved *Anomalophycus compactus* places these beds in the Allentown. About 1,400 feet west of the underpass the Allentown terminates below in a 5-foot pale gray bed. This rests upon cross-bedded calcarenite and is separated therefrom by an undulatory surface. The calcarenite is 3–4 feet thick and grades laterally into sedimentary breccia. Below the cross-bedded stratum are 25–30 feet of dark-gray, dolomitic limestone, remarkable for the presence of many quartz-filled vugs. These beds carry *Cryptozoön fieldii* and *Dolatophycus expansus* (?). *Archaeozoön undulatum* was found lower in the section. Because of the stromatolites, the beds below the undulatory surface are assigned to the Limeport, and that surface is taken to be the disconformity between Allentown and Limeport and presumably represents Franconian time.

In the fall of 1953, Mr. Kenneth A. Weiler accompanied the author in the study of a section of Upper Cambrian rocks along the Bushkill at Easton west from the Lafayette College campus (Fig. 4). The precise Allentown-Limeport contact is apparently concealed. However, the beds assigned to the upper part of the Limeport weather-stain bluish. This phenomenon, not observed in the overlying Allentown, was observed in the Limeport at its type locality in Bucks County. Because the thickness of the Limeport and Allentown are known, and because the Leithsville-Limeport contact was recognized in the Bushkill Valley to the west and could be projected east onto this section, an arbitrary division of the Upper Cambrian into its parts was made. The two formations are here distinguishable on their stromatolites. As calculated, the contact comes at a re-entrant in the bank of the stream where a prominent shale member quite unlike the dolomitic limestones crops out.

Intersystemic Contacts

BASAL CAMBRIAN CONTACT: Ingrained in the literature is the precept that the Cambrian is set off from the Precambrian by a great unconformity corresponding to Walcott's Lipalian interval. Recently, (Whittard, 1953; Snyder, 1947) heretical views have been voiced relative to this belief, because of the recognition of thick series of sedimentary rocks which appear to be transition between Cambrian and Precambrian. In Pennsylvania, no such thick series has been reported beneath the dated early Cambrian.

The contacts of the basal Cambrian Hardyston formation with underlying crystalline rocks is known from several Bucks, Northampton and Lehigh county exposures. Rogers (1858, p. 99) found the contact between his "Primal sandstone" and "gneissic system". One Second Pennsylvania Survey worker (Prime, 1883, p. 205–214) considered the "Potsdam sandstone" and the gneiss "transitional" because of confusing gneissic foliation with bedding. Except for Prime's statement, the nonconformable nature has been generally recognized.

The limestone valleys at Riegelsville and Durham Furnace (Fig. 1) are shut in by ridges of Precambrian crystalline rocks veneered by the Hardyston. Contact may be sharply exposed where the gneiss and quartzite have not weathered deeply. Movement has probably affected some contacts. Where granite-gneiss and arkosic quartzite are adjacent and weathered, the contact is often unrecognizable even in the best of exposures.

A contact, exposed some years ago on U. S. Highway 611 south of Durham Furnace, is

probably lost through slumping and growth of vegetation. At an elevation of 380 feet a bend in the road crossing the Northampton-Bucks county line 3½ miles west-southwest of Riegelsville, there is an excellent exposure; sharp, unfaulted. Six miles southwest from Riegelsville in the open valley west of Springtown, another contact in a small upfaulted block has been modified by slipping. A mile and three-quarters up the valley from Riegelsville, where a brook flows off the bordering northern ridge, a firmly welded contact between gneiss and quartzite was seen during low water. Along U. S. Highway 611, north of Riegelsville, the contact is indeterminate because of weathering, and a like situation obtains across the river in New Jersey. A sharp contact of Hardyston and hornblendic gneiss in the bed of the Delaware, south of Riegelsville on the New Jersey side, was called to the writer's attention by two former Lehigh students, David O. Beeler and M. M. Chow. It can be seen only during exceptionally low water.

The contact exposure lineally most extensive runs along the base of the northern shoulder of Morgan Hill 1 mile southeast of Easton (Miller, *et al.*, 1939a, p. 218):

> "Undoubtedly one of the most interesting exposures of the Hardyston in Northampton County is that on the eastern extremity of Morgan Hill just west of the highway along Delaware River. Here an old electric railway cut exposes the gneiss-Hardyston contact for several hundred feet, besides which there are two other definite outcrops higher up on the north side of the nose.
>
> The most characteristic Hardyston at the locality is an arkosic basal conglomerate, with quartz pebbles up to one and one-half inches in diameter. These pebbles are fairly well rounded. The matrix is arkose, but is rather altered, apparently to sericite and epidote. This basal conglomerate, resting on the gneiss with a sharp contact, is striking. A few inches of mashed gneissic material overlies the gneiss, and above the mashed zone there is a varying thickness of conglomerate. The conglomerate was not observed to be more than two feet thick at any point and at a few places is absent. Pegmatites have been found here."

This cut is impressive (Pl. 2, fig. 1). The conglomerate, more truly a pebbly arkose, directly overlies the undulatory upper surface of the gneiss. That this uneven surface is erosional rather than tectonic is attested by the bedding of the Hardyston which is tangent to the undulations. Further discussion of this contact and its relations to possible pegmatite intrusions has been published by D. M. Fraser (*in* Miller, 1939a, p. 198).

Another variation of the relation of the Hardyston with the gneiss is recorded where pinite separates the two rocks (Miller, *et al.*, 1941, p. 460):

> "*Pinite.*—At the base of the Hardyston formation in many places in the county [Lehigh], but especially along the north side of the mountain between Bethlehem and Allentown, there is a light-green amorphous, clay-like deposit up to a foot in thickness. This has been called serpentine. . . . As a result of microscopic examination and chemical analysis, E. T. Wherry determined it to be pinite, a variety of muscovite. In a few places it has been colored red by the precipitation of red iron oxides from circulating waters.
>
> Pinite is believed to be the metamorphosed ancient soil formed from the underlying gneiss and not removed before the deposition of the Hardyston sandstone.

The restricted distribution of the pinite is shown in three exposures of the Cambrian-Precambrian contact. The first, described by Miller and quoted above, is on the south side of the Lehigh west of Bethlehem (Fig. 1). Immediately across the stream behind the Central Railroad of New Jersey roundhouse, the Hardyston and gneiss are in contact without a trace of pinite. Yet, in Lehigh County on Little Lehigh Creek, about 5 miles to the southwest, a well-developed pinite separates the gneiss from the basal Hardyston, here a coarse conglomerate made up of ellipsoidal pebbles.

CAMBRIAN-ORDOVICIAN CONTACT: In eastern Pennsylvania, contact between the Allentown and Beekmantown formation is synonymous to that between the Cambrian and Ordovician systems. In this limited region it changes from marked disconformity to apparently perfect transition. The second condition must always be qualified with the statement that fossils have not been identified from the lowest Beekmantown beds. Of the Allentown, the unique faunule of Trempealeauian fossils in northeastern Northampton County demonstrates its age.

Until Wherry (1909) successfully broke down the valley limestones, the intersystemic contact was unrecognized. Peck (1911), albeit he used Allentown and "Coplay" (Beekmantown), failed to describe the contact. Hills (1935) was noncommittal. Miller dismissed the matter

briefly in 1925, but later (1939a, p. 240) discussed it more fully:

"The Allentown strata pass beneath the Beekmantown and again there seems to be perfect conformity. This contact is well shown in the exposed section along the Delaware River road about one and a half miles north of Chestnut Hill. It is difficult to determine the particular place to draw the separation line inasmuch as certain transitional beds might with almost equal reason be included in either formation but within a few feet distinctions are sufficiently great for ready differentiation of the two."

This seemingly contradictory statement about a recognized contact which cannot be identified precisely is actually correct. In this section, which the author has several times reviewed, the contact is not clear, and, as a matter of fact, there is considerable reason for thinking it to be a normal fault.

In the Lehigh County report, Miller (1941, p. 199) amplified his ideas:

"Along the Lehigh Valley R.R. in the south part of Fullerton there is a fine exposure of overturned strata. The beds strike N. 68°E., dip 41°SE. The north end of the section is Beekmantown dipping beneath Allentown at the south end. The overturning is shown by the upside-down heads of *Cryptozoa*. . . . Besides the *Cryptozoa* the Allentown beds show the alternating light and dark beds, and the Beekmantown formation is identified by the interbedded high- and low-magnesian strata. There seems to be perfect conformity throughout and there is some question where the exact boundary line should be drawn. At track level the line is drawn about 30 feet to the north of a small spring."

In the Lehigh County report (Miller, 1941, Pl. 1), the geologic map shows the Allentown in thrust-fault relations with the Beekmantown in the Fullerton section. Yet, the fault is not mentioned in the text, nor has the present author seen evidence for such a structure.

Several good sections which include the Cambrian-Ordovician contact are known. The first is in Bucks County, whence they continue northward along the Delaware Valley to Easton, thence westward along the Lehigh Valley to eastern Lehigh County (Fig. 1). These represent successive development, for the sections are in a sense a recitation of contact evolution from disconformity to transition.

The northeast end of the limestone lowland known as Buckingham Valley in eastern Bucks County 2 miles up river from New Hope and a quarter of a mile below the village of Limeport is the type locality of the Limeport formation (Fig. 2). West of State Highway 32 are two abandoned quarries in the formation. The first is visible from the highway, the second lies a few hundred feet southwest of the first. All beds dip north. In the first opening (Fig. 2, Quarry A), the Limeport limestone passes upward into an anomalous 40–50 feet of partially brecciated dolomite, brown silicarenite, red shale with ripple marks and mud cracks, and arenaceous beds marked by peculiar, concentric, gray-white lines (Pl. 2, fig. 2). At the top of the north face of the quarry these Cambrian red beds underlie the Triassic Stockton arkose, conglomerate and red shale. When first studied, the red beds in the Limeport were confused with those of the Stockton. In this quarry, bluish weather-stain may be seen on the Limeport, a condition duplicated along the Bushkill at Easton. Toward the western end of this quarry, near the floor, in normal dolomitic beds below the abnormal strata diagnostic *Cryptozoön fieldii* and *Archaeozoön undulatum* have been reported (Howell *et al.*, 1950, p. 1360). In the second opening (Fig. 2, Quarry B) which is entirely in the dolomitic beds and is stratigraphically slightly lower than

PLATE 1.—OUTCROPS, EASTERN PENNSYLVANIA

FIGURE 1.—ALTERNATING COLOR BANDING IN LIMEPORT FORMATION

A quarry face ¼ mi. S. of Lahaska, Bucks County

FIGURE 2.—PORTION OF BIOHERM OF CRYPTOZOÖN FIELDII

¾ mi. E. of Lahaska, Bucks County

PLATE 2.—OUTCROPS, EASTERN PENNSYLVANIA

FIGURE 1.—CAMBRIAN-PRECAMBRIAN CONTACT, MORGAN HILL, NORTHAMPTON COUNTY

Hammer at contact, gneiss below, pebbly arkose above

FIGURE 2.—INTERBEDDED DOLOMITIC LIMESTONE AND RED BEDS, NORTH WALL, QUARRY A, LIMEPORT, BUCKS COUNTY

FIGURE 1

FIGURE 2

OUTCROPS, EASTERN PENNSYLVANIA

FIGURE 1

FIGURE 2

OUTCROPS, EASTERN PENNSYLVANIA

FIGURE 1

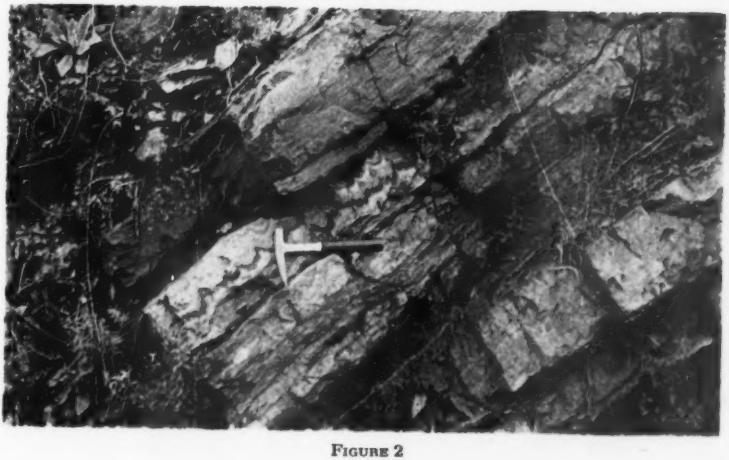

FIGURE 2

OUTCROPS, EASTERN PENNSYLVANIA

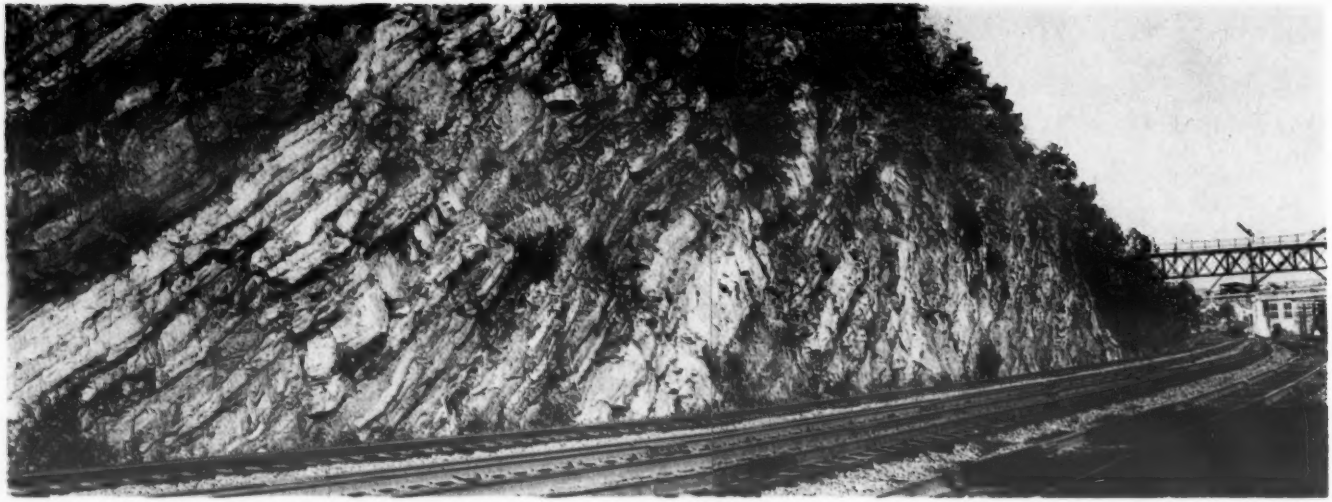

FULLERTON SECTION ALONG LEHIGH VALLEY R. R., LEHIGH COUNTY, PENNSYLVANIA

Quarry A, Howell obtained the invertebrate faunule on which he based the Dresbachian age of the Limeport (Howell *et al.*, 1950, p. 1360).

The red beds at the top of the Limeport were traced for approximately 2 miles southwestward in Buckingham Valley, where they yielded place to gray shale and silicarenite at the top of the formation. The next highest exposed beds are dolomitic limestone identical lithologically to the Beekmantown. The Beekmantown (?) is interpolated between the Cambrian and the Triassic westward. Unfortunately, no fossils have been reported from these highest, dolomitic beds. Their identity rests upon lithology and the fact that they overlie known Upper Cambrian. Thirty miles west, at Henderson Station 2 miles south of Norristown (Fig. 1), Bascom and coworkers (1909a, p. 5) collected Lower Ordovician fossils from beds believed to be the correlative of the Beekmantown (?) of Buckingham Valley. Furthermore, those who have seen the highest Buckingham Valley limestones agree that the beds are most likely Beekmantown (*cf.* Miller, 1934, p. 249; Bascom *et. al.*, 1931, p. 22–23; Willard, *et al.*, 1950. Of these references, some retain, some delete the question mark after the name).

The writer has never seen a Limeport-Beekmantown contact in Buckingham Valley. The nearest to one is 1 mile north from Aquetong (Fig. 2). Along a short northeast-southwest section of road, the shaly and sandy top Limeport beds are exposed at the south side. The Beekmantown (?) massive dolomite crops out in ledges in fields to the north of the road. The strikes and dips of the two formations are essentially identical.

In Buckingham Valley the youngest Cambrian identified is the Dresbachian Limeport formation. The Limeport is succeeded disconformably by dolomitic beds attributed to the Beekmantown. These are lithologically quite different from the known Allentown to the north. At the top of the easternmost exposed Limeport there is evidence of a profound change in sedimentation from normal carbonate to siliceous sand and red mud which connote a continental environment. A hiatus is deduced which includes Franconian and Trempealeauian time.

Two significant Cambrian-Ordovician sections are recognized in the Delaware Valley between Limeport and Easton (Fig. 3). Carpentersville, N. J., is about 20 miles up river from Limeport. Here, the Middle Ordovician, Jacksonburg limestone, delimits a synclinal axis (Lewis and Kümmel, 1931; Ludlum, 1940, Fig. 3). Abandoned quarries, road and railroad cuts strung out for a mile down river expose steeply south-dipping, northward-overturned strata of early Ordovician and Cambrian ages. In company with Mr. James R. Randolph and subsequently alone the author has studied this section.

Leithsville, largely concealed, overlies Hardyston in the southern end of the section. The Limeport occupies the middle and is overlain by the Allentown northward, to be followed by the Beekmantown. From one of the quarries in the Limeport, Weller (1899, p. 47–52; 1903, p. 13) obtained Upper Cambrian fossils which Howell (1945, p. 2; 1950, p. 1364) showed to be Dresbachian. No one has reported having rediscovered Weller's locality, so that the particular bed from which he collected remains an enigma.

The Limeport and Allentown carry characteristic algae. The Allentown itself is 400–500 feet thick and weathers to light- and dark-gray bands, but the Beekmantown remains a uniform gray, is heavier-bedded, and laced with gash veins, absent or rare in the Allentown. The northernmost quarry exposes slightly overturned Beekmantown. A road cut coincident

PLATE 3.—OUTCROPS, EASTERN PENNSYLVANIA AND NEW JERSEY

FIGURE 1.—ALLENTOWN-BEEKMANTOWN (CAMBRIAN-ORDOVICIAN) DISCONFORMITY, CARPENTERSVILLE, N. J.

FIGURE 2.—OVERTURNED CROPTOZOAN BED, ALLENTOWN FORMATION, SOUTH END OF SECTION AT FULLERTON, LEHIGH COUNTY, PA.

PLATE 4.—FULLERTON SECTION ALONG LEHIGH VALLEY R.R., LEHIGH COUNTY, PA.

Allentown limestone in foreground identified by alternate color banding, Beekmantown toward the signal bridge, transitional beds between. All beds overturned north (away from observer).

with the beds which form the south wall of this quarry, carries the section down into fossiliferous Allentown with color-alternating bands. Here are found the highest stromatolites seen in the section. In the south wall, of the quarry, is an undulatory surface parallel to the bedding. Above it, northward, the lithology is that of the Beekmantown (Pl. 3, fig. 1). No breccia, striations or other indications of faulting were seen at or near the surface, and the dips and strikes on opposite sides are concordant. Therefore, the Allentown-Beekmantown contact is drawn here as a disconformity. In this section, the Allentown is so thick it must nearly fill the Trempealeauian part of the hiatus noted in Buckingham Valley. Since the Allentown and Beekmantown at Carpentersville are in disconformity, there is still a diastem.

Across the Delaware River from Carpentersville is Raubsville, Pennsylvania (Fig. 3). The Northampton County geologic map (Miller, *et al.*, 1939a, Pl. 1) shows a limestone-floored, V-shaped, synclinal valley opening onto the river. "Tomstown" is mapped along both north and south sides, "Allentown" between. At the north border, limestone is interpreted as downfaulted against gneiss, eliminating the Hardyston. This interpretation disagrees with the mapping at Carpentersville.

North of Raubsville the limestone is undoubtedly in fault contact with the gneiss as mapped. However, this limestone is believed to be not "Tomstown" or Leithsville, but Beekmantown. Identification was made at exposures a quarter to half a mile west of Raubsville. The rest of the valley south to Coffeetown is underlain by undifferentiated Allentown and Limeport with Leithsville along its southern side. The beds dip steeply south (northward overturned) or are perpendicular. No syncline was observed. Exposures are confined mostly to a few abandoned quarries, and the section is inferior to that at Carpentersville.

The Beekmantown-Allentown contact is not exposed on this side of the River. Across the River at Carpentersville during low water, Randolph discovered a remarkably coarse breccia about 30 feet thick in the lower part of the Beekmantown. Its angular blocks of dolomitic limestone up to 3 feet across are firmly cemented in a dolomitic matrix. While this breccia is not an extension of the boundary fault above Raubsville, it may show movement affecting the Beekmantown.

The reinterpreted Raubsville region is complementary to that at Carpentersville. The limestone sequence is the same from south to north, and the attitude of the beds agrees. Where the Carpentersville section is continued north across a broad syncline, the Raubsville is faulted off. No data were obtained from the Raubsville section to confirm or deny the interpretation of the Allentown-Beekmantown contact described at Carpentersville.

In the vicinity of Easton, Pennsylvania, other Cambrian-Ordovician contacts were identified (Fig. 4). On the Northampton County geological map (Miller, *et al.*, 1939a, Pl. 1), a strip of Leithsville ("Tomstown") borders the foot of Chestnut Hill north of Easton, and another the north edge of Morgan Hill, the eastern end of South Mountain, south of the city. Between these two bands the map shows only Allentown (*sensu lato*) except at a point southwest of the City where a small, oval patch of Beekmantown overlies the Cambrian. The inferred structure is a syncline with the Beekmantown axial. The Allentown-Beekmantown contact could not be determined at this patch of Beekmantown, although narrowed down to a few feet.

A second area of Beekmantown was found along the Bushkill southwest of Lafayette College. Although barren, the rocks are characteristic of the Beekmantown and resemble closely those at Carpentersville and in the patch southwest of Easton. Structurally, this Beekmantown is synclinal. Northward from a meander along the Bushkill and the By-pass below Lafayette College, a fairly continuous section beginning in the Beekmantown descends through the Upper Cambrian.

The writer examined this section for the Allentown-Beekmantown contact. The bedding of the upper Allentown is uniformly about 1 foot thick. Strata which weather to contrasting grays carry *Anomalophycus compactus* and merge upward into barren beds of the Beekmantown. All observed oölite is in the Allentown. On the south side of the stream, the Beekmantown carries another coarse breccia

like that at Carpentersville. This section is best interpreted as transitional between Allentown and Beekmantown or Cambrian and Ordovician. The transitional beds may be only about 10–15 feet stratigraphically.

The By-pass runs east-west immediately north of Green Pond about midway between Easton and Fullerton (Fig. 1). On the Northampton County map a fault trace passes northeastward across Green Pond. Beekmantown spreads on both sides of the fault; the nearest Cambrian is half a mile to the east. Where a meridian road crosses the By-pass on an overhead bridge north of Green Pond, cuts, now covered, furnished fault contact. Before the cuts were covered, Mr. George L. Freeland and the writer examined and measured them.

Immediately west of the bridge along the south side of the By-pass there was a large cut in characteristic Beekmantown. The strike was nearly east-west, dip gently north. The same rock reappeared at the east side of the bridge. In both places, calcite-filled vugs up to 1 inch in diameter were distinctive. Four hundred feet east on the south side of the road, cuts exposed beds lithologically much like the Beekmantown but lacking the vugs and carrying poorly-preserved stromatolites suggestive of Roberts's form species A and *Anomalophycus compactus* (Howell *et al.*, 1950, Fig. 2). Floral evidence thus assigns these beds to the Allentown. They strike east-west but dip gently south. If projected north, they could pass above the Beekmantown. Between the Allentown and Beekmantown, some intermittent exposures of dolomitic limestone were assigned to the Allentown, but 100 feet east of the overpass bridge there was a brecciated interval. Many phenoclasts of the breccia were of Beekmantown lithology, but some carried traces of stromatolites. The interpretation of this section is that the Allentown was faulted against the Beekmantown. Presumably the movement was small. This fault contact is significant only in that similar contacts or near-contacts have been noted or deduced northeastward. One such is in the Bushkill Valley 3 miles northwest of Easton, and another along the west bank of the Delaware River 3½ miles north-northeast of Easton.

Near Fullerton, Pennsylvania, (Fig. 1) the last section to be described was investigated. This is along the west bank of the Lehigh southward from the town and three-quarters of a mile north of the northern limit of Allentown. Continuous cuts on the Lehigh Valley R.R. completely expose the succession (Pl. 4). The northern end of the section is in the Beekmantown. At the southern extremity the Allentown contains many stromatolites (Pl. 3, fig. 2). All beds are overturned north and dip 30°–40° S. This is the section which B. L. Miller discusses rather fully in the Lehigh County report (1941, p. 199).

Albeit abundant stromatolites stop abruptly about 50 feet north of the south end of the section, Allentown lithology with alternating light- and dark-gray beds continues for at least 200 feet, and among these strata one poorly-preserved stromatolite was found. Toward the upper (north) end of the cut the alternation of color gives way to laminated or shaly dolomitic limestone beneath more massive Beekmantown. Although the county map displays a prominent thrust fault at the Allentown-Beekmantown contact, no evidence of this was found, nor is it mentioned in the text of the County report. Miller drew the contact "about 30 feet north of a small spring" (1939a, p. 199).

Mr. Gerald D. O'Brien worked with the author on the Fullerton section, and ran a series of insoluble residue tests. He reported that below a specified horizon the residue consists of "white silt and rounded quartz grains", above it of "shale and gray silt particles". This change does not coincide sharply with the other data, paleontological or lithological, for determining the contact. In summing up all lines of evidence, it is believed that no definite Cambrian-Ordovician boundary can be drawn in this section and to all intents and purposes the Allentown and Beekmantown formations are transitionally related.

Summary and Conclusions

The Cambrian in eastern Pennsylvania is comprised of four formations:

Allentown
Limeport
Leithsville
Hardyston

Contacts between each pair are known and documented in the field. The Hardyston and Leithsville are conformable at all but one known contact where there is a local disconformity. The Leithsville interfingers with the overlying Limeport. The Limeport and Allentown meet in disconformity.

The relative ages of the Hardyston, Limeport, and Allentown are established upon paleontological evidence. No fossils have been identified from the Leithsville. Since the Hardyston is early and the Limeport early late Cambrian, the Leithsville should be chiefly middle Cambrian with some possible overlap into early and late Cambrian.

The basal contact of the Hardyston "quartzite" with the Precambrian gneiss changes in character from place to place, but is always nonconformable. The Cambrian-Ordovician contact is inconstant from south to north and thence west, thus:

Buckingham Valley	Carpentersville
Beekmantown (?)	Beekmantown
Disconformity	*Disconformity*
Limeport	Allentown
Easton	**Fullerton**
Beekmantown	Beekmantown
Transition?	*Transition*
Allentown	Allentown

These changes indicate that the Upper Cambrian wedged in from the west. That this was a sedimentary incursion rather than deposition followed by erosion is inferred from the red beds at the top of the Limeport in Bucks County where the Allentown is absent, from the Beekmantown-Allentown disconformity in the Delaware Valley, and from the gradual introduction of the Allentown from Carpentersville westward with the change of the Allentown-Beekmantown contact from a disconformity to apparent conformity.

References Cited

Ashley, George H., *et al.*, 1933, Classification and nomenclature of rock units: Geol. Soc. America Bull., v. 44, p. 423–459.

Bascom, F., Darton, N. H., Kümmel, H. B., Clark, W. B., Miller, B. L., and Salisbury, R. D., 1909a, Description of the Trenton quadrangle: U. S. Geol. Survey, folio 167.

—— 1909b, Description of the Philadelphia district: U. S. Geol. Survey, folio 162.

Bascom, F., Wherry, E. T., Stose, C. W., and Jonas, A. I., 1931, Geology and mineral resources of the Quakertown-Doylestown district, Pa. and N. J.: U. S. Geol. Survey Bull. 828.

Fenton, C. L., and Fenton, M. A., 1937, Cambrian calcareous algae from Pennsylvania: Am. Midland Naturalist, v. 18, p. 435–441.

Hills, J. M., 1935, The insoluble residues of the Cambro-Ordovician limestones of the Lehigh Valley, Pa.: Jour. Sed. Petrology, v. 5, p. 123–132.

Howell, B. F., 1945, Revision of the Upper Cambrian faunas of New Jersey: Geol. Soc. America Mem. 12, 46 p.

Howell, B. F., Roberts, Henry, and Willard, Bradford, 1950, Subdivision and dating of the Cambrian of eastern Pennsylvania: Geol. Soc. America Bull., v. 61, p. 1355–1367.

Kümmel, H. B., and Weller, Stuart, 1901, Paleozoic limestones of Kittatinny Valley, N. J.: Geol. Soc. America Bull., v. 12, p. 147–164.

Lesley, J. P., Sanders, R. N., Chance, H. M., Prime, F., and Hall, C. E., 1883, The geology of Lehigh and Northampton counties: Pa. (Second) Geol. Survey Report D3.

Lesley, J. P., *et al.*, 1892–1895, Summary description of the geology of Pennsylvania: Pa. (Second) Geol. Survey

Lewis, J. V., and Kümmel, H. B., 1931, Geologic map of New Jersey: N. J. Dept. Conserv. and Devel. Atlas, sheet 40, rev. ed., 1950.

Ludlum, J. C., 1940, Continuity of the Hardyston formation in the vicinity of Phillipsburg, N. J.: N. J. Dept. Conserv. and Devel., Geol. Survey Bull. 47.

Miller, B. L., 1925, Mineral resources of the Allentown quadrangle, Pa.: Pa. Topog. and Geol. Survey, 4th ser., Atlas 206.

—— 1934, Limestones of Pennsylvania: Pa. Topog. and Geol. Survey, 4th ser., Bull. M20.

Miller, B. L., Fraser, D. M., and Miller, R L., 1939a, Northampton County, Pa.; Geology and Geography: Pa. Topog. and Geol. Survey, 4th ser., Bull. C48.

Miller, B. L., Fraser, D. M., Miller, R. L., Willard, Bradford, Wherry, E. T., 1941, Lehigh County Pa.; Geology and Geography: Pa. Topog. and Geol. Survey, 4th ser., Bull. C39.

Peck, F. B., 1911, Preliminary report on the talc and serpentine of Northampton County and the Portland cement materials of the Lehigh district: Pa. Topog. and Geol. (Third) Survey, Rept. 5.

Prime, Frederick, Jr., 1875, Report of Progress on the brown hematite ore ranges in Lehigh County: Pa. (Second) Geol. Survey, Rept. D.

—— 1878, The brown hematite deposits of the Siluro-Cambrian limestones of Lehigh County: Pa. (Second) Geol. Survey, Rept. DD.

—— 1883, *in* The geology of Lehigh and Northampton Counties: Pa. (Second) Geol. Survey, Rept. 3D, p. 161–214.

Rogers, H. D., 1858, The Geology of Pennsylvania; Philadelphia: v. 1, 586 p.; v. 2, 1046 p.

Snyder, F. G., 1947, The problem of the Lipalian interval: Jour. Geology, v. 55, p. 146–152.

Stose, G. W., 1909, Description of the Mercersburg-Chambersburg district: U. S. Geol. Survey, folio 170, field ed.

Ulrich, E. O., 1911, Revision of the Paleozoic systems: Geol. Soc. America, Bull., v. 22, p. 281–680.

Weller, Stuart, 1899, Description of Cambrian trilobites from New Jersey: N. J. Geol. Survey An. Rept. 1899, p. 47–52.

—— 1903, Report on Paleontology, v. III, The Paleozoic faunas: N. J. Geol. Survey.

Wherry, E. T., 1909, The early Paleozoic of the Lehigh Valley district, Pa.: Science, n.s., v. 30, p. 416.

Whittard, W. E., 1953, The enigma of the earliest fossils: Bristol [England] Naturalists' Soc., Proc., v. 28, pt. 4, p. 289–304.

Whitcomb, Lawrence, 1948, An unusual Hardyston-Tomstown contact at Hellertown, Pa.: Pa. Acad. Sci., Proc., v. 22, p. 112–116.

Willard, Bradford, McLaughlin, D. B., *et al.*, 1950, Geologic map of Bucks County: Pa. Topog. and Geol. Survey, 4th ser.

Willis, Bailey, 1912, Index to the stratigraphy of North America: U. S. Geol. Survey Prof. Paper 71.

Wilmarth, M. Grace, 1938, Lexicon of geologic names of the United States: U. S. Geol. Survey Bull. 896, pts. 1 and 2.

Wolff, J. E., and Brooks, A. H., 1898, The age of the Franklin white limestone of Sussex County, N. J.: U. S. Geol. Survey An. Rept. 18, p 425–457.

Lehigh University, Bethlehem, Pa.

Manuscript Received by the Secretary of the Society, February 25, 1954

BULLETIN OF THE GEOLOGICAL SOCIETY OF AMERICA
VOL. 66, PP. 835-870, 11 FIGS. JULY 1955

MEASUREMENT OF THE DEFORMATION OF THE SIERRA NEVADA, CALIFORNIA, SINCE MIDDLE EOCENE

BY F. S. HUDSON

ABSTRACT

The main channel of the middle Eocene Yuba River is known from its mouth, a short distance east of the western edge of the Sierra Nevada, to the present range crest, immediately northwest of Donner Pass. Abrupt changes of gradient between variously directed reaches of this channel led Lindgren to conclude that the range had been tilted 60 feet per mile west-southwest as a rigid block. Faulting east of the summit seemed insufficient to account for such increase of slope, so he proposed uplift of an area greater than the present range with local sinking of moats. A corollary, not stated by him, is that both moats and mountains suffered absolute uplift.

The aggregate downthrow of faults east of the crest is actually 3550 feet, an amount more than enough to account for the 3300-foot uplift of the summit caused by a simple tilt of 60 feet per mile. A study of Lindgren's basic data and new information shows that uplift at Donner Pass was less than 2000 feet, or little more than half the sum of the downthrows on faults east of the pass. The deeper grabens east of the range must have suffered absolute depression since middle Eocene.

The uplift of the Sierra Nevada is not due to simple tilting of a rigid block. Gradient calculations indicate five zones of deformation on the western slope. Field studies confirm two of these, the more important being a north-trending fault zone situated about midway between the summit and the western edge of the range and extending 12 miles, from Forest Hill to near Dutch Flat.

CONTENTS

TEXT

	Page
Introduction	836
Formations	837
Middle Eocene South Fork of Yuba River	838
Tertiary and later deformation of the Sierra Nevada	841
General	841
Deformation calculated from the gradients of the channel	841
Deformation of the range by diverse movements in separate segments	844
Criticism of the mathematical method	850
Modification of the results of the uplift calculations	856
Internal deformation of the range	856
Folding	856
Inferred faults	856
Known faults	857
Crustal movements east of the crest	858
Summary of conclusions	859
References cited	859
Appendices:	
A. Gradient calculations	860
B. Examples of variance calculations	867

ILLUSTRATIONS

Figure	Page
1. Key map: part of northern Sierra Nevada	836
2. Profiles of middle Eocene Yuba River	839
3. Gradients of channels in Forest Hill region	842
4. Profile of modern Yuba River	843
5. Diagram of tilted channel segment	844
6. Amounts of uplift, projected onto vertical section connecting head and mouth of middle Eocene Yuba River	846
7. Structure map: part of northern Sierra Nevada	848
8. Structure map of Donner Summit region	849
9. Plat of part of modern Yuba River, where gradients average 37.2 feet per mile	850
10. Plat of part of modern Yuba River, where gradients average 15.6 feet per mile	851
11. Section across middle Eocene Yuba River, 3.4 miles above Station 5	854

TABLES

Table	Page
1. Sections of the Superjacent series	837
2. Present course of middle Eocene Yuba River	840
3. Summary of results of gradient calculations	845
4. Summary of calculations of post-middle Eocene uplift	847
5. Variances from average gradients	852
6. Correction factors	853
7. Modification of results of original calculations	855

Introduction

The Sierra Nevada Range extends 400 miles north-northwest along the east side of the Great Valley of California. Its abrupt eastern slope measures no more than one quarter, and in some places only one tenth, of the 50–75 mile total width.

This range was regarded for many years as the most noteworthy example of simple tilted blocks of the Basin Range type. According to this view it is a great block of the earth's crust, which has been rotated on an axis parallel to its length so that the eastern edge, dislocated from the region of the Great Basin, was elevated to make the crest of the range, while the western edge was depressed below sea level and buried by the deposits which underlie the Great Valley.

It was recognized long ago that the southern Sierra, in the latitude of Kern River, is not a simple, westward tilted block, when Lawson (1903, 1906) showed the range to be internally deformed by faulting of Quaternary age, and Anderson (1911) described a west-dipping normal fault of post-Pliocene age along the western edge of the mountains. Later, Hake (1928) described escarpments interrupting the continuity of the west slope of the southern and central parts of the range, and concluded that they are the eroded scarps of west-dipping normal faults.

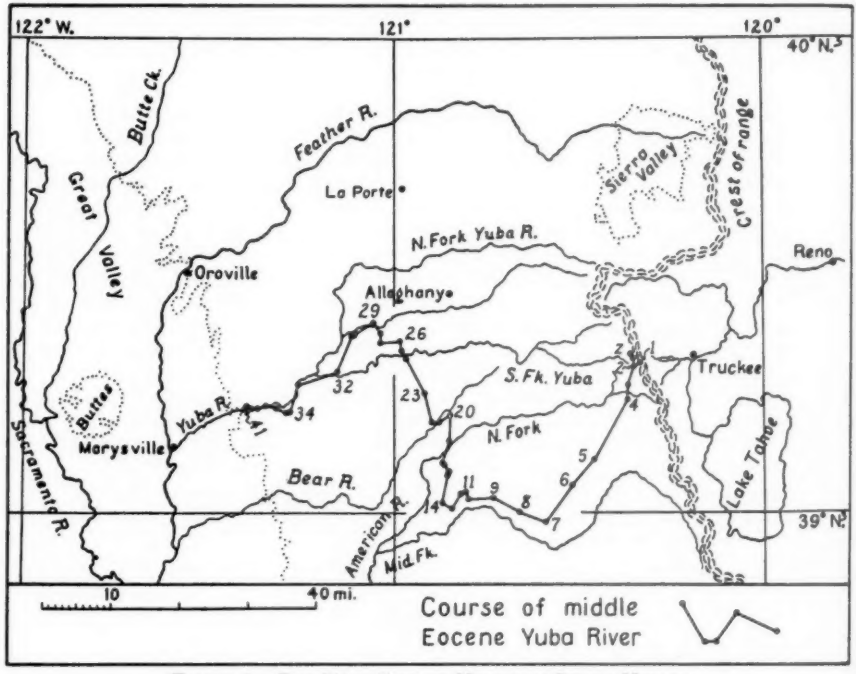

FIGURE 1.—KEY MAP: PART OF NORTHERN SIERRA NEVADA

It was to be expected that the structure of the northern Sierra, also, would eventually be shown to fail to conform with the theory of simple westward tilting. This expectation has been realized by the results of recent field work.

The region of the Sierra Nevada here considered was drained by the south (main) fork of the middle Eocene Yuba River, the headwaters of which are crossed by the upermost reaches of the present South Fork of Yuba River (Fig. 1). The ancient stream entered the body of fresh water in what is now the Great Valley, through the same canyon used by the modern stream. But here the resemblance ends.

The old stream flowed southwest, through an area now drained by the American River, then north-northwest across land now drained by the Bear River and the South Fork of the Yuba River, and finally southwest into the lower Yuba canyon. This course measures 109 miles. The modern stream flows west-southwest throughout, and its water travels only 75 miles in making the same journey.

The region drained by the ancient stream has yielded several hundred million dollars worth of placer gold, first from the bars of the present streams, later from the gravels of the Tertiary channels. The activity of placer mining was notably lessened about 70 years ago, and today it is insignificant. However, the records of the character of the gravels and of elevations along the channels collected over the years are essential for the solution of the orogenic problems of the Sierra.

These old records formed the basis for the first version of this paper (Hudson, 1948), which maintained that the uplift of the range at the present crest immediately northwest of Donner Pass has been only 1838 feet since middle Eocene time. These calculations have been revised, and correction factors have been devised, based on the gradients of the modern Yuba River. The basic calculations now indicate an uplift of 1684 feet. When corrected by the "most likely" factors, this becomes 1886 feet.

TABLE 1.—SECTIONS OF THE SUPERJACENT SERIES

	Donner-Castle Peak Stations 1-2-z (Hudson, 1951, p.937-945)		Forest Hill Divide Stations 10-14 (Lindgren, 1911, Pl. XXV and p.136, 138)		Gold Run North of Station 19 (Lindgren, 1911, p.145, and new observations)	
		feet*		feet		feet
Pliocene	Basalt	525				
	--unconformity--					
Pliocene-Miocene	Andesite agglomerate, minor tuffs and flows	1000	Andesite tuff, tuff breccia, and gravels	550	Andesite agglomerate and tuff	200
	---major unconformity---				--not in contact, but probable unconformity---	
Oligocene or Eocene	Andesite tuff	140			Gravel with sparse andesite boulders	70
	--unconformity--				--unconformity--	
Middle Eocene	Rhyolite tuff	1000	Rhyolite tuff with gravel beds	250		
	Pre-volcanic gravels	13	Pre-volcanic gravels	100	Bench gravels	160
					Deep gravels	60

*Maximum thicknesses in each area.

The earlier version claimed that the results of the calculations of uplift indicated zones of deformation within the western slope of the range. Two such zones have been discovered by field study in the Donner and Forest Hill-Dutch Flat areas. The latter appears to be an en echelon link between the Mother Lode and Alleghany faults.

The third major conclusion of the 1948 version, which is also unchanged, was that the faulting east of the range crest involved more depression of the Great Basin side than uplift of the Sierra.

FORMATIONS

The formations of the Sierra Nevada Range include the pre-Cretaceous Bedrock series of metamorphosed sediments and volcanic deposits intruded by deep-seated igneous rocks and the Superjacent series of Tertiary gravels, sands, clays, and volcanic materials.

BEDROCK SERIES: The slates, limestones, sandstones and cherts, and the associated lavas and tuffs of this series range from Carboniferous to upper Jurassic. They were closely folded, faulted, and intruded by granite, gabbro, and ultra-basic rocks during the Nevadan revolution (Taliaferro, 1942, p. 102). The gold-quartz veins of the Mother Lode, Alleghany, and other Sierra Nevada mining districts were formed at this time. The structural features of the metamorphic rocks, and the contacts between them and the intrusives, trend in general north-northwest and dip steeply eastward.

SUPERJACENT SERIES: The character of the deposits of this series at three localities on the middle Eocene Yuba River is given in Table 1.

Where the pre-volcanic gravels are best developed, the channel consists of a narrow gutter filled with the deep gravel, overlain by a wide deposit of bench gravel. At Indiana Hill (Fig. 1, sta. 19) the trough is 60 feet deep and about 400 feet wide, and the overlying bench gravels have a maximum depth of 160 feet and a width of almost a mile. The deep gravels consist of cobbles and boulders, as much as several feet in diameter, in a matrix of cemented sand. Quartz pebbles are present, but are generally subordinate to detritus of metamorphic and igneous rocks. The pebbles of the bench gravels are smaller, and quartz is often the dominant constituent.

Following the accumulation of these gravels volcanic materials buried the valleys and many intervening ridges. Erosion by recent streams has extended into the Bedrock series in many places, exposing the gravels and furnishing places of entry for mining by underground methods. Surface excavations increased the outcrop area, and underground (drift) mining disclosed evidence of the channel gradients.

The richest accumulations of placer gold were in the deep gravels and upon or in crevices in the underlying Bedrock; consequently the miners worked to Bedrock. To maintain proper gradients in the workings in order to remove water cheaply from the drift mines and transport and wash the gravel in the hydraulic pits at low cost, they made accurate measurements of elevation which are available today. The deep gravels are the oldest post-Cretaceous deposits of the range and are important in any study of the Tertiary and later deformation of the Sierra Nevada. Unless indicated otherwise, the word *channel*, hereafter, refers to the middle Eocene deep channel and elevations along the channel are those of the deepest part of the gutter.

Middle Eocene South Fork of Yuba River

Lindgren's earlier idea (1897, p. 6) was that the channel from Summit Valley to Russian Ravine (Fig. 1, stas. 2–6) constituted the headwaters of the North Fork of the Tertiary American River, which flowed directly southwestward. Later (1900, p. 5) he concluded that these upper reaches were the headwaters of the ancient South Fork of Yuba River which flowed southwest (stas. 6–7) from Russian Ravine to Clydesdale, then west-northwest to Yankee Jim (north of sta. 14) whence it ran north-northwest, then southwest past Sicard Flat (sta. 38) along the course of the present Yuba. (*See* Lindgren, 1911, Pls. I, X.)

In Figure 1, 21 of his 23 stations are used, while three lower reaches and two forking headwater branches of the stream as well as 16 intermediate stations are added. Figure 2A shows the profile calculated by Lindgren. Table 2 and Figure 2B give the writer's interpretation.

Le Conte (1880, p. 179, 182) thought the irregular hollows and frequent deep potholes in the bedrock of the channel were produced by swift currents carrying coarse detritus, at much higher velocities than those of modern streams of the Sierra. Much greater anomalies are exemplified by the channel between Indiana Hill and Thompson Hill (stas. 19, 20).

These anomalies and the character of the deep gravels led Le Conte (1880, p. 185, 190) and Haley (1922, p. 552) to believe that glaciation had affected the range at this time. Current ideas of Eocene climate give no support to this notion.

The large-scale anomalies can be explained by deformation of the channel and the underlying Bedrock, after the deposition of the gravels. Some smaller anomalies are undoubtedly due, following Le Conte, to scouring of weaker rock upstream from obstructions of

harder rock. But it is thought that post-middle Eocene deformation played a part here too. Finally it is suggested that the ancient stream, stream flowed north from Iowa Hill, past Indiana Hill, to Thompson Hill (stas. 18–19–20). The reach between stations 19 and 20 is the

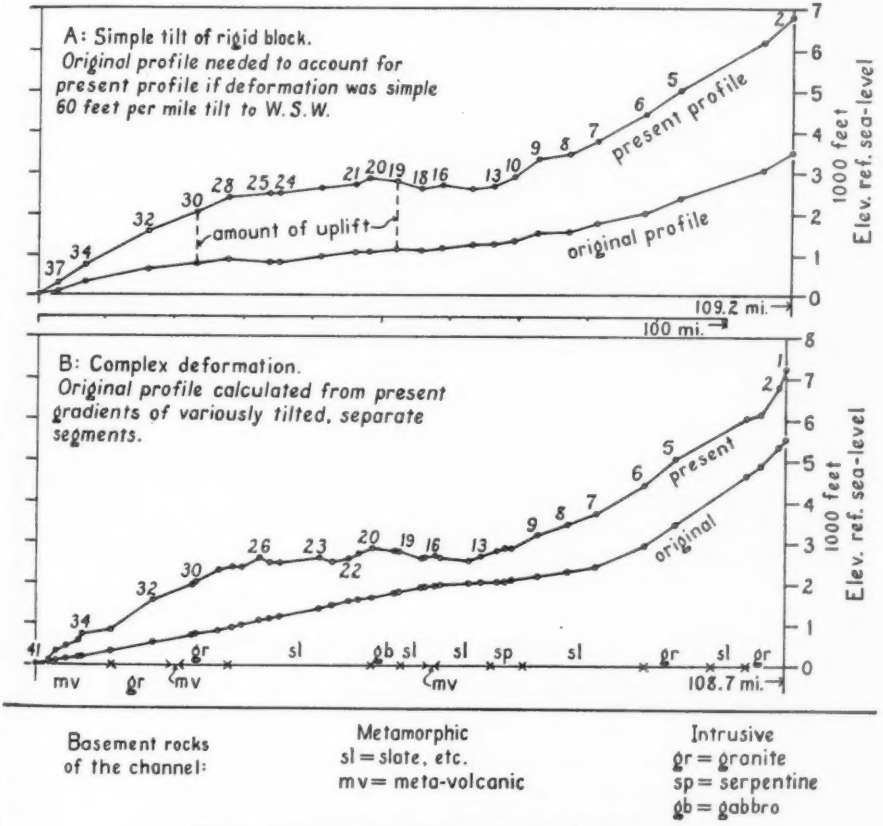
A: Simple tilt of rigid block.
Original profile needed to account for present profile if deformation was simple 60 feet per mile tilt to W.S.W.
present profile
amount of uplift
original profile
1000 feet
Elev. ref. sea-level
109.2 mi.
100 mi.
B: Complex deformation.
Original profile calculated from present gradients of variously tilted, separate segments.
present
original
1000 feet
Elev. ref. sea-level
mv gr mv sl gb sl sl sp sl gr sl gr mv
108.7 mi.
Basement rocks of the channel:
Metamorphic
sl = slate, etc.
mv = meta-volcanic
Intrusive
gr = granite
sp = serpentine
gb = gabbro

FIGURE 2.—PROFILES OF MIDDLE EOCENE YUBA RIVER

in establishing its course from Paragon to Thompson Hill (stas. 10–20), took advantage of a depression formed by faulting and had to fill in some irregularities in the Bedrock to make a through channel.

Despite minor anomalies in gradient, Hobson (1890, p. 418–422) thought that the channel ran from Forest Hill, by way of Morning Star and Iowa Hill (stas. 11–16–18), to a confluence with a south-flowing tributary from Gold Run past Indiana Hill (sta. 19), and thence southwest to the lowlands. Haley (1922, p. 552) followed Lindgren's latest idea that the ancient critical link in Lindgren's representation of the stream, as the gutter of the channel rises from 2792 to 3100 feet elevation in 2¾ miles north-northeast from station 19 and then declines to 2848 feet in 1 mile north-northwest, to station 20. One must consider the alternative that the high point between stations 19 and 20 was a middle Eocene divide, from which one stream flowed north as the ancient Yuba, and another south as a tributary of the ancient American, which drained southwest from Clydesdale (sta. 7) in accordance with Lindgren's first hypothesis.

The best way to solve this problem would be by direct evidence from the deep gravels, such as cross-bedding or shingle-stacking of pebbles. However, the underground mines are inaccessible, and the boulders of the surface workings were shifted, or even lifted out of the channel. Fortunately, pertinent evidence was found at the most critical locality. A mass of bench gravel 2 miles long, 500 feet wide, and 100 feet high, was left unmined at the head of the great Gold Run pit, and covers the high point of the channel, north of station 19. The deep channel passes from the south under this cover, and it appears again on the north side, so continuity is assured. The direction of flow was indicated by cross-bedding in the bench gravels at two localities: on the north side of the unmined mass, directly above the buried channel, a 1½ foot sand layer dips 4°S., but its well-developed cross-bedding shows it was deposited by a north-flowing stream; a quarter mile to the southwest, on the south side of the bench gravel remnant, the beds dip gently southwest but the cross-bedding again shows a northerly flowing stream.

Wherever observable along the channel the contact of bench gravel on deep gravel is conformable. Accordingly, Lindgren's idea of a continuous north-flowing deep channel between stations 19 and 20 is confirmed.

TABLE 2.—PRESENT COURSE OF MIDDLE EOCENE YUBA RIVER

Stations	Elev., feet ref. sea level	diff.	Miles		Grad. Ft/mi.
1. N.W. of Donner Pass	7232				
2. Summit Valley	6800	432	0.98	S 58 W	441
3. Onion Creek	6150	650	2.63	S 14 W	252
4. Soda Spg., 2 mi. W. of	6050	100	2.13	S 4 W	47
5. French Meadows	5050	1000	10.20	S 28 W	98
6. Russian Ravine	4440	610	4.54	S 44 W	134
7. Clydesdale	3750	690	6.97	S 34 W	99
8. Ralstons	3457	293	4.22	N 68 W	69
9. Michigan Bluff	3205	252	4.38	N 62 W	58
10. Paragon	2880	325	3.55	S 87 W	91
11. Under Forest Hill lava cap	2880	nil	1.14	N 20 W	nil
12. Under Forest Hill lava cap	2810	70	.89	S 70 W	79
13. Dardanelles	2670	140	2.58	S 32 W	54
14. Georgia Hill	2563	107	1.74	N 61 W	61
15. Gleeson	2625	u 62	4.12	N 11 E	r15
16. Big Dipper	2692	u 67	.62	N 18 E	r108
17. Iowa Hill, S. of	2640	52	1.46*	W of N	36
18. Iowa Hill, W. of	2631	9	.38	N 40 W	24
19. Indiana Hill	2792	u161	3.38	N 17 E	r48
20. Thompson Hill	2848	u 56	3.83	N 2 E	r15
21. Little York	2706	142	1.77	S 65 W	80
21. Little York	2706				
22. Hawkins Canyon	2595	111	1.38	S 89 W	80
23. Quaker Hill	2620	u 25	4.50	N 12 W	r 6
24. Blue Tent	2483	137	5.75	N 30 W	24
25. Grizzly Hill	2483	nil	1.33	N 25 W	nil
26. N. Bloomfield Jctn.	2626	u143	1.50	N 8 W	r96
27. Paterson	2395	231	2.53	S 86 W	91
28. Badger Hill	2391	4	1.40	N 5 E	3
29. N.W. of 28	2318	73	2.00	N 35 W	36
30. N. of N. San Juan	2033	285	3.25	S 55 W	88
31. W. of N. San Juan	1945	88	.50	S 77 W	176
32. French Corral	1579	366	5.70	S 23 W	64
33. Nigger Bar	862	717	6.00	S 70 W	119
34. Mooney Flat	750	112	4.30	S 13 W	26
35. Smartsville	575	175	.57	S 72 W	305
36. Timbuctoo	450	125	1.74	N 63 W	72
37. Sicard Flat	335	115	1.56	N 80 W	73
38. Under present Yuba River	94	241	1.12	S 70 W	215
39. Under present Yuba River	59	35	.97	S 84 W	36
40. Under present Yuba River	39	20	.71	N 65 W	28
41. Mouth	21	18	.42	S 38 W	43

u = up r = reversed gradient * not straight

Sources of information: 1, 14, 15, 33–41, new observations; 33, interpolated in conformity with existing denuded surface; 2, 5, 8, 10, 16, 18–21, 24, 25, 28, 30, and 32, Lindgren (1911, Pl. X); 10–13, Browne (1890, map); 17, new datum; 26, calculated from data of adjacent stations, and of Lindgren (1911, Pl. XX); from study of geologic maps of U.S.G.S. folios: 3 and 4, Truckee, Lindgren (1897); 6, 7, 9, Colfax, Lindgren (1900); 27, 29, 31, Smartsville, Lindgren and Turner (1895).

Near the mouth of the middle Eocene Yuba the logs of drill holes indicate a transition zone where tongues of gravel extend downstream from the main mass of the oldest auriferous gravels and interfinger with layers of clay which extend upstream from the eastern edge of the Ione freshwater sediments that underly the Great Valley. Elsewhere in the valley the Ione is both underlain and overlain by middle Eocene marine formations, and must have been deposited near sea level. Accordingly, the transition zone marks middle Eocene sea level at the mouth of the ancient Yuba.

Midway in the zone (Fig. 1, sta. 41), the gutter of the channel is 21 feet above present sea level. Presuming that sea level in this region was the same, geodetically, in the middle Eocene as today, this point has suffered 21 feet net uplift since middle Eocene time, and it can serve as a bench mark for measuring the post-

middle Eocene uplift of other points on the channel.

Tertiary and Later Deformation of the Sierra Nevada

General

Whitney (1880, p. 330–331) advanced the idea that the quartz veins of the Sierra Nevada were not formed until the range had been uplifted to nearly its present position, following which the region experienced few, if any, important orographic disturbances. He thought the Tertiary volcanic epoch was not inaugurated until the range had approximately its present form, so that the formation of the quartz veins in the Bedrock, and the covering of the auriferous gravel deposits with eruptive materials were very near each other in geologic time.

Le Conte (1886, p. 173) thought the auriferous gravel river system was obliterated at the end of the Tertiary by an immense flood of lava from fissures in the high Sierra. He believed that the displaced rivers then cut new channels, whose beds are 2000 to 3000 feet below the old ones, and concluded that, as this cutting was more rapid than the formation of the old channels, the height and slope of the range must have greatly increased contemporaneously with the lava flood. A few years later (1889, p. 262) he published his celebrated theory on the structure of the Basin Region. In this it was maintained that, at the end of the Tertiary the entire region from the Wasatch to the Sierra was lifted into a great arch, which *parri passu* collapsed into a series of basins and ranges, leaving the raw surfaces of the abutments (the Sierra and Wasatch scarps) facing one another across the Great Basin.

Aside from the dating of the vulcanism, Le Conte's ideas seem remarkably modern. But Whitney's views persisted as authoritative for some time. Thus Browne, after an unsuccessful attempt to prove tilting of the range from the gradients of the ancient rivers, concluded (1890, p. 444–445) that there had been no appreciable uplift of the range since these streams were active.

Lindgren (1897) and Turner (1897) confirmed Le Conte's idea by recognizing important faulting on the east side of the range crest. They thought most of the fault movement was pre-andesitic. Louderback, however, showed (1924, p. 23) that there was major normal faulting of quite recent (post-basaltic) date, northwest of Lake Tahoe. The latest work in this region has shown that the Tertiary and later deformation involved more than normal faulting with simple westward tilting. Durrell (1950, p. 1522) found that strike slip is far more important than dip slip on the so-called normal fault which marks the east edge of the range from Sierra Valley to a point 40 miles northwest. West of Truckee, along the west side of the zone of normal faults, the range was subjected to recurrent compressional deformations during Tertiary time, prior to the normal faulting (Hudson, 1951). Hall (1953) showed that the Union Valley damsite, 15 miles west of the summit of the range and near the south edge of the Figure 1 map, is on a part of the Sierra in which the tilt was eastward rather than westward, during the Pleistocene orogeny.

Although faulting in Tertiary deposits within the range has been recognized by most authors beginning with Browne (1890, p. 445), it has been generally considered of minor importance. Thus Lindgren (1900, p. 5) said the remarkable absence of faults over the western slope was a great aid to the interpretation of the gold channels. Actually, the channels have been deformed, certainly by faulting and also possibly by folding, and this hinders the interpretation of the channels.

Deformation Calculated from the Gradients of the Channel

Browne (1890, p. 445) in his work on the Forest Hill Divide pointed out that if Le Conte's ideas (1886; 1889) of uplift and increase of slope were correct then with westward tilt on a north-south axis, the effect on a sinuous channel would be: (1) a maintaining of the original grade where the course is north or south; (2) greatly increased grade where the course is west; and (3) little or no grade where the course is east. He considered the direction and gradient of eight exposed patches of channel and drew up a diagram (Fig. 3). He decided against an appreciable increase in the slope of the Sierra flank, and especially against an increase large enough to account *per se* for the

2000 feet deeper cutting of the modern river in the Forest Hill region.

Browne's basic idea is correct, but his data do not apply: (1) Gradients of short segments

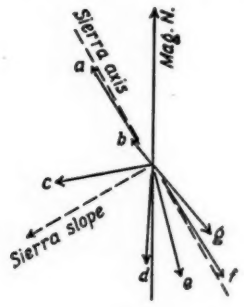

	ft./mi.		ft./mi.
a Pond	74	e Hidden Treasure	74
b Paragon	21	f Mountain Gate	85
c Yankee Jim	63	g Dardanelles	58
d Mayflower and Excelsior	63		

FIGURE 3.—GRADIENTS OF CHANNELS IN FOREST HILL REGION
After Browne

of the channel are misleading, because slope changes abruptly at many points; (2) The diagramed gradients of Mountain Gate and Hidden Treasure are on a tributrary which enters the main stream from the north at Michigan Bluff (Fig. 1, sta. 9), and the Pond locality is on a tributary which enters from the south at Georgia Hill (sta. 14); and (3) A fault separates Mountain Gate, Hidden Treasure, and Paragon, on the east, from the other localities on the west. One of these three defects, alone, might be enough to prevent solution of the problem from these data. Their combination was fatal.

In his earliest paper on the subject Lindgren (1893, p. 296–298) maintained that the profile of the present gradients of the Tertiary Middle Fork of Yuba River is composed of two curves, each convex upward, whereas the profile of the modern Yuba River, a much less mature stream crossing the same terrain, is uniformly concave upward. He attributed this to internal deformation of the range during the uplift of Le Conte's Sierra abutment block. Figure 4 shows that his basic premise of uniform upward concavity is far from true. It was perhaps a realization of this that led him to abandon his notion of internal deformation of the range. Had he held to this theory and gathered the evidence to support it, the present paper would be superfluous.

Lindgren (1900, p. 10), from a consideration of the elevations of the channel at Dutch Flat, Indiana Hill, Iowa Hill, and Yankee Jim (Fig. 1, stas. 14, 17, 18, and 19), concluded that the present gradients of this part of the stream are exactly what would necessarily result from a westward tilting of the Sierra block amounting to about 60 or 70 feet per mile. He later (1911, p. 46–50) gave consideration to the entire stream and concluded that actual tilting to the west-southwest and almost perfect rigidity of the range during this movement were established.

The reaches of Lindgren's profile (Fig. 2A) are straight lines connecting stations of known elevation. These lines cut across minor bends of the channel and pass below and above minor ups and downs of the gutter. It was only by using such generalized data that he succeeded where Browne had failed. Although his method of calculation is unknown, he probably merely applied a series of tilt factors to the reaches of the channel between Iowa Hill and Badger Hill (Fig. 1, stas. 18–28) and found that 60 to 70 gave the best results.

The idea of tilting of a rigid block may be tested mathematically. In Figure 5, AC is a straight reach of channel, affixed at point C to the horizontal, rectangular reference plane $BDFE$. β is the slope angle of reach AC.

When the reference plane, with the affixed reach, is tilted on the axis FE through the tilt angle α, the plane assumes the position $B'D'FE$ and the tilted reach is $A'C$.

A vertical plane through the tilted reach $A'C$ cuts the horizontal reference plane along line CG, and the tilted plane along line CH. $\measuredangle A'CG = \theta$ is the slope angle of the tilted reach.

$\measuredangle BCE = \delta_0$ and $\measuredangle GCE = \delta_1$ are the differences in azimuth between the direction of the axis of tilt and the directions of the pre-tilt and post-tilt reaches. Both are measured in the horizontal reference plane.

$$\theta = \measuredangle A'CH + \measuredangle HCG = \gamma + \epsilon \qquad (1)$$

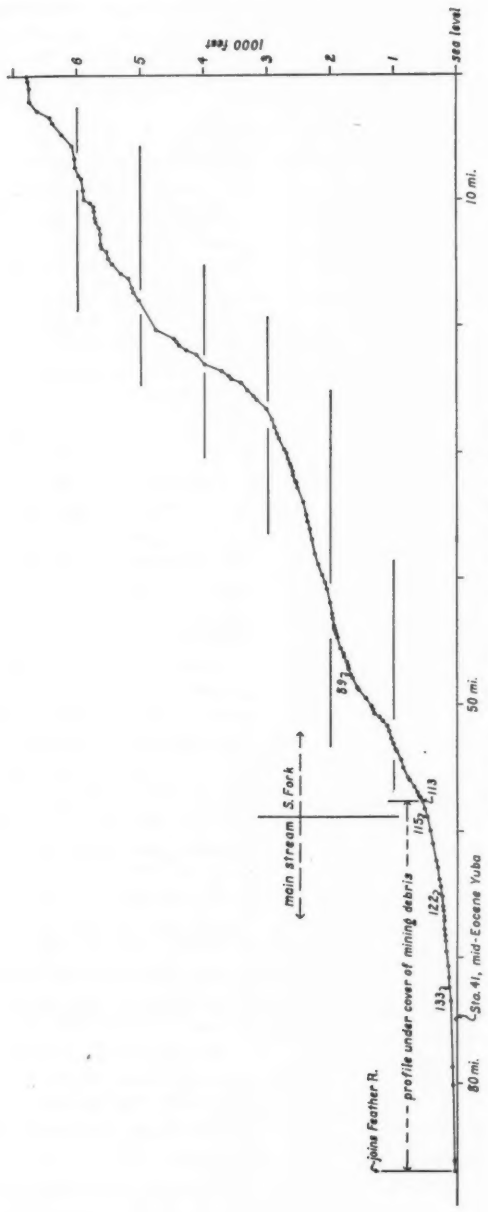

FIGURE 4.—PROFILE OF MODERN YUBA RIVER

$\measuredangle$'s CEG, EGH, and CGH are right angles, so

$$\tan \delta_1 = EG/CE, \tan \alpha = HG/EG,$$

$$HG = CE \cdot \tan \delta_1 \cdot \tan \alpha \quad (2)$$

and

$$\tan \epsilon = HG/CG, \text{ or } HG = CG \cdot \tan \epsilon \quad (3)$$

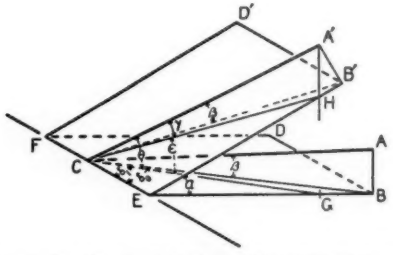

FIGURE 5.—DIAGRAM OF TILTED CHANNEL SEGMENT

Substituting (3) in (2) yields

$$CG \cdot \tan \epsilon = CE \cdot \tan \delta_1 \cdot \tan \alpha, \text{ or}$$

$$\tan \epsilon = \tan \delta_1 \cdot \tan \alpha \cdot CE/CG$$

but

$$CE/CG = \cos \delta_1$$

so

$$\tan \epsilon = \tan \delta_1 \cdot \cos \delta_1 \cdot \tan \alpha = \sin \delta_1 \cdot \tan \alpha$$

and

$$\epsilon = \tan^{-1}(\sin \delta_1 \cdot \tan \alpha) \quad (4)$$

Substituting (4) in (1) gives

$$\theta = \gamma + \tan^{-1}(\sin \delta_1 \cdot \tan \alpha) \quad (5)$$

Even when values far greater than those to be expected in nature are assigned to β and α, γ will differ from β by amounts much smaller than the errors arising from faulty measurement of channel distances and elevations. Accordingly, in (5) β may be substituted for γ, so that

$$\theta - \beta = \tan^{-1}(\sin \delta_1 \cdot \tan \alpha) \quad (6)$$

For the small values of θ and β that pertain to the channel of the ancient Yuba River, the tangent of the difference between the two angles is equal to the difference between the tangents of the two angles, so (6) may be written

$$\tan \theta - \tan \beta = \sin \delta_1 \cdot \tan \alpha \quad (7)$$

It is generally convenient to use gradients expressed in feet per mile instead of tangents of slope angles. The equation is then

$$S_1 - S_0 = T \cdot \sin \delta_1 \quad (8)$$

in which S_1, S_0 and T are respectively the present gradient, the original gradient, and the amount of tilt, expressed in feet per mile.

For each of Lindgren's channel reaches, the present gradient (S_1) and the difference (δ) between the direction of the reach and that of his assumed north-northwest axis of tilt are known. For the amount of tilt (T), the writer has adopted 60 feet per mile, the lower of the range of tilt values suggested by him. To solve for the pre-tilt gradient the formula is then

$$S_0 = S_1 - 60 \cdot \sin \delta$$

The length in miles of a reach, multiplied by the original gradient derived from this formula, gives the pre-tilt difference in elevation between the two stations that mark the ends of the reach. The lower line of Figure 2A shows the pre-tilt elevations of Lindgren's channel, calculated by this method.

In this profile the 23 feet per mile average gradient of the lower reaches is credible, and conforms to Lindgren's idea (1911, p. 41–45) that the original gradients of the middle and lower reaches were from 20 to 30 feet per mile. But between stations 24 and 28, and between stations 18 and 19, the stream runs uphill. Further, two reaches near the mouth seem too steep for that part of the channel. The reach which extends from 3 to 7 miles above the mouth has a gradient of 59 feet per mile, which is exceeded by only two reaches on the entire channel, and these lie 90 miles upstream. Finally a gradient of 2 feet per mile between stations 13 and 14 is improbably low.

Any appreciable increase or decrease of the assumed tilt of 60 feet per mile increases the difficulties. The theory of simple tilting of a rigid block is considered untenable.

Deformation of the Range by Diverse Movements in Separate Segments

Internal deformation seems most probable, and can also be tested mathematically by an elaboration of the single reach equation.

TABLE 3.—SUMMARY OF RESULTS OF GRADIENT CALCULATIONS

Channel segments, marked by stations:	Original gradients: ft./mi.	Amount of tilt: ft./mi.	Bearing of tilt axis:	Miles of channel: Solved by method A	B	C
1-2	212.5	254.7 W.	N. 5.7°W.	.98		
2-3	164.2					2.63
3-4-5-6	115.9	130.4 W.	N.35.9°E.	16.87		
6-7	73.6					6.97
7-8	31.3	80.3 W.	N.39.6°W.		4.22	
8-9-10-11	27.0	80.3 W.	N.39.6°W.	9.07		
11-12	18.3					.89
12-13-14-15	9.7	66.6 W.	N. 10.0°W.	8.44		
15-17	21.9					2.42
17-18-19-19A	34.9	90.4 W.	N.47.0°W.	4.34		
19A-20	35.4					3.25
20-21-22-22A	36.8	44.5 W.	N. 12.4°W.	5.57		
22A-27	36.3					13.23
27-28-29-30	35.7	52.0 W.	N.34.1°W.	6.65		
30-32	33.6					6.20
32-34	31.2					10.30
34-36	29.2					2.31
36-38	28.5					2.68
38-39-40-41	27.8	15.5 S.	N.63.4°W.	2.10		
				54.02	4.22	50.88

A. Triplets solved by formula 54.02 mi.
B. By assuming continuity in rigidity with block of a solved triplet 4.22
C. By interpolating between segments solved by A or B method 50.88
Total - 109.12 mi.

Assume that there are three consecutive reaches of the channel, which originally had the same gradient (S_0), and that these reaches lie on a block which acted as a rigid unit when tilted in the amount T feet per mile. S_0, T, and the direction of the axis of tilting will have values common to the three reaches. But each reach will have its own δ (deviation in azimuth from the direction of the tilt axis), and its own present gradient. So there will be three δ's and three S's, which may be distinguished by the subscripts 1, 2, and 3. By applying the single reach equation to each of the three reaches, a set of three simultaneous equations, from which the unknown S_0 is eliminated, result:

$$\left.\begin{aligned} S_1 - S_0 &= T\cdot\sin\delta_1 \\ S_2 - S_0 &= T\cdot\sin\delta_2 \\ S_3 - S_0 &= T\cdot\sin\delta_3 \end{aligned}\right\} \quad \begin{aligned} S_1 - S_2 &= T(\sin\delta_1 - \sin\delta_2) \quad \text{(a)} \\ S_1 - S_3 &= T(\sin\delta_1 - \sin\delta_3) \quad \text{(b)} \end{aligned}$$

By dividing (a) by (b), T is eliminated, giving:

$$\frac{S_1 - S_2}{S_1 - S_3} = \frac{\sin \delta_1 - \sin \delta_2}{\sin \delta_1 - \sin \delta_3} \qquad (c)$$

This equation may be solved. All of the S's are known and, although the values of the δ's

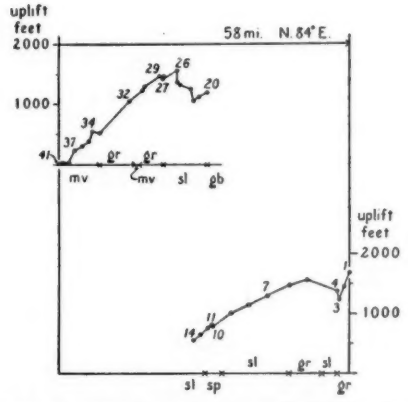

FIGURE 6.—AMOUNTS OF UPLIFT, PROJECTED ONTO VERTICAL SECTION CONNECTING HEAD AND MOUTH OF MIDDLE EOCENE YUBA RIVER
See Figure 2 for definition of symbols

are unknown, the value of each δ in terms of each other δ is known. So, only one or the other of the δ's is unknown. Having determined the δ's, a pair of them is introduced into equation (a) or (b) to solve for T, and that quantity, with the appropriate δ, is used in one of the single-reach equations to find the value of S_0.

In applying these formulae a triplet of reaches was selected, and, if no solution resulted, a reach was dropped from one end and one added at the other end to form a new triplet of consecutive reaches. Eight triplets having an aggregate length of 54.0 miles yielded solutions (Table 3). No quadruplets were solved, but a credible original gradient was determined for a reach of 4.2 miles length by assuming its continuity in rigidity with the block of an adjacent solved triplet. The original gradients of the 18 reaches that make up the remaining 50.9 miles of the 109.1 channel were determined by interpolation between the values found by the formulae for adjacent segments.

The calculations are presented in Appendix A. Their results, which are summarized in Tables 3 and 4, are the basis for the pre-deformational profile of the channel shown by the lower line of Figure 2B. As with the graph to illustrate Lindgren's solution, this profile is based on the assumption of geodetic equality between middle Eocene and present sea levels.

This profile is plausible. The lower reaches have an average gradient of about 30 feet per mile, which is the upper limit of Lindgren's idea of the range of slopes in this part of the stream. The upper reaches have steadily increasing gradients from station 10 to the headwaters. The middle reaches (stas. 11–29) form a huge upward convexity, much like that on the middle reaches of the modern South Fork of the Yuba River. (*See* Fig. 4.) The low gradients at the eastern end of the convexity of the ancient stream are believed to be due to the combined effect of the entrance of many tributaries, and the existence of grabens which were first formed in pre-middle Eocene time.

More important conclusions are to be drawn from a consideration of the amounts of uplift. These may be read from Figure 2B, by measuring the intercepts between the upper and lower graphs, but for easier study they are shown in larger scale on Figure 6. This shows the post-middle Eocene uplift from stations 1–14, and 20–41, projected onto a vertical section along the N.84°E. line which connects the mouth and head of the ancient stream. Stations 15–25 are omitted because their part of the channel trends about 90° from the line of the section. The amounts of uplift were used in connection with the calculated directions of tilt to construct the isobases of Figure 7, which also shows the known and inferred faults of the region.

By referring to Figure 6 for a general view and to Table 4 for precise data, one may see that the uplift at station 1 is 1684 feet and that, in passing downstream only 3½ miles to station 3, it decreases to 1242 feet. A secondary maximum occurs at station 5 and a local minimum of 786 feet at station 10. The slight rise between stations 10 and 11 is followed by a decline to station 14 at a rate much greater than the graph slope between stations 5 and 10.

The points of abrupt change of slope are at places where the channel has been affected by faulting. A fault cuts the channel just west

TABLE 4.—SUMMARY OF CALCULATIONS OF POST-MIDDLE EOCENE UPLIFT

Sta.	Distance: miles	Pre-tilt Gradients: ft./mi.	Pre-tilt Diff. elev.: feet	Elevations ref. sea level of mid-Eocene: feet	Elevations ref. present sea level: feet	Uplift: feet
41				nil	21	21
	2.10	27.8	58			
38				58	94	36
	2.68	28.5	76			
36				134	450	316
	2.31	29.2	67			
34				201	750	549
	10.30	31.2	321			
32				522	1579	1057
	6.20	33.6	208			
30				730	2033	1303
	6.65	35.7	237			
27				967	2395	1428
	13.23	36.3	480			
22A				1447	2520	1073
	5.57	36.8	205			
20				1652	2848	1196
	3.25	35.8	116			
19A				1768	2800	1032
	4.34	34.9	151			
17				1919	2640	721
	2.08	22.3	46			
15				1965	2625	660
	8.44	9.7	82			
12				2047	2810	763
	0.89	18.3	16			
11				2063	2880	817
	9.07	27.0	245			
8				2308	3457	1149
	4.22	31.3	132			
7				2440	3750	1310
	6.97	73.6	513			
6				2953	4440	1487
	16.87	115.9	1955			
3				4908	6150	1242
	2.63	164.2	432			
2				5340	6800	1460
	0.98	212.5	208			
1				5548	7232	1684
	108.78		5548			
2				5340	6800	1460
	3.03	212.5	644			
Z				5984	7400	1416

of station 11 (Fig. 7). Above station 3 the stream approaches two faults, which cut the channel between stations 3 and 2. Uplift increases rapidly beyond this point as the channel nears the main reverse fault of the Donner Summit region (Fig. 8).

Between stations 14 and 20 (*See* Table 4 and Fig. 7) the amount of uplift increases rather regularly from 558 feet to a local maximum of 1196 feet, perhaps effected by an important fault immediately east of the station 19–20 reach. Proceeding northwesterly, the increase

continues, but at a lesser rate, to station 26, where the uplift of 1567 feet is but little less than at the head of the stream.

Locke (1912, p. 85) showed that, where the Mother Lode is crossed by the Table Mountain lava flow between Jamestown and Rawhide,

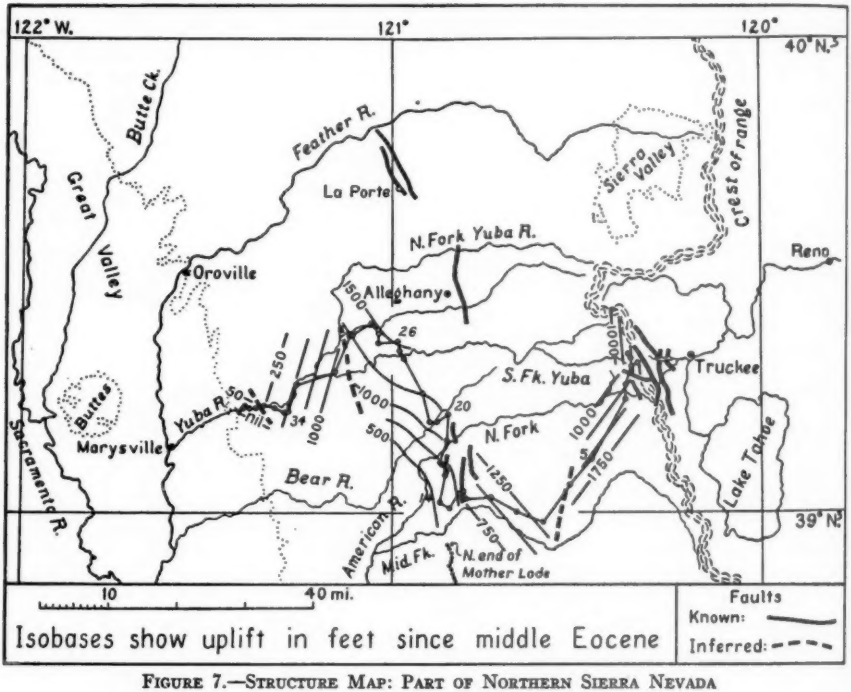

FIGURE 7.—STRUCTURE MAP: PART OF NORTHERN SIERRA NEVADA

At station 26 the channel makes its closest approach to the Alleghany fault. This was described by Ferguson and Gannett (1932, p. 21) as a major, N.20°W.-trending reverse fault, which dips 80°–90°E. They mentioned no evidence of Tertiary or later movement on this fault nor anywhere else in the Alleghany area. However, there have been relatively recent movements on the Mother Lode fault, the northern known end of which is near the south edge of the Figure 7 map. This fault is similar in trend and dip to the Alleghany fault, and the early major movements on the two were directionally the same, namely uplift of their eastern hanging-wall sides. Ransome concluded (1900, p. 8) that there had been repeated thrust movements on faults subsidiary to the main Mother Lode reverse fault, and probably subordinate reversal movements, *i.e.* normal faulting, on the same faults. He believed that the latter movements are still going on.

post-volcanic faulting has depressed the eastern block about 50 feet with respect to the western. Recent study of this locality indicates that, although the main movement occurred on the west side of a thick quartz vein which represents the Mother Lode here, at least eight minor faults affect a zone a half mile wide on the west side of the major fault. Study of air-photos suggests that there was right lateral-slip movement on the main fault amounting to about 150 feet. The lava involved in this faulting is the youngest member of the Tertiary sequence in this part of the range. With these facts in mind it is suggested that the noteworthy uplift in the vicinity of station 26 is due to movements on the Alleghany fault or some one or more nearly related fractures.

The upper graph of Figure 6 shows that decrease in the amount of uplift is fairly uniform between stations 27 and 37, and more rapid approaching station 38. From the pre-tilt

gradients, determined by interpolation between stations 30 and 38, it was calculated that the bearings of the axes of tilting for the segments 32–34, 30–32, and 34–37 are respectively: N.16°E., N.13°E., and N.56°W. As the course 32–34 makes up over one half of the section under consideration, the N.16°E. axial direction is used for the entire stretch from station 37 to a point between stations 32 and 31 in constructing the isobases of Figure 7. The abrupt decrease in uplift between stations 37 and 38, together with the nearly 90° difference in direction of tilt axes between segments 32–34 and 38–41, suggests faulting between the two segments. As no substantiating field evidence is known, an inferred fault is shown here on Figure 7. The abrupt change in direction of tilt axis between the segments 27–30 and 32–34 also suggests faulting. This fault on Figure 7 was placed at the contact between granite on the east and metamorphosed volcanics on the west, one mile west of North San Juan. (*See* Lindgren and Turner, 1895, map.) No attempt was made to confirm this in the field.

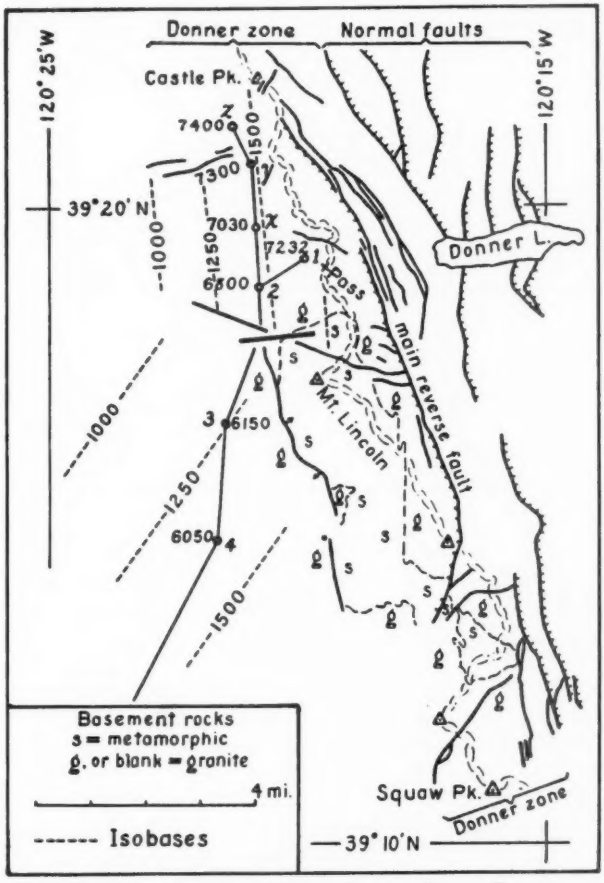

FIGURE 8.—STRUCTURE MAP OF DONNER SUMMIT REGION

That the mathematical method employed is appropriate to the problem and its results credible, has been shown by (1) the plausible character of the pre-deformational profile produced by it, (2) the solving for original gradient of more than one-half of the length of the ancient channel, and (3) the relation between loci of

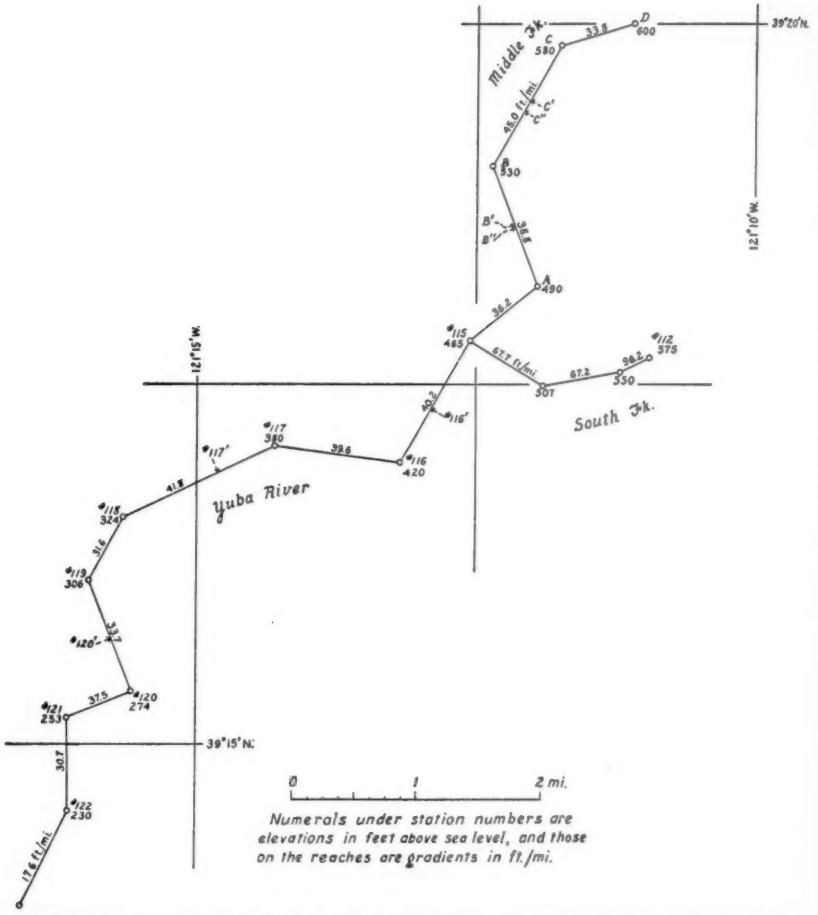

FIGURE 9.—PLAT OF PART OF MODERN YUBA RIVER, WHERE GRADIENTS AVERAGE 37.2 FEET PER MILE

deformation determined by the calculations and known faults.

Criticism of the Mathematical Method

By assuming the equality of the original gradients of the three reaches of a triplet, a set of three simultaneous equations, containing three unknowns, was produced. These can always be solved, but often produce absurd results, such as negative gradients, or absurdly high gradients or amounts of tilt, which had to be discarded. The remainder were regarded as proper solutions. This method does not yield the actual original gradient of a triplet of reaches, but *what the original gradient would have been if the three reaches had a common gradient and lay on a block that remained rigid during tilting.*

In order to learn the probable effect of lack of equality of the original gradients of the members of the solved triplets, one must first decide upon the probable amounts of variance from equality. This was done by studying the parts of the modern Yuba River where the gradients approximate those found for the eight usable triplets of the ancient stream. The calculated original gradients of five of these

range from 27.0 to 36.8 feet per mile and their average is 32.3 feet per mile. A close analogue on the modern stream is the 9.75 mile stretch of the main Yuba from station 122 through station 115 to station D (Fig. 9), as it existed

The calculations for the triplet 27-28-29-30 are given to illustrate the determination of variance factors. This triplet includes about 6 miles of the channel and the lengths of its reaches are in the approximate ratio 1:2:3.

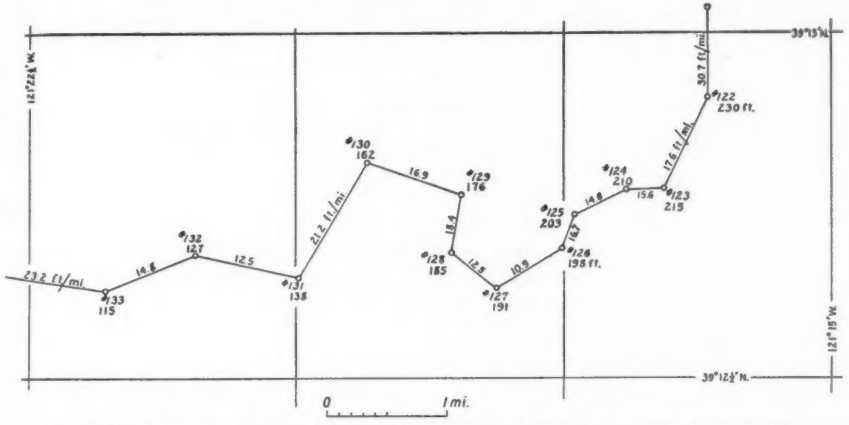

FIGURE 10.—PLAT OF PART OF MODERN YUBA RIVER, WHERE GRADIENTS AVERAGE 15.6 FEET PER MILE
See Figure 9 for explanation

before burial under hydraulic mining debris. The eleven reaches of this stretch have gradients ranging from 30.7 to 45.0 feet per mile and averaging 37.2 feet per mile.

A segment 10 miles long between stations 89 and 113 on the modern stream has gradients which are near the 115.9-feet-per-mile value determined for the triplet 3-4-5-6, that is from 41.7 to 250.0, and averaging 114.7 feet per mile. But the data of this stretch have no critical value, so the plat of its reaches is withheld.

The triplet 12-13-14-15, with calculated original gradient of 9.7 feet per mile, has no analogue on the modern stream. It is most nearly matched by the span of 7.2 miles between stations 122 and 133 (Fig. 10), in which the gradients average 15.6 feet per mile. Accordingly, the data of this span are used as the base for criticism of the triplet calculations.

The original gradient of the course between stations 1 and 2 of the ancient stream was determined by solving a triplet formed by combining 1–2 with two reaches of a tributary. The modern Yuba furnishes no suitable comparative data.

Sets of three consecutive reaches, measuring approximately 1, 2 and 3 miles each, were made by stepping from station to station along the modern channel, between stations 122 and D (Fig. 9). In order to simulate the data of the ancient channel, these steps by-passed stations where necessary to produce a reach of the required length. The three reaches may be arranged in six ways: 1:2:3, 1:3:2, 2:1:3, 2:3:1, 3:2:1, and 3:1:2. A set of triplets was produced for each such arrangement.

Each arrangement of reaches yielded from three to six triplets (Appendix B). After the average of the gradients of the three members of a triplet was found, the variances of its high and low gradients from that average gradient were calculated, first in feet per mile, and then as percentages of the average gradient. The average of these two percentages is taken to be the variance from average gradient in the triplet. For the reach arrangement 3:2:1, the variances from average gradient of its three triplets are 10.7, 13.7, and 13.8 per cent. The average of these three values, 12.7 per cent, is the average variance from average gradient

for this reach arrangement, and 10.7 per cent and 13.8 per cent are the extreme variances.

The average variance from average gradient and the two extreme values of each reach arrangement were summarized, and the average of each of the three categories determined.

Table 5.—Variances from Average Gradients
Feet per mile

Triplets:	3-6	8-11	12-15	17-19A	20-22A	27-30	38-41
Variances:							
Most likely	21.4	2.9	1.7	6.3	3.2	3.1	3.2
Less probable	>29.0	>3.8	>2.3	>8.0	>4.3	>4.2	>4.8
	<15.6	<1.8	<1.2	<4.5	<2.1	<2.0	<1.3
Improbable	>46.3	>5.1	>3.0	>8.4	>5.1	>4.9	>5.2
	<8.8	<1.0	<0.6	<4.3	<0.8	<0.7	<0.8

The average of the average variances from average gradient, 8.6 per cent, is considered the "most likely" variance for the aggregate of the six cases of reach arrangement. The averages of the two extreme variance columns, 5.7 per cent and 11.8 per cent, are regarded as the lower and upper limits of probability. Finally, the extreme individual values, 2.1 per cent and 15.1 per cent are taken to represent the lower and upper limits of possibility.

For the next step the variance factors must be converted to feet per mile. This procedure is illustrated in Appendix B for the triplets 17–19A, 20–22A and 27–30. Using the latter as an example, the "most likely" variance of 8.6 per cent becomes 3.1 feet per mile when applied to the 35.7-feet-per-mile calculated value of original gradient; the 11.8 per cent variance, representing the upper limit of probability, becomes "less probably, greater than 4.2 feet per mile"; and so on. (*See* Table 5.)

The next step is to learn the effect of the variances on the original calculations of pre-tilt gradients. Continuing with triplet 27–30 as an example, the present gradients of its three reaches are $S_a = 2.9$, $S_b = 36.5$, and $S_c = 87.7$ feet per mile. (*See* Appendix A.) Here, as in the succeeding calculations, a, b, and c refer, respectively, to the upstream, middle, and downstream reaches. The calculated pre-tilt gradient, S_0, is 35.7 feet per mile. Selecting 4.9 as the variance for the example, assume that the middle reach actually had the pre-tilt gradient 35.7, whereas the original slopes of the upstream and downstream reaches were 4.9 less and 4.9 more than that amount. The original gradients were thus:

$$S_{0_a} = 30.8 \qquad S_{0_b} = 35.7 \qquad S_{0_c} = 40.6$$

Now assume that a triplet with these gradients, but with unchanged reach bearings, was tilted on the same axis and in the same amount as those determined in the original calculation, namely axial bearing N.34.1°W. and tilt 52.0 feet per mile west. From equation (8) the post-tilt gradients would be:

$$S'_a = S_{0_a} - T \cdot \sin \delta_a = 30.8 - (52.0)(.631) = 30.8 - 32.8 = -2.0$$

$$S'_b = S_{0_b} + T \cdot \sin \delta_b = 35.7 + (52.0)(.016) = 35.7 + .08 = 36.5$$

$$S'_c = S_{0_c} + T \cdot \sin \delta_c = 40.6 + (52.0)(1.000) = 40.6 + 52.0 = 92.6$$

Assuming that these values are the present gradients of the reaches and introducing them and the appropriate δ's into equation (c), the result is $S'_0 = 33.8$ feet per mile, or 5.3 per cent less than the average of the three unequal gradients. This shows that, if the original gradients varied from equality in the assumed manner, the assumption of a common pre-tilt gradient leads to a calculated value of S_0 which is 5.3 per cent less than the average of the true, unequal values. This error may be corrected by multiplying the S'_0 result by the factor

$$1/(100.0 - 5.3) = 1/94.7 = 105.6\%$$

There are six possible ways of arranging the three unequal reaches. Calculations were made for each arrangement, first with the extreme variance of 4.9 feet per mile, and then with

TABLE 6.—CORRECTION FACTORS

Triplets:	8-11		12-15		17-19A	
Variances, ft./mi.	5.1	2.9	2.3	1.7	8.0	6.3
Factors:						
Extreme	43.0%	55.4%	84.3%	90.6%	26.7%	31.4%
Extreme	121.0	450.0	134.8	124.3	125.5	119.9
Average	61.7	98.6	105.0	105.0	43.2	48.6

Triplets:	20-22A		27-30		38-41	
Variances, ft./mi.	5.1	3.2	4.9	3.1	4.8	3.2
Factors:						
Extreme	63.1%	73.6%	78.1%	85.0%	88.0%	96.6%
Extreme	118.7	104.3	143.2	120.2	118.7	111.5
Average	79.7	84.9	100.1	99.4	101.0	103.6

the "most likely" variance of 3.1 feet per mile. Following is a summary of the results.

Arrangement of reaches:		Relation of calculated S_0 to average of true S_0's: variance 4.9 ft./mi. (per cent)	variance 3.1 ft./mi. (per cent)
c > b > a		94.7	96.9
b > c > a		69.8	83.2
c > a > b		122.4	114.2
b > a > c		78.4	88.0
a > b > c		105.9	103.7
a > c > b		128.0	117.6
	average	99.9	100.6
Correction factors by which S_0 from original calculation is to be multiplied.	extreme	143.2	120.2
	extreme	78.1	85.0
	average	100.1	99.4

Similar calculations gave seemingly useful correction factors for five of the other solved triplets. These with the results for triplet 27–30 are summarized in Table 6. The two remaining triplets require special consideration.

TRIPLET 3-4-5-6: Of the six possible arrangements of reaches, only two could be solved when the lower of the calculated variances were used and only one yielded a solution with higher variances. These results are as follows.

Arrangement of reaches:	Correction factors: variance 46.3 ft./mi. (per cent)	variance 29.0 ft./mi. (per cent)	variance 21.4 ft./mi. (per cent)
c > b > a	43.8	55.0	62.4
a > b > c		460.6	241.5

The two additive correction factors were rejected as absurdly large. The three subtractive factors were derived from triplets, the reaches of which, in profile, form an upward convexity. This arrangement is not unusual for the short, natural reaches of the stretch of the modern Yuba between stations 89 and 113 that was chosen as the basis for criticizing the calculations for triplet 3–6. It exists there in six of the total 22 triplets. But the proper comparison is with the long, artificial reaches which were produced from the data of the modern stream by by-passing stations, so as to simulate the 2, 4.5, and 10 mile lengths of the members of triplet 3–6. Of the 27 triplets so produced, only one had the reach arrangement in question, and it was a marginal case, the relation of a:b:c being (110.5):(130.0):(131.0), which suggests that the subtractive correction factors also are not useful.

The idea is confirmed by geologic evidence. From the data of Lindgren's map of the Truckee quadrangle (1897), three structure sections were made across the channel between stations 4 and 5. Each passed through a pair of points, one on either side of the channel, where andesitic deposits overlap the contact of rhyolite tuff on Bedrock. In the region north of station 3 the interval between the rhyolite and andesite was one of strong erosion, subsequent to activity on the main reverse fault of the Donner, zone and on the

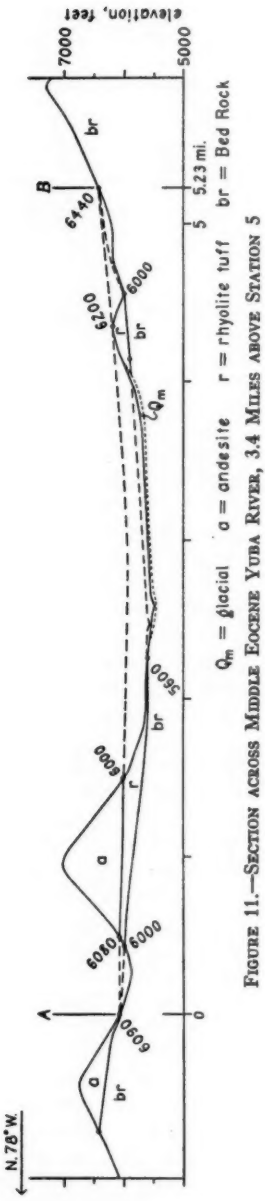

FIGURE 11.—SECTION ACROSS MIDDLE EOCENE YUBA RIVER, 3.4 MILES ABOVE STATION 5

oblique fault which passes between stations 2 and 3. There was also tilting, but its importance decreased southward and appears nil in the area one to two miles north of station 3. (Hudson, 1951, section C-C′, Pl. 1.) In the region between stations 4 and 5 the erosion in this interval decreased southward to an undetectable amount along A-B, the southern of the three structure sections (Fig. 11). This, and the bilateral symmetry of the rhyolite mass in all three sections, indicate there was little, if any, tilting during the andesite/rhyolite interval in the area south of station 4. Thus, there is sound basis for the assumption that the pairs of points of overlap of andesite on rhyolite in the three sections are indices of post-rhyolite tilting. The measure of the latter is the same as that of post-middle Eocene tilting, as it was the deposition of the rhyolite that stopped the activity of the Eocene stream. Following are the data of the sections.

Section:	Location of channel crossing:	Direction of section:	Amount of tilt along line of section:
A–B	3.4 mi. above sta. 5	N. 78°W.	350/5.23 = 67.0 ft./mi.
C–D	2.5 mi. below sta. 4	N. 32°W.	160/1.74 = 92.0
E–F	0.4 mi. below sta. 4	N. 67°W.	160/1.75 = 91.5

These values are the projections of the true tilts on the planes of the sections. If the assumptions were sound and the data perfect, the true amount and direction of tilting could be found by solving simultaneous equations. But only approximation is possible, which gives: T = 95 ft./mi. in the direction N.50°W., that is to say, on a N.40°E. axis. When these factors and the present gradients of the three reaches are introduced into equation (8), the results obtained are:

Reach:		Original gradient:
a		102.8 ft./mi.
b		117.7
c		127.7
	average	116.0 ft./mi.

The basic calculations indicated a pre-tilt gradient of 115.9 feet per mile, a chance but significant similarity with that derived from the structure sections.

TRIPLET 1-2-y-z: As this is formed from the

forking headwaters, to which the modern stream provides no analogue, it is not subject to the mathematical scheme of criticism. However, the results of the calculation of original feet per mile, and that of the base of the welded tuff is 106 feet per mile. Along this line there can be little or no unconformity between the two tuffs, as the thickness of the welded tuff

TABLE 7.—MODIFICATION OF RESULTS OF ORIGINAL CALCULATIONS

		Original calculation		Modification by factors derived from "most likely" variances								
				Extreme			Extreme			Average		
Sta.	miles	gradient ft/mi.	diff. elev.	factors %	gradient ft/mi.	diff. elev.	factors %	gradient ft/mi.	diff. elev.	factors %	gradient ft/mi.	diff. elev.
41	2.10	27.8	58	111.5	31.0	65	96.6	26.9	56	103.6	28.8	60
38	2.68	28.5	76	–	31.7	85	–	27.1	73	–	29.2	78
36	2.31	29.2	67	–	33.1	76	–	27.5	64	–	30.0	69
34	10.30	31.2	321	–	36.6	377	–	28.5	293	–	31.9	329
32	6.20	33.6	208	–	41.2	255	–	29.8	185	–	34.5	214
30	6.65	35.7	237	120.2	42.9	285	85.0	30.3	202	99.4	35.5	235
27	13.23	36.3	480	–	40.6	535	–	28.7	379	–	33.4	441
22A	5.57	36.8	205	104.3	38.4	214	73.6	27.1	151	84.9	31.3	174
20	3.25	35.8	116	–	40.1	130	–	19.0	62	–	19.1	62
19A	4.34	34.9	152	119.9	41.8	181	31.4	11.0	47	48.6	17.0	74
17	2.08	22.3	46	–	26.9	56	–	9.9	21	–	13.6	28
15	8.44	9.7	82	124.3	12.1	102	90.6	8.8	74	105.2	10.2	86
12	.89	18.3	16	–	66.8	59	–	11.9	11	–	18.4	16
11	9.07	27.0	245	450.0	121.5	1102	55.4	15.0	136	98.6	26.6	242
8	4.22	31.3	132	450.0	141.0	595	55.4	17.3	73	98.6	30.9	130
7	6.97	73.6	513	–	128.4	895	–	66.6	467	–	73.4	512
6	16.87	115.9	1955	–	115.9	1955	–	115.9	1955	–	115.9	1955
3	2.63	164.2	432	–	164.2	432	–	164.2	432	–	164.2	432
2	.98	212.5	208	–	212.5	208	–	212.5	208	–	212.5	208
1												
Sta. 1, mid-Eocene elev.			5549 ft.			7607 ft.			4859 ft.			5345 ft.
present elev.			7232			7232			7232			7232
change since mid-Eocene:		Uplift	1683 ft.		Depression	375 ft.		Uplift	2343 ft.		Uplift	1887 ft.

gradient of the reaches of this triplet may be evaluated by geologic evidence.

From station 1 westward the ancient channel is overlain by rhyolite tuff, which increases in thickness from 38 to 250 feet in three quarters of a mile (Hudson, 1951, Pl. 1), owing to overlap to the east of older layers by younger deposits. The top of the rhyolite tuff sequence is a sheet of welded tuff. This is overlain conformably by thinly bedded, even-grained andesite tuff, apparently deposited in water. The contact of the andesitic on the rhyolitic deposits must have been originally horizontal. The reach between stations 1 and 2 runs S.58°W. with a present gradient of 441 feet per mile. The component of dip of the rhyolite-andesite contact, in the same direction, is 121 decreases by only 6 feet, from 36 to 30 feet, in a half a mile southwest from station 1. So the tilt of the base of the andesite tuff is an index of the post-middle Eocene tilt of the area and, from this geologic evidence, the original gradient of the reach 1-2 was

$$441 - 121 = 320 \text{ feet per mile.}$$

This is 108 feet per mile greater than the value of 212 feet per mile determined by the original gradient calculations. If this larger value were adopted, the calculated uplift of the range at station 1 would be reduced by about 100 feet. This would be a moderate correction, but in the direction most likely to provoke adverse criticism. Accordingly, the

geologic evidence is offered only to confirm the original result of 212 feet per mile.

Modification of the Results of the Uplift Calculations

The variance factors are probably larger than those which actually pertained to the ancient stream, as it was more mature and, presumably, more evenly graded than the modern Yuba River. Accordingly, only modification by the factors based on the "most likely" variances will be considered. From these results (Table 7), the most likely modified value for the uplift at station 1 is 1887 feet, and a value of more than 2343 feet is improbable. The other extreme modification, leading to a depression of 375 feet, is geologically absurd, as it calls for the incredibly high gradients of 121.5–141.0 feet per mile between stations 6 and 11 where thick gravel masses accumulated. This depression value is, however, as sound arithmetically as the 2343 feet uplift value and emphasizes the probability of the 1887 feet result.

The illustrations showing amounts of uplift (Figs. 3, 6, 7, 8) are based on the unmodified results of the basic calculations. As shown in the following tabulation, the corrections do not change the form of uplift in any part of the channel, or greatly affect its amount except in the upper reaches.

Stations	Uplift, feet:							
	38	26	20	14	10	5	3	1
Basic results	36	1567	1196	558	786	1571	1242	1684
Modifications:								
Most likely	34	1556	1248	757	984	1774	1445	1887
Extreme additive	38	1680	1445	994	1245	2230	1901	2343

Internal Deformation of the Range

Folding

In the Mount Lincoln-Castle Peak area, at the headwaters of the middle Eocene Yuba, rocks of the Superjacent Series have been folded where they rest on foliated members of the bedrock and also where they overlie massive Bedrock but are separated from it by a basal "mattress" of faulted Superjacent rock. The forking headwater reaches (stas. 2-1 and 2-z) lie on a structural block in which the youngest Superjacent formation, basalt, has been folded, whereas the underlying andesite and rhyolite, which separate the basalt from the granitic Bedrock, have been tilted and faulted, but not folded. A short distance to the south, in the vicinity of Mount Lincoln, the Bedrock is steeply inclined schist, and the entire Superjacent Series is gently folded (Hudson, 1951, p. 948).

Nearly two thirds of the channel is on foliated metamorphic rock (Fig. 2). About one third of the remainder is on serpentine and gabbro, which are severely fractured and in part schistose. With the Mount Lincoln example in mind, folding of the Superjacent Series on the western slope of the range also can be assumed.

Folding seems most probable for the block which extends north from Dardanelles toward Alleghany (sta. 13 past sta. 26), as it contains no granite, being composed of metamorphosed sediments, with minor amounts of serpentine, gabbro, and metamorphosed volcanics. For this reason, and also because it is the simplest construction from the evidence now at hand, the isobases of this block are shown on Figure 7 as curves. Their representation by straight lines elsewhere in the range was, again, to have simplicity of construction, and without implication that folding is precluded.

Inferred Faults

The abrupt change in direction and amount of tilt between triplets 3-4-5-6 and 8-9-10-11 is shown on Figure 7 as taking place on a north-northeast-trending fault, assumed to mark the contact between granite on the east and metamorphic rock on the west, which is crossed by the channel immediately west of station 6. Folding can be substituted for this faulting by constructing the isobases in the form of a broad anticlinal nose with its axis striking slightly north of west and passing with westerly plunge through station 6. Indeed, metamorphic rock here does wrap around a westward bulge of the granite in much the same form as the isobasic lines.

To explain the change in tilt between triplet

27–30 and channel segment 32–34, the north-northwest-trending contact between granite and metamorphosed volcanics, which is crossed by the channel west of station 31, is considered a fault. This contact is rather straight over a distance of several miles so, although the swing in tilt direction could be explained by folding, faulting seems more likely.

The fault considered necessary to explain the great difference in tilt between channel segments 38-41 and 34-37, as well as the rapid decrease in amount of uplift between stations 37 and 38, is shown with N.30°W. strike to accord with the local strike of the Bedrock. An east-west trend may be more appropriate, as that is the strike of the veins in the Brown's Valley mining district (a few miles northwest of station 38), and also of minor faults which cut the ancient gravels at Smartsville, near station 35.

Known Faults

The representation of the Alleghany fault on Figure 7 is from Ferguson and Gannett (1932, Pl. 3). The faults extending northwest from LaPorte were determined by study of the contact of the Superjacent Series on Bed Rock shown on Turner's (1897) map of the Downieville quadrangle.

Many of the other known faults on the western slope of the range were found from the gradient calculations. Abrupt changes in tilt between adjacent segments of the channel, and failure to form solvable triplets from certain reaches, indicated deformation in the Summit region and in the zone from Forest Hill to Dutch Flat, near the middle of the western slope, and field work has confirmed this.

The principal faults on the west slope of the range in the vicinity of Donner Summit (Fig. 8) were significant in the deformation of the channel. The middle and western members of the fault zone, which extends N.70°W. from the main reverse fault on the north side of Mount Lincoln, cut the channel 0.75 and 0.9 mile, respectively, south of station 2. The north-northwest-trending fault, west of the mountain, terminates against the middle member of the fault zone. The combined effect of these faults is 230 feet relative downthrow of the channel on the south side of the middle member of the zone.

Ten faults have been identified in a zone 2–5 miles wide, which extends north 12 miles from between Forest Hill (sta. 13) and the Paragon Mine (sta. 10) to the east side of the Gold Run pit, a short distance south of Dutch Flat (sta. 20). On Figure 7 these are shown, in generalized form, by four lines.

The easternmost line represents a single fault, with varying direction of dip, which marks the western edge of the principal serpentine mass of the Forest Hill district. A small body of pre-volcanic gravel was observed in downthrown position on the west side of the fault. The amount of movement could not be determined. There has been no post-andesitic activity.

The southern part of the next fault line to the west on Figure 7 is the trace of a fault exposed on the Mosquito Ridge road, 0.9 mile S.25°W. of the Paragon pit (sta. 10). Here it strikes N.20°W., dips 83°E., and forms the contact between gabbro on the west and serpentine on the east. It is marked by a 1-foot zone of talcose gouge and, for 50 feet to the east, the serpentine is crushed and stained by limonite. A half mile to the north this fault cuts a contact of andesite on serpentine Bedrock. Here its trend is due north and its effect on the andesite has been 120 feet downthrow to the west. It is presumed to continue northward, crossing the channel between stations 11 and 12, as a fault of this character is needed there to account for the difference in tilt between channel segments 8–11 and 12–15. North of the channel crossing the fault is presumed to continue 4½ miles, through the sites of three gold quartz veins in the Bedrock. According to Lindgren (1900, p. 8) these veins strike N.W. and dip steeply N.E. As the general strike of the country rock here is N.-S., the fractures filled by the veins are believed complementary to a north-south-trending master fault. This role is most readily filled by prolonging the fault from the channel crossing.

Two other important faults are exposed on the road one quarter and three quarters of a mile southwesterly from the first locality. The former is a vertical, N.48°W.-striking fault in

serpentine, which has caused a downthrow of 150 feet to the southwest on the base of the andesite where it cuts that contact a short distance northwest of the road. The latter, where serpentine on the east comes against schist on the west, strikes N.5°E. and dips 88°E. A zone of severe brecciation with limonitic and quartzose mineralization extends 10 feet on either side of the main fracture, and eight subsidiary faults are situated from 90 to 260 feet east of it. The last movement on this fault was pre-andesitic.

These faults east of Forest Hill illustrate how pre-Cretaceous mineralized zones, buried under Tertiary formations, might be found through study of the deformation of the younger rocks.

The principal fault recognized in the Dutch Flat area is east of, and approximately parallel with, the 19–20 reach of the channel. Its trend is slightly west of north, and its dip is steep and of varying direction. At the east edge of the Gold Run pit, 2 miles north of station 19, the contact of bench gravel on Bed Rock is downthrown 100 feet to the west along this fault. One and a half miles south, a subsidiary fault was identified, 800 feet west of the main fault. It strikes N.N.W., dips 87°W., and separates two parts of an erosional remnant of bench gravel, the western part being downthrown 30 feet. Another fault was found, cutting the gutter of the channel, 1¾ miles north of station 19. This fault strikes N.N.E., dips 83°W., and causes 75 feet downthrow to the west on the base of the gravel.

These faults are insufficient to account for the deformation of the channel in the Dutch Flat region. Additional faulting seems necessary in the area north and east of station 20. Ferguson and Gannett, having discovered the Alleghany fault, and noting its similarity to the Mother Lode fault, suggested the continuity of the two. They examined the railway cuts east of Towle (2 miles east of sta. 20) for evidence. Although unsuccessful in their search, they report (1932, p. 22) having found "nothing incompatible with the presence of such a fault." Present evidence denies continuity, but supports the idea of connection through a chain of en echelon faults. That the Forest Hill-Dutch Flat zone is part of such a chain is attested by its position on the straight path between the now-recognized ends of the Alleghany and Mother Lode faults and by similarities in trend, ages of activity and mineralization. These geological considerations support the idea that there must be additional faulting northeast of station 20, if the deformation of the channel is to be fully explained.

Crustal Movements East of the Crest

If the direction and amount of tilt calculated for triplet 1-2-z pertain to the entire block from station 1 eastward to the Donner reverse fault (Fig. 8), and the unmodified value of 1684 feet is used for the uplift at station 1, the uplift since middle Eocene time has been 1783 feet at Donner Pass and 1987 feet on the west side of the main reverse fault. If the modified value of 1887 feet is used for station 1, the results for the Pass and the west side of the fault become 1986 and 2190 feet, respectively. The reverse fault here is composed of a pair of overlapping fractures. The base of the andesite on the east side of this pair has been depressed 1250 feet with respect to the west side. Here, as well as in the region to the east, the basal contacts of the andesite and basalt are used as indices of Tertiary and later deformation, because the rhyolite is not preserved along the line of section and the ancient gravels are not seen. From this point eastward to the western end of Donner Lake, the base of the andesite drops about 800 feet. Beyond this to the east is a zone of normal faulting, 1½ miles wide. The base of the basalt on the east side of this zone is 1500 feet below its position immediately west of the zone. (*See* Hudson, 1951, p. 948-950 and section C-C′, Pl. 1.) The total downthrow of the base of the Superjacent series, from the west side of the main reverse fault to the east end of Donner Lake, is thus 3550 feet. This is thought to be a minimum estimate of the downthrow of the Tahoe-Truckee moat in the latitude of Truckee, because the geographic axis of that depression is several miles east of Donner Lake.

Believing the amount of faulting east of the summit to be insufficient to account for the 3300 feet of crestal uplift which would result from simple 60 feet per mile tilt of the range,

Lindgren (1911, p. 41 and 46) proposed uplift of an area greater than the present range, with local sinking of moats. A necessary corollary, not stated by him, is that both moats and mountains suffered absolute uplift. But the fault movements east of the summit are more than adequate to match his 3300 feet of uplift, and are nearly twice the amount of post-middle Eocene uplift at the crest determined by the gradient calculations.

It is evident that the deeper grabens east of the summit have suffered absolute depression. The Great Basin has been growing at the expense of the Sierra Nevada. This conforms with Le Conte's theory of a collapsed arch and adds to the confirmation of that idea by Lindgren (1911, p. 41) who concluded, from physiographic evidence, that the scarps along the east front of the range are not due to uplift of the western block.

Summary of Conclusions

The gradient calculations indicate that the uplift of the summit of the range at Donner Pass has been 1783 feet since middle Eocene time. After applying correction factors, it was concluded that the most likely value for the uplift at this point is 1986 feet.

The present form of the channel of the ancient Yuba River cannot be explained by simple tilting of a rigid Sierra Nevada block. The results of gradient studies show five zones of internal deformation. The existence of two of these has been confirmed by the discovery of fault zones in the Donner Summit and Forest Hill-Dutch Flat regions. The latter is believed to be a link between the Mother Lode and alleghany faults.

The Tertiary and later movements on the western slope of the range probably included folding.

The faulting east of the range crest involved more downthrow on the Great Basin side than uplift of the Sierra Nevada side.

Some faults which were the loci of pre-Cretaceous mineralization in this region had renewed activity in Tertiary or later time. Such mineral deposits, where buried under Tertiary formations, might be discovered by studies of the deformation of the younger rocks.

References Cited

Anderson, F. M., 1911, The Neocene deposits of Kern River, California, and the Temblor Basin: Calif. Acad. Sci., 4th ser., v. III, p. 73–148.

Browne, Ross E., 1890, The ancient river beds of the Forest Hill Divide (Placer Co.): Calif. St. Min. Bur. Ann. Rept. 10, p. 435–465.

Durrell, Cordell, 1950, Strike-slip faulting in the eastern Sierra Nevada near Blairsden, California (Abstract): Geol. Soc. America Bull., v. 61, p. 1522.

Ferguson, H. G., and Gannett, R. W., 1932, Gold quartz veins of the Alleghany District, California: U. S. Geol. Survey Prof. Paper 172, p. 1–139.

Hake, B. F., 1928, Scarps of the southwestern Sierra Nevada, California: Geol. Soc. America Bull., v. 39, p. 1017–1030.

Haley, C. S., 1922, Tertiary sluice robbers: Calif. St. Mineralogist Rept. 1922, p. 550–554.

Hall, C. E., 1953, Engineering geology—Union Valley damsite, El Dorado County, California (Abstract): Geol. Soc. America Bull., v. 64, p. 1507.

Hobson, J. B., 1890, Placer County: Calif. St. Min. Bur. Bull. 90, p. 410–434.

Hudson, F. S., 1948, Measurement of deformation of the Sierra Nevada since middle Eocene (Abstract): Geol. Soc. America Bull., v. 59, p. 1373.

—— 1951, Mount Lincoln—Castle Peak area, Sierra Nevada, California: Geol. Soc. America Bull., v. 62, p. 931–952.

Lawson, A. C., 1903, Geomorphogeny of the upper Kern Basin: Bull. Dept. Geol. Univ. Calif., v. 3, p. 291–376.

—— 1906, The geomorphic features of the middle Kern: Univ. Calif. Pub., Bull. Dept. Geol., v. 4, p. 397–409.

Le Conte, J., 1880, The old river beds of California: Am. Jour. Sci., 3rd ser., v. 19, p. 176–190.

—— 1886, Post-Tertiary elevation of the Sierra Nevada, shown by the river beds: Am. Jour. Sci., 3rd ser., v. 23, p. 167–181.

—— 1889, The origin of normal faults and of the structure of the Basin Region: Am. Jour. Sci., 3rd ser., v. 28, p. 256–263.

Lindgren, W., 1893, Two Neocene rivers of California: Geol. Soc. America Bull., v. 4, p. 257–298.

—— 1897, Truckee folio, California: U. S. Geol. Survey Folio 39.

—— 1900, Colfax folio, California: U. S. Geol. Survey Folio 66.

—— 1911, The Tertiary gravels of the Sierra Nevada of California: U. S. Geol. Survey Prof. Paper 73, p. 1–266.

Lindgren, W., and Turner, H. W., 1895, Smartsville folio, California: U. S. Geol. Survey Folio 18.

Locke, Augustus, 1912, Tuolumne Table Mountain: Min. and Sci. Press, v. 105, p. 85.

Louderback, G. D., 1924, Period of scarp production in the Great Basin: Univ. Calif. Pub., Bull. Dept. Geol. Sci., v. 15, p. 1–44.

Ransome, F. L., 1900, Mother Lode District folio, California: U. S. Geol. Survey Folio 63.

Taliaferro, N. L., 1942, Geologic history and correlation of the Jurassic of southwestern Oregon and

California: Geol. Soc. America Bull., v. 53, p. 71–112.
Turner, H. W., 1897, Downieville folio, California: U. S. Geol. Survey Folio 37.
Whitney, J. D., 1880, The auriferous gravels of the Sierra Nevada of California: Harvard Coll. Mus. Comp. Zoology Mem. 6, no. 1, p. 1–659.

SOURCES OF DATA OF MODERN YUBA RIVER

Figure 4:
Above 2800 ft. el.:
Plan and profile of South Fork Yuba River, Jones Bar to Soda Springs, U. S. Geol. Survey, 1940, Sheets 1, 2, 9.
Below 2800 ft. el., to junction with Middle Fork:
Washington, 1951, North Bloomfield, 1951, Nevada City, 1950, and French Corral, 1950, quads., U. S. Geol. Survey, 1:24,000.
Figure 4, Middle Fork to junction with Feather River, and Figures 9, 10:
Gilbert, G. K., 1917, Hydraulic mining debris in the Sierra Nevada: U. S. Geol. Survey Prof. Paper 105, Figure 4, p. 47.
Parks Bar, 1922, Browns Valley, 1911, and Yuba City, 1934, quads., U. S. Geol. Survey, 1: 31,680.
Unpublished sources.

2304 WASHINGTON ST., SAN FRANCISCO, CALIF.
MANUSCRIPT RECEIVED BY THE SECRETARY OF THE SOCIETY OCTOBER 29, 1953

APPENDIX A. GRADIENT CALCULATIONS

Sta. 1 to 2 to x-y-z:

Sta.:	Elevation:	Diff.:	Reach:	Bearing:	Length:	Gradient: ft./mi.	Angle between directions of reach and tilt axis:
1	7232						
		432	a	S.58°W.	0.95 mi.	440.8	$\delta_a = 58° + B$
2	6800						
		230	b	S. 4° E.	1.09	211.0	$\delta_{b'} = B - 3.5°$
x	7030						
		270	c	S. 3° E.	1.16	232.8	
y	7300						
		100	d	S.25°E.	0.78	128.2	$\delta_d = 25° - B$
z	7400						

Combine b & c into one course, b', S.3.5°E., 2.25 mi., gradient = 500/2.25 = 222.2 ft/mi.

$$S_a = S_0 + T \cdot \sin\delta_a$$
$$S_{b'} = S_0 + T \cdot \sin\delta_{b'}$$
$$S_d = S_0 - T \cdot \sin\delta_d$$

$$S_a - S_{b'} = T(\sin\delta_a - \sin\delta_{b'})$$
$$S_{b'} - S_d = T(\sin\delta_{b'} + \sin\delta_d)$$

$$\frac{S_a - S_{b'}}{S_{b'} - S_d} = \frac{\sin\delta_a - \sin\delta_{b'}}{\sin\delta_{b'} + \sin\delta_d}$$

$\delta_a - \delta_{b'} = 61.5°$, $\delta_{b'} = \delta_a - 61.5°$
$\delta_a + \delta_d = 83°$, $\delta_d = 83° - \delta_a$

Introducing these and the gradient values into the foregoing equation, one has:

$$\frac{440.8 - 222.2}{222.2 - 128.2} = \frac{218.6}{94.0} = 2.326 = \frac{\sin\delta_a - \sin(\delta_a - 61.5°)}{\sin(\delta_a - 61.5°) + \sin(83° - \delta_a)}$$

$$\sin\delta_a = 3.326 \sin(\delta_a - 61.5°) + 2.326 \sin(83° - \delta_a)$$
$$\delta_a = 63.7°$$

Azimuth of tilt axis, $B = \delta_a - 58° = 63.7° - 58° = 5.7°$, or N.5.7°W.

Amount of tilt, $T = (S_a - S_{b'})/(\sin\delta_a - \sin\delta_{b'}) = \frac{218.6}{.8965 - .0384} = \frac{218.6}{.8581}$
= 254.7 ft./mi., westerly

Pre-tilt gradient, $S_0 = S_a - T \cdot \sin\delta_a = 440.8 - (254.7)(.8965) = 440.8 - 228.3$
= 212.5 ft./mi.

Sta. 3 to 6:

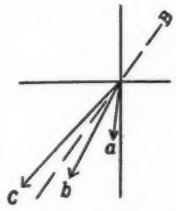

Sta.	Reach:	Direction:	Gradient ft./mi.	Angle between direction of reach and tilt axis:
3				
4	a	S. 4°W.	47.0	$\delta_a = B - 4°$
	b	S. 28°W.	98.0	$\delta_b = B - 28°$
5	c	S. 44°W.	134.3	$\delta_c = 44° - B$
6				

$$(S_a - S_b)/(S_c - S_b) = (47-98)/(134.3-98.0) = -51/36.3 = -1.405 = \frac{\sin\delta_b - \sin\delta_a}{\sin\delta_b + \sin\delta_c}$$

$\delta_a + \delta_c = 40°$, $\delta_a = 40° - \delta_c$ $\qquad$ $\delta_b + \delta_c = 16°$, $\delta_b = 16° - \delta_c$

$$-1.405 \sin(16°-\delta_c) - 1.405 \sin\delta_c = \sin(16°-\delta_c) - \sin(40°-\delta_c)$$

$$1.405 \sin\delta_c = \sin(40°-\delta_c) - 2.405 \sin(16°-\delta_c)$$

$$\sin\delta_c = .7117 \sin(40°-\delta_c) - 1.7117 \sin(16°-\delta_c)$$

This is satisfied by $\delta_c = 8.1°$, so $B = 44° - 8.1° = 35.9°$, or N. 35.9° E.

Amount of tilt, $T = (S_c - S_b)/(\sin\delta_b + \sin\delta_c) = (134.3-98.0)/(.1374+.1409)$

$= 36.3/.2783 = 130.4$ ft./mi., westerly.

Pre-tilt gradient, $S_0 = S_a + T \cdot \sin\delta_a = 47 + (130.4)(.5284) = 47 + 68.9 = 115.9$ ft./mi.

Sta. 2 to 3: The original gradient of this reach cannot be found by calculations based on the tilts of adjacent reaches. It is accordingly considered to have been the average of the S_0's of the adjacent reaches, viz.

$$S_{0_{2-3}} = (212.5 + 115.9)/2 = (328.4)/2 = 164.2 \text{ ft./mi.}$$

Sta. 6 to 8:

Using tilt factors of Triplet #3-#6 $\quad S_{0_{6-7}} = 99.0 + (130.4)[\sin(35.9°-34.0°)] = 99.0 + 4.3 = 103.3$

" " " $\quad S_{0_{7-8}} = 69.5 - (130.4)[\sin(68.0°+35.9°)] = 69.5 - 126.6 = -57.1$

Triplet #8-#11 $\quad S_{0_{7-8}} = 69.5 - (80.3) \cdot \sin(68.0°-39.6°) = 69.5 - 38.2 = 31.3$

" " " $\quad S_{0_{6-7}} = 99.0 - (80.3) \cdot \sin(34.0°+39.6°) = 99.0 - 77.0 = 22.0$

The values accepted are: For Sta. 7-8, $S_0 = 31.3$ ft./mi.

For Sta. 6 to 7 the average between 31.3 and the S_0 of triplet #3-6, i.e. $(31.3 + 115.9)/2 = 147.2/2 =$ 73.6 ft./mi.

Sta. 8 to 11:

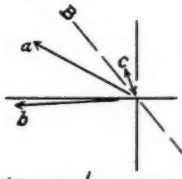

Sta.:	Reach:	Direction:	Gradient: ft./mi.	Angle between directions of reach and tilt axis:	
8	a	N.62°W.	57.6	$\delta_a = 62° - B$	$\delta_a = \delta_b - 31°$
9	b	S.87°W.	91.5	$\delta_b = 93° - B$	$\delta_c = 73° - \delta_b$
10	c	N.20°W.	nil	$\delta_c = B - 20°$	
11					

$(S_a - S_b)/(S_b - S_c) = (\sin\delta_a - \sin\delta_b)/(\sin\delta_b + \sin\delta_c)$

$(57.6-91.5)/(91.5+nil) = -33.9/91.5 = -0.3705 = \dfrac{\sin(\delta_b - 31°) - \sin\delta_b}{\sin\delta_b + \sin(73° - \delta_b)}$

$0.6295 \sin\delta_b = 0.3705 \sin(73° - \delta_b) + \sin(\delta_b - 31°)$

$\sin\delta_b = 1.588 \sin(\delta_b - 31°) + 0.588 \sin(73° - \delta_b)$

This is satisfied by $\delta_b = 53.4°$, so $B = 93° - 53.4° = 39.6°$, or N. 39.6°W.

Amount of tilt, $T = (S_a - S_b)/(\sin\delta_a - \sin\delta_b) = \dfrac{-33.9}{.381 - .803} = \dfrac{-33.9}{-.422}$

$= 80.3$ ft./mi., westerly

Pre-tilt gradient, $S_0 = S_a - T \cdot \sin\delta_a = 57.6 - (80.3)(.381) = 57.6 - 30.6$

$= 27.0$ ft./mi.

Sta. 11 to 12: No solution was obtained by combining this reach with either upstream or downstream reaches. Accordingly, the average of the S_0's of the adjacent reaches was accepted as the original gradient of #11-12, viz.

$S_0 = (27.0 + 9.7)/2 = 36.7/2 = 18.3$ ft./mi.

Sta. 12 to 15:

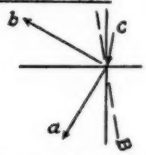

Sta.:	Reach:	Direction:	ft./mi.:		
12	a	S.32°W.	54.3	$\delta_a = 32° + B$	$\delta_b = 93° - \delta_a$
13	b	N.61°W.	61.5	$\delta_b = 61° - B$	$\delta_c = \delta_a - 21°$
14	c	N.11°E.	r 15.0	$\delta_c = 11° + B$	
15					

$(S_a - S_b)/(S_b - S_c) = (-7.2)/(76.5) = -.0941 = (\sin\delta_a - \sin\delta_b)/(\sin\delta_b + \sin\delta_c)$

$\sin\delta_a = .9059 \sin\delta_b - .0941 \sin\delta_c = .9059 \sin(93° - \delta_a) - .0941 \sin(\delta_a - 21°)$

$\delta_a = \sin^{-1}.669 = 42°$, $B = \delta_a - 32° = 42° - 32° = 10°$, or N.10°W.

$\sin\delta_b = .777$, $\sin\delta_c = .358$

$T = (S_a - S_b)/(\sin\delta_a - \sin\delta_b) = (54.3 - 61.5)/(.669 - .777) = (-7.2)/(-.108) = 66.6$

$S_0 = S_b - T \cdot \sin\delta_b = 61.5 - (66.6)(.777) = 61.5 - 51.8 = 9.7$ ft./mi.

Sta. 15 to 20:

The only solvable triplet in this stretch of the channel was produced by using Lindgren's data of Sta. 18, Iowa Hill, and Sta. 19, Indiana Hill, with two new stations: #17, south of Iowa Hill, and #19A, in the Stewart pit, north of Indiana Hill.

Sta. 17 to 19A:

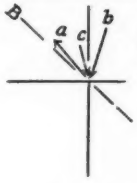

Sta.:	Elevation:	Diff.:	Reach:	Bearing:	Length: mi.	ft./mi.:	
17	2640						
		9	a	N.40°W.	0.38	23.7	
18	2631						
		u.161	b	N.17°E.	3.38	r. 47.6	$\delta_b = 57° + \delta_a$
19	2792						
		u. 8	c	N.15°W.	0.58	r. 13.8	$\delta_c = 25° + \delta_a$
19A	2800						

$$(S_a - S_b)/(S_b - S_c) = (23.7 + 47.6)/(-47.6 + 13.8) = (71.3)/(-33.8) = -2.110$$

$$= (\sin\delta_b - \sin\delta_a)/(\sin\delta_c - \sin\delta_b)$$

$$-2.110 \sin\delta_c + 2.110 \sin\delta_b = \sin\delta_b - \sin\delta_a$$

$$\sin\delta_a = 2.110 \sin(\delta_a + 25°) - 1.110 \sin(\delta_a + 57°)$$

This is satisfied by $\delta_a = \sin^{-1}(.122) = 7°$, B is N.47°W., $\sin\delta_b = .898$, $\sin\delta_c = .530$

$$T = (71.3)/(.898 - .122) = 71.3/.776 = 91.8$$
$$= (-33.8)/(.530 - .898) = -33.8/-.368 = 91.8 \Big\} \text{ 91.8 ft./mi.}$$

$$S_0 = 23.7 + (91.8)(.122) = 23.7 + 11.2 = 34.9$$
$$= -47.6 + (91.8)(.898) = -47.6 + 82.5 = 34.9 \Big\} \text{ 34.9 ft./mi.}$$

Sta. 15 to 17:

The original gradient is assumed to be the average of those found for the adjacent solved triplets, viz.

$$S_0 = (34.9 + 9.7)/2 = 44.6/2 = 22.3 \text{ ft./mi.}$$

Sta. 19A to 20:

By same method as the foregoing:

$$S_0 = (34.9 + 36.8)/2 = 71.7/2 = 35.8 \text{ ft./mi.}$$

Sta. 20 to 22A:

The only successful calculation on the stretch of channel between Sta. 20 and 27 was made by introducing Sta. 22A, Hunts Hill, between Hawkins Canyon and Quaker Hill. Lindgren showed the Hunts Hill working on his geologic map of the Colfax quadrangle and, in writing of it, said (1911, p.143) "the deepest channel is exposed by mining operations at about the level of the tailings in the river at an elevation of 2620 feet." The Chicago Park quadrangle map (U.S.Geol.Sur., 1951) shows the level of the tailings here to be within a few feet of 2520 feet, indicating that Lindgren's published datum is 100 feet in error. Accordingly, the lower value was accepted for the elevation of Sta. 22A.

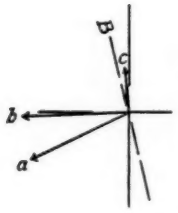

Sta.	Elevation:	Diff.:	Reach:	Bearing:	Length:	ft./mi.	
20	2848						
		142	a	S.65°W.	1.77mi.	80.2	$\delta_a = B + 65°$
21	2706						
		111	b	S.89°W.	1.38	80.4	$\delta_b = 91° - B$
22	2595						
		75	c	N. 5°W.	2.42	31.1	$\delta_c = B - 5°$
22A	2520						

$\delta_a + \delta_b = 156°$, $\delta_a = 156° - \delta_b$ $\qquad$ $\delta_b + \delta_c = 86°$, $\delta_c = 86° - \delta_b$

$$\frac{S_b - S_c}{S_a - S_c} = \frac{80.4 - 31.1}{80.2 - 31.1} = \frac{49.3}{49.1} = 1.004 = \frac{\sin\delta_b + \sin\delta_c}{\sin\delta_a + \sin\delta_c} = \frac{\sin\delta_b + \sin(86° - \delta_b)}{\sin(156° - \delta_b) + \sin(86° - \delta_b)}$$

$$1.004 \sin(156° - \delta_b) + 1.004 \sin(86° - \delta_b) = \sin\delta_b + \sin(86° - \delta_b)$$

$$\sin\delta_b = 1.004 \sin(156° - \delta_b) + .004 \sin(86° - \delta_b)$$

This is satisfied by $\delta_b = 78.6°$, so $B = 91° - 78.6° = 12.4°$, or N. 12.4° W.

Amount of tilt, $T = (S_b - S_c)/(\sin\delta_b + \sin\delta_c) = 49.3/(.9803 + .1288) = 49.3/1.1091$
$= 44.5$ ft./mi., westerly

Pre-tilt gradient, $S_o = S_b - T \cdot \sin\delta_b = 80.4 - (44.5)(.9803) = 80.4 - 43.6$
$= 36.8$ ft./mi.

Sta. 27-30:

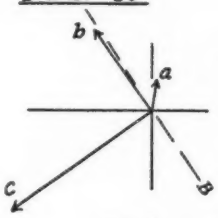

Sta.	Reach:	Direction:	Gradient: ft./mi:	Angle between direction of reach and tilt axis:	
27					
28	a	N. 5°E.	2.9	$\delta_a = B + 5°$	$\delta_a = \delta_c - 60°$
29	b	N.35°W.	36.5	$\delta_b = B - 35°$	$\delta_b = \delta_c - 90°$
30	c	S.55°W.	87.7	$\delta_c = B + 55°$	

$$\frac{S_c - S_b}{S_b - S_a} = \frac{87.7 - 36.5}{36.5 - 2.9} = \frac{51.2}{33.6} = 1.524 = \frac{\sin\delta_c + \sin\delta_b}{\sin\delta_a - \sin\delta_b}$$

$$\sin\delta_c = 1.524\sin\delta_a - 2.524\sin\delta_b$$
$$= 1.524\sin(\delta_c - 50°) - 2.524\sin(\delta_c - 90°)$$

This is satisfied by $\delta_c = 89.1°$, so $B = 89.1° - 55° = 34.1°$, or N.34.1°W.

Amount of tilt, $T = (S_c - S_b)/(\sin\delta_b + \sin\delta_c) = (87.7 - 36.5)/(-.0157 + .9999)$
$= 51.2/.984 = 52.0$ ft./mi.

Pre-tilt gradient, $S_0 = S_a + T\cdot\sin\delta_a = 2.9 + (52)(.631) = 2.9 + 32.8$
$= 35.7$ ft./mi.

Sta. 22A to 27, and 30 to 38: The original gradients of these two stretches of the channel are assumed to be the values found by interpolating between the S_0's determined for the triplets #20-#22A, #27-#30, and #38-41.

Sta. 38 to 41:

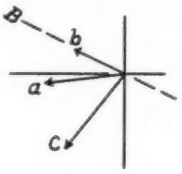

Sta.	Reach:		ft./mi.	
38				
39	a	S. 84°W.	$S_a = 36.1$	$\delta_a = 96° - B$
40	b	N. 65°W.	$S_b = 28.2$	$\delta_b = 65° - B$
41	c	S. 38°W.	$S_c = 42.9$	$\delta_c = 142° - B$

$$\frac{S_a - S_b}{S_b - S_c} = \frac{36.1 - 28.2}{28.2 - 42.9} = \frac{7.9}{-14.7} = -0.537 = \frac{\sin\delta_a - \sin\delta_b}{\sin\delta_b - \sin\delta_c}$$

$$\delta_a - \delta_b = 31^\circ \qquad \delta_b = \delta_a - 31^\circ$$

$$\delta_c - \delta_a = 46^\circ \qquad \delta_c = 46^\circ + \delta_a$$

$$-.537 \sin(\delta_a - 31^\circ) + .537 \sin(46^\circ + \delta_a) = \sin\delta_a - \sin(\delta_a - 31^\circ)$$

$$\sin\delta_a = .463 \sin(\delta_a - 31^\circ) + .537 \sin(46^\circ + \delta_a)$$

$$\sin\delta_a = .539\ , \quad \delta_a = 32.6^\circ, \quad B = 96^\circ - 32.6 = 63.4^\circ, \text{ or } N.63.4^\circ W.$$

$$\sin\delta_b = .028 \qquad \sin\delta_c = .980$$

$$T = (S_a - S_b)/(\sin\delta_a - \sin\delta_b) = 7.9/(.539 - .028)$$

$$= 7.9/.511 = 15.5 \text{ ft./mi. southerly}$$

$$S_0 = S_c - T \cdot \sin\delta_c = 42.9 - (15.5)(.980) = 42.9 - 15.1$$

$$= 27.8 \text{ ft./mi.}$$

Appendix B. Examples of Variance Calculations

Triplet 17 to 19A:

Total length 4.3 mi., divided in the approx. proportion ½ : 4 : ½

reach arrangement 4:½:½

sta.	grad.	variance from avg.	
115-120	49.1	+10.0 or +25.6%	23.6%
120-121	37.5		
121-122	30.7	−8.4 or −21.5%	
avg.	39.1		
A-119	43.0	+4.9 or +12.9%	12.2
119-120	33.7	−4.4 or −11.5%	
120-121	37.5		
avg	38.1		
A-118	43.8	+7.4 or +20.3%	16.7
118-119	31.6	−4.8 or −13.2%	
119-120	33.7		
avg.	36.4	3	52.5
avg. variance from avg. grad.			17.5%

arrangement ½ : ½ : 4

D-C	33.8	−9.8 or −22.5%	20.8%
C-C'	45.0		
C'-117	51.9	+8.3 or +19.0%	
avg.	43.6		
C''-B	45.0		
B-B'	38.8	−10.1 or −23.0%	16.2
B'-118	48.0	+4.1 or +9.3%	
avg.	43.9		
B''-A	38.8		
A-115	36.2	−5.2 or −12.5%	15.7
115-120	49.2	+7.8 or +18.8%	
avg.	41.4		
A-115	38.8	−4.0 or −9.4%	12.5
115-116	40.2		
116-122	49.5	+6.7 or +15.7%	
avg.	42.8	4	70.2
avg. variance from avg. grad.			17.6%

arrangement ½ : 4 : ½

sta.	grad.	variance from avg.	
116'-116	40.2		
116-121	50.2	+9.9 or +24.6%	24.2%
121-122	30.7	−9.6 or −23.8%	
avg.	40.3		
A-115	36.2	−8.2 or −20.0%	20.0
115-120	49.1	+8.2 or +20.0%	
120-121	37.5		
avg.	40.9		
A-115	36.2		
115-119	44.2	+6.2 or +16.3%	13.8
119-120'	33.7	−4.3 or −11.3%	
avg.	38.0		
B''-A	38.8		
A-118	43.8	+5.7 or +15.0%	16.1
118-119	31.6	−6.5 or −17.1%	
avg.	38.1		
D-C	33.8	−8.4 or −19.9%	20.3
C-117	50.9	+8.7 or +20.6%	
117-117'	41.8		
avg.	42.2	5	94.4
avg. variance from avg. grad.			18.9%

Summary of the three cases:

	Avg.	Extremes:	
4 : ½ : ½	17.5%	12.2%	23.6%
½ : ½ : 4	17.6	12.5	20.8
½ : 4 : ½	18.9	13.8	24.2
averages	18.0%	12.8%	22.9%

		ft./mi.
Calculated S_0		34.9
Variance from avg. grad.		
Most likely	18.0%	6.3
Less probable	>22.9%	> 8.0
	<12.8%	< 4.5
Improbable	>24.2%	> 8.4
	<12.2%	< 4.3

Triplets 20-22A and 27-30:

Each has total length of about 6 mi., with reach lengths in the approx. proportion 1:2:3.

reach arrangement 3:2:1

sta.	grad.	variance from avg.	
B-117	53.0	+6.9 or +15.0%	13.8%
117-120	44.6		
120-122	40.7	-5.4 or -11.7%	
avg.	46.1		
B-117	53.0	+6.2 or +13.3%	13.7
117-119	40.2	-6.6 or -14.1%	
119-121	47.3		
avg.	46.8		
C-116	44.8	+3.7 or +9.0%	10.7
116-118	42.5		
118-120	36.0	-5.1 or -12.4%	
avg.	41.1		3 / 38.2

avg. variance from avg. grad. 12.7%

arrangement 3:1:2

sta.	grad.	variance from avg.	
B-117	53.0	+7.2 or +15.7%	12.2%
117-118	41.8	-4.0 or -8.7%	
118-121	42.5		
avg.	45.8		
C-116	44.8		
116-117	39.6	-4.1 or -9.4%	8.2
117-120	46.7	+3.0 or +6.9%	
avg.	43.7		
D-115	47.3	+4.0 or +9.2%	8.2
115-116	40.2	-3.1 or -7.2%	
116-118	42.5		
avg.	43.3		3 / 28.6

avg. variance from avg. grad. 9.5%

arrangement 2:3:1

sta.	grad.	variance from avg.	
A-116	49.1		
116-120	51.8	+4.6 or +9.8%	11.8%
120-122	40.7	-6.5 or -13.8%	
avg.	47.2		
A-116	41.4	-2.5 or -5.7%	6.8
116-119	42.9		
119-121	47.3	+3.4 or +7.8%	
avg.	43.9		
C-115	46.5	+3.9 or +9.2%	12.4
115-118	45.3		
118-120	36.0	-6.6 or -15.5%	
avg.	42.6		3 / 31.0

avg. variance from avg. grad. 10.3%

arrangement 1:3:2

sta.	grad.	variance from avg.	
115-116	40.2	-2.3 or -5.4%	5.1%
116-119	42.9		
119-122	44.5	+2.0 or +4.7%	
avg.	42.5		
B-115	46.1	+1.4 or +3.1%	4.0
115-118	45.4		
118-121	42.5	-2.2 or -4.9%	
avg.	44.7		
C-B	45.0	-3.2 or -6.6%	8.4
B-117	53.0	+4.8 or +10.0%	
117-120	46.7		
avg.	48.2		3 / 17.5

avg. variance from avg. grad. 5.8%

20-22A and 27-30, cont.

reach arrangement 1:2:3

sta.	grad.	variance from avg.	
B-115	46.1		
115-117	48.0	+1.8 or +3.9%	3.7%
117-122	44.6	-1.6 or -3.5%	
avg.	46.2		
B-A	38.8	-4.0 or -9.3%	7.1
A-117	44.9	+2.1 or +4.9%	
117-122	44.6		
avg.	42.8		
B-115	46.1	-0.7 or -1.5%	2.1
115-117	48.0	+1.2 or +2.6%	
117-121	46.3		
avg.	46.8		
B-A	38.8	-4.4 or -10.2%	15.1
A-116	39.1		
116-120	51.8	+8.6 or +19.9%	
avg.	43.2		
B-A	38.8	-1.5 or -3.7%	5.1
A-116	39.1		
116-119	42.9	+2.6 or +6.5%	
avg.	40.3		
C-B	45.0		
B-116	44.4	-2.0 or -4.3%	5.8
116-121	49.8	+3.4 or +7.3%	
avg.	46.4		6 / 38.9

avg. variance from avg. grad. 6.5%

arrangement 2:1:3

sta.	grad.	variance from avg.	
A-116	39.1	-2.6 or -6.2%	8.6%
116-117	39.6		
117-121	46.3	+4.6 or +11.0%	
avg.	41.7		
B-116	44.4		
116-117	39.6	-3.8 or -8.8%	7.8
117-121	46.3	+2.9 or +6.7%	
avg.	43.4		
C-115	46.5	+2.5 or +5.1%	6.9
115-116	40.2	-3.8 or -8.6%	
116-120	45.4		
avg.	44.0		
C-115	46.5	+3.3 or +7.6%	7.3
115-116	40.2	-3.0 or -6.9%	
116-119	42.9		
avg.	43.2		
D-B	43.8	-1.3 or -2.9%	2.6
B-115	46.1	+1.0 or +2.2%	
115-118	45.4		
avg.	45.1		5 / 33.2

avg. variance from avg. grad. 6.6%

Summary of the six cases:

	Avg.:	Extremes:	
3:2:1	12.7%	10.7%	13.8%
2:3:1	10.3	6.8	12.4
3:1:2	9.5	8.2	12.2
1:3:2	5.8	4.0	8.4
1:2:3	6.5	2.1	15.1
2:1:3	6.6	2.6	8.6
averages	8.6%	5.7%	11.8%

Variances:

		20-22A ft./mi.	27-30 ft./mi.
Calculated S_0		36.8	35.7
Var. from avg. grad.:			
Most likely	8.6%	3.2	3.1
Less probable	>11.8%	>4.3	>4.2
	<5.7%	<2.1	<2.0
Improbable	>15.1%	>5.6	>5.4
	<2.1%	<0.8	<0.7

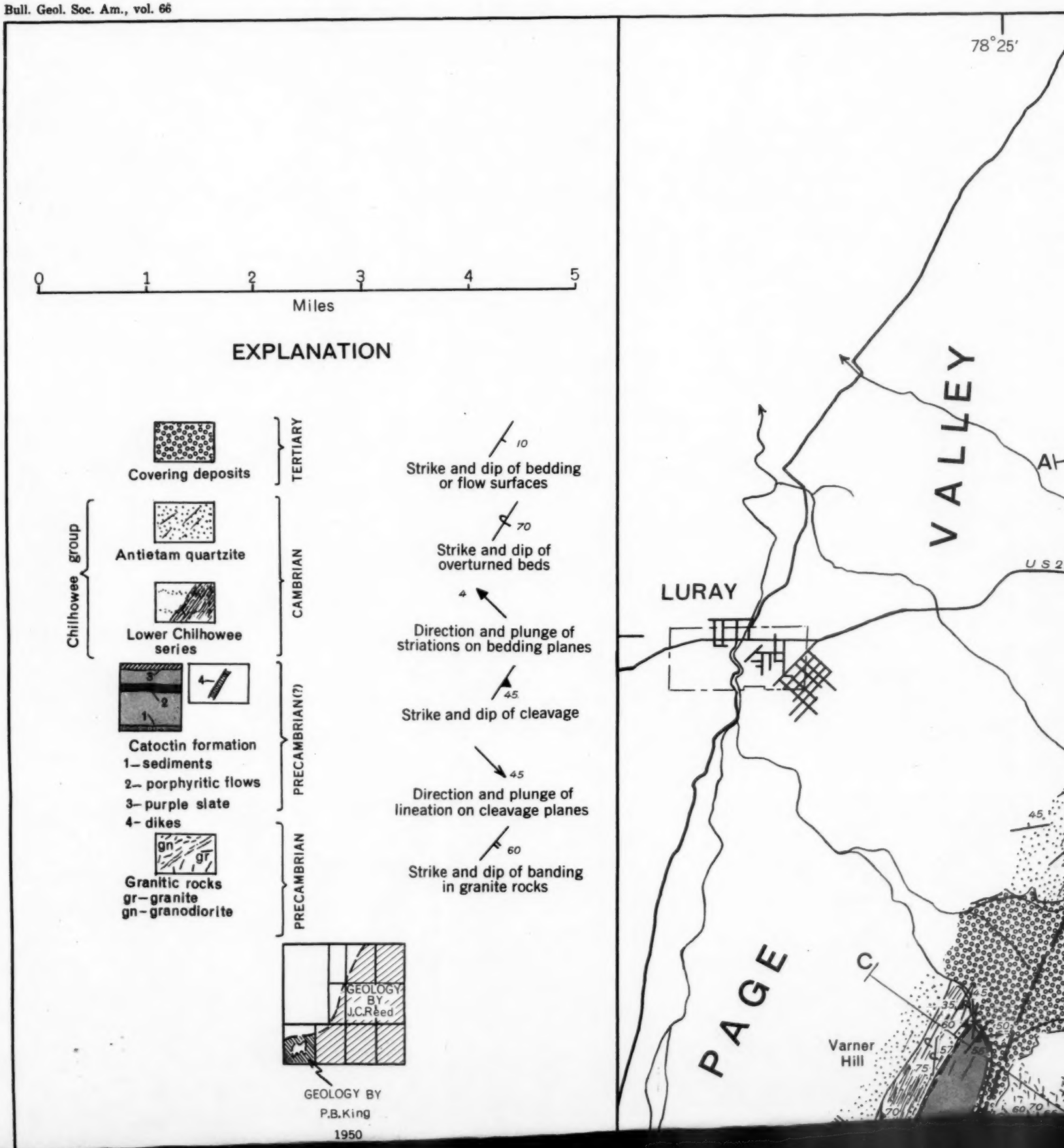
0 1 2 3 4 5
Miles
EXPLANATION
Covering deposits
TERTIARY
Chilhowee group
Antietam quartzite
Lower Chilhowee series
CAMBRIAN
Catoctin formation
1—sediments
2—porphyritic flows
3—purple slate
4—dikes
PRECAMBRIAN(?)
Granitic rocks
gr—granite
gn—granodiorite
PRECAMBRIAN
Strike and dip of bedding or flow surfaces
Strike and dip of overturned beds
Direction and plunge of striations on bedding planes
Strike and dip of cleavage
Direction and plunge of lineation on cleavage planes
Strike and dip of banding in granite rocks
GEOLOGY BY J.C.Reed
GEOLOGY BY P.B.King 1950
78°25'
VALLEY
LURAY
US 2
PAGE
Varner Hill

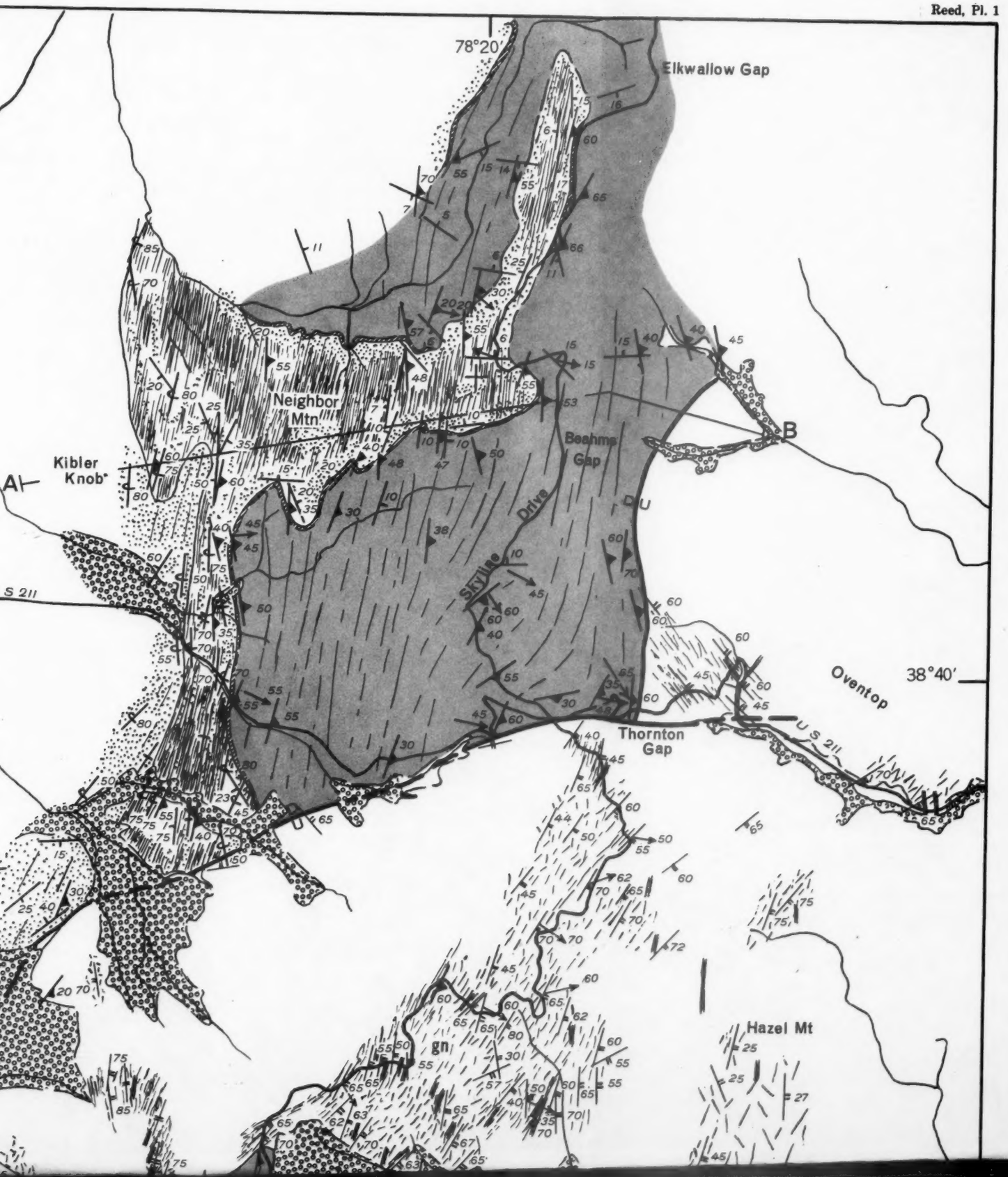
78°20'
Elkwallow Gap
Neighbor Mtn
Kibler Knob
A
A'
Beahms Gap
B
B'
Skyline Drive
S 211
38°40'
Oventop
Thornton Gap
U S 211
Hazel Mt
gn

Catoctin formation
1—sediments
2—porphyritic flows
3—purple slate
4—dikes

PRECAMBRIAN

gn gr

Granitic rocks
gr—granite
gn—granodiorite

PRECAMBRIAN

45
Direction and plunge of lineation on cleavage planes

60
Strike and dip of banding in granite rocks

GEOLOGY BY J.C.Reed

GEOLOGY BY
P.B.King
1950

PAGE

Varner Hill

Hersberger Hill

78° 30′

gn

Big Meadows

Skyline

Tanners Ridge

Chapman Mt.

SHENANDOAH SALIENT

A

B

C

E

gn

gn

GEOLOGIC MAP AND CROSS SECTIONS OF

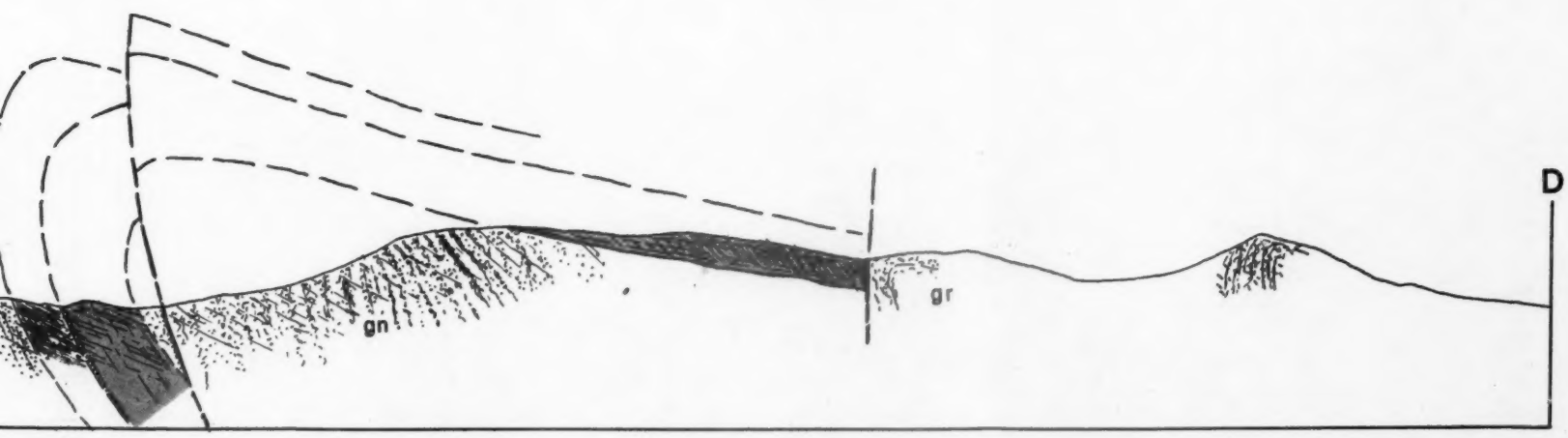

OF THE BLUE RIDGE NEAR LURAY, VIRGINIA

BULLETIN OF THE GEOLOGICAL SOCIETY OF AMERICA
VOL. 66, PP. 871-896, 10 FIGS., 3 PLS. JULY 1955

CATOCTIN FORMATION NEAR LURAY, VIRGINIA

BY JOHN C. REED, JR.

ABSTRACT

In the Blue Ridge Province of northern Virginia, Maryland, and southern Pennsylvania the established lower Cambrian beds are underlain by a thick sequence of greenstone and interbedded sedimentary rocks known as the Catoctin formation. In an effort to determine the thickness of the formation, its relationship to overlying and underlying rocks, and the original nature of the lavas from which the Catoctin greenstone was derived, an area near Luray, Virginia, was studied. There the Catoctin formation lies unconformably on granitic rocks. Its basal sedimentary layer ranges from a few inches to 150 feet thick and contains pebbles of underlying plutonic rocks. The erosion surface beneath the Catoctin is irregular, and in several places hills up to 750 feet high were buried beneath the Catoctin lavas. No important time break is indicated between the deposition of the Catoctin formation and of the overlying Cambrian sediments, and the Catoctin may be early Cambrian.

Mineralogy, chemical composition, and primary structures indicate that the original Catoctin lavas were basaltic in composition and were probably normal plateau basalts. Columnar joints, amygdules, sedimentary dikes, flow breccias, low-dipping primary joints, and other primary structures are well preserved, and the flows in this area are believed to have been subaerial.

CONTENTS

TEXT

	Page
Introduction	872
Area studied	875
Acknowledgments	875
General geology of the Luray area	875
Structural setting	875
Rocks underlying the Catoctin formation	876
General character	876
Relation to the Catoctin formation	877
Rocks overlying the Catoctin formation	878
General character	878
Relation to the Catoctin formation	878
General character of the Catoctin formation	879
Catoctin formation in the Big Meadows-Stony Man area	879
General structure	879
Sedimentary members	880
Volcanic flows	881
Primary structures	883
Introduction	883
Columnar jointing	883
Low-dipping primary joints	884
Amygdules	884
Sedimentary dikes	885
Flow breccias	886
Petrography and mineralogy of the flows	887
Dikes of greenstone	890
Purple volcanic slate	891
Original nature of the Catoctin lavas	893
Metamorphism	894
Conclusions	895
References cited	896

ILLUSTRATIONS

Figure	Page
1. Index map	873
2. Possible stratigraphic relationships of the Catoctin formation	874
3. Stratigraphic relationship of the Catoctin formation to the granitic basement rocks	877
4. Cross sections of the lower three Catoctin flows at Franklin Cliffs and Crescent Rocks	882
5. Axes of deformed columns	884
6. Cleavage and lineation	884
7. Poles of flat primary joints in greenstone	885
8. Sketch of a portion of a sedimentary dike	886
9. Mud-lump breccia	887
10. Volume percentage of various minerals plotted against grain size as measured by average length of groundmass plagioclase in Catoctin greenstones	895

Plate	Facing page
1. Geologic map and cross sections of the Blue Ridge near Luray, Virginia	871
2. Primary structures of the Catoctin formation	884
3. Photomicrographs	885

TABLES

Table	Page
1. Micrometric analyses of greenstone of the Catoctin formation	889
2. Chemical analyses of Catoctin greenstones	891
3. Chemical analyses of volcanic slate	892
4. Atoms associated with 160 oxygen atoms in the average Catoctin greenstone and the average tholeiitic basalt	894

Introduction

In the central Appalachians, as in several other areas in North America, the lowermost fossiliferous Cambrian rocks are underlain not by high-grade metamorphic and igneous rocks of the early Precambrian basement but by great thicknesses of volcanic and unfossiliferous sedimentary rocks which are similar in metamorphic grade to the fossiliferous Cambrian rocks. Where the break between fossiliferous rocks and unfossiliferous rocks is a definite unconformity the base of the Paleozoic is usually placed at this unconformity. Where no such break occurs, however, the question arises as to what criteria should be used in defining the base of the Cambrian. Should it be placed at the lowest Cambrian fossil? Should it be placed at the first major unconformity below? If so, what is a "major unconformity"? Or, should it be placed somewhere between?

The oldest Cambrian fossils known in the central Appalachians are trilobites and brachiopods collected from the upper part of the Chilhowee group[1], a conformable sequence of sandy and shaly sediments between 2500 and 7000 feet thick which underlies the Cambrian and Ordovician carbonate sequence of the Appalachian Valley (King, 1949). The Chilhowee group can be subdivided into at least three formations: a clean, white, sugary quartzite at the top, passing downward into shale and siltstone (in most places slightly metamorphosed and slaty or phyllitic in character), and a basal sequence of graywacke and conglomerate. North of Roanoke, Virginia, these units are the Antietam quartzite, Harpers formation, and Weverton formation respectively. Southwest of Roanoke they are called the Erwin quartzite, Hampton shale, and Unicoi formation.

In a few places these Chilhowee rocks rest on a plutonic basement consisting of granites, granodiorites, and granitelike gneisses which in places show relic sedimentary structures suggesting that they are at least in part derived from granitization of a sedimentary series (Jonas, 1935). In most places in southern Pennsylvania, Maryland, and northern Virginia, however, the Cambrian sedimentary rocks are underlain by metamorphosed volcanic rocks and associated sedimentary rocks known as the Catoctin formation. In the area in northern Virginia discussed in this paper, most of the volcanic rocks of the Catoctin are believed to be basaltic, but in the Mount Rogers area in southwestern Virginia and in South Mountain, Pennsylvania, large thicknesses of rhyolitic volcanics have been described (Stose, 1938; Bascom, 1896). Discontinuous sedimentary members are inter-bedded with the volcanics, and a basal sedimentary member up to several hundred feet thick commonly is present. Such basal sedimentary rocks have received several formation names including Swift Run tuff (Stose and Stose, 1946) and Oronoco formation (Bloomer and Bloomer, 1947).

The Catoctin formation unconformably overlies the basement rocks, but its relationship to the overlying Chilhowee rocks has been subject to much discussion. Most authors have postulated a major unconformity at the top of the Catoctin; several recent workers have questioned this and pointed out that the Catoctin may be early Cambrian. The present evidence on this question is inconclusive.

In northern Virginia the Catoctin formation and the overlying Cambrian rocks are exposed on the limbs of the Catoctin Mountain-Blue Ridge anticlinorium, a major structural unit which extends from southern Pennsylvania southwestward into central Virginia (Fig. 1). The core of the anticlinorium is composed of the granitic basement rocks. The western limb is marked by the lower Cambrian and Catoctin rocks of the main Blue Ridge; the eastern limb is marked by similar sediments and volcanics exposed in a line of lower ridges which include Catoctin Mountain in Maryland, Bull Run Mountain near Warrenton, and Southwest Mountain near Charlottesville. Folds within the anticlinorium are shear folds overturned to the northwest. Cleavage strikes north or

[1] The term Chilhowee group was first applied in Tennessee. The extension of the term to northern Viriginia is open to question since the sequence referred to is composed of different formations than the Chilhowee group of the type area. However, the term has been applied by King (1950) in the Elkton area and it is used in this paper as a convenient designation for the clastic sedimentary rocks which overlie the Catoctin formation and underlie the Tomstown dolomite.

northeast and dips to the southeast; lineation lies in the cleavage plane and plunges down the dip in the "a" direction. This pattern is common to all rocks within the anticlinorium.

Catoctin formation and the Glenarm series are Precambrian and are separated from the Paleozoic rocks by a major unconformity, marking the base of the Cambrian (Fig. 2A). Another

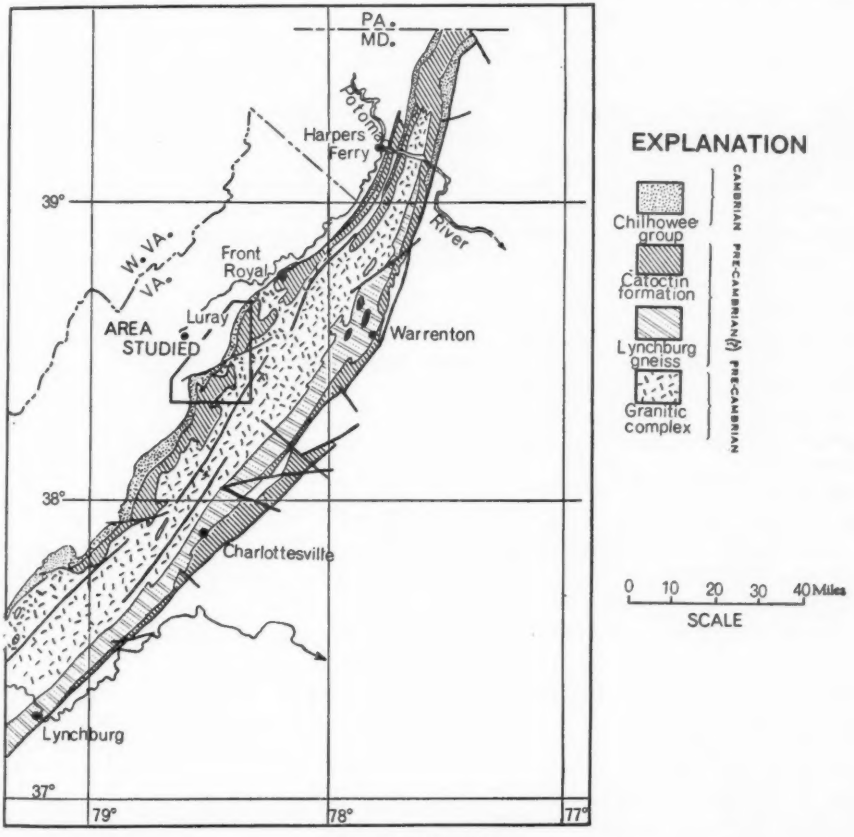

FIGURE 1.—INDEX MAP

The Catoctin Mountain-Blue Ridge anticlinorium in Maryland and northern Virginia; modified from Jonas and Stose, 1939

Because of its widespread distribution in the Blue Ridge province, the Catoctin formation is an important reference horizon in attempts to correlate the thick sequence of crystalline schists, marble, and quartzite (Glenarm series) of the Piedmont with the better known stratigraphic column of the Appalachians west of the Blue Ridge. A number of possibilities exist; some of these are illustrated in Figure 2. The older interpretation assumed that both the possibility is that the Chilhowee group overlies the Catoctin formation without unconformity, and that the Catoctin is therefore either early Cambrian or late Precambrian, while the Glenarm series is an eastern facies of the Cambrian and Ordovician sediments which has undergone a higher degree of metamorphism (Fig. 2B). A third interpretation, proposed by Bloomer (1950) is that the Catoctin interfingers with the Wissahickon schist (an important unit in the

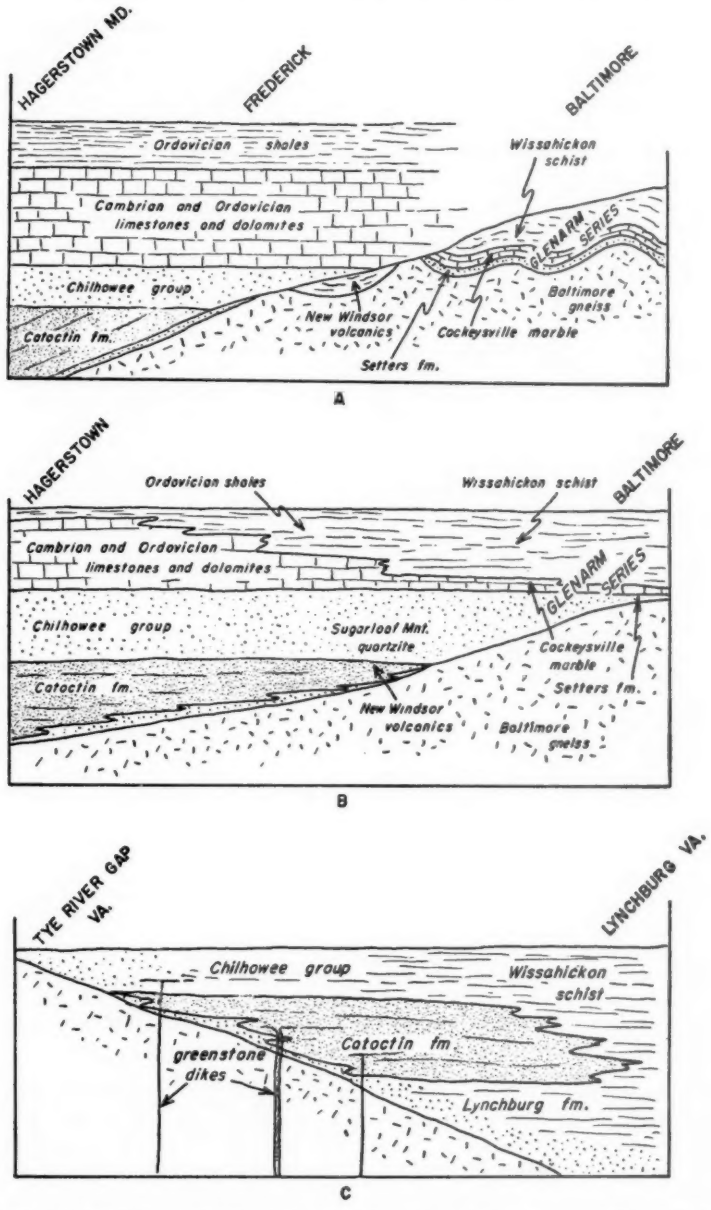

FIGURE 2.—POSSIBLE STRATIGRAPHIC RELATIONSHIPS OF THE CATOCTIN FORMATION

A. Catoctin formation and Glenarm series Precambrian; modified from Swartz (1948)

B. Catoctin Cambrian or Precambrian, Glenarm series Cambrian and Ordovician; modified from Swartz (1948)

C. Catoctin and Glenarm both Cambrian or Precambrian; modified from Bloomer and Bloomer (1947)

Glenarm series), whereas the Lynchburg formation, a thick sedimentary series underlying the Catoctin near Lynchburg, Virginia, grades upward into the Glenarm series in areas where the Catoctin is absent (Fig. 2C).

Detailed studies of the stratigraphic relationships and origin of the Catoctin may have a bearing not only on the geologic history of the Blue Ridge province but also on the larger problems of the position of the lower boundary of the Paleozoic in the Appalachians and the age of the Glenarm series.

The Catoctin is here considered in a limited area in the Blue Ridge in northern Virginia, on the western limb of the Catoctin Mountain-Blue Ridge anticlinorium. In an effort to determine the original character of the lavas and their mode of eruption, petrology and primary structures of the Catoctin greenstones are emphasized as are the stratigraphic relationships of the Catoctin formation to the overlying and underlying rocks.

Area Studied

The area described lies in the Blue Ridge province of northern Virginia about 50 miles southwest of Harpers Ferry and 70 miles west-southwest of Washington, D. C. Most of this area lies within the Shenandoah National Park. The maximum relief is about 3900 feet from the floor of the Page Valley to the crest of the Blue Ridge. The country is heavily wooded except where former farm lands have been included within the park area. The Skyline Drive furnishes easy access to many parts of the area, and more remote sections can be reached from fire roads and trails.

The Catoctin greenstones and interbedded sedimentary rocks are well exposed on the steep western slopes of the Blue Ridge and in the deep stream canyons on the gentler eastern slopes. Large talus slopes and boulder trains cover many mountainsides. Most of them are completely overgrown with large trees, but a few talus slopes may be currently active on a small scale. The boulder trains extend far down into the stream valleys where they blend into or overlie the normal valley fill. Many of the boulders are 20 feet or more in diameter and some of them must have been transported several miles. A periglacial climate during Pleistocene time might account for the development of boulder trains and talus slopes.

A total of 22 weeks was spent in the field in the summer of 1952 and the summer and fall of 1953.

Acknowledgments

The field work was supported in part by a predoctoral fellowship from the National Science Foundation. Members of the National Park Service were co-operative during the course of the field work. Paul G. Favour, Thomas Norris, and Carl Stoddard were particularly helpful and their continued interest is much appreciated.

Ernst Cloos and A. C. Waters of the Johns Hopkins University made valuable suggestions and accompanied me on several trips to the area. Assistance in the preparation of the illustrations and typing of the manuscript was received from Margaret L. Keister and Shirley Jackson of the Potomac Appalachian Trail Club. R. E. Fellows first suggested the problem.

General Geology of the Luray Area

Structural Setting

The major structural feature of the Blue Ridge in northern Virginia is a large asymmetrical anticline trending north or northeast. The eastern limb of the fold is gently dipping; the western limb is vertical or overturned (Pl. 1). In the Luray area most of the crest of the Blue Ridge is capped by greenstone of the Catoctin formation in the upper limb of the anticline, but 5 miles between Thornton Gap and Stony Man the Catoctin formation has been removed by erosion, and the underlying granitic gneisses form the crest of the ridge. The steep western limb of the fold is marked by a series of low foothills composed of resistant rocks of the Catoctin formation and lower Cambrian quartzites with bedding vertical or overturned to the east. In the area between Ingham and Big Meadows the gentle upper limb of the anticline has smaller folds superimposed and is complicated by the wedging out of the Catoctin beneath the Cambrian sediment. The anticline is cut by

several high-angle faults (Pl. 1). The Stanley fault, which cuts the structure diagonally, brings the lower Cambrian sedimentary rocks into contact with the plutonic basement rocks—a relationship that in the past has been explained as due to a major overthrust along the western foot of the Blue Ridge. No such overthrust is believed to be present in the Luray area or in the Elkton area to the south described by King (1950).

Between Tanners Ridge and U. S. Highway 211, granitic basement is exposed over wide areas on the western slopes of the Blue Ridge in the core of the anticline. On the gentle eastern limb of the structure the Catoctin is cut off by steeply dipping faults which bring up the granitic basement in the peaks of Oventop, Hazel Mountain, and Old Rag Mountain to the east of the main Blue Ridge.

The pattern of cleavage and lineation in the Catoctin formation and Chilhowee rocks is closely related to the anticlinal structure and conforms to the pattern in the rest of the Catoctin Mountain-Blue Ridge anticlinorium. Cleavage strikes north or northeast and dips to the southeast; dips of 50° or 60° are common on the eastern limb, whereas dips of 30° or 40° predominate on the overturned western limb of the anticline. Local variations in the dip of the cleavage are related to differences in lithology or to fanning in subsidiary folds. Lineation lies in the cleavage plane and plunges down the dip to the east or southeast, normal to the fold axes. In the sedimentary rocks it is marked by the elongation of phyllite fragments, parallel orientation of minerals, or a faint grooving of the cleavage planes. In the volcanic rocks it is marked by parallel orientation of chlorite blebs which represent mashed amygdules.

Slickensiding on bedding planes and flow surfaces normal to the fold axes was found in a few places, indicating that flexure folding, as well as shear folding, played a part in the deformation of the area.

Rocks Underlying the Catoctin Formation

General character.—Two major lithologic types were recognized in the granitic basement underlying the Catoctin formation. The first of these, mapped as hypersthene granodiorite on the geologic map of Virginia (Stose *et al.*, 1928), is exposed chiefly along the crest of the Blue Ridge and on the western flank of the mountains; the second, designated the Old Rag granite by Furcron (1934) for exposures on Old Rag Mountain, is exposed in the area east of the crest of the Blue Ridge.

The hypersthene granodiorite is an altered medium- to coarse-grained granitic rock, light greenish gray where fresh, weathering to light brownish gray or white. The rock is composed of plagioclase, quartz, hypersthene, biotite, chlorite, magnetite, and garnet with minor amounts of epidote and albite. The chlorite forms dark-green patches, probably derived from alteration of ferromagnesian minerals. The feldspars are generally greenish white although where alteration has been minor they may be clear and show twin striations. The texture is hypidiomorphic granular; the average grain size is 0.5–2 cm. In most places shearing has shattered the feldspars and mashed the chlorite clots.

Most of the granodiorite exposed on the western slopes of the Blue Ridge is only faintly foliated. Along the Skyline Drive between Hughes River Gap and Thornton Gap the granodiorite is well foliated, the foliation being defined by parallel clots and layers of light and dark minerals from 1 mm to 10 cm thick. Augen structure is well developed locally. In some types the dark minerals are in parallel spindle-shaped clots which give the rock a spotted appearance where broken across the lineation. A few pegmatitic stringers and pods lie parallel to the foliation in the gneissic facies of the granodiorite. At several places along U. S. Highway 215 east of Thornton Gap gneissic granodiorite contains layers composed of quartz. Locally, hydrothermal alteration of the granodiorite has produced a rock composed of epidote, pink feldspar, and blue quartz, called unakite. Jonas and Stose (1939) have suggested that the granodiorite is at least in part derived from granitization of a sedimentary series.

The Old Rag granite of Furcron is considerably coarser-grained than the hypersthene granodiorite; individual feldspars are up to 3 cm long. The only abundant minerals are milky-white unstriated feldspar and dark-gray or blue smoky quartz. A very small amount of chlorite is present, but no primary ferromagne-

sian minerals remain. The rock commonly is light gray or white; foliation is defined by parallel stringers or elongate patches of dark quartz. Along faults the Old Rag granite is commonly intensely sheared and in places is reduced to a fine-grained white mylonite.

of the Catoctin formation rest on an eroded surface of granodiorite and granite with a relief of as much as 1000 feet. Valleys in the erosion surface contain a layer of clastic sediments up to 150 feet thick beneath the greenstone. In other places the sediments may be only a few inches

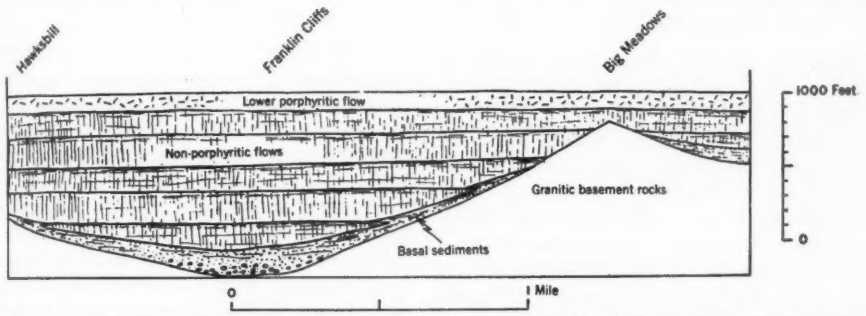

FIGURE 3.—STRATIGRAPHIC RELATIONSHIP OF THE CATOCTIN FORMATION TO GRANITIC BASEMENT ROCKS
The relationships along the western edge of the Catoctin outcrop area between Hawksbill and Big Meadows

The contact between the granodiorite and the Old Rag granite is gradational over a distance of several miles. Near the transition zone the granodiorite takes on a gneissic character which is finer-grained and much richer in biotite. Garnet seems to be confined exclusively to this zone. Dikelets and pods of blue-quartz granite similar to the Old Rag granite occur in gneissic granodiorite at several places along Skyline Drive on the flanks of Marys Rock and along the fire road west of Skyland.

The foliation or layering of the granitic rocks is rudely parallel to the cleavage in the overlying Catoctin formation over wide areas, but locally there is a distinct divergence between the two structures. A faint fracture cleavage in the basement rocks in many areas is believed related to the cleavage in the overlying rocks.

Pebbles of foliated granodiorite in the basal sedimentary member of the Catoctin formation show that the foliation of the basement rocks antedated the deposition of the Catoctin sediments. The fracture cleavage in the basement rocks was probably formed at the same time as the cleavage in the Catoctin and overlying rocks. The low-grade metamorphism of the basement rocks probably dates from this period.

Relation to the Catoctin formation.—The flows

thick. Hills of granitic rocks buried in the Catoctin and exposed in valleys of Whiteoak Run and Rose River superficially resemble stocks, but a widespread basal sedimentary layer surrounding them contains pebbles of gneiss and granite, showing that the contact is sedimentary.

Figure 3 shows the relationship of the basal sedimentary member of the Catoctin formation to the pre-Catoctin erosion surface as exposed on the western slopes of the Blue Ridge between Hawksbill Mountain and Big Meadows. The diagram is based on a series of well-exposed sections from the base of the lowest porphyritic flow in the Catoctin to the base of the formation. The flood-like character of the lavas and the thickening of the basal sedimentary member in the lower areas in the pre-Catoctin surface are well illustrated in this area. These relationships are typical of those observed wherever the bottom contact of the Catoctin formation was examined.

Several authors have described localities at which they believe granitic rocks intruded the Catoctin. The writer has not been able to find the exposures described but has seen several places in which a hurried examination might suggest this relationship. In every case this appearance is due either to the intersection of an

irregular contact with an outcrop surface in such a way as to simulate blocks of greenstone included in granite, or else to a network of sedimentary dikes of arkose which might be confused at first glance with dikes of granite injecting the greenstone.

Rocks Overlying the Catoctin Formation

General character.—The lower Cambrian sedimentary sequence has been well described in other areas in northern Virginia and Maryland (King, 1950; Stose and Stose, 1946; Cloos *et al.*, 1951) and only a general description is necessary here. With the exception of the Shenandoah salient and a few small areas around Chapman Mountain on the south and Neighbor Mountain on the north, all the Chilhowee exposures in the area studied are confined to the nose and lower limb of the Blue Ridge anticline where shearing has been intense and outcrops are poor. The Weverton and Harpers formations have been grouped together and mapped as a single unit in Plate 1. The lower beds (equivalent to the Weverton formation) are coarse-grained, thick-bedded, ferruginous quartzites and graywackes, commonly dark-gray, brown, purple, or bluish with color banding parallel to bedding. Scattered quartz pebbles are common and cross-bedding is present in many exposures. Dark-colored slaty interbeds are common. These beds grade upward into a poorly exposed sequence of buff or light-gray sandy phyllite and argillite with thin quartzite beds representing the Harpers formation. Bedding in the Harpers formation is obscured by cleavage except where competent quartzite beds are present. The upper part of the formation is characterized by jet-black, blue, or purple quartzite beds in the phyllite sequence. The thickness of the lower Chilhowee measured by the writer along U. S. Highway 211 is about 2300 feet; in the Shenandoah salient and in the Elkton area just to the south, King found the thickness to be between 1900 and 2500 feet.

The Antietam quartzite is a medium- to fine-grained sugary-white vitreous orthoquartzite forming prominent cliffs and ledges in areas where it has not been completely shattered during deformation. Where shattering has been intense outcrops of the Antietam are rare, and the ground is littered with quartzite fragments a few inches in diameter. The upper part of the formation contains abundant *Scolithus* tubes oriented normal to bedding, but they are absent in the lower part. Megascopic cleavage is poorly developed and bedding is obscure in many outcrops. According to King (1950) the Antietam is about 800 feet thick in the Elkton area; no reliable estimate was made in the Luray area. It passes upward through a few feet of shaly beds into the Tomstown dolomite of well-established early Cambrian age which marks the bottom of the great Cambrian and Ordovician carbonate sequence of the Appalachian Valley.

Relation to the Catoctin formation.—The contact between the Catoctin formation and the overlying sedimentary beds is marked by a layer of purple or blue slate up to 150 feet thick which was mapped by King (1950) as the Loudoun formation in the Elkton area. The volcanic nature of this rock is clear; it contains numerous amygdules and in thin section shows a relic basaltic fabric. Furcron and Woodward (1936) have described this as an altered rhyolite flow, but the fabric and composition indicate that it is more probably derived from an andesite or basalt. Its petrographic character will be discussed in more detail, but its stratigraphic relations have an important bearing on the relation of the Catoctin formation to the overlying rocks. In the western part of the Shenandoah salient the greenstone of the Catoctin is absent and the purple slate lies directly on granodiorite. Still farther to the west the slate is absent and the basal beds of the Chilhowee rest directly on faintly foliated coarse-grained granodiorite. The purple slate is thus present in several places where the greenstone is absent. Furcron and Woodward consider this to be due to an angular unconformity beneath the Chilhowee and the purple slate. However, as no discordance was noted between the Catoctin and Chilhowee the writer prefers to attribute the relationship to overlap of the Catoctin formation on a topographic high of basement rocks; the purple slate can then be assigned to the Catoctin formation where its volcanic character and similarity to other rocks in the volcanic sequence seem to indicate that it belongs.

Along the Skyline Drive about 4 miles north of Thornton Gap, the slate is absent, and the

basal quartzite of the Chilhowee contains rounded cobbles of fine-grained massive Catoctin lava, indicating erosion preceding deposition of the Chilhowee sedimentary rocks. However, evidence of a major unconformity is lacking. Cloos *et al.* (1951) report that volcanic rocks are interlayered with the Chilhowee sedimentary rocks in some areas in Maryland and that conglomerates at the base of the Weverton formation contain phyllitic lenses elongated parallel to the cleavage of the enclosing rock. If their phyllitic character were the result of deformation preceding the deposition of the conglomerate, the elongation should be parallel to bedding, not to cleavage. Bloomer (1950) has pointed out the similarity of the volcanic rocks of the Catoctin to the volcanic flows within the Chilhowee group near Tye River Gap and the James River as evidence that no major erosion interval occurred.

General Character of the Catoctin Formation

In the Luray area, most of the Catoctin formation consists of greenstone altered from lava flows by low-grade regional metamorphism. Sedimentary members are common but not extensive, and none of these interbeds is more than 40 feet thick, although the basal sedimentary layer locally reaches 150 feet. The greenstone is green, blue, purple, or gray and generally so fine-grained that only chlorite and epidote can be recognized with the hand lens. Porphyritic varieties with plagioclase phenocrysts up to 1 cm. long are present in several places in the greenstone sequence. In thin section the chief minerals of the greenstone can be identified as albite, chlorite, epidote, actinolite, and sphene, with minor amounts of pyroxene, magnetite, hematite, and ilmenite. Most exposures show a well-developed cleavage, but cleavage is absent in some places. Primary structures such as amygdule bands, columnar and platy jointing, and sedimentary dikes are preserved where deformation has not been intense. Flow breccias are common. Veinlets of epidote, milky quartz, and anthophyllite cut the greenstone in many places. Complete replacement of greenstone by irregular pods and veinlets of epidote and quartz has formed yellowish-green epidosite which is very common in some areas. Sedimentary members of the formation are mostly arkoses, graywackes, and conglomerates derived from the underlying granitic rocks and sericite phyllites which may be derived from volcanic ash layers.

Investigation of the Catoctin formation was concentrated in the southern half of the Stony Man quadrangle where excellent exposures of the volcanic sequence occur along the crest of the Blue Ridge between Stony Man and Big Meadows. Here the Catoctin formation lies on the upper limb of the Blue Ridge anticline where deformation has been at a minimum. North of Thornton Gap the Catoctin was not studied in detail.

Catoctin Formation in the Big Meadows-Stony Man Area

General Structure

The general attitude of the formation was determined by tracing the basal sedimentary member and two coarsely porphyritic flows in the volcanic sequence. None of the sedimentary interbeds is continuous enough to serve as a marker horizon.

The structure of the formation is simple. North of the Rose River the porphyritic flows and the sedimentary members show a homoclinal dip of 15–20° E.-SE. The western boundary of the formation is the outcrop of the pre-Catoctin erosion surface and is marked by a few inches to 150 feet of sediments containing pebbles of the underlying granodiorite. On the east the formation is cut off by a steeply dipping fault along which the Old Rag granite is intensely sheared and in places reduced to a dense white mylonite. There is a reversal of dip of the Catoctin formation near this fault.

At least two minor faults cut the formation in this area. One extends from Hawksbill Gap down Cedar Run; the other goes through Franklin Cliffs and down the valley of Rose River. They are commonly marked by zones of anomalous northwest-trending cleavage.

In the Big Meadows area, south of the Rose River, the dip of the Catoctin is 10°–15° S. Southwest of Big Meadows the greenstone crops out for several miles down Tanners Ridge. There the structure is a gentle anticline on the upper limb of the main Blue Ridge fold. Poor exposures and more intense shearing make it

impossible to trace the porphyritic flows in this area, but the anticlinal structure is indicated by the lower contact of the formation on the north slopes of Tanners Ridge. The top of Chapman Mountain, just south of Tanners Ridge, is capped by several hundred feet of flat-lying lower Chilhowee sedimentary rocks on the crest of the subsidiary fold. They are underlain by 50–150 feet of purple, red, or blue volcanic slate. The entire thickness of the greenstone in that area is only about 500 feet, as compared with at least 1800 feet at Big Meadows, where the top of the formation has been removed.

Throughout the Big Meadows-Stony Man area cleavage strikes north or northeast and dips 30°–60° E., except near faults. Lineation plunges east or southeast down the dip of the cleavage planes in the "a" direction; it is marked by dark-green elongate chlorite blebs, faint striations on the cleavage, parallel orientation of actinolite needles in greenstone and by elongated phyllite fragments in sediments.

Sedimentary Members

The sediments associated with the greenstones of the Catoctin formation occur both at the base of the sequence and in thin interbeds between flows. The sediments locally form clastic dikes penetrating overlying and underlying flows.

Jonas and Stose (1939) described a sedimentary layer near the base of the greenstone near Swift Run Gap which has later been called the Swift Run formation. Bloomer and Bloomer (1947) recognized similar sediments near Rockfish Gap and named them the Oronoco formation. In the Big Meadows-Stony Man area a sedimentary layer occurs beneath the lowest flow, but because it is discontinuous and closely related to the sediments interbedded with the overlying greenstones, it is not considered here as a separate formation.

The basal sediments of the Catoctin formation are mostly poorly sorted arkoses, conglomerates, and graywackes (Pl. 3, figs. 1 and 2). The graywackes contain angular to subrounded grains of glassy quartz and feldspar 0.1–3 mm in diameter in a grayish-green phyllitic matrix of sericite and chlorite. This matrix material makes up 20–50 per cent of the rock. Conglomerates with pebbles and cobbles of vein quartz and underlying gneisses in a matrix of graywacke are common. Pink, green, and gray phyllite fragments and small greenstone fragments occur locally. Detrital magnetite and hematite are common.

The arkosic sediments are composed principally of angular to subrounded grains of clear quartz and white feldspar with a small amount of matrix material, mainly epidote; most arkoses are better sorted than the graywackes and many are cross-bedded. Where the basal sediments are thick they are generally graywackes or conglomerates; where they are thin they are arkoses or phyllites.

Near the head of Hawksbill Creek west of Big Meadows the basal Catoctin sedimentary rocks are about 100 feet thick and consist of graywacke and purple phyllite interbedded with finely laminated gray argillite. Each lamination in the argillite grades upward from the light-greenish-gray layer of coarse siltstone to a dark-gray argillite layer. The upper contact of the argillite layer is sharp and is overlain by the coarse silt layer of the next couplet of laminations. Thiesmeyer (1939) has described slates with similar laminations from Fauquier County, Virginia. He assigned them to the Loudoun formation, apparently on the basis of Keith's geologic map of the Harpers Ferry quadrangle (Keith, 1894a), but a brief visit to his locality indicates that these sediments are probably part of the basal Catoctin sedimentary rocks. Thiesmeyer gives an excellent description of the structures and concludes that they are freshwater varves, possibly related to glaciation. Although the general appearance of the laminations near Big Meadows and the gradation from coarse light-colored material at the bottom of each set to fine dark material at the top are very suggestive of glacial varves, no striated pebbles or rafted grains have been found associated with them, and a glacial origin is therefore unproven.

At many places the lower contact of the basal sediments is obscure. Graywackes with angular detrital grains grade downward into slightly sheared and altered gneiss with angular quartz and feldspar grains in a matrix of chlorite and sericite derived from alteration of some of the feldspars and the ferromagnesian minerals.

Fifty or 100 feet below the sediments the gneiss is fresh and contains large feldspar and quartz grains with little sericite. This effect may be due to weathering of the gneiss on the pre-Catoctin erosion surface, and much of the overlying sediment may be only slightly reworked from this weathered mantle.

The basal sedimentary layer of the formation has a well-developed cleavage and lineation marked by flattened and elongated phyllite fragments and parallel orientation of micaceous minerals. Quartz pebbles in the conglomerates are not visibly deformed, but their surfaces commonly have fine striations parallel to the lineation of the enclosing rock caused by flowage of the matrix. Banding in the granodiorite pebbles in the sediments is not parallel to the cleavage of the enclosing rock.

The pre-Catoctin erosion surface has more than 1000 feet of relief along the western boundary of the Catoctin outcrop area between Big Meadows and Stony Man. The thickest sections of the basal sedimentary rocks occur near the low areas in the erosion surface, indicating that this relief is not due to later deformation (Fig. 3). In two places streams have cut through Catoctin rocks and exposed hills of granitic rocks in the erosion surface which were flooded beneath the Catoctin lavas. The hill in Whiteoak Canyon had a relief of 450 feet, while the one in Hogcamp Branch was at least 750 feet high.

The sediments between the lava flows are similar petrographically to the basal sediments but are not extensive and are commonly only a few inches thick. Phyllites in the interbedded sediments are common. They are generally gray but may be green, blue, or purple and contain few detrital grains. Phyllites of different colors are interbedded within a single outcrop and they may show complex interfingering relationships. They are composed almost exclusively of sericite and probably were derived from alteration of volcanic-ash layers.

Volcanic Flows

In several places it has been possible to recognize and map individual flows within the greenstone sequence. At Franklin Cliffs, Crescent Rocks, on Stony Man, and in Whiteoak Canyon massive greenstone layers form series of cliffs up to 150 feet high separated by talus-covered benches (Fig. 4). Near the top of each cliff the greenstone is schistose, but a few feet down it is massive and irregularly jointed. Locally columnar jointing is well developed. Low-dipping joint sets similar to the flat primary joints in recent lava flows are commonly present, especially just below the schistose upper zone. The rock in the schistose layers is commonly a highly sheared breccia with fragments of amygdaloidal greenstone, silver phyllite, and aphanitic red argillite. The matrix is either epidote, greenstone, or phyllite. Locally thin beds of sandstone occur in the sheared zones between the greenstone layers. The character of these breccias may not be apparent except on polished surfaces of hand specimens.

The sheared zones mark boundaries between lava flows, and probably represent surface breccias, scoriaceous zones, soil horizons, and thin sedimentary beds at the top of one flow developed before extrusion of the next flow. Loose blocks of lava and pieces of sediment torn up and churned into the base of the succeeding flow during its advance also make up part of the breccias. Deformation was concentrated at the flow boundaries, which left the greenstone near the centers intact and permitted preservation of primary structures in many places.

In sections at Franklin Cliffs and Crescent Rocks, both of which expose the lower three flows, all but one flow have a thickness between 150 and 200 feet. The second flow at Franklin Cliffs is about 270 feet thick (Fig. 4). Northwest of Big Meadows seven flows have a total stratigraphic thickness of 1500 feet, an average thickness of 215 feet each.

It is generally difficult to trace an individual flow in the greenstone sequence because of the lack of continuous exposures, but the two porphyritic flows can be easily traced in float and therefore furnish excellent horizon markers.

Because the pre-Catoctin erosion surface is irregular the stratigraphic interval between the lowest of the porphyritic flows and the base of the Catoctin formation varies. On Hawksbill Mountain the lowest prophyritic flow is the sixth flow from the bottom of the formation. North of Big Meadows it is the fourth, and west of Big Meadows the second or third flow from the bottom. At the head of the Rose River

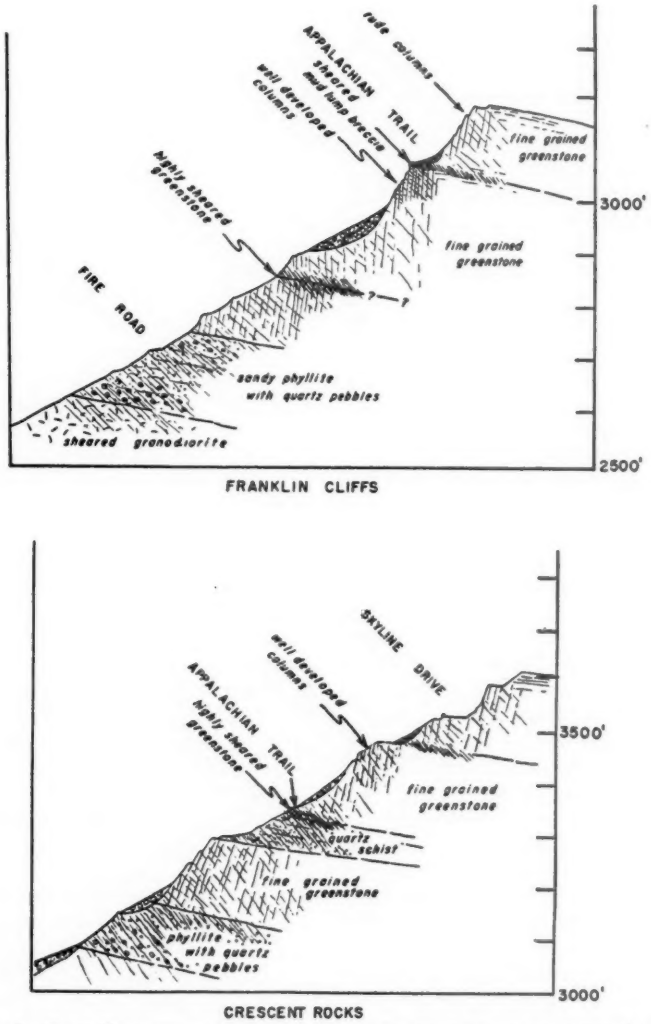

FIGURE 4.—CROSS SECTIONS OF THE LOWER THREE CATOCTIN FLOWS AT FRANKLIN CLIFFS AND CRESCENT ROCKS

the flow probably abuts against the granodiorite hill exposed in the canyon of Hogcamp Branch.

The flows below the lowermost porphyritic flow are the best exposed in the volcanic sequence. The greenstone of these flows is fine grained and generally nonporphyritic, although sparse small plagioclase phenocrysts are present locally. Interbedded phyllitic sediments are common. Columnar jointing is well developed in one flow and distinguishable in several others. Flow boundaries exposed in the cliffs are marked by intensely sheared zones of volcanic breccia. Most of the primary structures described below are best observed in this group of flows.

The greenstone of the lower porphyritic flow has a medium- or coarse-grained groundmass with plagioclase crystals about 1 mm long. The plagioclase phenocrysts (now albite) are 5 mm-

1½ cm long and make up 15–30 per cent of the rock. They generally occur individually or in groups of two or three, but may be collected in clots of five or ten. The flow has been traced for more than 6 miles, though its position is indefinite in areas where outcrops are poor or where epidotization or intense shearing have obscured the porphyritic character. The flow commonly forms cliffs even where exposures of the other flows are poor. On Tanners Ridge southwest of Hawksbill Creek the flow could not be traced because of poor outcrops and intense shearing. The porphyritic character becomes less distinct to the north near Stony Man. The flow must have covered an area of at least 15 square miles.

The upper porphyritic flow lies between 400 and 800 feet stratigraphically above the lower. From three to five flows may be present between the two porphyritic flows. The greenstone between the porphyritic flows is slightly coarser-grained than that below the lower porphyritic flow; groundmass feldspar laths may reach several mm and scattered phenocrysts up to 1 cm long occur locally. Sedimentary interbeds are sparse in this part of the formation. The upper porphyritic flow cannot be traced as extensively as the lower. In most outcrops this flow closely resembles the lower porphyritic flow, but its petrographic character is more variable. In some places the phenocrysts reach several cm in length and make up as much as 50 per cent of the rock. They tend to be concentrated in bands a few cm thick or in clots several cm in diameter.

The flows above the upper porphyritic flow are poorly exposed and the maximum number still preserved is undetermined. Much of this sequence consists of fine-grained and nonporphyritic greenstone, but coarse-grained types with scattered phenocrysts are common. A few sedimentary interbeds less than a foot thick occur. Approximately 700 feet of greenstone is preserved above the upper porphyritic flow on the slopes south of Spitler Hill. The Catoctin is at least 1800 feet thick in this area and the top has been removed by erosion. This is believed to be the maximum thickness preserved in the Big Meadows-Stony Man area.

Primary Structures

Introduction.—The preservation in the greenstone of some of the typical primary structures of more recent basalt flows is of interest both because these structures afford important clues to the origin of the greenstone and also because their preservation indicates the small amount of deformation which some of the rocks have undergone.

Columnar jointing.—A flow with unusually well-developed columnar jointing can be traced discontinuously near the bottom of the greenstone sequence from Big Meadows to Stony Man. The columns are approximately a foot in diameter and as much as 20 feet long (Pl. 2, fig. 1). The faces of the columns are commonly marked by faint grooves normal to the axes, but ball and socket joints across the columns have not been observed. Most of the columns are broken along cleavage planes. In most exposures of this flow the axes of the individual columns are parallel, but in a few places, for example at Crescent Rocks, the axes are curved and randomly oriented.

Many flows show rude columnar jointing; generally the columns are 2 or 3 feet in diameter and considerably shorter than those in the flow just described. No good example of two-tier columnar jointing was found, but some flows have large columns near the base and smaller ones near the top.

The axes of the columns are no longer perpendicular to the flow boundaries but plunge to the south or southeast, making an angle of as much as 50° with the normal to the flow surface. Figure 5 is an equal area projection of the axes of columns in the southern part of the Stony Man quadrangle. The poles of cleavage planes and lineations in the same area are summarized in Figure 6. The close geometric relationship between these structures indicates a probable genetic connection, and the regional plunge of the column axes is interpreted as being due to the deformation which produced the cleavage and lineation. The inclination of the axes is due to movement of the upper ends of the columns to the west or northwest with respect to the lower parts, and this direction of relative movement is the same as that indicated by drag on the cleavage planes at flow boundaries and slickensiding on bedding planes in sediments.

Many of the columns are flattened parallel to a plane determined by the long axes of the columns and the intersection of the flow surfaces and the cleavage.

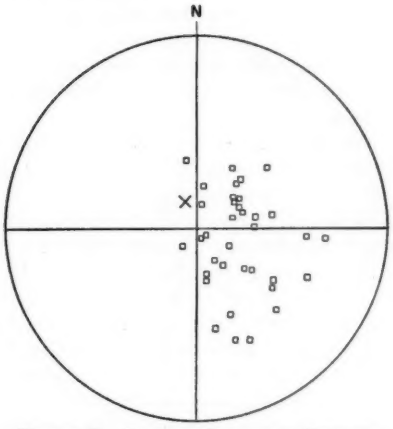

FIGURE 5.—AXES OF DEFORMED COLUMNS

Equal area projection on lower hemisphere of axes of deformed joint columns in the Big Meadows-Stony Man area. Cross indicates pole of average attitude of bedding in sedimentary members of Catoctin formation.

Low-dipping primary joints.—Many greenstone exposures have a prominent low-dipping joint set which gives the outcrops a steplike appearance. Figure 7 is a plot of the poles of these joints in the Big Meadows-Stony Man area. Poles of bedding in sedimentary rocks associated with the flows are plotted for comparison. The close parallelism between these structures indicates that the joints are related to flow surfaces and that they may be used in the field to determine the approximate attitude of the flows. They are probably analogous to the original joints parallel to flow surfaces common in recent basalt flows. The joints are spaced anywhere from a few inches to several

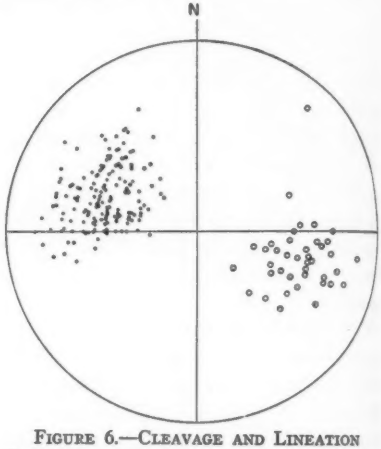

FIGURE 6.—CLEAVAGE AND LINEATION

Equal area projection and "a" lineations (open circles) of poles of cleavage (solid dots) in the Big Meadows-Stony Man area

feet apart and are most pronounced near the top of a flow. Farther down in a flow they are generally absent.

Amygdules.—Amygdules occur in almost every greenstone outcrop, and are especially abundant in zones near flow tops. The characteristic minerals in the amygdule fillings are milky quartz, epidote, albite, calcite, and chlorite (Pl. 2, figs. 2 and 3). An amygdule may be filled with a single mineral or with several minerals in concentric layers or irregular intergrowths. Epidote, quartz, and albite are com-

PLATE 2.—PRIMARY STRUCTURES OF THE CATOCTIN FORMATION

FIGURE 1.—COLUMNAR JOINTING

Near top of the second flow above the base of the formation at Franklin Cliffs, about 40 feet below the Appalachian Trail

FIGURE 2.—AMYGDULES

Typical amygdules in greenstone; albite rims (white) surround cores of epidote (dark); 200 yards south of Whiteoak Canyon parking overlook, Skyline Drive

FIGURE 3.—CHLORITE AMYDGULES

Chlorite with faint radiating structure surrounds open cavity at top of amygdules; probably chlorite has replaced original chlorophaeite; lower porphyritic flow at altitude 3000 north of Big Meadows; (plain light, ×11)

FIGURE 4.—PORPHYRITIC GREENSTONE

White plagioclase phenocrysts and dark chlorite amygdules in lower porphyritic flow; mile 47.35, Skyline Drive

FIGURE 1

FIGURE 2

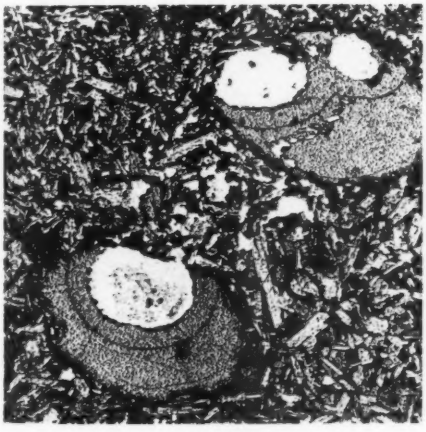

FIGURE 3

FIGURE 4

PRIMARY STRUCTURES OF THE CATOCTIN FORMATION

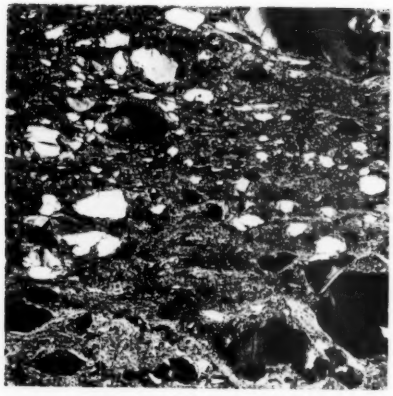

FIGURE 1

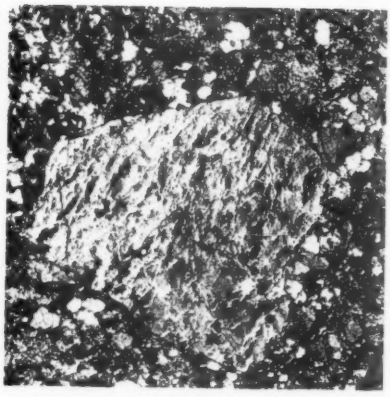

FIGURE 2

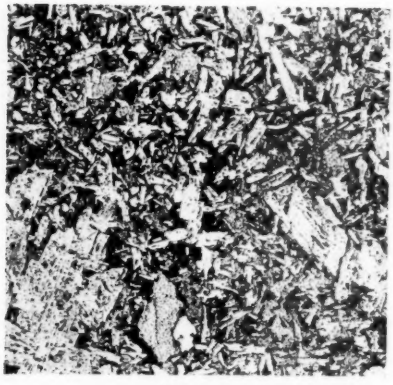

FIGURE 3

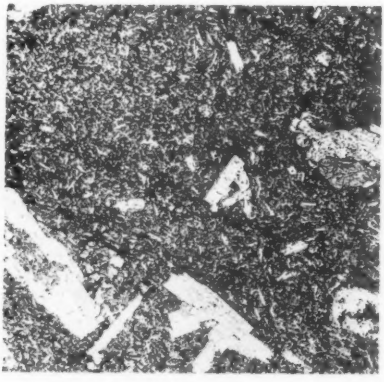

FIGURE 4

FIGURE 5

FIGURE 6

PHOTOMICROGRAPHS

monly associated in the amygdule fillings. Chlorite and albite are common associates, albite forming the rim and chlorite the core of the amygdule. Chlorite occurs alone in some amygdules. Chlorite-filled amygdules appear in the same outcrop as epidote-quartz amygdules.

In thin section the chlorite filling commonly shows an outer layer composed of a fibrous aggregate of chlorite in which the long axes of the fibers are perpendicular to the walls of the amygdule. The core is composed of a structureless aggregate of chlorite of the same color and birefringence. This relationship is similar to that in chlorophaeite amygdules in unaltered basalts, and the chlorite amygdule fillings may have been derived from chlorophaeite. Chlorite is a common metamorphic product of chlorophaeite; little change of composition is involved in the transformation.

Amygdules in the greenstone are generally ellipsoidal or almond-shaped where scattered but in the highly amygdaloidal zones they are irregular or amoeboid in outline. Some of the larger amygdules have rounded upper surfaces and flat bottoms parallel to the flat primary jointing. In some places the amygdules are arranged in layers which are probably related to flow planes in the lava.

Where a pronounced cleavage has developed the quartz and epidote-filled amygdules are little deformed, but the chlorite amygdules are streaked out into dark-green blebs which are aligned down the dip of the cleavage planes.

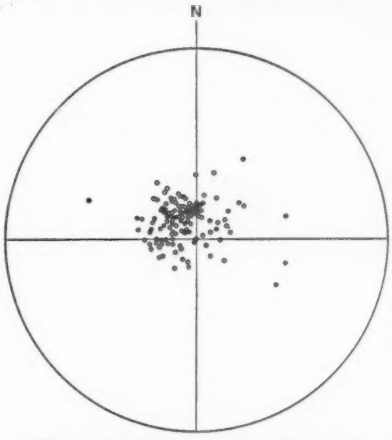

FIGURE 7.—POLES OF FLAT PRIMARY JOINTS IN GREENSTONE

Equal area projection of poles of flat primary joints (open circles) in greenstone and of bedding (solid dots) in sedimentary members of the Catoctin formation in the Big Meadows-Stony Man area.

Sedimentary dikes.—Interbedded sedimentary members of the Catoctin formation commonly show complex and confusing relations to the greenstone. Near the top of a flow, sediments from an overlying lens may extend down-

PLATE 3.—PHOTOMICROGRAPHS

FIGURE 1.—GRAYWACKE

Angular grains of strained quartz (probably derived from Old Rag granite) in matrix of sericite and chlorite; sedimentary interbed in the Catoctin formation at altitude 2000 above the Rose River 0.5 miles west of the Shenandoah National Park boundary; (X-nicols, ×4.5)

FIGURE 2.—CONGLOMERATE

Quartzite pebble in graywacke matrix in the basal sedimentary member of the Catoctin formation; foliated gneiss pebbles occur at the same locality; altitude 2500 below first hairpin turn in fire road west of Fishers Gap; (X-nicols, ×4.5)

FIGURE 3.—COARSE-GRAINED PORPHYRITIC GREENSTONE

Albite laths in matrix of secondary chlorite; lower porphyritic flow north of Big Meadows; (plain light, ×11)

FIGURE 4.—FINE-GRAINED PORPHYRITIC GREENSTONE

Plagioclase phenocrysts clouded with chlorite and zoisite and fresh pyroxene phenocrysts (center right) in matrix of plagioclase laths, chlorite and actinolite, lower porphyritic flow north of Hawksbill Gap; (plain light, ×11)

FIGURE 5.—ZONING IN PLAGIOCLASE

Core of crystal is about An_{62}, rim about An_{42}; float from dike at altitude 2680, Saddle Trail, Old Rag Mountain; (X-nicols, ×4.5)

FIGURE 6.—HOUR-GLASS STRUCTURE IN AUGITE

Dike just east of summit of Old Rag Mountain; (X-nicols, ×11)

ward along cracks 5 or 10 feet into the greenstone. These sedimentary dikelets are up to 3 inches wide and contain sediments similar to those immediately overlying the flow. They forming a network of sedimentary dikes. On polished surfaces the greenstone can be seen to be dark and aphanitic for a few mm away from the contact with the sedimentary rocks,

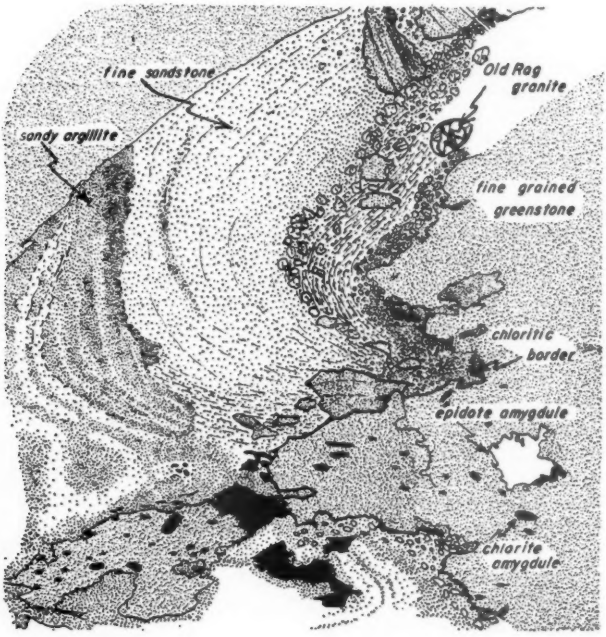

FIGURE 8.—SKETCH OF A PORTION OF SEDIMENTARY DIKE

Note thin chloritic border of the greenstone at the contact, the chlorite amygdules, and the pebble of Old Rag granite of Furcron in the sediment. Polished surface of specimen from 5 feet above contact of Catoctin formation and Old Rag granite at alt. 2000 feet on Nigger Run

probably represent sand and mud that sifted down into cracks soon after solidification of the flows.

Sedimentary dikes of a different type occur near the bases of some of the flows (Fig. 8). There sedimentary rocks project upward into the greenstone in a network of anastomosing veins which extend 10 or 15 feet above the base of the flow where they gradually die out in solid greenstone. These dikes were probably formed as a result of the advance of a flow over wet sediments. Steam pressure and the weight of the overlying lava would force the soft, unconsolidated sediments up into cracks in the abruptly chilled lava at the base of the flow, whereas farther away it is greenish gray and coarser-grained. The dark aphanitic border probably represents a thin selvage of glass formed when the lava came in contact with the wet sediments, but the glass has been devitrified to a dense, fine-grained aggregate consisting mostly of chlorite.

Flow breccias.—Flow boundaries are generally marked by zones up to 20 feet thick of breccia containing fragments of amygdaloidal greenstone, purple phyllite, and red or pink sandy argillite. Angular fragments of specular hematite are common in some of the breccias. The two most common types of breccia are "epidote-amygdaloid breccia" and "mud-lump breccia."

The "epidote-amygdaloid" type is composed of angular or irregular rounded fragments of purple, red, or blue-gray amygdaloid set in a matrix of quartz and epidote. The amygdules are filled with milky quartz. Fragments range from two inches up to several feet across. This breccia probably represents a scoriaceous crust formed on the lava flow and broken up by further movement of the still liquid lava beneath. Later hydrothermal solutions, finding especially easy access along these zones, have almost completely replaced the breccias with epidote and quartz.

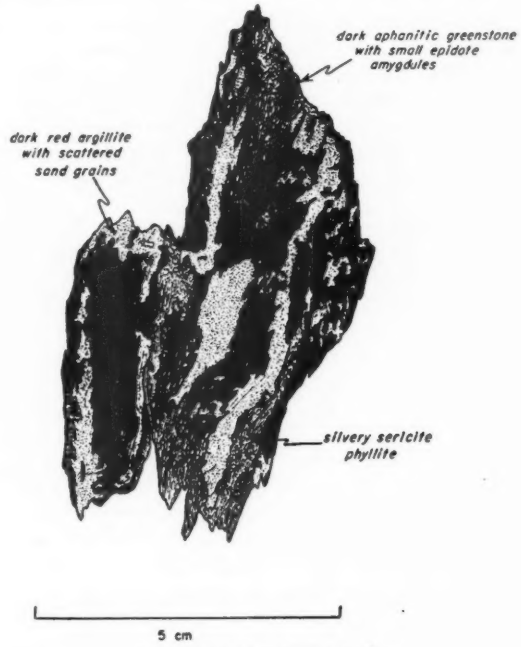
dark aphanitic greenstone with small epidote amygdules
dark red argillite with scattered sand grains
silvery sericite phyllite
5 cm

FIGURE 9.—MUD-LUMP BRECCIA

Sketch of sheared mud-lump breccia from base of third flow; north end of Little Stony Man Cliffs along Appalachian Trail

The "mud-lump" breccias consist of angular or subangular fragments of pink or reddish-brown sandy argillite or sandstone in a matrix of fine-grained schistose greenstone or silver phyllite and contain only minor amounts of epidote (Fig. 9). On slightly weathered surfaces the "mud-lumps" stand out in relief. Most are dense aphanitic pink or red rocks whose sedimentary character is not apparent except where thin sandy stringers are present or where there is a gradation from sandstone into aphanitic red argillite containing scattered sand grains. The "mud-lumps" may be pieces of a thin soil mantle or sedimentary layer developed on top of one flow and later churned into the base of the next flow. The red "mud" which formed the bulk of the sedimentary material may well have been derived from weathering of underlying lava; the sand grains, mostly quartz, must have been derived from some outside source, probably some nearby granitic hill still unburied by lava. The silvery phyllite probably represents tuffaceous material. In a few places thin layers of material similar to the "mud-lumps" are found undisturbed between flows, possibly indicating old soil horizons.

Petrography and Mineralogy of the Flows

Feldspar laths, chlorite, and epidote are seen with a hand lens in coarse greenstone, but in

the fine-grained greenstone none of the rock minerals can be identified megascopically. Native copper occurs in minute flakes at a few localities.

Some flows contain scattered phenocrysts of plagioclase, but phenocrysts are rare at most localities. At least two flows are coarsely porphyritic and contain plagioclase phenocrysts up to 1 cm long; the phenocrysts make up as much as 30 per cent of the rock and occur both singly and in glomeroporphyritic clots (Pl. 3, fig. 4). On freshly broken surfaces the phenocrysts may be obscure, but they weather bone white and are conspicuous on slightly weathered surfaces. The unusual porphyritic texture of these flows has made it possible to distinguish them from the other flows in the lava sequence and trace them for considerable distances.

The greenstone is commonly cut by veinlets of quartz and epidote which are also the typical minerals in the amygdule fillings. In many places the greenstone has been completely replaced by epidote and quartz, forming a hard yellowish-green epidosite. This rock is characteristically cut by narrow, nearly horizontal gash fractures containing quartz and fibrous anthophyllite. The veins are generally only a few mm thick, but reach several cm at a few localities.

The epidote-quartz rock occurs in large pods and irregular masses associated with epidote-quartz veinlets. The contact of these masses with the normal greenstone may be sharp, in which case it is usually a joint plane, or gradational over several inches. Where this type of alteration has occurred amygdules and plagioclase phenocrysts have been replaced by quartz.

Minor amounts of native copper appear in the greenstones of the Catoctin formation, and unsuccessful attempts at copper mining were made at several localities. Two prospects within the area were worked in 1854–56 and are described briefly by Weed and Watson (1906). One of these, located just north of the summit of Stony Man, was opened by a shaft of unknown depth which has now been filled. The other is on the nose north of the confluence of the Rose River and Hogcamp Branch in the zone of northwest-trending cleavage which is believed to mark the Rose River cross fault. Its workings comprise a few shallow prospect trenches and a shaft that is flooded to the surface. Judging from the size of the dump it is only a few feet deep.

In thin section, the chief minerals of the normal greenstone are seen to be chlorite, actinolite, epidote, albite, magnetite, specular hematite, sphene, and pyroxene. Small amounts of quartz and calcite are also common. Only the pyroxene and part of the magnetite are believed to be primary minerals of the original lava. The albite is pseudomorphic after the original calcic plagioclase.

The approximate modal compositions of several apparently typical greenstone specimens are given in Table 1. The compositions were determined by the point-count method, probably accurate only to within a few per cent since most of the rocks are fine-grained.

Where the greenstones are not sheared the texture is that of the original lava (Pl. 3, figs. 3 and 4). The rock consists of interlocking plagioclase laths (now albite) in an interstitial mat of chlorite, actinolite, epidote, sphene, leucoxene, and magnetite. Original pyroxene grains are common between the laths in some specimens, but in most of the finer grained rocks the pyroxene is almost completely altered. This texture suggests the typical basaltic textures in which the spaces between the plagioclase are filled with either granular crystals of pyroxene (intergranular) or basalt glass (intersertal). The present texture of the greenstone is probably the result of the alteration of the interstitial fillings between plagioclase laths to secondary minerals. Large irregular patches of chlorite are fairly common in the greenstone and some of them resemble the chlorophaeite patches of fresh basalts.

In most of the greenstones the groundmass plagioclase laths average about 0.05 by 0.4 mm; plagioclase phenocrysts in the porphyritic flows generally average less than a cm in length. The plagioclase laths are from 5 to 10 times as long as they are wide. Polysynthetic twinning is common, especially in the larger phenocrysts. The smaller plagioclase crystals do not contain more than one or two twin lamellae, but the larger phenocrysts contain several. Most plagioclase crystals are cloudy with minute

inclusions of zoisite or clinozoisite. No trace of zoning was noted in any of the crystals from the flows.

needles are oriented with their long axes parallel to the cleavage planes; other minerals do not show dimensional orientation. Rarely the relic

TABLE 1.—MICROMETRIC ANALYSES OF GREENSTONE OF THE CATOCTIN FORMATION
(in per cent)

Number	Albite	Chlorite	Epidote	Actinolite	Pyroxene	Ores	Talc	Quartz	Sphene and Leucoxene
1	27	14	3	12	18	7	1	1	.....
2	40	19	6	13	6	8	.....	.....	7
3	20	18	10	17	19	4	.....	.....	12
4	55	28	1	....	....	15	.....	1	.....
5	32	5	21	16	3	18	.....	1	4
6	6	24	10	12	22	4	8	3	10
7	29	23	21	5	3	6	.....	.....	14
8	32	19	10	11	9	9	.....	.....	10
9	42	18	23	4	....	7	.....	.....	5
10	24	7	12	21	7	10	.....	.....	18
11	21	39	4	18	....	10	.....	.....	8

1. Porphyritic greenstone, lower porphyritic flow north of Hawksbill Gap
2. Coarse-grained greenstone, lower porphyritic flow on south flank of Stony Man
3. Fine-grained greenstone, near top of second flow above base of the formation at Crescent Rocks
4. Porphyritic greenstone, lower porphyritic flow north of Big Meadows
5. Coarse-grained greenstone, alt. 2390 on north side of Rose River canyon near mouth of Hogcamp Branch
6. Fine-grained greenstone, mile 47.5, Skyline Drive, from flow beneath the lower porphyritic flow
7. Porphyritic greenstone, lower porphyritic flow, mile 47.4, Skyline Drive
8. Porphyritic greenstone, Whiteoak Falls fire road just below junction with Skyline Drive
9. Porphyritic greenstone, lower porphyritic flow on north side of Rose River near mouth of Hogcamp Branch
10. Porphyritic greenstone, upper porphyritic flow near summit of Spitler Hill
11. Fine-grained greenstone, abandoned quarry along Skyline Drive on south slope of Stony Man

The groundmass in the porphyritic greenstones is similar to the nonporphyritic types although commonly coarser-grained. The phenocrysts are either single or in clots of up to 10 crystals. By far the largest number of phenocrysts are plagioclase, but pyroxene phenocrysts are common. They are generally smaller than the plagioclase phenocrysts and in places are clustered around plagioclase crystals. Locally the phenocrysts make up as much as 30 per cent of the rock, but they are generally less abundant.

In the more schistose greenstone the original texture has been destroyed, and the rock consists of actinolite needles and equidimensional grains of epidote, sphene, and opaque minerals in a chloritic matrix. Small irregular grains of plagioclase are generally present. Actinolite

fabric can be detected in the orientation of a few ragged feldspar laths. The actinolite needles cut across this old fabric and many of them penetrate several plagioclase crystals. Pyroxene grains have survived in some specimens after almost all of the plagioclase has been altered.

The plagioclase was determined by universal stage methods in several thin sections and checked in other sections by measurements of extinction angles on the flat stage and by index of refraction determinations in crushed fragments. All determinations indicate a plagioclase well within the albite range, usually less anorthitic than An_5. The determinations are considered reliable although they conflict with those of several authors who reported the plagioclase in the Catoctin formation to be andesine.

Optic angles and extinction angles of pyroxenes were determined on the universal stage. Augite with 2V = 45–50° and Z ∧ C = 40–49° is the predominant pyroxene, but pigeonite with 2V = ca. 10° and Z ∧ C = 30–35° is also very common. In a few of the larger phenocrysts of pyroxene a faint zoning can be detected in which the core has a larger optic angle and different extinction position than the rim. Twinning on the 100 face is common, especially in phenocrysts.

Where the greenstone is completely replaced by epidote and quartz the rock has a granoblastic texture with sutured boundaries between epidote and quartz grains. In plain light the basaltic fabric may still be seen almost perfectly preserved. Feldspar laths are entirely replaced by fine-grained aggregates of quartz, and the interstitial minerals are replaced by epidote and quartz. Outlines of amygdules are preserved, but their fillings have been replaced by mosaics of a fine-grained quartz. In some specimens large amounts of opaque minerals are scattered through the rock giving it a slightly purplish color in hand specimen instead of the common light-greenish-yellow characteristic of the epidotized greenstone.

In some specimens the plagioclase is almost completely altered to chlorite and actinolite but the pyroxene is little affected. The rock may consist of as much as 20 per cent pyroxene grains set in a matrix of chlorite and actinolite with only a few small remnants of unaltered albite. In such rocks some of the plagioclase is replaced by quartz which preserves the rectangular outlines of the plagioclase laths.

Epidote occurs in variable amounts both as small grains in the chloritic mat between feldspars and in large scattered grains which at first glance resemble olivine or pyroxene phenocrysts. Several early workers who reported olivine in the greenstone may have been deceived by these large epidote grains. Most of the epidote has a $(-)2V \cong 80°$ and a slightly anomalous yellowish interference color suggesting the presence of manganese.

Chlorite from a typical porphyritic greenstone near Big Meadows has $n_y = 1.624 \pm 0.002$, (+)2V, and dispersion r > v.

Optical properties of the actinolite were not measured because of the extremely small size of the needles and their intimate association with chlorite and epidote.

Iron-ore grains are scattered through the chloritic groundmass. The ore minerals include magnetite, specular hematite, and probably some ilmenite. The magnetite is locally abundant enough to affect a compass held within several feet of the outcrop. Ore minerals also occur in hemispherical concretions in amygdule fillings.

A few published analyses of greenstone of the Catoctin are presented in Table 2. Descriptions of the hand specimens are not available in most cases, but several of the analyses, especially those high in CaO are believed to represent completely epidotized greenstone.

Dikes of Greenstone

The granitic rocks underlying the Catoctin formation are cut by dikes of greenstone from a foot to 50 feet or more in width. Most of the dike rocks are fine-grained and megascopically resemble the greenstones of the Catoctin flows. Many dikes show columnar jointing normal to the walls; some show a faint cleavage parallel to that in the rocks overlying the granitic basement. Most dikes have a thin fine-grained margin, probably caused by chilling against the walls. Several dikes on Old Rag Mountain contain phenocrysts of plagioclase up to 1 cm across.

Good examples of these dikes are found along the Skyline Drive in the road cut north of Shavers Hollow parking area where at least six crop out within 1500 feet. Two large dikes, one of them 50 feet thick, cut through the granite of the summit of Old Rag Mountain; they are less resistant to erosion than the granite and form deep notches in the summit ridge. A dike 15 feet thick with columnar jointing is exposed at the north end of the tunnel on the Skyline Drive about three quarters of a mile south of Thornton Gap. The attitude of the dikes is generally difficult to determine precisely, but most strike north and dip 65°–90° either E. or W.

The greenstone in the dikes is composed of pyroxene and plagioclase in a mat of secondary chlorite with minor amounts of calcite, quartz, and epidote. In specimens in which alteration

is incomplete the texture is intergranular or ophitic. Chlorite replaces plagioclase in many places, leaving isolated rounded grains of pyroxene in a chloritic mat.

ences in grain size and the difference in environment during metamorphism, i.e., protection from shearing by the surrounding granite and gneiss and scarcity of water in the basement

TABLE 2.—CHEMICAL ANALYSES OF CATOCTIN GREENSTONES

	1	2	3	4	5	6
SiO_2	51.89	50.36	46.79	51.08	50.00	50.83
TiO_2	0.91	3.10	1.66	2.67	2.08	2.03
Al_2O_3	15.28	17.37	14.22	11.37	14.56	14.07
Fe_2O_3	3.10	8.13	5.10	11.17	6.87	2.88
FeO	3.60	4.33	9.20	5.64	5.69	9.00
MgO	8.68	3.57	5.86	3.96	5.51	6.34
CaO	7.38	4.29	10.14	5.20	6.75	10.07
Na_2O	3.27	4.74	2.38	5.54	3.98	2.23
K_2O	2.57	0.08	0.77	1.50	1.23	0.82
H_2O	2.54	2.99	3.52	1.50	2.63	0.91
P_2O_5	0.61	0.63	0.35	0.39	0.49	0.23
Other	0.38	0.24	0.18	0.22	0.25	0.18
Total	100.21	99.73	100.39	100.24		

1. Catoctin schist, Bechtel copper shaft, South Mountain, Pa. (Stose and Stose, 1946, p. 21, quoted from G. H. Williams)

2. Metabasalt, Northwest of Devils Racecourse, Fairfield quadrangle, Pa. (Stose and Bascom, 1929, p. 5) "Massive bluish green amygdaloid . . . plagioclase is andesine (?), and the other constituents are magnetite, ilmenite, chlorite, quartz, and epidote. The fabric tends toward the trachytic, and the rock is more andesitic than basaltic."

3. Metabasalt, 2½ miles west of triangulation station on Green Ridge, Fairfield quadrangle, Pa. (Stose and Bascom, 1929, p. 5) ". . . dark yellowish-green nonamygdaloidal schistose rock, containing actinolite, chlorite, epidote, ilmenite, magnetite, finely granular feldspar, and apatite. The original fabric has been obliterated by development of actinolite."

4. Andesite (?), 3 miles east of Front Royal, Va. (Keith, 1894b, p. 305)

5. Average of 1–4

6. Average tholeiitic basalt (Nockolds, 1954)

Measurements of extinction angles in the plagioclase indicate a composition of about An_{80} in most specimens. Composition zoning is well developed in some crystals (Pl. 3, fig. 5). The pyroxene includes both pigeonite and normal augite with $2V = 40–50°$ and $Z \wedge C = 30–40°$. Both pyroxenes are present in all specimens studied. Many of the larger pyroxene crystals show distinct zoning from normal augite in the center to pigeonite at the rim. Some specimens contain augite showing hour-glass structure (Pl. 3, fig. 6).

The field relationships of the dikes to the greenstone of the Catoctin formation suggest that the dikes were feeders through which the Catoctin lavas were erupted. Original differrocks may account for the more calcic composition of the plagioclase in the dikes compared with that of the Catoctin flows and for the preservation of zoning in the plagioclase and pyroxene in the dikes.

Purple Volcanic Slate

In most places between the Catoctin formation and the overlying Chilhowee sedimentary rocks there is a purple or reddish-brown volcanic slate described by Furcron and Woodward (1936) as a basal Cambrian lava flow. King (1950) mapped the slate in the Elkton area as the Loudoun formation and considered it to be of pyroclastic origin. This rock under-

lies the Chilhowee sedimentary rocks that cap Chapman Mountain; it crops out in a narrow belt west of Lucas Gap on Tanners Ridge and discontinuously along the upper contact of the

TABLE 3.—CHEMICAL ANALYSES OF VOLCANIC SLATE*

	1	2
SiO_2	47.3	44.2
Al_2O_3	15.7	16.6
FeO	2.1	2.4
Fe_2O_3	15.3	17.2
MgO	2.2	3.0
CaO	1.5	1.5
Na_2O	.08	.06
K_2O	7.3	6.8
TiO_2	3.6	3.4
P_2O_5	.72	.11
MnO	.04	.07
CO_2	<.05	<.05
H_2O	2.9	3.6
Sum.....	99	99

*H. F. Phillips, P. D. Elmore, K. E. White, Analysts; analyses by rapid methods

1. Purple volcanic slate, south slope of Chapman Mountain

2. Purple volcanic slate, north side of Knob Mountain along fire road

Catoctin at least as far north as Knob Mountain, north of Jeremys Run. The slate averages 50–100 feet thick, but locally reaches 200 feet. North of Beahms Gap it is absent in several places, and the lower beds of the Chilhowee group rest directly on greenstone of the Catoctin. Furcron and Woodward (1936) state that the slate

"... has been found ... above granodiorite in the absence of any greenstone—a fact that strongly suggests that the extrusive is later or younger than either the greenstone or granodiorite. Indeed, no other interpretation is possible except to identify the amygdaloid with the greenstone in apparent contradiction to the lithologic and stratigraphic evidence."

If one assumes, as Furcron and Woodward did, that there is a major unconformity between the Catoctin and the Chilhowee group and that the granodiorite intrudes the greenstone, the volcanic slate would have to be assigned to the early Cambrian. However, if no major unconformity exists at the base of the Chilhowee, the slate can equally well be assigned to the top of the Catoctin formation, and its presence immediately overlying granodiorite can be interpreted as being due to normal overlap of the Catoctin formation on to an irregular erosion surface of granodiorite.

The volcanic slate is purple, reddish, or chocolate brown, generally intensely cleaved with green chloritic blebs elongated down the dip of the cleavage, conforming to the deformation plan of the overlying and underlying rocks. In a few exposures on the south flank of Neighbor Mountain the rock is massive with a faint parting parallel to bedding in immediately overlying Chilhowee sedimentary rocks. The rock is characteristically spotted; white spots 1 or 2 mm in diameter appear on polished surfaces as circles or oval with light rims and darker cores.

In thin section the rock commonly shows rectangular laths, probably representing original plagioclase now completely replaced by sericite, in a matrix of sericite and dark opaque material. Scattered throughout the rock are green chlorite clots, probably representing either amygdules or chloritized ferromagnesian phenocrysts. Small wedge-shaped crystals of sphene are common, and a few unaltered remnants of pigeonite occur. The spots which appear white in the hand specimen are dark and nearly opaque in thin section. They are oval in general plan, but in detail their boundaries are highly irregular and spongelike. They include sericitized plagioclase laths, some of which extend across the boundaries of the spots. Where shearing has destroyed or modified the fabric of the rock as a whole, the replaced plagioclase laths within the spots preserve a basaltic texture. This suggest that the material forming the spots has protected and preserved the fabric of the rock it included. In some cases sericitized feldspar laths in the groundmass have been bent around one of the spots, which indicates that the spots may have acted as resistant knots during deformation subsequent to growth. The spots appear to be porphyroblasts of ottrelite (chloritoid), cloudy with minute inclusions, which replaced the original basaltic fabric prior to deformation.

In several areas the slate does not show

volcanic textures and contains rounded quartz grains. Locally it is interbedded with arkose and quartzite of the overlying Weverton formation.

Two chemical analyses of specimens of the slate showing volcanic textures are given in Table 3.

Field relationships and petrography suggest that the slate is a metamorphosed saprolite developed at the top of the Catoctin formation prior to deposition of the overlying sediments. Where the weathered material was reworked during deposition of the basal bed of the Chilhowee the volcanic texture was lost, but where the saprolite was not disturbed the texture is locally preserved. Chemical analyses show slightly more Al_2O_3 and iron than normal greenstone and less SiO_2 MgO, CaO, and Na_2O; this supports the hypothesis that the slate is derived from a saprolite. The high K_2O as compared with Na_2O suggests that there has been some subsequent hydrothermal alteration.

Thin layers of similar slate and purple argillite lie between flows in the greenstone of the Catoctin, and veinlets of jasper with detrital sand grains penetrate the greenstone near the tops of some flows. Weathering of basalts commonly leads to the formation of similar jasper veinlets. King (1950) reports jasper masses in the slate in the Elkton area.

That the slate immediately overlies the granitic rocks in a few places may merely indicate that a thin Catoctin flow was completely weathered in place before deposition of the Chilhowee beds.

Original Nature of the Catoctin Lavas

The volcanic nature of the greenstones of the Catoctin formation has long been recognized, but little has been published concerning the original composition of the Catoctin lavas and their mode of eruption. Most authors agree that the bulk of the lavas were basalts, although Bloomer and Bloomer (1947) concluded that they were andesites on the basis of the composition of the plagioclase, which they reported as being about An_{40}. Determinations by the writer, however, indicate that the plagioclase is secondary, with a composition of $An_{0\text{-}10}$. At any rate, conclusions about the original character of the Catoctin lavas cannot reasonably be based on the present composition of the plagioclase. Relic textures strongly indicate that the lavas were basalts, and this conclusion is supported by the mineralogy of the rocks and by the available chemical analyses.

In the Mull Memoir of the Geological Survey of Scotland, Bailey *et al.* (1924) recognized three main basalt magma types. The Catoctin lavas closely resemble their "non porphyritic central type", which is characterized by sparseness or absence of olivine, occurrence of both pigeonite and normal augite, and a plagioclase in the labradorite range. This magma type, which is perhaps more commonly referred to as the tholeiitic type (Kennedy, 1933) by most authors, is widespread on the great lava plateaus of the world, including the Columbia River plateau, the Deccan plateau, and the Tholean province. It is also characteristic of the flows and dikes of Triassic age in the eastern United States. Tholeiitic basalt flows are generally from 150 to 200 feet thick and commonly show well-developed two-tier columnar jointing. They are floodlike and have enormous area and volume. They are commonly associated with parallel dike swarms which were the feeders for the flows.

The Catoctin lavas are believed to have been tholeiitic basalts erupted from fissures in the basement rocks. The thickness and extent of the flows, subaerial origin, absence of known central volcanoes, and floodlike character agree with the characteristics of plateau basalt accumulations. The sparseness of any relics that might suggest olivine, and the occurrence of pigeonite are very suggestive of a tholeiite-basalt association.

The association of the greenstone of the Catoctin with the sedimentary rocks of the Appalachian geosyncline brings up the question of its relationship to spilitic lavas so characteristic of the early stages of many geosynclines. Mineralogically the spilites are characterized by albitic feldspars, chloritization of ferromagnesian minerals, and abundance of epidote and calcite. Although the origin of the albite in spilites has been much debated many recent authors agree that it is secondary because partially replaced labradorite cores are common in some of the albite crystals and because

albite and pyroxene would probably not crystallize simultaneously from a magma (Gilluly, 1935).

TABLE 4.—ATOMS ASSOCIATED WITH 160 OXYGEN ATOMS IN THE AVERAGE CATOCTIN GREENSTONE AND THE AVERAGE THOLEIITIC BASALT

	Average Greenstone (Column 5 of Table 2)		Average tholeiitic basalt (Nockolds, 1954) (Column 6 of Table 1)	
Si	48.35		46.37	
Ti	1.73		1.38	
Al	15.38		15.12	
Fe^{+++}	5.01	9.61	1.97	8.89
Fe^{++}	4.60		6.92	
Mg	7.93		8.61	
Ca	7.00		10.20	
Na	7.48		3.95	
K	1.52		.93	
H	8.49		5.54	
P	.40		.12	
Total.....	107.89		101.11	

The greenstone of the Catoctin is similar to some spilites in certain respects, but it differs from them in other important features. First, the Catoctin flows were clearly subaerial as is shown by the presence of columnar jointing, absence of pillow structure, areal extent of individual flows, and relatively thin breccia zones between flows, whereas typical spilites are submarine and show well-developed pillow structure. Secondly, spilites are characteristically associated with great thicknesses of graywackes and bedded cherts containing occasional limestone lenses, whereas the sedimentary members of the Catoctin formation are insignificant and are arkoses derived from local sources in the nearby granitic rocks. Thirdly, there is no evidence that the albite and other secondary minerals were formed during or immediately following consolidation of the flows. Alteration did not occur until after soil zones had formed, and the overlying sediments were deposited. For these reasons the mineralogy of the Catoctin greenstone can best be explained as the result of low-grade regional metamorphism of an accumulation of plateau basalts of tholeiitic type without important change in the bulk composition.

Metamorphism

Lack of reliable chemical data on the greenstone is the Luray area prevents any detailed discussion of the metamorphic processes which affected the original Catoctin lavas. Only four complete analyses of Catoctin greenstones are available (analyses 1–4, Table 2). and three of these are from southern Pennsylvania, more than 100 miles away, so that any conclusions based on these data are tentative.

For comparison the average of these four analyses has been expressed in terms of a unit cell of 160 oxygen atoms according to the method of Barth (1952) in column 1, Table 4. Column 2 is the average composition of tholeiitic basalts given by Nockolds (1954) expressed in the same manner. Comparing the two columns we see that the derivation of an average greenstone of the Catoctin formation (if the average of the four analyses is truly an average greenstone) from an average tholeiitic basalt would not involve large changes in composition during metamorphism. Changes in Ti, Al, Mg, P, and total Fe would involve less than one atom of each element in every unit cell of 160 oxygen atoms. Si differs by less than two atoms. More extensive changes would include addition of Na, K, and H, removal of some Ca, and change of the oxidation state of the Fe.

Derivation of the greenstone from the original basaltic lavas involved the conversion of the mineral assemblage labradorite-augite-pigeonite into albite, chlorite, actinolite, and epidote, an assemblage characteristic of the greenschist facies of Turner (1948). The metamorphic reactions were not complete, for large amounts of relic primary pyroxenes remain in some of the greenstone of the flows, and a few of the dikes also contain small relics of labradorite.

Figure 10 illustrates the relationship between grain size of the original basalts and the degree to which metamorphism has approached completion. The albite occurs in laths which are pseudomorphic after the original plagioclase and therefore furnish a measure of the original grain size. In Figure 10 the percentages of various minerals are plotted against the average length of plagioclase laths in nine specimens of greenstone. Relic pyroxene is

higher in the finer-grained rocks, while the metamorphic minerals albite and chlorite tend to be more abundant in the coarser-

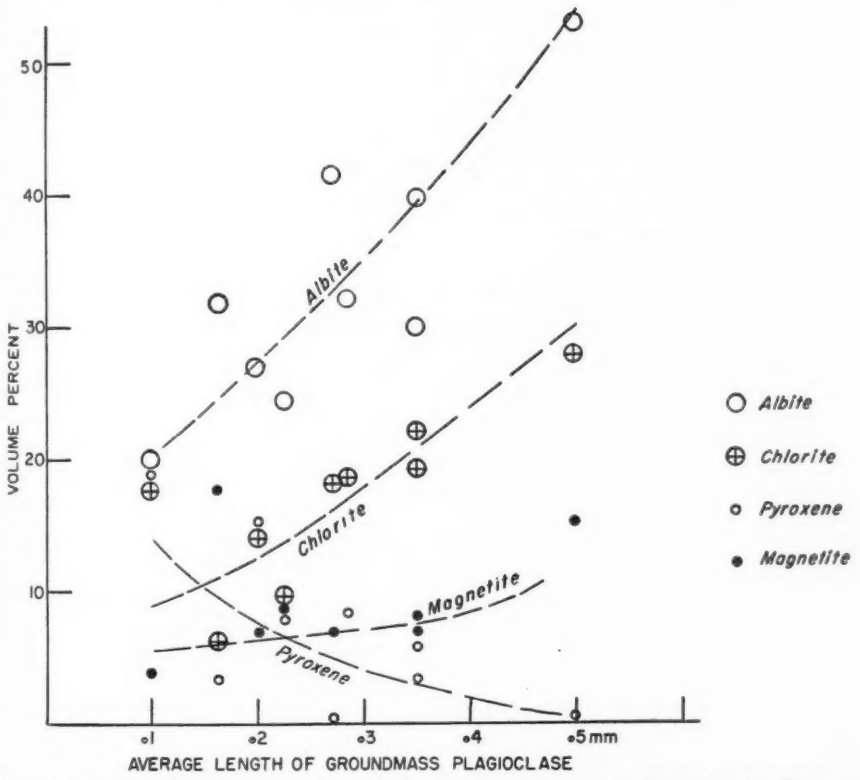

FIGURE 10.—VOLUME PERCENTAGE OF VARIOUS MINERALS PLOTTED AGAINST GRAIN SIZE AS MEASURED BY AVERAGE LENGTH OF GROUNDMASS PLAGIOCLASE IN CATOCTIN GREENSTONES

grained specimens. This may be due to the higher permeability of the coarser grained rocks which would facilitate metamorphic reactions.

CONCLUSIONS

The Catoctin formation unconformably overlies the granitic basement rocks in the Luray area and is not intruded by them as was suggested by some earlier workers. The Catoctin lavas were subaerial flows poured out on an erosion surface of considerable relief, drowning the valleys, but at least in the earlier stages leaving projecting hills of granitic rocks. Several thousand feet of basaltic lava flows and interbedded tuffaceous and sedimentary material accumulated before volcanic activity ceased, and the entire area was submerged beneath the sea in which the sediments composing the Chilhowee were deposited. A period of weathering which formed a saprolite up to 150 feet thick may have followed the end of Catoctin vulcanism, but no evidence was found in the Luray area of a major time interval between the Catoctin and the Chilhowee. The Catoctin may therefore be at least in part early Cambrian.

Because of its stratigraphic position beneath the early sediments of the Appalachian geosyncline the greenstone of the Catoctin formation is sometimes mentioned as marking volcanic activity associated with the early stages

of formation of the geosyncline (Bucher, 1933). The present study indicates, however, that the Catoctin lavas resemble basalt accumulations characteristic of nonorganic areas, and that they should not be considered as belonging to the Appalachian geosynclinal cycle. The Catoctin greenstones are probably remnants of a great basaltic plateau which foundered beneath the advancing early Cambrian seas during the initial stages of formation of the Appalachian geosyncline.

References Cited

Bailey, E. B., *et al.*, 1924, The Tertiary and post-Tertiary geology of Mull, Loch Aline, and Oban: Scotland Geol. Survey Mem.

Barth, Tom F. W., 1952, Theoretical Petrology: N. Y., John Wiley & Sons, Inc.

Bascom, Florence, 1896, The ancient volcanic rocks of South Mountain, Pennsylvania: U. S. Geol. Survey Bull. 136.

Bloomer, R. O., 1950, Late pre-Cambrian or lower Cambrian formations in central Virginia: Am. Jour. Sci., v. 248, p. 753–783.

Bloomer, R. O., and Bloomer, R. R., 1947, The Catoctin formation in central Virginia: Jour. Geology, v. 55, p. 94–106.

Bucher, W. H., 1933, Deformation of the Earth's Crust: Princeton, N. J., Princeton Univ. Press.

Cloos, E., *et al.*, 1951, Physical features of Washington County: Md. Dept. of Geology, Mines and Water Resources.

Furcron, A. S., 1934, Igneous rocks of the Shenandoah National Park area: Jour. Geology, v. 42, p. 400–410.

Furcron, A. S., and Woodward, H. P., 1936, A basal Cambrian lava flow in northern Virginia: Jour. Geology, v. 44, p. 45–51.

Gilluly, James, 1935, Keratophyres of eastern Oregon and the spilite problem: Am. Jour. Sci., v. 29, Pt. I, p. 225–252; Pt. II, p. 336–352.

Jonas, A. I., 1935, Hypersthene granodiorite in Virginia: Geol. Soc. America Bull., v. 46, p. 47–60.

Jonas, A. I., and Stose, G. W., 1939, Age relations of the pre-Cambrian rocks in the Catoctin Mountain-Blue Ridge and Mt. Rogers anticlinoria in Virginia: Am. Jour. Sci., v. 237, p. 575–593.

Keith, A., 1894a, Description of the Harpers Ferry sheet [Va.-Md.-W. Va.]: U. S. Geol. Survey folio 10.

Keith, A., 1894b, Geology of the Catoctin belt: U. S. Geol. Survey 14th Ann. Rept., pt. 2, p. 285–395.

Kennedy, W. Q., 1933, Trends of differentiation in basaltic magmas: Am. Jour. Sci., v. 25, p. 239–256.

King, P. B., 1949, The base of the Cambrian in the southern Appalachian, Pt. 1: Am. Jour. Sci., v. 247, p. 514–530; Pt. 2: v. 247, p. 622–645.

King, P. B., 1950, Geology of the Elkton area, Virginia: U. S. Geol. Survey Prof. Paper 230.

Nockolds, S. R., 1954, Average chemical compositions of some igneous rocks: Geol. Soc. America Bull., v. 65, p. 1007–1032.

Swartz, F. M., 1948, Trenton and sub-Trenton in outcrop areas in New York, Pennsylvania, and Maryland: Am. Assoc. Petroleum Geologists Bull., v. 32, p. 1493–1595.

Stose, A. J., and Stose, G. W., 1946, The physical features of Carroll County and Frederick County: Md. Dept. of Geology, Mines, and Water Resources.

Stose, G. W., 1938, Late pre-Cambrian volcanic rocks and lower Cambrian sediments in the Blue Ridge province of Virginia and Maryland (abstract): Geol. Soc. America Bull., v. 49, p. 1961–1962.

Stose, G. W., and Bascom, F., 1929, Description of the Fairfield and Gettysburg quadrangles, U.S. Geol. Survey folio 225.

Stose, G. W. *et al.*, 1928, Geologic map of Virginia: Va. Geol. Survey.

Thiesmeyer, L. R., 1939, Varved slates in Fauquier County, Virginia: Va. Geol. Survey Bull. 51, p. 109–118.

Turner, F. J., 1948, Mineralogical and structural evolution of the metamorphic rocks: Geol. Soc. America Mem. 30.

Weed, W. H., and Watson, T. L., 1906, The Virginia copper deposits: Econ. Geology, v. 1, p. 309–330.

United States Geological Survey, 2648 Interior Building, Washington 25, D. C.

Manuscript Received by the Secretary of the Society, June 11, 1954.

BULLETIN OF THE GEOLOGICAL SOCIETY OF AMERICA
VOL. 66, PP. 897-912, 9 FIGS. JULY 1955

TRANSFORMATION OF INDICES IN TWIN GLIDING

BY A. PABST

ABSTRACT

For computation the most convenient form to express transformation of indices attending twin gliding is that of a matrix comparable to matrices used in connection with changes in the axes of reference. The matrix can be obtained by the usual equations, first derived by Mügge (1889a, p. 286–294), or directly from the changes of indices of a suitable set of three faces. These can usually be chosen by inspection when the elements of twin gliding are established.

The reciprocal lattice and the gnomonic projection are used to represent the several types of twin gliding.

Transformation of crystal forms, of the lattice, and of the crystal structure are illustrated by stereographic projections and diagrams. Geometric criteria can sometimes be used not only to determine the possibility of twin gliding but also to decide the sense of the glide.

Simple shear describes twin gliding megascopically, but this concept requires modification in describing known cases of atom movements. Structures at the moving twin boundary are related to polymorphs of the crystal undergoing gliding in certain cases.

CONTENTS

TEXT

	Page
Introduction	897
Acknowledgments	898
Symbols and procedures	898
Use of reciprocal lattice and gnomonic projection	900
Twin gliding in S sections—criteria of possibility of twin gliding	902
Examples	904
General	904
Calcite	904
Dolomite	907
Atom movements in twin gliding	909
Previous work	909
Calcite	909
Sphalerite	909
Concluding remarks	911
References cited	911

ILLUSTRATIONS

Figure	Page
1. Definition and relations of the elements of twin gliding	898
2. Twin gliding in the reciprocal lattice and in the direct lattice	900
3. Twin gliding of TYPES I and II and twin gliding in diopside	901
4. Twin gliding in a cubic face-centered lattice shown in S section	903
5. Morphological changes in calcite caused by twin gliding	905
6. Sections through dolomite structure parallel to $(1\bar{2}10)$	908
7. Twin gliding in dolomite shown in S section	908
8. S section through calcite showing rearrangement of structural units attending twin gliding	910
9. Structure of sphalerite twin projected onto a $(1\bar{1}0)$ section	911

TABLE

Table	Page
1. Summary of index transformations corresponding to twin gliding on $\{01\bar{1}2\}$	906

INTRODUCTION

Recent work by F. J. Turner and associates on the role of twin gliding in the deformation of marble, especially the work of Borg and Turner (1953), has once again directed attention to the problem of index transformation in twin gliding. This problem was dealt with by Bell (1941) who gave a brief historical account of the study of twin gliding and published a derivation of two sets of equations for what he referred to as "TWINNING OF TYPE I" and "TWINNING OF TYPE II". These relations for the transformation of face indices were first derived by Mügge (1889a) for the two cases which he designated α and β. The two sets of equations are strictly analogous, and some authors, including Schmid and Boas

(1935; 1950), Tertsch (1949, p. 91), Niggli (1924, p. 299; 1929, p. 436), and Johnsen (1914a, p. 243), give only one set of equations. Derivations have also been given by Wallerant (1909) and by Johnsen (1913).

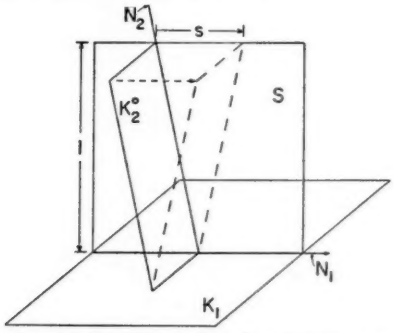

FIGURE 1.—DEFINITION AND RELATIONS OF THE ELEMENTS OF TWIN GLIDING

Wallerant (1904) derived the relations for transformation of zonal indices (co-ordinates of points) which have been quoted by Niggli, Tertsch, and Schmid and Boas. This problem was not considered by Bell. It will be seen later that there is no need for a separate statement of such relations.

ACKNOWLEDGMENTS

The writer is indebted to his colleagues, Professor F. J. Turner and Dr. R. M. Douglass, for many helpful discussions. The work has been supported by the Office of Naval Research under a project on "the crystal chemistry of minerals" and by the Committee on Research of the University of California.

SYMBOLS AND PROCEDURES

Familiarity with Bell's paper or some equivalent treatment of twin gliding such as that of Johnsen (1913) is here presupposed. The symbols and terms of Bell are used with slight modification:

K_1—Slip plane
K_2—Other plane of no distortion
N_1—Slip direction
N_2—Intersection of K_2 and S
S—Plane of deformation
s—Amount of slip or shear, the displacement of a point at unit distance from K_1, equal to $2\cot 2\varphi$, where 2φ is the angle between K_1 and K_2°

The relations of these lines and planes, which may conveniently be referred to as elements of twin gliding, are shown in Figure 1. The names given are those used by Bell. He did not name N_2. For N_1 and N_2 the symbols η_1 and η_2 appear in Bell's Figures 5 and 6. These are the symbols most frequently used. Mügge designated these directions by σ_1 and σ_2. Bell does not give the symbol S in his list (Bell, 1941, p. 254–255) but he uses it in a footnote (p. 256) and elsewhere designates the plane normal to both K_1 and K_2 as the "plane of deformation". In most German works, including that of Schmid and Boas (1935), this plane is designated *Schiebungsebene* or *Ebene der Schiebung*. Unfortunately, in the 1950 translation of that work the anonymous translator has used four different names for the S plane. Following Barrett (1952, p. 383) it will be convenient to identify "the other plane of no distortion" in its original position by a superscript, thus: K_2°.

Following Mügge (1889a, p. 286–294) Bell derived two sets of equations for calculating the indices of a plane after twin gliding, from its original indices and the indices of certain of the elements of twin gliding. His equations 6a are in terms of the indices of K_1 and N_2, and equations 8a are in terms of K_2° and N_1. Since these are identical in form, a single set of equations covers either case:

$$\rho \cdot h' = 2H(uh + vk + wl) - h(uH + vK + wL)$$
$$\rho \cdot k' = 2K(uh + vk + wl) - k(uH + vK + wL)$$
$$\rho \cdot l' = 2L(uh + vk + wl) - l(uH + vK + wL),$$

where HKL are the indices of K_1 or K_2°, uvw the indices of N_2 or N_1, hkl the indices before transformation of the plane under consideration, $h'k'l'$ the indices sought, and ρ a "proportionality factor". Wallerant's (1909, p. 44) relations can be rearranged to the same form but lacking the factor of proportionality. This may be omitted since it serves only to indicate that the indices $h'k'l'$ may not be coprime in all instances. Niggli (1924, p. 299; 1929, p. 436) also employs a form lacking the proportionality factor.

Since rational indices $h'k'l'$ are obtainable

for transformed planes when only K_1 and N_2 or only K_2° and N_1 are known, two cases may be distinguished, designated α and β by Mügge (1889a), and referred to by Bell as "TWINNING OF TYPE I" and "TWINNING OF TYPE II". Mügge's (1889a, p. 294) contrasting descriptions may be abbreviated as follows:

	α		β
K_1	rational glide plane	K_1	irrational glide plane
K_2°	irrational "other plane of no distortion"	K_2°	rational "other plane of no distortion"
N_1	irrational slip direction	N_1	rational slip direction
N_2	rational intersection of K_2° and S twin axis normal to K_1 is irrational.	N_2	irrational intersection of K_2° and S twin plane normal to N_1 is irrational.

These cases are distinct when the conditions here specified exist, as they may in crystals of low symmetry. In case α, K_1 is the rational twin plane. In case β, N_1 is the rational twin axis. Case α would correspond to albite twinning, K_1 (010) N_2 [010], and case β to pericline twinning, K_2 (010) N_1 [010], in plagioclase. Twinning in plagioclase may not be the result of twin gliding, though it has been considered as such. Both pericline and albite twinning are listed with a question mark under twin gliding in the tabulations of Niggli (1924, p. 302) and Seifert (1927) but are included by Tertsch (1949, p. 59) without question. Mügge and Heide (1931) artificially produced lamellae in anorthite which they attributed to twin gliding resulting in albite and pericline twins. Mügge (1927, footnote p. 747) had pointed out that the "rhombic section" would be expected as the composition plane in pericline twins formed by twin gliding. It is then the irrational glide plane K_1 parallel to the rational slip direction N_1, here [010]. On the other hand plagioclase twinned on [010] with (001) as composition plane, according to the acline law, must not be considered as resulting from twin gliding.

Most authors have failed to emphasize that the distinction between the two cases is lost when both K_1 and K_2 are rational, as shown explicitly by Wallerant (1909, p. 49) and Friedel (1926, p. 488). Schmid and Boas (1935; 1950) state only that in cases of high symmetry both K_1 and N_1 may be rational and that twin gliding of TYPE II is restricted to crystals of low symmetry. More specifically, in isometric crystals a distinction between the two cases cannot exist; all elements of twin gliding must be rational. The proof of this proposition may be followed with the aid of Figure 1. If K_1 and N_2 are rational, a minimum requirement, the normal to K_1 in S, is rational since in isometric crystals there are rational axes normal to all rational planes. Then S is a rational plane since it contains two rational lines, this normal and N_2. The normal to S, which is the intersection of K_1 and K_2, is rational. Then K_2 is rational because it contains two rational lines, N_2 and the normal to S. Finally N_1 is rational since it is the intersection of the rational planes K_1 and S. At the other extreme, in triclinic crystals, twin gliding of TYPE I and TYPE II are ordinarily distinct because, in general, rational planes do not exist normal to other rational planes in such crystals. In the remaining systems the two types of twin gliding may or may not be distinct. They will merge in all cases where S is a symmetry plane or is normal to a symmetry axis, for instance where S is (010) of a monoclinic crystal.

In applying the relations for transformation of indices to particular cases it is convenient to use special forms for each case rather than to substitute in the equations given for transforming indices of each face. Many workers have done this, but Bell (1941, footnote page 256), in dealing with an example from calcite, substitutes directly in the general equations. Wallerant (1909, p. 66) gives this special form of the transformation for the common twin gliding of calcite referred to rhombohedral axes:

$$\begin{gathered} q - q' = r - r' = q + r \\ s = s' \end{gathered}$$

This may be written in the form of a matrix, $0\bar{1}0/\bar{1}00/001$. Relations of this sort can be derived in various ways without the use of Mügge's equations. In fact Liebisch (1889, p. 117–120) gave several such special rela-

tions, though not in matrix form, shortly before Mügge published his widely quoted equations.

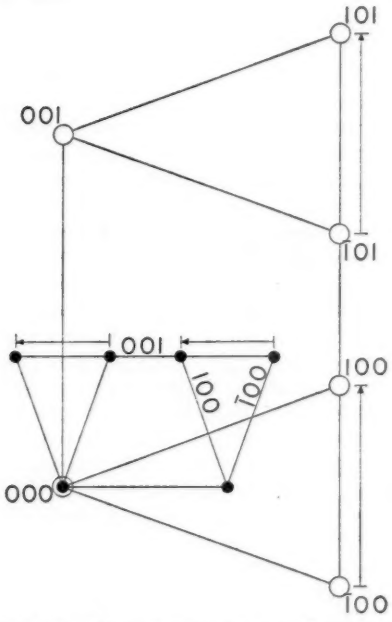

FIGURE 2.—TWIN GLIDING IN THE RECIPROCAL LATTICE AND IN THE DIRECT LATTICE

Solid circles represent points in the direct lattice, open circles points in the reciprocal lattice.

Giving specifications for the transformation of indices in a particular case in matrix form amounts to considering the twin gliding as a change of reference axes. This is justified since all rows in the lattice in twin orientation, including those chosen as axes, were rows before the twinning. They have, in general, been displaced by the twin gliding and their indices changed. The matrix is a statement of the coordinates of the unit distances on the new axes referred to the old axes. Such a statement might be obtained by inspection of a model, particularly one representing the twin glide operation, or from Mügge's equations. In many cases the matrix can be obtained from the known changes of indices of any three noncozonal faces just as with other transformations of axes.[1] Generally three suitable faces will be known when the twin glide elements have been established, for instance K_1 and any two faces in the zone of N_1.

The matrix necessarily has certain properties. The unit cell does not change volume, so the matrix has the modulus unity. As twin gliding is reversible (Mügge, 1883, p. 81) with restoration of faces to their original orientation and indices, the inverse matrix must be identical with the direct matrix. The matrix multiplied by itself must yield the identity transformation, 100/010/001. The identity of direct and inverse matrices has a useful corollary. Since the rows in the direct matrix for transformation of coordinates or position, zonal, or axis indices are the columns of the inverse matrix for transformation of indices or faces, all four matrices for transformation back and forth are known as soon as one is known when the direct and inverse matrix are identical. The relations for transformation of zonal indices can then be dispensed with.

USE OF RECIPROCAL LATTICE AND GNOMONIC PROJECTION

Gnomonic projections can aid in the consideration of twin gliding. Such projections represent the reciprocal lattice projected upon a plane at unit distance from the origin by lines connecting each reciprocal lattice point with the origin. Figure 2 shows a section through an oblique unit cell and the simple shearing of this cell involved in twin gliding. With this is shown a section through a portion of the reciprocal lattice and of this lattice transposed to a new orientation with the shearing of the direct cell. This involves a shear of the reciprocal lattice at right angles to the shear of the direct lattice. It is possible and even advantageous in certain situations to describe twin gliding in terms of suitable elements in the reciprocal lattice.

In Figure 3 three cases of twin gliding are represented by means of one gnomonic projection and by two sections through the respective reciprocal lattice normal to the gnomonic plane and normal to each other. In each case the gnomonic plane has been chosen normal to the glide in the direct lattice so that movement of face poles (reciprocal lattice points) is parallel to the plane of the gnomonic pro-

[1] Readers unfamiliar with the use of matrices in crystallography may refer to Buerger (1942, Chapter 2) or to Henry and Lonsdale, (1952, p. 15–21).

FIGURE 3.—TWIN GLIDING OF TYPES I AND II AND TWIN GLIDING IN DIOPSIDE

Each of the three cases is represented by a gnomonic projection marked by a scale circle and by two sections through the reciprocal lattice normal to the plane of the gnomonic projection.

jection. Figures 3A and 3B represent twin gliding of TYPE I and TYPE II in hypothetical triclinic lattices dimensioned and oriented so as to enable comparison with the known twin gliding of diopside, in which all elements are rational and no distinction of types is to be made (Fig. 3C). For Figures 3A and 3C the reciprocal lattice sections to the left of the gnomonic projections are in the S plane which is common for the direct and reciprocal lattices, while the sections shown below are normal to what may be called N_1^*, the slip direction in the reciprocal lattice. In Figure 3B the lower section is normal to the slip plane of the reciprocal lattice and includes b^*; the section at left is normal to this and to the gnomonic plane. Of the six sections only the S plane section for diopside coincides with a rational plane in the reciprocal lattice. The reciprocal lattice points shown in the other sections have been projected orthographically. In the gnomonic projections lower semicircles represent face poles in original position, and upper semicircles the same poles after twin gliding. The same convention is used in the sections beside the gnomonic projections. In both of these, filled circles or semicircles represent reciprocal lattice points at their appropriate level. Open circles or semicircles have been used for those poles in the gnomonic plane which can be thought of as projected onto this plane from a different level in the reciprocal lattice, as shown by dashed lines in some of the sections.

In simple shear each plane parallel to the slip plane is displaced in proportion to its distance from the origin. The reciprocal lattice suffers such shear in twin gliding. Accordingly, as seen in several of the sections, the displacement of (201) is double that of (101). In the gnomonic plane, however, the displacement of all points is the same.

At the top of each section of Figure 3 are given the twin glide elements for both the direct and the reciprocal lattice. Spaces for the symbols of elements which are not rational have been left blank. Symbols corresponding to those previously defined but modified by the addition of an asterisk designate comparable elements in the reciprocal lattice. The rational elements in the reciprocal lattice in twin gliding of TYPES I and II are perpendicular to those which are rational in the direct lattice. Figure 2 shows that this must be so. In TYPE I, for instance, the slip direction in the reciprocal lattice is c^* which is normal to (001), the slip plane in the direct lattice. In symbolizing the plane elements of twin gliding in the reciprocal lattice, forms such as $(hk0)^*$ have been used meaning the reciprocal lattice planes which are the loci of points of the type indicated.[2]

In each section of Figure 3 the transformation matrix is given below the twin glide elements, so that the slip plane becomes a symmetry plane for the twin in TYPE I, whereas the slip direction becomes a digonal axis for the twin in TYPE II, the usual description of the two cases. For diopside the matrix is given as for TYPE II. The matrix may be multiplied through by minus one, corresponding to the operation of a center of symmetry, if this is in accord with the symmetry of the crystals involved.

Twin Gliding in S Sections—Criteria of Possibility of Twin Gliding

The reorientation of the lattice or structure in twin gliding may best be shown by sections parallel to S. Figure 4 shows such a section through a face-centered cubic lattice; S is $(\bar{1}10)$, K_1 (111), and N_1 $[11\bar{2}]$. The transformation matrices given in the figure are those which correspond to lattice orientations if the senses of the [111] axes in the two parts of the twin are parallel, not opposed, the twinning corresponding superficially to 180° rotation on this axis as in an articulating model. If the indices are to correspond as by reflection in the twin plane it is necessary only to multiply the matrices through by minus one. This amounts to adding inversion to 180° rotation resulting in reflection on the plane normal to the rotation axis.

The twinning represented in Figure 4 has been reported for several metals, including copper, silver, and gold, with only the twin glide elements just mentioned specified. The

[2] The writer does not insist upon this form of describing twin gliding elements in the reciprocal lattice. He has merely sought to give symbols which would not readily be subject to misinterpretation.

figure shows the possibility of two interpretations. At the level of the first row of lattice points seen in the section above the labelled twin plane, the twinned lattice may be obtained by a slip to the right of two thirds $[\frac{2}{3}\frac{2}{3}1]$, as shown at BB′. It may also be obtained by slip to the left of one third $[\frac{1}{3}\frac{1}{3}\bar{1}]$, as shown at EE′. The figures within the brackets here symbolize the identity distance in the slip direction and the sense of the slip. It is thus possible to make the description of slip direction and amount unambiguous.

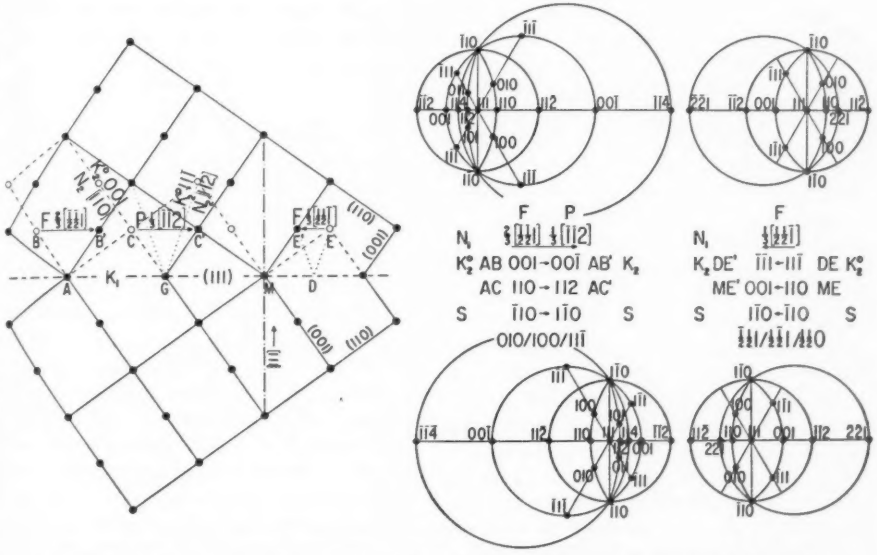

FIGURE 4.—TWIN GLIDING IN A CUBIC FACE-CENTERED LATTICE SHOWN IN S SECTION
Paired stereographic projections at right illustrate changes in the indices of faces for two cases discussed in text.

Though either of these mechanisms gives the same twin relations, the index transformation differs as indicated by the matrices given at the right of Figure 4 where the changes for selected planes are also shown by pairs of stereographic projections. Presentation of these alternatives does not mean that both are realized. The first alternative would require the movement of an atom from B to B′ through a position closer to A than the initial distance between these atoms, a distance determined by close packing. Such a mechanism must obviously be rejected. It has been suggested (Barrett, 1943, p. 315)[3] that certain types of twin gliding are excluded in cubic metals not because of transitory shortening of interatomic distances during slip, but because they would greatly shorten distances between atoms in the first layer above the twin plane and those in the first layer below.

In some cases another criterion can be used to exclude certain twin glide mechanisms. Wallerant (1904, p. 172–173) has shown that a condition for the possibility of twin gliding is that the distances in the direction N_2 between points in the untwinned lattice must be halved by planes in the direction K_1; he has expressed this analytically.[4]

Figure 4 illustrates Wallerant's criterion. If lattice points at face centers are eliminated

[3] Reference is here made to the earlier edition of Barrett's book in which he was more explicit about this matter. His statement in the earlier edition can be checked by constructions similar to those of Figure 4, but for some cases atoms in adjacent planes must be considered as well. These can be projected onto the same section as shown in Figure 9.

[4] Another formulation of criteria to determine whether a lattice is transformed into itself by twin gliding has been given by Johnsen (1916).

and only those at cube corners—intersections of lattice lines in the drawing—are considered, the figure can be taken to represent a $(\bar{1}10)$ section through a simple cubic lattice. Twin gliding with slip that moves cube corner C to C′ meets the Wallerant criterion. The slip is now symbolized by $\frac{1}{3}$ $[\bar{1}\bar{1}2]$, because the identity distance in this direction in a simple cubic lattice is twice that in a face-centered lattice. Hindrance because of overshortening of interatomic distances during slip does not arise as it does for the like mechanism in the face-centered case because there are no atoms in positions such as G. Twin gliding of this sort has not been reported in any material having a simple cubic lattice, and it may never occur; however its possibility cannot be excluded by the simple tests here considered. On the other hand, twin gliding in structures with a simple cubic lattice such that E moves to E′ with corresponding movements of other lattice points does not lead to reconstruction of the lattice in twin position. In this case N_2 would be [112], represented by ED in the section. No lattice point exists in a simple lattice below the twin plane at the point required to satisfy Wallerant's criterion.

It may be that lattice criteria for the possibility of twin gliding are met but that structural features exclude a particular mechanism. Thus Bradley, Burst, and Graf (1953, Fig. 4) have shown from a consideration of atomic arrangements that twin gliding on $(01\bar{1}2)$, as in calcite, is impossible in dolomite. A similar approach can be used to test the possibility of a particular twin glide mechanism in all cases where the crystal structure is fully known.

Examples

General

Of the many compilations of data on twin gliding perhaps the most comprehensive are those of Seifert (1927) and of Tertsch (1949). The former covers both minerals and artificial materials. The latter gives data on translation gliding and twin gliding for about 80 minerals and a few metals not known as minerals. An article by Buerger (1930, p. 61–64) includes a table in which "fundamental elements" are given for a number of minerals and artificial substances and designated by the letters "*t*" and "*T*" which have generally been used in connection with translation gliding only. The table also includes data on twin gliding for a few substances such as calcite; the appropriate indices for N_1 and K_1 appear in it under the headings *t* and *T*.

Calcite

In Figure 5A is shown a calcite crystal with all the forms having "simple" indices when referred to rhombohedral axes. Above it is its stereographic projection on which are entered both rhombohedral and hexagonal indices. Figure 5B shows a similar crystal and its stereographic projection reoriented so that (101) is horizontal. Figure 5C shows the same crystal after "complete" twinning by gliding. Such complete transformation of a crystal was accomplished by Mügge (1883) but is difficult to realize. Ordinarily this twin gliding is demonstrated experimentally only by shearing of a small section of a rhombohedron as shown in pictures in some textbooks (Ford, 1932, Fig. 516; Niggli, 1924, Fig. 362).

Figure 5 shows that whereas the faces of the unit rhombohedron still belong to the same form after twin gliding this is not the case with all the faces of the prism $\{10\bar{1}\}$ or $\{11\bar{2}0\}$. Other changes can be followed out from the pictures and projections. With the combination of forms shown all changes are accompanied by other complementary changes, and the transformed crystal has the same habit as the initial crystal. This will not generally be the case. In the transformation of a crystal with only the forms $\{10\bar{1}1\}$ and $\{01\bar{1}2\}$ the unit rhombohedron would transform into itself, but the faces of the other rhombohedron would transform as follows:

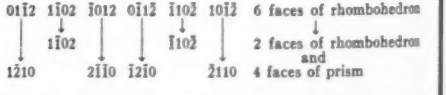
01$\bar{1}$2 1$\bar{1}$02 $\bar{1}$012 0$\bar{1}\bar{1}$2 $\bar{1}$10$\bar{2}$ 10$\bar{1}\bar{2}$ 6 faces of rhombohedron
1$\bar{1}$02 $\bar{1}\bar{1}$02 2 faces of rhombohedron
and
$\bar{1}$2$\bar{1}$0 2$\bar{1}\bar{1}$0 $\bar{1}\bar{2}\bar{1}$0 $\bar{2}$110 4 faces of prism

Mügge (1883, p. 85; 1885, p. 44) pointed out that such relations would distinguish mechanical twins from growth twins, since the two parts of a mechanical twin will in general not appear symmetrical with respect to the

twin plane in cases where growth twins might and often do appear thus.

Recently Borg and Turner (1953) have described calcite deformed by twin gliding in indices by inspection. As given in Figure 5 it again corresponds to rotation of the twinned part 180° on the normal to the twin plane as in an articulating model. The matrix for

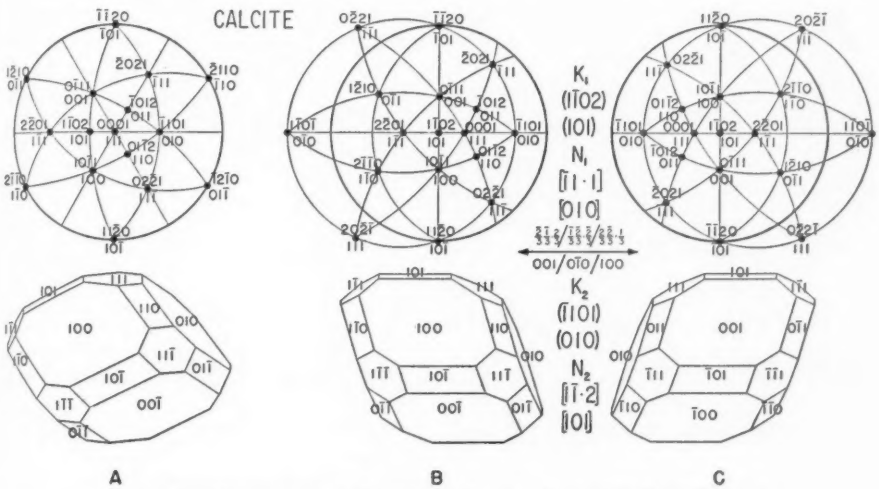

FIGURE 5.—MORPHOLOGICAL CHANGES IN CALCITE CAUSED BY TWIN GLIDING

A. Calcite showing all forms having "simple" indices in rhombohedral indexing
B and C. Calcite crystals showing the same forms as A; B is transformed into C by twin gliding and vice versa.

which they report lamellae, designated L_2, parallel to faces of the $\{11\bar{2}0\}$ prism. They have interpreted these as twin lamellae on *e* $(01\bar{1}2)$ rotated by further twinning on other twin surfaces of the same form as clearly shown in their Figures 2, 3, and 4. An excellent drawing explaining the change produced by successive twin gliding on two surfaces of $\{01\bar{1}2\}$ was published by Mügge (1883, Fig. 4), who also reported parting in calcite parallel to faces of the $\{11\bar{2}0\}$ prism. Later Mügge (1889b) reported that these partings occur parallel to four of the prism faces only and that they are associated with twin lamellae parallel to all three face directions of $\{01\bar{1}2\}$. The features observed by Mügge probably arose by the mechanism described by Borg and Turner. The case of transformation previously described explains why Mügge found parting parallel to just four faces (two face directions) of the prism.

The transformation matrix for twin gliding in calcite can be given for rhombohedral transforming hexagonal indices is not so readily obtained. It may be computed by the methods previously mentioned or by conversion of the rhombohedral matrix. This is done by multiplying the known matrix for converting hexagonal to rhombohedral indices by the rhombohedral twin glide matrix and then multiplying the product by the known matrix for converting rhombohedral to hexagonal indices. The resulting matrix is shown in Figure 5. Obviously this is a case where the use of rhombohedral axes is advantageous.

For twin gliding on other planes of $\{01\bar{1}2\}$ the transformation matrices must be suitably modified. Three possible forms can be used for the hexagonal matrix depending on which of the hexagonal *a* axes is eliminated as redundant. A full tabulation of the several cases that arise is given in Table 1. This shows the three possible sets of K_1 and N_1 together with the appropriate matrices. For the hexagonal matrices all three alternatives are given for each set, the choice of reference axes being

indicated by dots in suitable positions in the matrices. A similar scheme is used in describing the directions of N_1. Bell (1941, footnote p. 256) completed the indices [12.1] and [12.2] to [12$\bar{3}$1] and [12$\bar{3}$2]. This is incorrect since [*uvxw*] would not indicate the same direction as [*uv*.*w*], *x* being supplied by the assumption that $u + v + x = 0$, except in the special case that *u* and *v* have the same value though they may differ in sign. Even then the symbols may not be equivalent if they are to be taken as representing vectors. In other words, the symbol for the direction [*uv*.*w*] may be filled out in the manner referred to without changing its directional signification only in those cases in which the direction coincides with a symmetry axis of the hexagonal lattice.

All the rhombohedral matrices are symmetrical, columns may be interchanged with rows, and one matrix serves for transforming either face or axis indices. Among the hexagonal matrices only those are symmetrical in which the reference axes are taken symmetrically to the glide direction. The hexagonal matrix shown in Figure 5 is of this type. All the matrices for twin gliding on the several possible K_1 planes can be derived from those for gliding on one of these by suitable permutations.

The indices and matrices used here are those appropriate to calcite when it is referred to a unit form corresponding to the cleavage rhombohedron. The correct structural unit is a steep rhombohedron with $a_{rh} = 6.36$ and $\alpha = 46° 6'$, corresponding to {40$\bar{4}$1} in the morphological setting. The matrix for the transformation is given by Palache, Berman, and Frondel (1951, p. 158) as "morphology to structure, 1000/0100/0010/0004." Modified to the form used here this becomes 10.0/01.0/00.4. The corresponding rhombohedral matrix is 211/121/112. Each of these matrices has the modulus 4 requiring that the structural cell have four times the volume of the morphological cell. In the usual representations of the calcite structure (Bragg, 1937, Fig. 66; Ewald and Hermann, 1931, Fig. 140) and in Figure 8 the structure cell has half the volume of the morphological cell which corresponds to a face-centered rhombohedron containing $4CaCO_3$. The matrices for the transformation corresponding to this description would be $\frac{1}{2}0.0/0\frac{1}{2}.0/00.2$ and $1\frac{1}{2}\frac{1}{2}/\frac{1}{2}1\frac{1}{2}/\frac{1}{2}\frac{1}{2}1$. Each matrix has the modulus one half. The apparent discrepancy may be resolved by considering the rhombohedral unit for the morphological setting as having half the edge length usually pictured and containing but half a $CaCO_3$. With the use of the matrix given by Palache, Berman, and Frondel (1951, p. 158) the indices of the cleavage

TABLE 1.—SUMMARY OF INDEX TRANSFORMATIONS CORRESPONDING TO TWIN GLIDING ON {01$\bar{1}$2}

Hexagonal Axes			Rhombohedral Axes		
K_1	N_1	Transformation Matrix	K_1	N_1	Transformation Matrix
($\bar{1}$012)	[21·1]	$\frac{1}{3}1\cdot\frac{2}{3}/0\bar{1}\cdot0/\quad/\frac{4}{3}\frac{2}{3}\cdot\frac{1}{3}$	(011)	[100]	$\bar{1}00/001/010$
	[1·$\bar{1}$1]	$\frac{2}{3}\cdot\frac{1}{3}\frac{2}{3}/\quad/\frac{1}{3}\cdot\frac{2}{3}\frac{2}{3}/\frac{2}{3}\cdot\frac{2}{3}1$			
	[·$\bar{1}$21]	$/\cdot\bar{1}00/\cdot\frac{1}{3}\frac{1}{3}\frac{2}{3}/\cdot\frac{2}{3}\frac{4}{3}1$			
(1$\bar{1}$02)	[$\bar{1}$1·1]	$\frac{2}{3}\frac{1}{3}\cdot\frac{2}{3}/\frac{1}{3}\frac{2}{3}\cdot\frac{2}{3}/\quad/\frac{2}{3}\frac{2}{3}\cdot\frac{1}{3}$	(101)	[010]	$001/0\bar{1}0/100$
	[2·$\bar{1}$1]	$\frac{1}{3}\cdot1\frac{2}{3}/\quad/0\cdot\bar{1}0/\frac{4}{3}\cdot\frac{2}{3}1$			
	[·211]	$/\cdot\frac{1}{3}1\frac{2}{3}/\cdot0\bar{1}0/\cdot\frac{4}{3}\frac{2}{3}1$			
(01$\bar{1}$2)	[1$\bar{2}$·1]	$\bar{1}0\cdot0/1\frac{1}{3}\cdot\frac{2}{3}/\quad/\frac{2}{3}\frac{4}{3}\cdot\frac{1}{3}$	(110)	[001]	$010/100/00\bar{1}$
	[1·21]	$\bar{1}\cdot00/\quad/1\cdot\frac{1}{3}\frac{2}{3}/\frac{2}{3}\cdot\frac{4}{3}1$			
	[·$\bar{1}$11]	$/\cdot\frac{2}{3}\bar{1}2/\cdot\frac{1}{3}\frac{2}{3}\frac{2}{3}/\cdot\frac{2}{3}\frac{2}{3}1$			

rhombohedron referred to the structural cell become $\{10\bar{1}4\}$, but with use of the matrix $\frac{1}{2}0.0/0\frac{1}{2}.0/00.2$ its indices become $\{\frac{1}{2}0\frac{1}{2}2\}$. The former matrix is more convenient, and indices referred to the structure cell are given accordingly.

Twin gliding in calcite on the plane truncating the terminal edges of the cleavage rhombohedron with glide direction parallel to the truncated edge is described in terms of the hexagonal and rhombohedral structure cells by the following parameters:

	K_1	N_1	
Hexagonal	$(1\bar{1}\cdot 8)$	$[\bar{2}4\cdot 1]$	$\frac{4}{3}\cdot\frac{1}{3}/\frac{1}{3}\cdot\frac{4}{3}/\frac{4}{3}\cdot\frac{1}{3}$
Rhombohedral	(323)	$[\bar{1}3\bar{1}]$	$\frac{1}{3}\frac{4}{3}\frac{1}{3}/1\bar{2}1/\frac{4}{3}\frac{1}{3}\frac{1}{3}$

in the case illustrated by Figure 5. By suitable permutations alternatives corresponding to those given in Table 1 may be obtained. Bradley, Burst, and Graf (1953) have discussed twin gliding of calcite in terms of the structure cell. Their statement "that the (222) and one of the (110) directions interchange" is an example of the index changes obtainable by applying one of the permutations of the rhombohedral matrix. The indices of the zone represented by the horizontal line in the stereographic projections of Figure 5 referred to the structural cells remain [11.0] or $[10\bar{1}]$, the same as when referred to the morphological cells. The indices of the faces in this zone as shown in Figure 5B become:

$1\bar{1}0\bar{4}$	$1\bar{1}02$	$1\bar{1}08$	0001	$\bar{1}104$
$\bar{1}2\bar{1}$	101	323	111	121

They interchange upon twin gliding as indicated in Figures 5B and 5C.

Dolomite

Polysynthetic twinning of dolomite on $(02\bar{2}1)$ was first attributed to twin gliding by Johnsen (1902), though his efforts to produce it artificially were unsuccessful. Rogers (1929) described the morphological criteria for recognizing this type of twinning but did not mention its origin.

Johnsen (1902) discussed the mechanism of twin gliding in dolomite, using a diagram purporting to represent the distribution of two kinds of "molecules" in the S plane. Fairbairn and Hawkes (1941, Fig. 1A) and Fairbairn (1949, Fig. 10-6(a)) used the same diagram, referring to the two sets of points shown by Johnsen as representing "*Ca* atoms" and "*Mg* atoms". The arrangement of cations in dolomite was first suggested by Bragg (1914). In Figure 6A the Johnsen diagram shows an S section through dolomite corresponding to Figure 10-6(a) of Fairbairn (1949, p. 139). In Figure 6B a similar section shows the distribution of Ca and Mg ions in accord with the structure suggested by Bragg and now generally accepted.

Fairbairn (1949, p. 140) refers to the "direction-sense of slip" for twin gliding in dolomite as being "the reverse of that for calcite". This "direction-sense" is indicated by an arrow with a question mark in his Figure 10-6(b). Some doubt has persisted as to this "direction sense", but Turner, Griggs, Weiss, and Heard (1954, p. 482, 486) have recently shown that the original suggestion of Fairbairn and Hawkes (1941, p. 628–629) repeated by Fairbairn (1949, p. 140) is correct.

Bradley, Burst, and Graf (1953, Fig. 5) discuss twin gliding in dolomite, using a diagram of the structure projected onto an S plane. Half the ions represented in their diagram lie in a plane parallel to (110); the other half lie in an adjacent plane and are projected orthographically.

Figure 7 shows a section through a dolomite twin in the plane of deformation S. The indices of N_1 give the direction sense B to B′. By changing the signs of all the indices within the brackets the opposite direction sense, B to B″, would be indicated. For the slip B to B′, $K_2°$ is $(\bar{1}101)$, and s is equal to 0.5874. If the slip were B to B″, $K_2°$ would be (0001), and s would be 1.0408. The corresponding transformation matrix, determined from the transformation of the three known planes K_1, $K_2°$, and S, would be $\frac{1}{3}\bar{1}\frac{1}{3}/\frac{1}{3}0\frac{1}{3}/\frac{1}{3}\bar{1}\frac{1}{3}$ for rhombohedral indices. From this it may be calculated that (100) would have to be converted to $(\bar{1}\bar{1}1)$ and vice versa. If the dolomite structure is considered to be face-centered with a distribution of cations and anions analogous to that of NaCl, the indicated conversion could probably not be realized since structural planes corresponding to (100) have a checkerboard

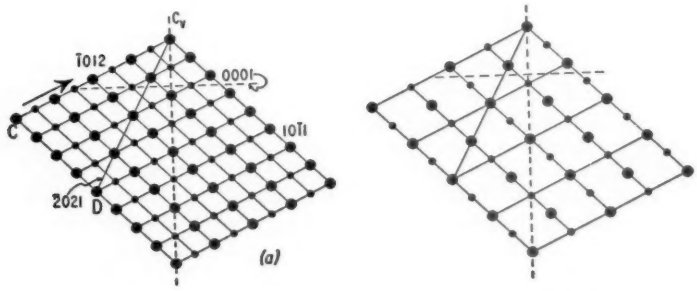

FIGURE 6.—SECTIONS THROUGH DOLOMITE STRUCTURE PARALLEL TO $(1\bar{2}10)$
A. After Figure 10-6(a) of Fairbairn (1949)
B. Arrangement of cations corresponding to structure suggested by Bragg (1914)

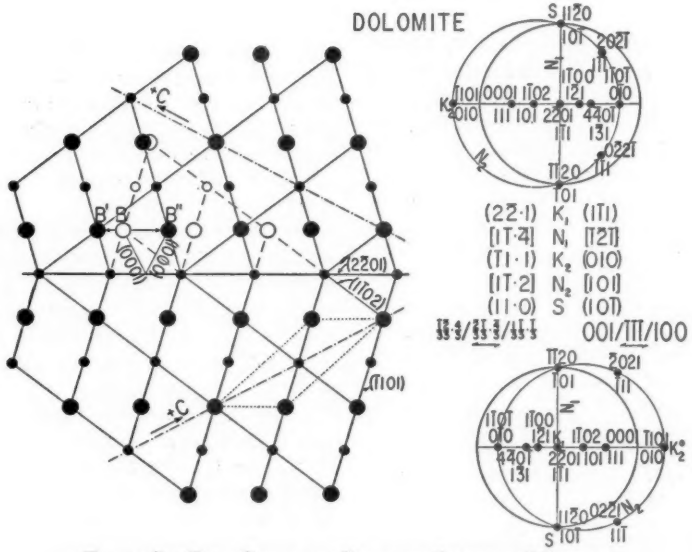

FIGURE 7.—TWIN GLIDING IN DOLOMITE SHOWN IN S SECTION
Cations only are shown by filled circles. Open circles indicate positions of some cations before gliding. Dotted lines in lower part of figure outline one structure cell.

arrangement of anions and cations, whereas structural planes parallel to $(\bar{1}\bar{1}1)$ are made up either entirely of cations or entirely of anions. Such a slip would involve the selection of rows of like ions as new axes, as may be seen from inspection of the matrix. This will not occur when the direction sense of slip is B to B′, found experimentally. In this case the new axes are rows along which cations and anions alternate as required by the structure. This can be seen from the rhombohedral matrix.

Bradley, Burst, and Graf (1953, Fig. 4) have shown, with the aid of a projection of the dolomite structure onto an S plane, why twin gliding of the type known in calcite cannot occur in dolomite. They also suggest a mechanism to account for the changes induced in dolomite by grinding. This involves the long-known translation gliding on (111) and what they refer to as "unit glide on (110)". They use indices referred to the structure cell. Their "unit glide on (110)" becomes gliding

on $(11\bar{1})$ in the direction $[\bar{1}\bar{1}2]$ referred to the edges of the cleavage rhombohedron as axes. However, as may be seen from their Figure 6, the s of their "unit glide" is not identical with that of the known twin gliding involving the same elements. It seems that their "unit glide" is specially postulated to fit into a mechanism which will account for the effects of grinding on the DTA behavior and X-ray diffraction of dolomite.

Atom Movements in Twin Gliding

Previous Work

Bell (1941, p. 253) stated:

> This theory of simple shear explains all of the facts which can be observed on mechanically twinned crystals. However, it should be emphasized that this may not represent the actual movement of atoms, molecules, ions or other units in the crystal structure."

Wallerant (1904, p. 174) pointed out that "molecules" in the twinned part are not turned 180° on an axis normal to the glide plane as was suggested by the idea that the two parts of the twin must be related as are the two parts of articulating twin models.

Niggli (1929, p. 426, Fig. 3) suggested that the relation of the two parts in a glide twin must require "movements additional to" (*zusätzliche Bewegungen*) simple shear, and Tertsch (1949, p. 151) in copying Niggli's figure specifies that this must be "rotation" (*Drehung*). This view is not tenable. Hochschild (1908) made careful observations on sphalerite and showed that the polar axes normal to the twin plane (111) are parallel, not antiparallel, in these twins. Such twins might arise by twin gliding without rotation.

Calcite

At most only atom centers (or lattice points) are rearranged by simple shear (translation an amount proportional to the distance from the glide plane) in twin gliding. Because of the existence of indeformable spherical atoms or indeformable structure units twin gliding cannot be simple shear on an atomic scale (Friedel, 1926, p. 486). As soon as Bragg (1914) determined the crystal structure of calcite Johnsen (1914) showed that, whereas the movement of the centers of Ca and C atoms here involves only simple shear, the O atoms must also be rotated about the C atoms to which they belong so that the planar CO_3 groups become oriented normal to the newly constituted c axis. Friedel (1926, p. 486) pointed out that these groups are rotated through 52°30′ on the normal to the plane of deformation.

Figure 8 shows a section through the calcite structure parallel to an S plane. In the upper right-hand corner is a portion of the structure that has been brought into twin orientation by gliding; the original position of the structural units is shown by dotted lines and circles. This shows that a rotation such as that prescribed by Friedel must take place. As Bradley, Burst, and Graf (1953, p. 214) describe this, "CO_3 ions rotate according to the steric requirements". A comparable rotation occurs in twin gliding of dolomite, in this case through 54°59′.

Sphalerite

Buerger (1928, p. 35–41) has shown that sphalerite suffers twin gliding on {111}, the slip direction being $[11\bar{2}]$. Figure 9 shows two planes through the cell projected orthographically. In the lower part of the twin two small rectangles are shaded to show correspondence to the picture of a unit cell at lower right. Solid circles indicate atoms on a $(1\bar{1}0)$ plane; open circles indicate atoms on a parallel plane at a distance $a_0\sqrt{2}/4$.

The one choice of direction sense for N_1 in face-centered structures is indicated in Figure 9. A twin structure is achieved by the gliding of successive slices consisting of a sheet of Zn's with an adjacent sheet of S's. Beginning with the sheet of Zn's connected by a continuous horizontal line, all the Zn centers undergo simple shear to the left. Similarly all S centers undergo such shear with respect to the sheet of S's indicated by the continuous horizontal line. No single plane of reference can be given with respect to which all atom centers in the twinned part are shifted by simple shear. It is often stated that twins are joined at a twin plane and that atoms or lattice points in this plane are common to the two parts of the twin. In this case two twin planes, one of

Zn atoms and another of S atoms, would be common to the two parts of the twin. This would give rise to an orientation of the two parts of the twin to each other corresponding to that reported by Hochschild (1908) for sphalerite.

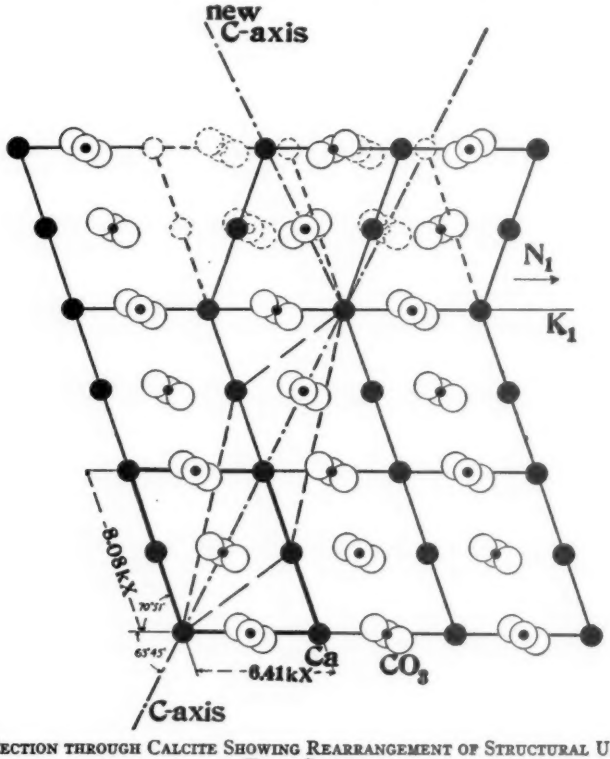

FIGURE 8.—S SECTION THROUGH CALCITE SHOWING REARRANGEMENT OF STRUCTURAL UNITS ATTENDING TWIN GLIDING

Heavy lines at lower left outline a unit containing $4CaCO_3$ and bounded by surfaces parallel to the cleavage rhombohedron. Dashed lines extending from lower left outline a structure cell. At the top is shown a section reoriented by twin gliding.

Aminoff and Broomé (1931) have shown by the consideration of twins of several minerals of simple structure that the two parts of the twin have in common a portion of the structure, a slice parallel to the contact plane, and that along the twin boundary a structure exists which is different from the normal untwinned structure. They maintained that the "contact structure" which characterizes the boundary zone must correspond to a structure that is realized in nature, a polymorph, or to some plausible structure. In the case of sphalerite this contact structure was shown by Aminoff and Broomé to correspond to wurtzite.

The stacking of successive ZnS slices in wurtzite parallel to (0001) is that of hexagonal close packing, whereas the stacking of ZnS slices parallel to (111) in sphalerite is that of cubic close packing, and the two cases can be represented by the sequences ABABAB . . . and ABCABCABC . . . respectively. At the left of Figure 9 successive slices of ZnS are labelled by appropriate letters, and it is indicated that the lower sphalerite sequence, ABCA . . . , reading from the middle A down, overlaps the upper sphalerite sequence, ABCA . . . , reading up from the middle A. The BAB sequence corresponds to the wurtzite contact structure

pointed out by Aminoff and Broomé. Other wurtzite structures are now known (Frondel and Palache, 1950) involving yet other stacking regularities of the ZnS slices. Two of these are designated wurtzite-4H and wurtzite-6H using the nomenclature devised by Ramsdell (1947, p. 65) for polymorphs of SiC. These have the "*zig-zag* sequences" 22 and 33 respectively which can be recognized in Figure 9 as the stacking sequences CBABC and ACBABCA. The two parts of a sphalerite twin are joined not only by the wurtzite contact structure recognized by Aminoff and Broomé but also by thicker sequences of wurtzite-4H or wurtzite-6H. Twin gliding in sphalerite consists of the progress of a segment of wurtzite-6H through the structure with successive sheets passing from the original sphalerite to sphalerite in the twin part through the wurtzite-6H structure.

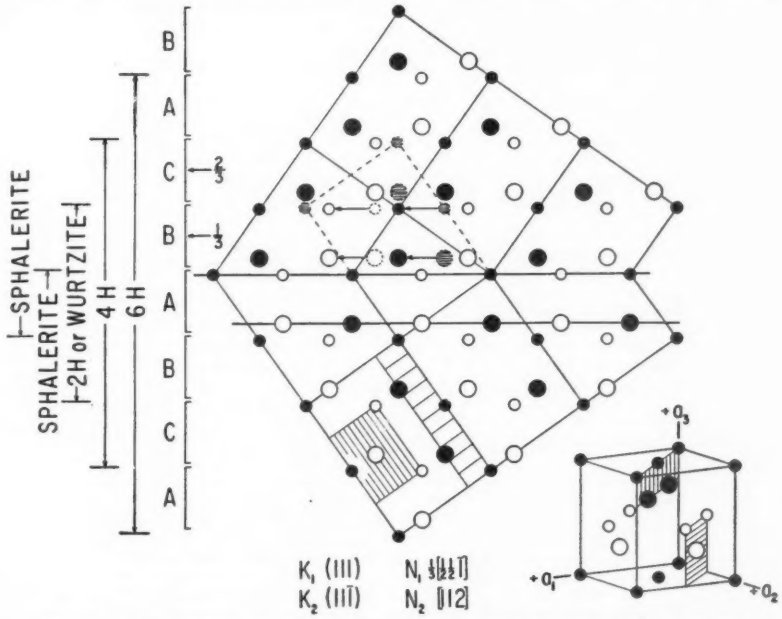

FIGURE 9.—STRUCTURE OF SPHALERITE TWIN PROJECTED ONTO A (1$\bar{1}$0) SECTION

Dashed lines, ruled and broken circles in upper part of figure show a small section of structure before twin gliding. Compare drawing at lower right for correlation of solid and open circles.

CONCLUDING REMARKS

As Friedel (1926, p. 489) has pointed out, the atomic rearrangements attending twin gliding are undeterminable except where the structure is known. Three distinct cases have been considered here: in twin gliding of gold only simple shear of atom centers is involved; in calcite a rotation of CO_3 groups also occurs; and in sphalerite ZnS slices are affected. Study of twin gliding in other materials of known structure should reveal variants of these mechanisms.

REFERENCES CITED

Aminoff, G., and Broomé, B., 1931, Strukturtheoretische Studien über Zwillinge, I.: Zeitsch. Krist., v. 80, p. 355–376.

Barrett, C. S., 1943, Structure of metals: N. Y., McGraw-Hill, 567 p.

—— 1952, Structure of metals: N. Y., McGraw-Hill, 2d ed., 661 p.

Bell, J. F., 1941, Morphology of mechanical twinning in crystals: Am. Mineralogist, v. 26, p. 247–261.

Borg, I., and Turner, F. J., 1953, Deformation of Yule marble: Part VI—Identity and significance of deformation lamellae and partings in calcite grains: Geol. Soc. America Bull., v. 64, p. 1343–1352.

Bradley, W. F., Burst, J. F., and Graf, D. L., 1953,

Crystal chemistry and differential thermal effects of dolomite: Am. Mineralogist, v. 38, p. 206–217.

Bragg, W. L., 1914, The analysis of crystals by the X-ray spectrometer: Roy. Soc. Proc., v. 89a, p. 468–489.

—— 1937, Atomic structure of minerals: Ithaca. N. Y., Cornell Univ. Press, 292 p.

Buerger, M. J., 1928, Plastic deformation of ore minerals: Am. Mineralogist, v. 13, p. 1–17, 35–51.

—— 1930, Translation-gliding in crystals: Am. Mineralogist, v. 15, p. 45–64.

—— 1942, X-ray crystallography: N. Y., John Wiley & Sons, 531 p.

Ewald, P. P., and Hermann, C., 1931, Strukturbericht 1913–1928: Ak. Verlagsges. Leipzig, 818 p.

Fairbairn, H. W., 1949, Structural petrology of deformed rocks: Cambridge, Mass., Addison Wesley, 344 p.

Fairbairn, H. W., and Hawkes, H. E., 1941, Dolomite orientation in deformed rocks: Am. Jour. Sci., v. 239, p. 617–632.

Ford, W. E., 1932, Dana's textbook of mineralogy: N. Y., John Wiley & Sons, 851 p.

Friedel, G., 1926, Lecons de cristallographie: Paris, Berger-Levrault, 602 p.

Frondel C., and Palache, C., 1950, Three new polymorphs of zinc sulfide: Am. Mineralogist, v. 35, p. 29–42.

Henry, N. F. M., and Lonsdale, K., 1952, International tables for X-ray crystallography Vol. I: Birmingham, Kynoch Press, 558 p.

Hochschild, P., 1908, Studien an Zinkblende: Neues Jahrb., Beil.-Bd. 26, p. 151–212.

Johnsen, A., 1902, Biegungen und Translationen: Neues Jahrb., 2, p. 133–153.

—— 1913, Die Struktureigenschaften der Kristalle: Fortsch. Min., v. 3, p. 93–140.

—— 1914a, Schiebungen und Translationen in Kristallen: Jahrb. der Radioaktivität und Elektronik, v. 11, p. 226–262.

—— 1914b, Die Massengitter des Kalkspates: Physik. Zeitsch., v. 15, p. 712–715.

—— 1916, Die Deformation der Raumgitter durch Schiebung: Centralbl. Mineralogie, p. 121–130.

Liebisch, Th., 1889, Ueber eine besondere Art von homogenen Deformationen: Neues Jahrb., Beil.-Bd. 6, p. 105–120.

Mügge, O., 1883, Beiträge zur Kenntniss der Structurflächen des Kalkspathes und über die Beziehungen derselben untereinander und zur Zwillingsbildung am Kalkspath und einigen anderen Mineralien: Neues Jahrb., 1, p. 32-54, 81–85.

—— 1885, Zur Kenntniss der durch secundäre Zwillingsbildung bewirkten Flächen-Verschiebungen: Neues Jahrb., 2, p. 44–58.

—— 1889a, Ueber homogene Deformationen (einfache Schiebungen) an dem Triklinen Doppelsalz $BaCaCl_4.4aq.$: Neues Jahrb., Beil.-Bd. 6, p. 274–304.

—— 1889b, Mineralogische Notizen: Neues Jahrb., 1, p. 230–251.

—— 1927, Mikroskopische Physiographie der petrographisch wichtigen Mineralien: Stuttgart, Schweitzerbart, 810 p.

Mügge, O., and Heide, F., 1931, Einfache Schiebungen am Anorthit: Neues Jahrb., Beil.-Bd. 64A, p. 163–170.

Niggli, P., 1924, Lehrbuch der Mineralogie, I. Allgemeine Mineralogie: Berlin, Borntraeger, 2d ed., 712 p.

—— 1929, Geometrisches zur Theorie der Kristallschiebungen, Translationen und Zwillingsbildungen: Zeitsch. Krist., v. 71, p. 413–451.

Palache, C., Berman, H., and Frondel, C., 1951, System of mineralogy: N. Y., John Wiley & Sons, 7th ed., Vol. II, 1124 p.

Ramsdell, L. S., 1947, Studies on silicon carbide: Am. Mineralogist, v. 32, p. 64–82.

Rogers, A. F., 1929, Polysynthetic twinning in dolomite: Am. Mineralogist, v. 14, p. 245–250.

Schmid, E., and Boas, W., 1935, Kristallplastizität; Berlin, Springer, 373 p.

—— 1950, Plasticity of crystals: London, Hughes, 353 p. (A translation of the original German of 1935 by an anonymous translator)

Seifert, H., 1927, Spaltbarkeit, Translationen und einfache Schiebungen nach Gleitflächen: Landolt Börnstein Physikalisch-chemische Tabellen, 5th ed., 1er Ergänzungsband, p. 35–47.

Tertsch, H., 1949, Die Festigkeitserschienungen der Kristalle: Vienna, Springer, 310 p.

Turner, F. J., Griggs, D. T., Heard, H., and Weiss, L., 1954, Plastic deformation of dolomite rock at 380°C: Am. Jour. Sci., v. 252, p. 477–488.

Wallerant, F., 1904, Des macles secondaires et du polymorphisme: Bull. Soc. Fran. Min., v. 27, p. 169–189.

—— 1909, Cristallographie: Paris, Beranger, 523 p.

Department of Geological Sciences, Univ. of Calif., Berkeley 4, Calif.

Manuscript Received by the Secretary of the Society June 1, 1954.

BULLETIN OF THE GEOLOGICAL SOCIETY OF AMERICA
VOL. 66, PP. 913-948, 22 FIGS. JULY 1955

CRUSTAL STRUCTURE AND SURFACE-WAVE DISPERSION

PART IV: ATLANTIC AND PACIFIC OCEAN BASINS

BY JACK E. OLIVER, MAURICE EWING, AND FRANK PRESS

ABSTRACT

Properties of the suboceanic crust are deduced from dispersion of earthquake surface waves. Love waves and Rayleigh waves on seismograms of the Honolulu station from shocks occurring in the circum-Pacific earthquake belt show typical oceanic crust throughout the Pacific Ocean. They do not reveal anomalous areas of continental proportions which may once have stood above sea level. Similar results are obtained for parts of the North Atlantic. The method, however, is insensitive to relatively small or thin structures. The Easter Island Rise is somewhat anomalous and possibly represents a deviation toward the continental type of crust.

Some earthquakes cause a short-period train of surface waves to predominate over the more common long-period surface waves for purely oceanic paths. The beginning of the train is identified definitely as Love-wave motion. The later part of the train, which is apparently a noncoherent mixture of Love and Rayleigh waves, with periods of 6 to 9 seconds, is similar in character to long-period microseisms. These waves are sharply attenuated at continental margins but propagate easily through either continents alone or oceans alone.

From the coast of North America to the Easter Island Rise shocks generally produce short-period surface waves at Honolulu, and other Pacific shocks produce long-period waves. Hawaiian shocks produce short periods on the North American coast.

CONTENTS

TEXT

	Page
Introduction	914
Acknowledgments	914
Instrumentation	915
Experimental procedure	915
Selection of records	915
Identification of wave trains	915
Method of reading dispersion	922
Continental correction	922
Epicentral location	922
Theory	922
General	922
Rayleigh waves	926
Love waves	929
Choice of constants	930
Experimental results	932
Rayleigh waves	932
Love waves	940
Short-period surface waves	942
Geographical factors relating to presence or absence of various surface-wave types	943
Conclusions	945
References cited	946

FIGURES

Figure		Page
1.	Map of epicentral locations of selected earthquakes	925
2.	Dimensionless phase and group velocity, Rayleigh and first-shear modes	927
3.	Group velocity, Rayleigh and first-shear modes, dimensions pertinent to earthquakes	928
4.	"G" waves	929
5.	Seismograms	931
6.	Dependence of Rayleigh waves on liquid depth for Case II	932
7.	Sediment thicknesses in the Pacific	932
8.	Rayleigh-wave dispersion, Marianas	934
9.	Rayleigh-wave dispersion, Philippines	934
10.	Rayleigh-wave dispersion, Formosa, Luzon	935
11.	Rayleigh-wave dispersion, Japan	935
12.	Rayleigh-wave dispersion, Kuriles	936
13.	Rayleigh-wave dispersion, Alaska	936
14.	Rayleigh-wave dispersion, Washington	937
15.	Rayleigh-wave dispersion, Mexico to Peru	937
16.	Rayleigh-wave dispersion, Chile	938
17.	Rayleigh-wave dispersion, Tongas, Fijis	938
18.	Rayleigh-wave dispersion, New Guinea, Solomons	939
19.	Rayleigh-wave dispersion, Atlantic	939
20.	Short-period surface waves, Berkeley records	941
21.	Short-period surface-wave dispersion	942
22.	Short-period surface waves, Palisades and Bermuda records	944

TABLES

Table		Page
1.	Shocks recorded at Honolulu	916
2.	Hawaiian shocks recorded in North America	922
3.	Atlantic shocks	923
4.	Constants used in calculation of theoretical curves	927
5.	Computed points on first shear-mode curve	928
6.	Compressional and shear wave velocities corresponding to various values of Poisson's ratio	929
7.	Liquid, water, and sediment thickness for Atlantic shocks	933

Introduction

Although surface waves are the most conspicuous feature on most seismograms, and have received careful study by a few seismologists, there remain many unexplained or partially understood surface-wave arrivals. Most early writers on Rayleigh waves confined their attention to the period and velocity of the beginning of the Rayleigh wave train and attached little importance to its duration.

Ewing and Press (1950; 1952a; 1952b) showed that, in the normal-mode theory of propagation of elastic waves in a liquid layer overlying a homogeneous solid substratum, the gravest mode explained the entire train of ordinary Rayleigh waves (periods 15–40 sec.) propagated over oceanic paths. In this paper the writers follow Haskell (1951) and call this the Rayleigh mode, and the corresponding waves Rayleigh waves. Higher modes will be called the first-shear mode, second-shear mode, and so on, since these waves have a cutoff at the velocity of shear waves in the bottom.

The theory of Love waves has been known for some time, and several investigators (Gutenberg and Richter, 1936; Wilson, 1941; Evernden, 1952b; and Byerly, 1930) have deduced oceanic crustal structure from Love-wave dispersion.

The purpose of this study is to consider all types of surface waves having a preponderance of oceanic path, with a view toward (1) description and geographic correlation of surface-wave types, (2) experimental investigation of the mechanism of propagation, (3) reconciliation of crustal structures obtained from surface-wave dispersion and that deduced from explosion seismology, (4) reconnaissance of oceanic areas to detect variations in crustal structure.

With these objectives in mind, a collection of records from the Honolulu installation was obtained. This station has the following advantages: (1) it is uniquely located near the center of the Pacific so that oceanic paths prevail at all azimuths, (2) its location near the center of the Pacific earthquake belt provides, over a period of a few years, shocks of suitable magnitude at practically all azimuths, (3) the instrumentation includes matched long-period horizontal seismometers with reasonably good response at the surface-wave frequencies. Its chief disadvantage is the absence of a matched long-period vertical instrument for the separation of Rayleigh and Love waves. A further difficulty is due to the restriction to one recording station; it becomes necessary to utilize sources that may be dissimilar, but this is outweighed by the advantage of a single set of invariable instrumental constants. The consistency of the results is proof of the validity of this approach.

Although the Honolulu collection accounted for most of the data, supplementary information for the Pacific Ocean was obtained from the Berkeley and Fresno stations, and from the Bermuda, Palisades, Ottawa, and Kew installations for the Atlantic Ocean.

Almost all seismograms used could be classified into two types according to surface-wave periods. The long-period type (15 to 40 sec.) and the short-period type (6 to 15 sec.) are designated in data tabulations by *LP* and *SP* respectively. In the few cases where both types of surface waves are present the two trains are readily separable, even in the exceedingly rare cases where they have comparable amplitudes.

Acknowledgments

The authors wish to thank the U. S. Coast and Geodetic Survey, in particular Frank Neumann and L. M. Murphy, for the loan of the Honolulu seismograms and for other valuable assistance. Similar acknowledgments

are due the Berkeley, Bermuda, Ottawa, and Kew stations for the use of their records.

Instrumentation

The Honolulu station is operated by the U. S. Coast and Geodetic Survey. Under normal conditions two modified long-period Milne-Shaw horizontals and one short-period Neumann-Labarre horizontal are recording. The Milne-Shaws have a 12-second free period, gain (static magnification) of about 130, damping ratio of 20:1, and are oriented N.-S. and E.-W. The Neumann-Labarre has a free period of 1.2 sec., gain of 4800, damping ratio of 8:1, and is oriented E.-W. All three drums run at a paper speed of 30 mm/min. For a few months at the end of 1949 and the beginning of 1950, short- and long-period vertical Sprengnethers were operated, producing some records used in this study.

Background from microseisms is particularly bad at Honolulu, especially during the winter months. For this reason the long-period instruments have a low gain. Selection of sources is restricted to earthquakes of fairly high magnitude.

At Bermuda there are two Milne-Shaw horizontals oriented NE.-SW. and NW.-SE. with a free period of 12 seconds, gain of 250, damping ratio about 16:1, and paper speed of 8 mm/min. There are also three component Benioff seismometers, both long- (T_o = 1, T_g = 90 sec) and short-period (T_o = 1, T_g = 0.2 sec) as well as a Columbia University vertical seismograph with T_o = 12, T_g = 15 sec. The latter instruments were installed during 1951 and 1952, so that the backlog of earthquake records from them is scanty.

The Palisades records used in this study were taken by a matched three-component set of Columbia University seismometers with T_o = 12, T_g = 15 sec. The vertical is identical with the instrument at Bermuda. Long- and short-period Benioff records are also available at Palisades.

Only the Galitzin records from Berkeley were studied. These are similar in response to the Columbia instruments and have T_o = 12, T_g = 12 sec for all three components. Fresno has a three-component set of Sprengnethers.

Ottawa has two Milne-Shaw horizontals and a Benioff vertical, both long and short period. Kew has a three-component set of Galitzins with the free period of the seismometer and of the galvanometer equal. The periods of the Kew instruments all fall in the range of 12–23 seconds.

Experimental Procedure

Selection of Records

Tables 1, 2, and 3 list earthquakes used in this study. Figure 1 shows their geographic distribution. Most of the Pacific earthquakes are limited to the years 1947–1950. Those which made Rayleigh waves at Honolulu are plotted as squares. They were chosen for selected azimuths and paths, and general clarity, and do not represent all the earthquakes making this type of surface wave during the four-year period. Triangles designate earthquakes that made the short-period surface waves. These represent all earthquakes of this type in the Pacific belt during the four-year period which were of sufficient magnitude to be located and to be recorded at Honolulu. The reason for the more thorough search for this type is their rather peculiar geographical distribution to be discussed later. Open circles represent earthquakes which made both types of surface waves at Honolulu.

To take advantage of the superior instrumentation, several records of Hawaiian earthquakes recorded at Berkeley and Fresno were added to the Pacific collection.

The Atlantic earthquakes were restricted to 1950–1952 because of the recent additional instrumentation at Bermuda, and because the Palisades station has been in operation only during that period.

Identification of Wave Trains

The absence of a long-period vertical at the Honolulu station (to distinguish Love and Rayleigh waves) is the greatest difficulty in the entire study. To overcome this, the first records studied were chosen from quakes at azimuths nearly due north, south, east, or west. With this orientation, Love waves appear only, or in practice much more strongly, on the transverse

TABLE 1.—SHOCKS RECORDED AT HONOLULU

No.	Date Day	Month	Year	Hour GCT	Lat.	Long.	Depth in km	Mag.	Surface-Wave Type	Location	G	Δ in km	Δ Cont. in km
1	1	Apr	46	12 29 04	53°N	162.7°W	50±		S. P.	off Alaska Peninsula			
2	10	Nov	46	17 43 00	7.8°S	77.8°W			L. P.	N. Peru	?	9300	330
4	2	Apr	47	05 39 46	1.8°S	138.3°E			L. P.	Pacific Ocean N. of New Guinea	No	7380	
5	13	June	47	20 24 51	19°N	146°E			L. P.	400 mi N of Guam	No	5880	
6	19	June	47	07 34 39	21.7°N	145°E			L. P.	600 mi N of Guam	Weak	5820	
7	15	Oct	47	02 09 45	64.5°N	148,8°W			L. P., S. P.	400 mi SW of Fairbanks	No	4860	
8	1	Nov	47	14 58 54	10.8°S	74.5°W			L. P.	150 mi NE of Lima	Yes	9720	
8a	14	Jan	48	02 25 36	8.9°S	108.7°W			S. P.	1200 mi N of Easter Isl.			
9	24	Jan	48	17 46 46	10.8°N	121.9°E			L. P.	Philippines	Yes	8570	
10	3	Mar	48	09 09 54	18 1/2°N	119°E	Norm	7.2	L. P.	Philippines	Yes	8600	390
11	13	Mar	48	20 02 35	1 1/2°N	126 1/2°E	60	7.1	L. P.	Molucca Passage	Yes	8460	
12	14	May	48	22 31 49	54.7°N	160.2°W			L. P., S. P.	? N Pacific Ocean off Alaskan Peninsula	Possibly		

											Ocean off Alaskan Peninsula	Possibly		

TABLE 1 (Cont.)

No.	Day	Month	Year	Hour GCT	Lat.	Long.	Depth in km	Mag	Surface-Wave Type	Location	G	Δ in km	Δ Cont in km
13	28	June	48	07 13 30	36.1/2°N	136°E	Norm	7.3	L. P.	Honshu, Japan	Yes	6540	610
14	2	Sept	48	23 34 50	10°N	125 1/2°E	Norm	7.0	L. P.	Philippines	Yes	8240	
15	8	Sept	48	15 09 14	21.0°S	174.2°W			L. P.	Tonga Region	Weak	5020	
16	10	Sept	48	13 48 34	43 1/2°N	147°E	40	7.1	L. P., S. P.	Pacific Ocean E. of Hokkaido, Japan	No	5620	
17	16	Mar	49	22 15 13	5 1/2°S	151°E	60	7.1	L. P.	New Britain Isl.	No	6320	390
18	17	Mar	49	21 05 03	5 1/2°S	151°E	60	7.0	L. P.	New Britain Isl.	No	6320	
19	24	Mar	49	20 56 58	41.9°N	124.8°W			S. P.	Pacific Ocean off N. Calif. Coast		3850	
20	27	Mar	49	06 34 05	3 1/2°N	127 1/2°E	Norm	7.0	L. P.	S of Mindanao	No	8280	
20a	13	Apr	49	19 55 40	47.1°N	122.6°W			L. P., S. P.	Pacific NW	No	4280	
21	20	Apr	49	03 29 0	38°S	72 1/2°W	70-700	7 1/2	L. P.	Chile	No		
22	2	July	49	19 57 13	16°N	148°	50	7.2	L. P.	Marianas	No	5710	
23	5	Aug	49	19 08 47	1°S	78°W			L. P.	Central Ecuador	No	8990	280
24	14	Sept	49	19 50 20	3/4°N	126°E	50?	7.2	L. P.	Celebes Region	Yes	8550	450
25	27	Sept	49	15 30 43	60°N	149°W		7	L. P., S. P.	S. Alaska	Possibly	4370	
26	27	Nov	49	08 42 16	18°S	173°W			L. P.	Tonga Isl. Region	Possibly	4660	
27	17	Dec	49	15 07 53	54°S	71°W		7 1/2, 7 1/4	L. P.	Punta Aremas	Yes	1170	

TABLE 1 (Cont.)

No.	Day	Date Month	Year	Hour GCT	Lat.	Long.	Depth in km	Mag	Surface-Wave Type	Location	G	Δ in km	Δ Cont in km
27a	17	Dec	49	06 53 29	54°S	71°W			L. P.	Punta Arenas	Yes		
28	29	Dec	49	03 03 55	18 1/2°N	121°E	Norm	7.2	L. P.	N. Tip of Luzon	No	8400	
29	17	May	50	18 13 13	21°S	169°E	40	7.0		New Hebrides		5830	
30	25	May	50	18 35 00	13°N	142 1/2°E	100	7 1/4 Pas	L. P.	150 mi W of Guam	Yes	6370	
31	24	June	50	22 25 34	20 1/2°S	169 1/2°E	40	7.2	L. P.		Weak	8340	
31a	25	June	50	11 05 51	5°N	127°E		6 1/2	L. P.	S. of Mindanao	Weak	8270	
31b	29	July	50	14 36 33	33°N	115 1/2°W			S. P.			4360	
32	31	Aug	50	07 05 35	6°N	126°E		7	L. P.	Off S. coast of Mindanao	Weak	8340	
33	29	Sept.	50	06 32 14	19°N	107°W		7	S. P.	Off Colima	Yes	5300	
33a	4	Oct	50	00 41 07	18 1/2°S	170°E			L. P.	New Hebrides	No	5640	
34	5	Oct	50	16 09 31	11° N	85°W	Norm	7.7	L. P., S. P. ?	Costa Rica	Yes	7840	
35	5	Nov	50	17 37 27	33 1/4°N	134 3/4°E	Norm	6.9	L. P.	Japan	Yes	6700	
36	8	Nov	50	02 18 12	10°S	159 1/2°E	Norm	7 1/4	L. P., S. P. ?	Solomons	Yes	5810	
37	17	Nov	50	19 28 18	17°N	100 1/2°W		6 3/4-7	L. P.	Near west coast of Mexico	No	6010	
38	5	June	51	16 57 47	30°N	132°E	100	6 3/4-7	L. P.	S of Kyushu	No	7000	

38	5	June	51	16 57 47	30°N	132°E	100	6 3/4-7	L. P.	S of Kyushu	No	7000	

TABLE 1 (Cont.)

No.	Day	Date Month	Year	Hour GCT	Lat.	Long.	Depth in km	Mag	Surface-Wave Type	Location	G	Δ in km	Δ Cont in km
40	17	June	51	23 26 58	44 1/2°N	130°W		5 1/2	S. P.	300 mi off coast of Oregon		3640	
41	8	July	51	05 44 20	11°N	122°E		6 1/2	L. P.	Panay Isl. Philippines	Yes	8560	400
42	21	Oct	51	21 34 13	11°N	122°E			L. P.	Formosa	Yes	8120	
42a	22	Oct	51	03 29 26	24°N	122°E			L. P.	Formosa	Yes	8120	
42b	22	Oct	51	05 43 01	24°N	122°E			L. P.	Formosa	No	8120	
43	6	Nov	51	16 40 06	47°N	154°E			L. P., S. P.	Kurile Isl.	No	5170	
45	8	Nov	51	13 45 09	54 1/2°N	160°W		6 1/4	S. P.	Aleutians	Possibly	3710	
46	24	Nov	51	18 50 19	23°N	121°E		7 1/4	L. P.	Formosa	No	8150	
47	10	Apr	47	15 58 04	35°N	116. 6°W			S. P.	Mojave Desert, Cal.		4290	
48	2	May	47	02 19 06	53. 8°N	164. 3°W	50±		S. P.	N Pacific Ocean off Unimak Isl		3690	
49	27	Aug	47	13 37 48	37. 8°S	179. 1°E			S. P.	Off SE coast N. Isl. New Zealand		6990	
50	23	Sept	47	13 52 58	40. 2°N	125. 8°W			S. P.	Cape Mendocino, Cal.		3690	
51	20	Oct	47	01 43 17	64°N	147. 9°W			L. P., S. P.	Fairbanks & Mt. McKinley area		4780	
52	2	Nov	47	07 00 26	40°N	127°W			S. P.	Cape Mendocino, Cal.		3590	
53	21	Nov	47	03 54 15	19°N	107°W			S. P.	Off Mexico		5290	

TABLE 1 (Cont.)

No.	Day	Month	Year	Hour GCT	Lat.	Long.	Depth in km	Mag	Surface-Wave Type	Location	G	Δ in km	Δ Cont in km
54	28	Feb	48	01 58 05	53.2°N	133°W		6 1/2	S. P.	Queen Charlotte Isl.		4170	
55	14	May	48	22 31 49	54.7°N	160.2°W			S. P.	N. Pacific Ocean off Alaskan Peninsula		3720	
56	17	May	48	17 48 42	54.8°N	160.1°W	75		L. P., S. P.	N. Pacific Ocean off Alaskan Peninsula		3770	
57	26	May	48	19 16 58	55.8°N	152.6°W		6	S. P.	Pacific Ocean off Alaskan Peninsula		3880	
57a	15	July	48	11 02 15	11°N	104°W	100		S. P.	550 mi W. of Mexico coast		5870	
58	22	July	48	20 05 27	49 1/2°N	130 1/2°W			S. P.	Pacific Ocean W. of Vancouver Isl.		3960	
58a	22	July	48	20 52 39	50°N	130°W			S. P.	Pacific Ocean W. of Vancouver Isl.		3960	
59	7	Aug	48	14 40.2	34°N	142°E			L. P., S. P.	Off Honshu Isl., Japan		6020	
60	19	Aug	48	13 50 52	62.7°N	149.1°W	100	6 1/4	S. P.	Near Anchorage		4540	
60a	30	Dec	48	23 49 53	51.5°N	130°W		6.6	S. P.	Queen Charlotte Isl.		4140	
61	22	Aug	49	04 01 12	54°N	133°W		7 1/2-8	S. P.	Queen Charlotte Isl.		4140	
62	23	Aug	49	19 43 35	53°N	132°W		6 1/2	S. P.	Queen Charlotte Isl.		4170	
62a	24	Aug	49	06 07 14	43 1/2°N	127°W			S. P.	West of Oregon		3770	
62b	24	Aug	49	09 22 02	9°S	109°W			L. P., S. P.	1200 mi N of Easter Isl.		6290	

62a	24	Aug	49	06 07 14	43 1/2°N	127°W			S. P.	West of Oregon	3770
62b	24	Aug	49	09 22 02	9°S	109°W			L. P., S. P.	1200 mi N of Easter Isl.	6290

TABLE 1 (Cont.)

No.	Day	Month	Year	Hour GCT	Lat.	Long.	in km	Mag	Surface-Wave Type	Location	G	Δ in km	Δ Cont in km
63	31	Oct	49	01 39 32	56°N	135°W		6 3/4	S. P.			4310	
64	26	Dec	49	06 23 54	14 1/2°S	180°E		7	L. P., S. P.	Fiji Isl. Region		4650	
65	10	Jan	50	03 05 42	11°N	103°W		6 1/4	S. P.	Pacific Ocean off S. Coast of Mexico		5940	
66	12	Feb	50	22 44 55	19°S	178°E		6. 5 pas	S. P.	Fiji Isl. Region		5190	
67	9	July	50	12 34 15	33°S	112°W			S. P.	500 mi SW of Easter Isl.		7900	
67a	12	July	50	01 36 42	2°N	101°W			S. P.	700 mi NW of Galapagos		6510	
68	12	July	50	11 09 15	53°N	166°W		6 1/4	S. P.	Aleutian Isl.		3720	
70	22	Sept	50	07 52 07	25°S	114°W		6. 8, 6 1/2	S. P.	Easter Isl. Region		7040	
71	29	Sept	50	06 32 14	19°N	107°W		7	S. P.	Off Colima		5290	

instrument and Rayleigh waves on the longitudinal—*e.g.*, *see* Figure 5*A*, where the earthquake is nearly due west of Honolulu. Points *G* and *R* indicate the beginning of the Love- and Rayleigh-wave trains respectively. With experience, sight identification was virtually certain at the intermediate azimuths. The advantages of this procedure were described by Neumann (1929, p. 64). It is fortunate that, in general, the long-period Love-wave train, or *G* wave, has died away before the beginning of the Rayleigh waves. For the intermediate azimuths it is always possible to check the particle motion in the horizontal plane by combining the results of the two components.

The above statement is strictly true when applied to the long-period surface waves. When the short-period type predominates, the motion generally becomes incoherent, and the above criteria fail.

Method of Reading Dispersion

The method of reading and plotting the dispersed train of waves was discussed by Ewing and Press (1952b, p. 317) and Pekeris (1948, p. 8). The procedure is to assign consecutive numbers to each peak, or trough, or zero, beginning with the first and continuing until the train becomes ragged. Each number is then plotted against the arrival time of the corresponding point. The slope of the resulting curve at any point is a measure of the frequency at the time corresponding to the point. The group velocity is then calculated and plotted against the period. After the train becomes ragged, periods are obtained by averaging groups of five or six peaks that appear relatively undisturbed. The time is measured to the center of the group.

Continental Correction

For the portion of the path of known continental character (1000-fathom curve used as boundary) a correction was made using the continental, Rayleigh-velocity curve of Brilliant and Ewing (1954, p. 157) or Wilson and Baykal (1948, p. 50). These continental curves have some uncertainty and may vary somewhat from place to place, but in all cases studied here the differences between the curves are insignificant because the percentage of continental path is small.

TABLE 2.—HAWAIIAN SHOCKS RECORDED IN NORTH AMERICA

No.	Day	Month	Year	Hour	Lat.	Long.	Depth in km	Mag	Surface-Wave Type	Ben
A	30	May	50	01 16 16	19 1/2°N	156°W		6 1/4	S. P. (weak L. P.)	3830
B	23	Apr	51	00 52 51	19°N	155 1/2°W		6 1/2, 6	S. P.	3830
C	21	Aug	51	10 56 57 1/2	19 3/4°N	156°W		6 3/4, 7	S. P. (Fresno & Palisades)	
D	22	Aug	51	08 47 51	19 3/4°N	156°W			S. P. (Fresno)	

Epicentral Location

The preliminary epicentral determinations of the U. S. Coast and Geodetic Survey, occasionally supplemented by the preliminary locations of the Jesuit Seismological Association, were used throughout the investigation. The differences between these epicentral locations were in nearly all instances negligible in the present study. No earthquakes listed as deeper than 100 km were studied.

THEORY

General

Elastic theory provides for two types of waves at a free surface, now commonly called Love and Rayleigh waves after their discoverers. Love or *SH* waves are shear waves polarized horizontally. They depend for their existence on horizontal layering and are always dispersive—*i.e.*, different periods travel with

TABLE 3.—ATLANTIC SHOCKS

No.	Date Day	Month	Year	Hour GCT	Lat.	Long.	Depth	Mag	Surface-wave Type Berm.	Pal.	Location	Δ Berm.	Δ Pal.
1	9	Mar	50	10 03 39	16°N	60°W			S. P.		Leeward Isl.	1880	3090
2	20	May	50	09 37 27	29°N	43 1/2°W			S. P.	L. P.	N. Atlantic	2050	3050
4	23	July	50	23 32 28	21°N	64°W			S. P.		200 mi N. of Puerto Rico	1260	2410
4a	25	July	50	18 15 00	31°N	42°W				L. P.	Mid Atlantic Ocean		3000
5	26	July	50	08 31 28					S. P.		Off E. Coast Dominican Republic		
6a	6	Oct	50	08 16 02	20°N	66°W			S. P.	L. P.	Off N. Coast Puerto Rico	1380	2440
6b	28	Oct	50	16 40 36	32°N	41°W				L. P.	Mid Atlantic Ocean		2970
7	19	Oct	50	03 48 25	19°N	68°W			S. P.	L. P.	Off NE Coast of Puerto Rico	1490	2670
7a	20	Oct	50	07 44 30	19°N	68°W			S. P.	L. P.	Off NE Coast of Puerto Rico	1490	2670
7b	31	Oct	50	19 15 22	1°N	26°W				L. P.	Mid Atlantic Ocean		6450
8	1	Dec	50	14 51 00	14°N	47°W	100	7 1/4-7.4	S. P. (off scale)		Mid Atlantic 800 off NE Coast of Brazil	2720	3990
9	29	Dec	50	20 16 29	17°N	63°W	100		S. P.,	L. P.,	L. P. Leeward Isl.	1720	2890
10	30	Jan	51	19 00 30	15 1/2°N	99°W		6 1/4-6 1/2	S. P.	L. P.	Off S. Coast of Mexico	3490	3660
11	31	Jan	51	11 51 46	21°N	46°W			S. P.		N. Atlantic Ocean	2240	3440

TABLE 3 (Cont.)

No.	Date Day	Month	Year	Hour GCT	Lat.	Long.	Depth	Mag	Surface-wave Type Berm.	Pal.	Location	Δ Berm.	Δ Pal.
12	19	Mar	51	03 07 31	35 1/2°N	35°W			S. P.		N. Atlantic Ocean	2750	3440
15	27	May	51	04 30 55	23 1/2°N	45° W			S. P.	L. P.	N. Atlantic Ocean	2160	3250
16	18	July	51	09 06 16	1°N	27°W		6 1/2-6 1/4	S. P. L. P. on R2	L. P.	Mid Atlantic Ocean	5260	6400
17	10	Aug	51	05 32 33	8 1/2°N	40°W		6	S. P.		Atlantic Ocean	3680	4900
18	8	Sept	51	06 42 40	29°N	43 1/2°W			S. P.	L. P.	N. Atlantic Ocean	1870	3000
19	22	Sept	51	23 40 37	16 1/2°N	47°W			S. P. (hint of S. P.)	L. P.	N. Atlantic Ocean	2500	3780
20	3	Oct	51	02 00 06	16 1/2°N	61°W			S. P.		Leeward Isl.	1810	3110
21	12	Nov	51	09 36 36	17°N	61°W			S. P.		Leeward Isl.	1750	2950
22	30	Nov	51	07 51 17	32°N	41°W			S. P.		N. Atlantic Ocean	2220	3050
26	19	Jan	52	06 25 51					L. P.		700 mi N. of Azores		
27	23	Feb	52	21 35 65	29°N	43°W			S. P.		N. Atlantic Ocean		
28	1	May	52	16 10 41	28°N	43 1/2°W			L. P., S. P.		N. Atlantic Ocean		

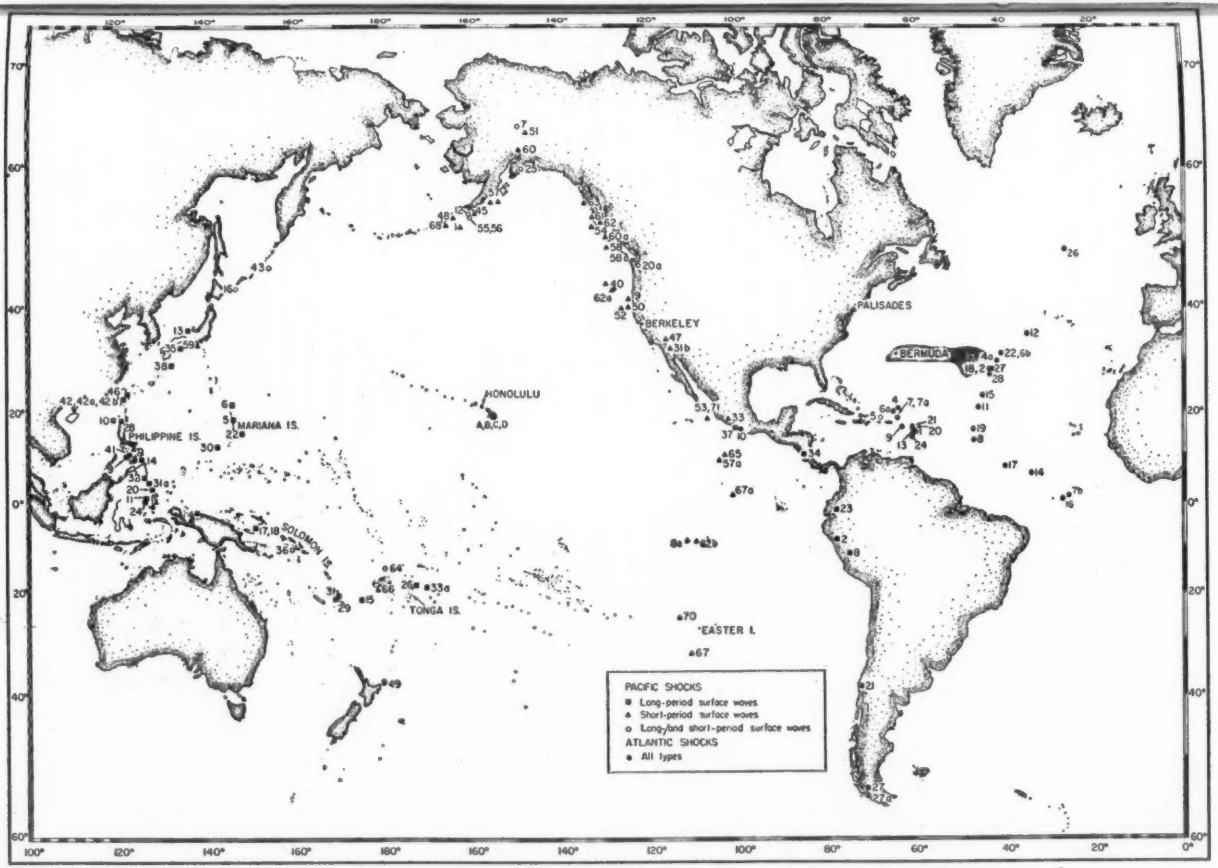

FIGURE 1.—MAP OF EPICENTRAL LOCATIONS OF SELECTED EARTHQUAKES

different phase and group velocities. Rayleigh wave particle motion at the surface is retrograde elliptical in the plane of propagation. Rayleigh waves can exist at the free surface of a homogeneous, semi-infinite solid, in which case they are nondispersive, but in the actual case of the layered earth they too are dispersive. This is evident intuitively because the shorter wave lengths are confined largely to the upper layer and derive their velocity from its elastic properties, whereas the longer wave lengths penetrate deeper and are more affected by the properties of the deeper layer. Some consideration will be given to the higher modes of these wave types, which can exist under certain conditions. We will consider each type separately in the following discussion. The symbols used are:

α = compressional wave velocity in a solid
β = shear wave velocity
V = compressional wave velocity in water
σ = Poisson's ratio
H = layer thickness
λ = wave length
$k = \frac{2\pi}{\lambda}$ = wave number
f = frequency
$\gamma = \frac{Hf}{V} = \frac{H}{\lambda}$ = nondimensional term proportional to frequency
C = phase velocity
U = group velocity
ρ = density

Subscripts $_1$, $_2$, and $_3$ refer to layers numbered from top to bottom and $_n$ refers to number of mode.

Rayleigh Waves

Several investigators have examined the problem of elastic-wave propagation in a water layer overlying a semi-infinite solid layer. A bibliography and a brief review of earlier results is found in Press *et al.* (1950, p. 113). The earlier papers, in general, do not contain numerical results suitable for application in the present study. The Ewing-Press theory considers a liquid layer having the elastic properties appropriate to the material below the Mohorovičić discontinuity. In this simplified structure the sediments are lumped with the water as the liquid layer, and the bottom material is considered an average for any layering present in the bottom. They used the following equation, first given by Stoneley (1926, p. 353), which is a relation between phase velocity and wave length:

$$\tan\left(k_n H\sqrt{C_n^2/V^2-1}\right) = \frac{\rho_2\beta_2^4\sqrt{C_n^2/V^2-1}}{\rho_1 C_n^4\sqrt{1-C_n^2/\alpha_2^2}}$$

$$[4\sqrt{1-C_n^2/\alpha_2^2}\sqrt{1-C_n^2/\beta_2^2}-(2-C_n^2/\beta_2^2)$$

The group velocity is obtained by graphical or numerical differentiation from

$$U = C + kHdC/d(kH).$$

These curves are shown in Figure 2 in dimensionless form. The values assigned to the constants are tabulated in Table 4 as Case II. The method of solution is to choose a C and then solve for kH. Since the tangent function is oscillatory there will be an infinite number of solutions. The order of each solution or mode is designated by the subscript $_n$. In practice only the lower orders are encountered, and only the first two are shown on the graph.

The depth of the source is an important factor in deciding how much energy is put into each mode, and Press *et al.* (1950) showed that in the case of a flat bottom only the gravest mode is significant if the source lies farther below the bottom than the depth of the water.

Figure 6 shows a family of curves for the gravest mode in which group velocity is plotted against period and the depth of water is taken as a parameter. The shorter wave lengths are most sensitive to the depth of the liquid so that the steep portion of the curve on the left is most useful in determining this quantity experimentally (Fig. 6). The curve is so steep that it is possible to estimate the depth simply by measuring the period anywhere along the late, long-drawn-out coda.

The long wave lengths, virtually unaffected by the water depth, are sensitive to the shear velocity of the basement rocks. A variation of this quantity would raise or lower the flat portion of the curve, which is asymptotic to the Rayleigh wave velocity ($= 0.92\beta$ for $\sigma = \frac{1}{4}$) in the lower medium.

An intermediate layer or layers, not con-

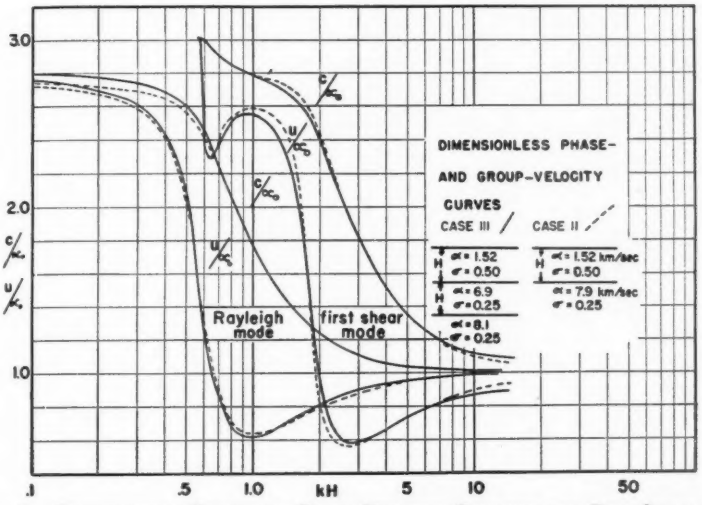

FIGURE 2.—DIMENSIONLESS PHASE AND GROUP VELOCITY, RAYLEIGH AND FIRST-SHEAR MODES

TABLE 4.—CONSTANTS USED IN CALCULATIONS OF THEORETICAL CURVES

Case	I	II	III
V	1.52 km/sec	1.52	1.52
α_2	5.5	7.90	6.9
α_3	8.1	----	8.1
H_2	$=H_1$	$=\infty$	$=H_1$
ρ_2	$2.67\rho_1$	$3.0\rho_1$	$2.67\rho_1$
ρ_3	$3.0\rho_1$	----	$3.0\rho_1$
σ	1/4	1/4	1/4

sidered in the original theory, would have its greatest influence on the wave lengths between the two extremes. To determine the magnitude of the effect of such a layer, Jardetzky and Press (1953) solved the three-layer problem of a liquid layer overlying two solids for the two cases listed in Table 4. Case III represents the results of refraction shooting in the North Atlantic Basin. In Case I the velocity of the intermediate layer is what might be expected from a granitic material. Their results showed that for the range of periods involved it is impossible to distinguish Case III from the simpler two-layer case of Ewing and Press (1950). Case I could be differentiated from the others only if the thickness of the intermediate layer were at least as great as the depth of the water. For a layer of continental-type granitic rock to be detected under the Pacific Basin by Rayleigh-wave dispersion a 5½-km average thickness over the entire path would be necessary.

The first-shear mode of the period equation of Jardetzky and Press was calculated using the constants of Case III (Figs. 2, 3; Table 5). The only appreciable deviation from the two-

TABLE 5.—COMPUTED POINTS ON FIRST-SHEAR MODE CURVE

c/α_0	kH	c/α_0	kH	c/α_0	kH
1.20	6.944	2.00	2.620	2.73	1.265
1.30	5.558	2.05	2.530	2.75	1.173
1.40	4.701	2.10	2.447	2.77	1.079
1.50	4.115	2.20	2.289	2.80	.947
1.60	3.677	2.30	2.144	2.83	.842
1.65	3.495	2.40	2.006	2.85	.789
1.70	3.333	2.50	1.862	2.875	.738
1.75	3.187	2.55	1.777	2.90	.700
1.80	3.054	2.60	1.680	2.95	.646
1.85	2.932	2.65	1.555	3.00	.608
1.90	2.820	2.70	1.389	3.0766	.557
1.95	2.716				

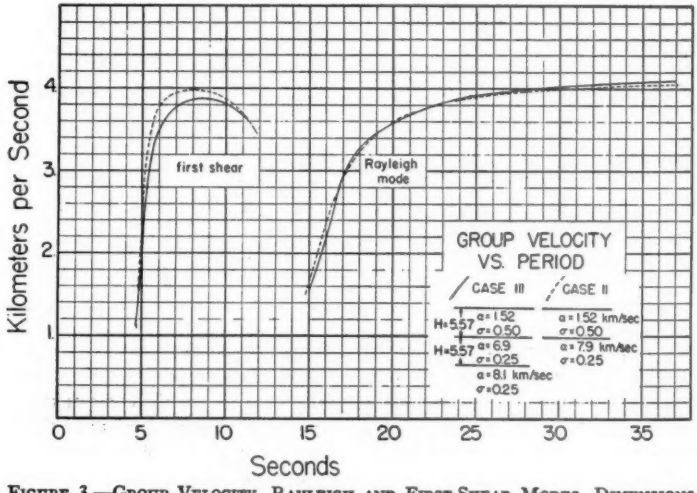

FIGURE 3.—GROUP VELOCITY, RAYLEIGH AND FIRST-SHEAR MODES, DIMENSIONS PERTINENT TO EARTHQUAKES

layer case falls in the period ranges 5½ to 8 seconds for $H = 5.57$ km. The magnitude of the difference is of the order of the experimental error so that if a first-shear mode train were definitely identified, it is improbable the dispersion would give useful information about the intermediate layering unless the variations in dimensions or elastic constants were greater than those chosen for the calculations.

For the simple two-layer case, particle motion

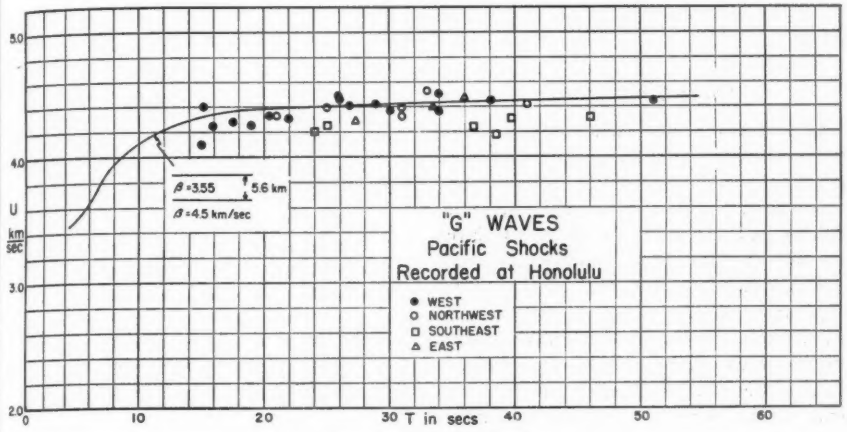

FIGURE 4.—"G" WAVES

TABLE 6.—COMPRESSIONAL AND SHEAR-WAVE VELOCITIES CORRESPONDING TO VARIOUS VALUES OF POISSON'S RATIO

σ	α	β	α	β	α	β	α	β
.23	8.1	4.80	7.9	4.68	6.9	4.09	6.5	3.85
.25	8.1	4.68	7.9	4.56	6.9	3.98	6.5	3.75
.27	8.1	4.55	7.9	4.43	6.9	3.87	6.5	3.65
.28	8.1	4.48	7.9	4.37	6.9	3.81	6.5	3.59
.30	8.1	4.33	7.9	4.22	6.9	3.69	6.5	3.47

at the surface of the solid was shown to be retrograde elliptical for both the Rayleigh and first-shear modes (Press *et al.*, 1950). For the three-layer case calculations were not carried out owing to prohibitive time and labor required. However, at least for the long waves, the particle motion of the Rayleigh mode is probably also retrograde elliptical at the surface of the upper solid. It also seems probable that this is the case for the first-shear mode as well. Sezawa's M_2 wave (Sezawa and Kanai, 1935), which the writers would term first-shear mode for the case of a solid layer over a semi-infinite solid, was shown to have progressive elliptical motion. However, the branch of the equation corresponding closest to M_2 for the three-layer case falls at a shorter period than the two branches studied here—*i.e.*, out of the recorded surface-wave periods.

Love Waves

The theory of Love-wave propagation is well known (Bullen, 1947, p. 90). The period equation for the two media case is

$$\mu_2(1 - C^2/\beta_2^2)^{\frac{1}{2}} - \mu_1(C^2/\beta_1^2 - 1)^{\frac{1}{2}} \tan kH_1(C^2/\beta_1^2 - 1)^{\frac{1}{2}} = 0$$

Figure 4 shows the curve for Case III. The second mode was computed for Case III, but the values of the periods fall well below the range covered in this investigation. The chief features of the curve are that (1) the long waves are asymptotic to the shear velocity in the lower medium, and (2) the duration of the train is determined largely by the contrast of the two-shear velocities. The effect of a change in layer thickness is to rearrange in a simple

manner the distribution of periods in this time interval.

Choice of Constants

The accuracy of the values of the elastic constants chosen for the calculations determines the degree of usefulness of the method. Constants chosen for the calculations have the following basis: Case II, the simple two-layer case, was the first Rayleigh-wave dispersion curve calculated because the equations and computations are the simplest. The value of 7.9 km/sec. for the compressional wave velocity is representative of the early seismic-refraction results in the Atlantic Ocean basin. Improvements in the refraction techniques enabling longer profiles to be carried out resolved the original single-basement layer into two layers of compressional velocities 6.9 and 8.1 km/sec. respectively. These numbers were used in the three-layer computation, Case III, of Jardetzky and Press. More recent refraction results (Officer *et al.*, 1952, Ewing *et al.*, 1950) in the Atlantic have centered about a mean of 6.5 and 7.9, although the values run from 6.27 ± .17 to 6.63 ± .17, and 7.56 ± .18 to 8.27 ± .27 km/sec. In the Pacific, Raitt (1951) has given values of 6.75 and 8.1 for typical deep-water profiles between Hawaii and the west coast of North America. The value of 5.5 km/sec. was taken (Case I) as typical of continental rock. Recent measurements give velocities slightly above 6 km/sec. for the bulk of continental rocks.

As the surface-wave calculations for the three-layer case are long and tedious it is not practical to compute separate curves for the different values. However, the effect of small changes in the constants can be estimated fairly well. From the two three-layer cases in which the velocity of the intermediate layer was 5.5 and then 6.9 km/sec., resulting in curves differing by an amount barely discernible experimentally, it is evident that a change from 6.9 to 6.5 or 6.75 km/sec. will fall between the first two curves and nearly coincide with the latter. Thus the selection of an intermediate layer more in keeping with the results of recent refraction shooting will alter the theoretical curve only negligibly. However, a change of the bottom layer from 8.1 to 7.9

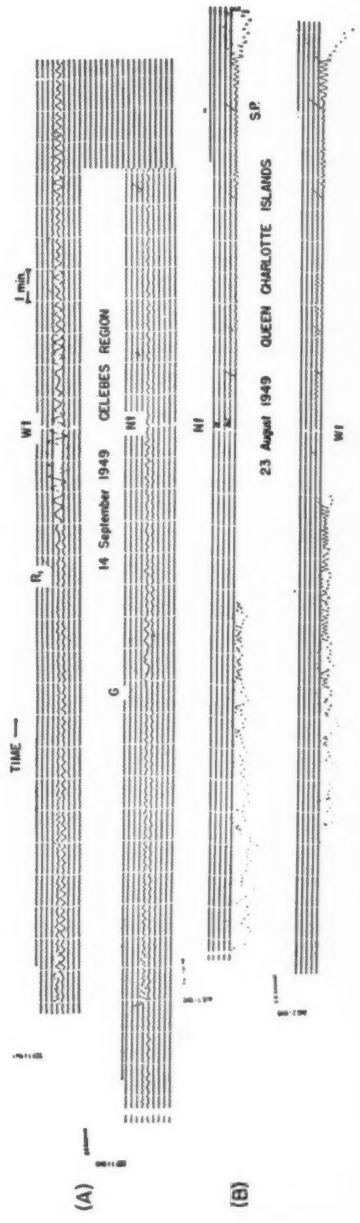

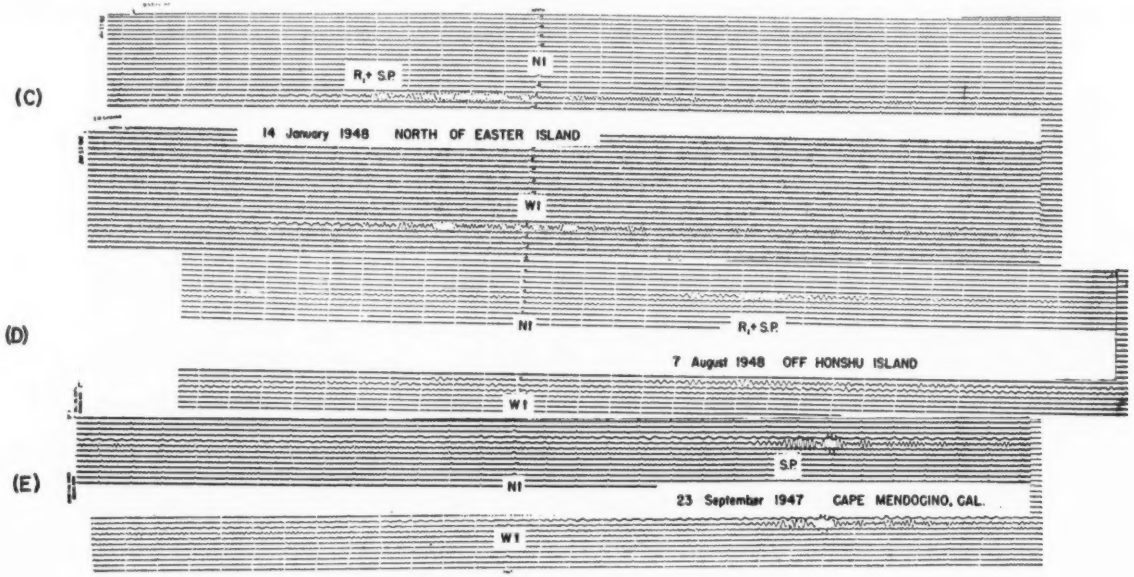

FIGURE 5.—SEISMOGRAMS

A. First-mode Rayleigh and Love waves B, E. Short-period surface waves C, D. Mixed long and short-period surface waves

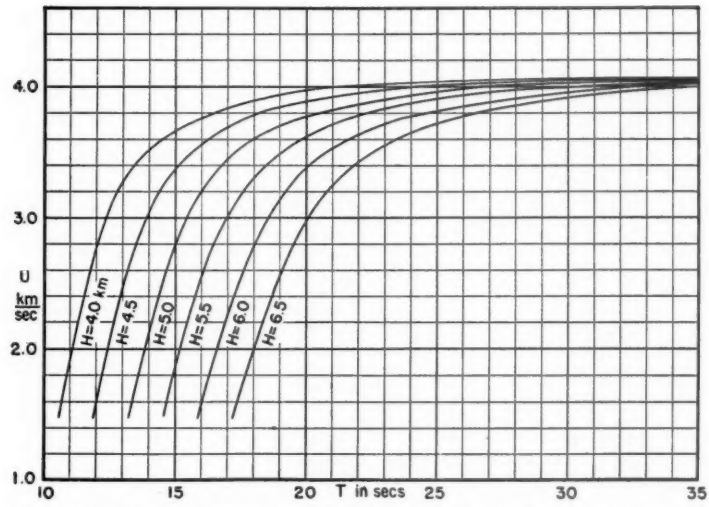

FIGURE 6.—DEPENDENCE OF RAYLEIGH WAVES ON LIQUID DEPTH FOR CASE II

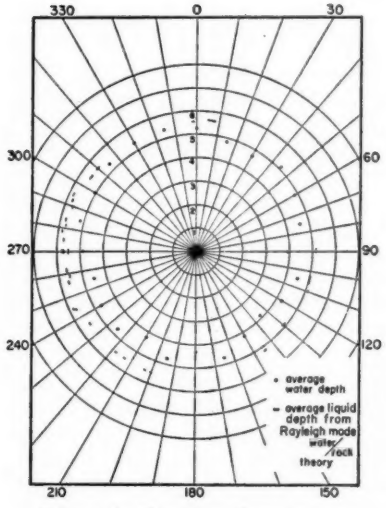

FIGURE 7.—SEDIMENT THICKNESSES IN THE PACIFIC
Sediment thickness = liquid depth = water depth.

gives a more pronounced effect. Using $\sigma = \frac{1}{4}$ the shear velocities are 4.68 and 4.56, and the Rayleigh-wave velocities for very long wave lengths 4.31 and 4.20 km/sec. The long-period end of the dispersion curve is asymptotic to these latter two values so as a first approximation the curves will differ by about 0.1 km/sec. for the long periods. This is about the margin of experimental error. The Love-wave curve will be affected in about the same manner and degree.

The validity of the 0.25 choice for Poisson's ratio also needs examination. From the well-known formula

$$1 + \frac{1}{1 - 2\sigma} = \frac{\alpha^2}{\beta^2},$$

the values in Table 6 may be obtained. The value for $\sigma = 0.25$ was chosen to simplify the calculations. Earthquake data (Bullen, 1947, p. 220, Gutenberg, 1951, p. 68) give a value for σ of about 0.27 for the depths and material considered here. A first approximation to the effect of a change can be estimated by observing the change in shear velocity as above and raising or lowering the curve by that amount. This is about 0.1 km/sec. for these two values of σ.

EXPERIMENTAL RESULTS

Rayleigh Waves (long period)

This train of waves is markedly sinusoidal and usually occupies a major portion of the seismogram (Fig. 5*A*). The periods range from about 35 to 15 seconds with corresponding

velocities varying from 4.1 to about 1.4 km/sec. Figures 8–19 show that in all cases the measured dispersion fits the theoretical curve. The particle motion, whenever determinable, is retrograde elliptical and is always in the general direction of the plane of propagation. Thus it is clear that the theory predicts the correct dispersion. Anomalies in amplitude which correspond to the absence of shorter-period waves of this type are the principal unexplained feature.

There are, however, small systematic differences correlating with azimuth from Honolulu. Figure 7 shows the thickness of the liquid layer (water + unconsolidated sediment) deduced from the low-velocity part of the train using Figure 6. The scatter is of the order of 0.2 km. Plotted on the same figure are average water depths at 15-degree intervals of azimuth taken from H.O. charts 0526, 0527, 0528, 0529, 0823, 0824, 0825, 0826, and 5951. There is some uncertainty in these values because (1) the water depths are not known to sufficient precision, and (2) there is some doubt as to precisely which path between epicenter and station should be followed because of lateral refraction of the surface waves. It seems reasonable that these averages might be in error by, at most, 0.2 km. These uncertainties limit the precision of the experiment, but a reliable estimate of the sediment thickness is possible from the plot.

The sediment thickness taken from Figure 7 ranges from 0.4 km due north of Honolulu to nearly 1.2 km to the southwest. These numbers agree with results of Raitt (1951) using the explosion seismic-refraction technique in the Pacific, and with results of similar studies in the Atlantic. Furthermore, a real trend toward thicker sediments is suggested in the southwest quadrant where atoll groups are plentiful. Also apparent from the plot are the greater basement depths in the western half of the Pacific. However, the data are scanty to the east and almost lacking in the entire northeast quadrant owing to the absence of earthquakes generating Rayleigh waves, so that the last statement needs verification.

TABLE 7.—LIQUID (WATER + SEDIMENT), WATER, AND SEDIMENT THICKNESS FOR ATLANTIC SHOCKS

No.	Day	Month	Year	Recording Station	Liquid	Water	Sediment
4A	25	July	50	Palisades	5.3 km	4.8 km	0.5 km
6B	8	Oct	50	Palisades	5.3 km	4.8 km	0.5 km
6B	8	Oct	50	Palisades	5.3 km	4.8 km	0.5 km
7B	31	Oct	50	Palisades	5.1 km	4.0 km	1.1 km
8	1	Dec	50	Palisades	5.5 km	4.9 km	0.6 km
8	1	Dec	50	Ottawa	5.5 km	4.9 km	0.6 km
8	1	Dec	50	Kew	4.8 km	4.2 km	0.6 km

The sediment thicknesses in the Atlantic are shown in Table 7. Water depths are from H.O. charts 0955, 0956, 0955a, and 0956a. This survey is not so complete as the Pacific one because of the less convenient location of earthquakes and stations. However, the thicknesses are of the same order of magnitude, ranging from 0.5 to 1.1 km. Only one value is more than 0.6 km, and in that case the path includes a sizable portion of the Mid-Atlantic Ridge where the error in the water depth may be greater.

The second phase of exploration with Rayleigh waves would involve determination of the shear velocity in the deep-rock layer from the longer wave lengths; however, the instrumental response and perhaps the frequency spectrum of energy released at the source prevent recording of wave lengths that are long enough to be insensitive to the intermediate layer or layers.

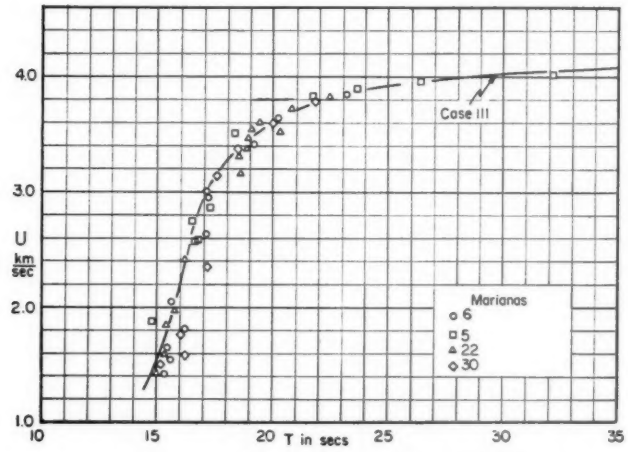

FIGURE 8.—RAYLEIGH-WAVE DISPERSION, MARIANAS (Table 1)

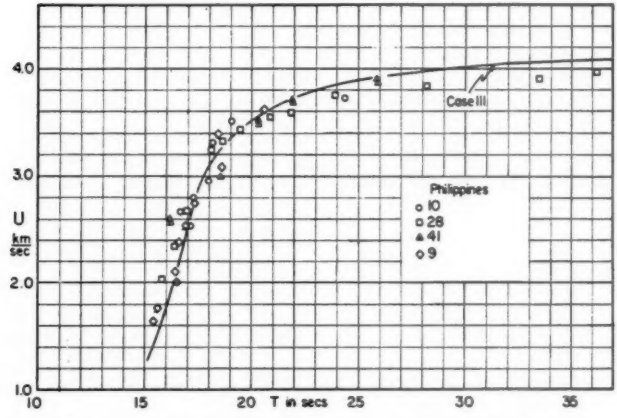

FIGURE 9.—RAYLEIGH-WAVE DISPERSION, PHILIPPINES (Table 1)

Thus we cannot isolate the deep-layer shear-velocity problem from the intermediate-layer problem.

To study these questions the earthquakes have been grouped geographically. Figure 8 is a plot of Rayleigh-wave group velocity *vs.* period for earthquakes in the Marianas. This group fits the three-layer case III quite well. The path is clearly entirely oceanic. Plotted in Figure 9 are earthquakes on the prolongation of the great-circle path to the Marianas—*i.e.*, the Philippine Island shocks. The points at the long-period end in general lie somewhat below those for the Mariana shocks. Since it will be seen later that there is a general tendency for the long-period observations to fall on or about .1 km/sec. below the theoretical curve of Case III, the margin is near the limit of experimental error. It is difficult to say whether a slightly different type of layering is indicated beneath the Philippine Sea, but it may safely be concluded that layers having continental properties and dimensions are absent. These results are supported by Love-wave observations given in a later section. This negates the conclusions of some geologists (*see* Umbgrove, 1947, p.

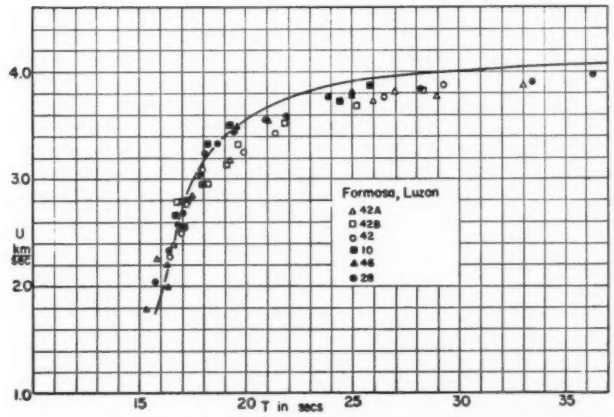

FIGURE 10.—RAYLEIGH-WAVE DISPERSION, FORMOSA LUZON (Table 1)

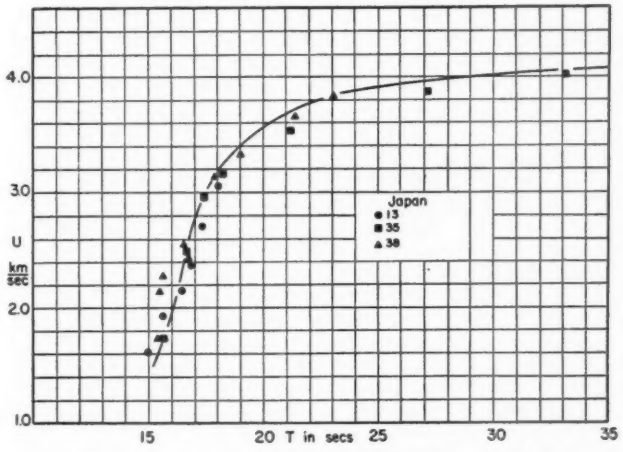

FIGURE 11.—RAYLEIGH-WAVE DISPERSION, JAPAN (Table 1)

228, for references) concerning the existence of the submerged Melanesian continent.

The Formosan shocks nos. 42, 42*A*, 42*B*, and 46 (Fig. 10) also fall slightly below the theoretical curve. However, interpretation here is further complicated by the presence of a segment of the Ryukyu island arc over a significant portion of the great-circle path to Honolulu. The correction for such a structure in such an orientation is so uncertain that deductions concerning slight deviations from the layering assumed in Case III are not reliable. The Japanese shocks 13, 35, and 38 (Fig. 11) fall on the theoretical curve quite well although only one shock, 35, gave waves of more than 25-second period. Shocks 16 and 43 in the Kuriles (Fig. 12) gave virtually identical results with the Japanese shock although waves of more than 25-second period were lacking from both. Shocks 7, 12, and 25 in the Alaskan area (Fig. 13) also fit the theoretical curve well. Shocks 7 and 25 produced waves of 30–35-second period although the former required a large continental correction. Shock 20*A* near Tacoma (Fig. 14) also gave an excellent fit with periods up to 30 seconds.

The next group of shocks (Fig. 15) subtends a fairly large angle from southern Mexico to

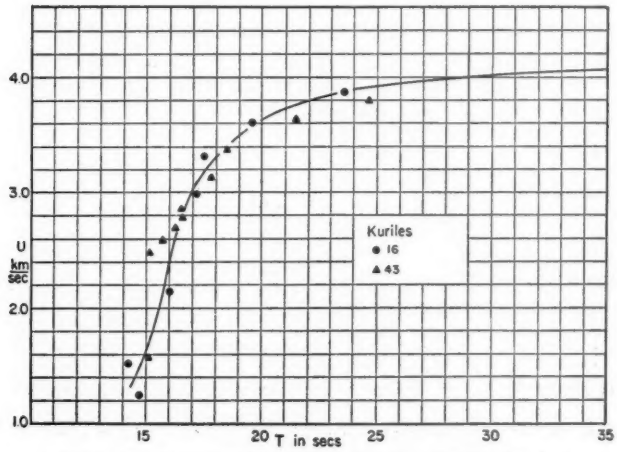

FIGURE 12.—RAYLEIGH-WAVE DISPERSION, KURILES (Table 1)

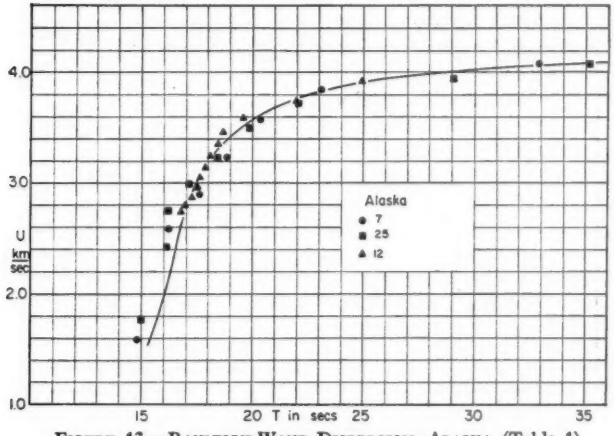

FIGURE 13.—RAYLEIGH-WAVE DISPERSION, ALASKA (Table 1)

central Peru and also agrees with the theoretical curve. The next group of earthquakes to the south includes one in Chile and two, a main shock and an aftershock, at the tip of South America (Fig. 16). Only for the latter two were waves of more than 25-second period recorded. These fall below the general trend of observations by the minimum detectable amount. Probably they have been affected by the Easter Island Rise indicating a possible thickening of the intermediate layer or an additional material of slower velocity, or both. This conclusion is supported by data from Love waves to be given in a later section.

The six earthquakes in the next group (Fig. 17) stretching from the Tongas to the Loyalty Islands plot close to the theoretical curve but slightly below it. From refraction studies near this area Raitt has found some slow-velocity material (4.5–5.0 km/sec.) near volcanic islands or submerged mountains which he has tentatively identified as volcanic rock. Possibly there is enough of this material throughout Polynesia to account for the slightly slower surface-wave velocities there. Such would also be the case for the remaining shocks, nos. 4, 17, 18, and 36 (Fig. 18) which also plot slightly low. Shocks 17 and 18, however, off New Britain,

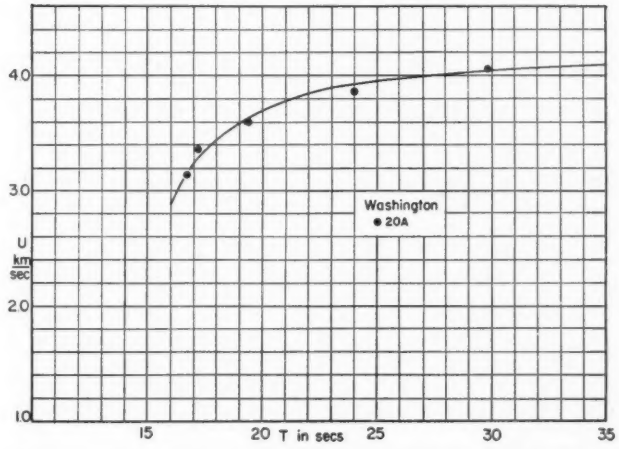

FIGURE 14.—RAYLEIGH-WAVE DISPERSION, WASHINGTON (Table 1)

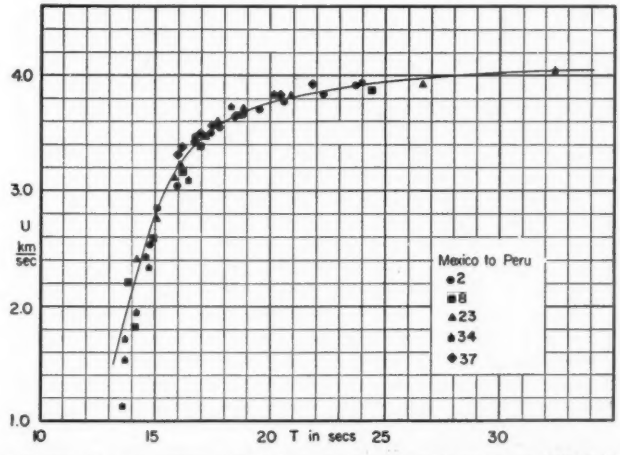

FIGURE 15.—RAYLEIGH-WAVE DISPERSION, MEXICO TO PERU (Table 1)

need allowances for the land and shallow-water path. The same can be said for no. 36 in the Solomons. No. 4 (Pacific Ocean, north of New Guinea) fits the curve as it stands.

In summary, although slight deviations in the long-period end of the Rayleigh-wave dispersion curve can be detected at different azimuths from Honolulu, these deviations are small and cannot be used with certainty to deduce minor changes in crustal structure over small segments of the path. In spite of these limitations, however, the data show conclusively that there are no major variations in the crustal structure throughout the Pacific Ocean—*i.e.*, no submerged continental structure of significant proportions. The slightly low velocity of the long Rayleigh waves from the quakes at the tip of South America is interpreted as due to a lower-velocity material in the Easter Island Rise. The slightly low velocity for paths crossing the Philippine Sea would admit at most the possibility of a thin low-velocity layer, but Love-wave data show no indication of its presence. The Pacific is com-

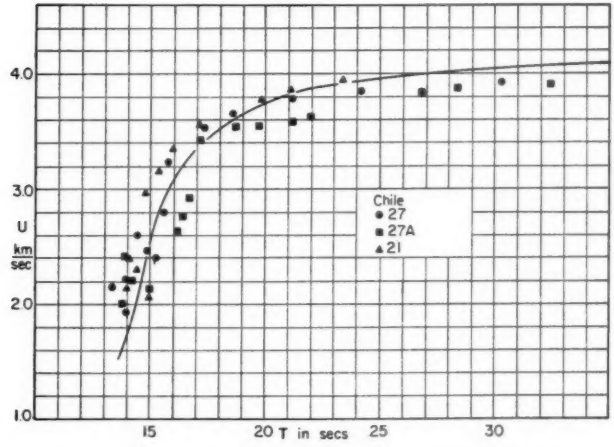

FIGURE 16.—RAYLEIGH-WAVE DISPERSION, CHILE (Table 1)

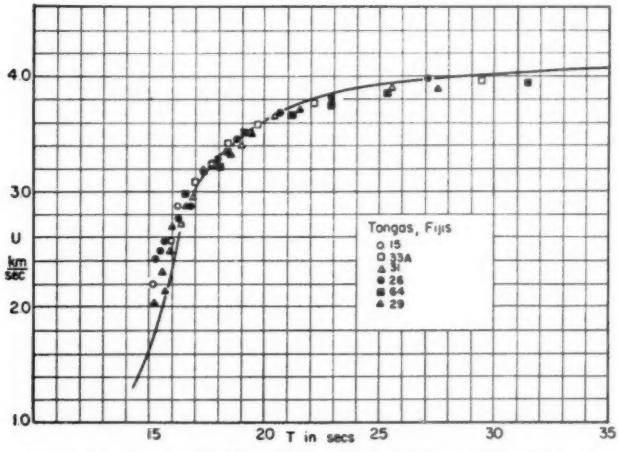

FIGURE 17.—RAYLEIGH-WAVE DISPERSION, TONGAS, FIJIS (Table 1)

monly divided into two sections on petrologic evidence. These sections are separated by the "andesite line", so called because volcanic islands between the continents and the line frequently contain andesitic rocks, whereas those on the ocean side of the line are of olivine basalt. Although this study indicates that the areas on either side of the andesite line are similar with respect to the propagation of surface waves, it does not preclude the possibility of petrologic changes, providing the dimensions of the rocks involved are small in the sense described in the section on Theory.

For most of the plots the points corresponding to long-wave lengths tend to fall below the theoretical curve. This indicates a shear velocity for the material below the Mohorovičić discontinuity about 1–3 per cent lower than that assumed for Case III.

The Atlantic data are plotted in Figure 19. Scatter of the order of 0.2 km/sec. is evident at the long-period end of the curve, about the same order of magnitude as in the Pacific data. However, the same dispersion curve fits both oceans so that no difference between the Atlantic and the Pacific is shown by the Rayleigh-wave data.

Previous work on Rayleigh-wave dispersion

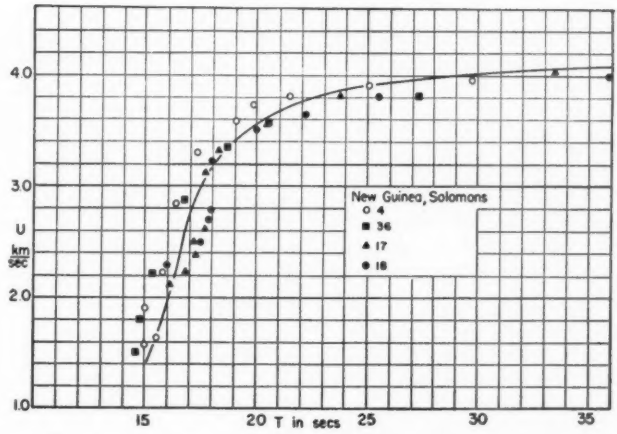

FIGURE 18.—RAYLEIGH-WAVE DISPERSION, NEW GUINEA, SOLOMONS (Table 1)

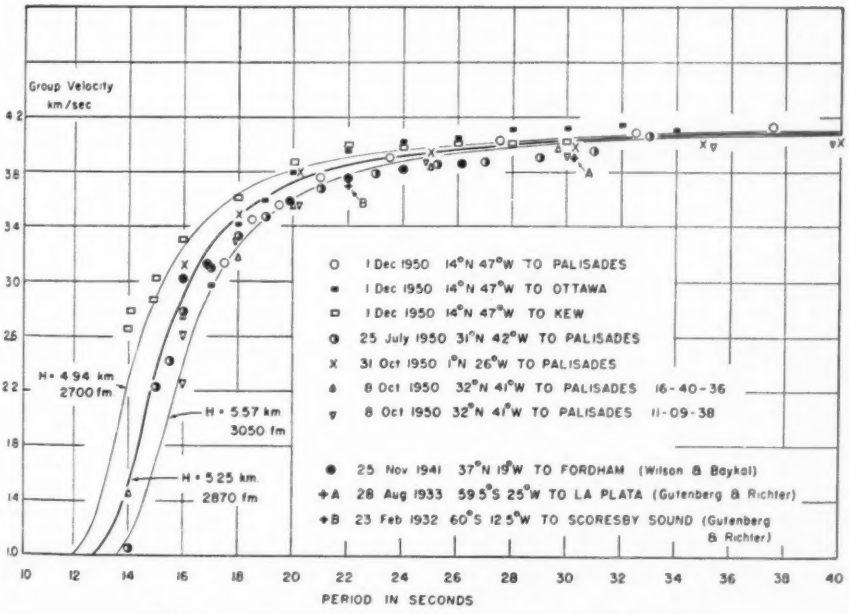
Group Velocity km/sec
PERIOD IN SECONDS
H = 4.94 km 2700 fm
H = 5.57 km 3050 fm
H = 5.25 km 2870 fm
○ 1 Dec 1950 14°N 47°W TO PALISADES
■ 1 Dec 1950 14°N 47°W TO OTTAWA
□ 1 Dec 1950 14°N 47°W TO KEW
◑ 25 July 1950 31°N 42°W TO PALISADES
X 31 Oct 1950 1°N 26°W TO PALISADES
▲ 8 Oct 1950 32°N 41°W TO PALISADES 16-40-36
▽ 8 Oct 1950 32°N 41°W TO PALISADES 11-09-38
● 25 Nov 1941 37°N 19°W TO FORDHAM (Wilson & Baykal)
✦A 28 Aug 1933 59.5°S 25°W TO LA PLATA (Gutenberg & Richter)
✦B 23 Feb 1932 60°S 12.5°W TO SCORESBY SOUND (Gutenberg & Richter)

FIGURE 19.—RAYLEIGH-WAVE DISPERSION, ATLANTIC (Table 3)

in the Atlantic (Wilson and Baykal, 1948) considered the shock of 25 November, 1941. Their readings from the Fordham seismogram plotted in Figure 19 are concordant with the new data. The readings used by Gutenberg and Richter (1936) from the South Atlantic earthquakes of 28 August, 1933, recorded at La Plata, and 23 February, 1932, recorded at Scoresby Sound, also agree (Fig. 19). The other Atlantic data of Gutenberg and Richter are not shown because large corrections for continental paths would be required.

Rothe (1951) concluded that the Mid-Atlantic Ridge forms the boundary between an eastern basin underlain by continental rocks and a western basin underlain by ultra-

basic rocks. Although the present study gives little coverage of the eastern basin, the data show no evidence of a submerged continent. Available Rayleigh-wave evidence favors similarity of the two basins. Coverage of the Mid-Atlantic Ridge is more nearly complete. The Ridge produces no effect on the dispersion curves except those due to water depths.

Evernden (1952a) presented evidence to show that lateral refraction of Rayleigh waves could account for the deviation of the direction of approach from the azimuth of the epicenter. Qualitative observations of this study verify his conclusions and further indicate the increasing magnitude of the effect as the period of the waves decreases. An investigation of waves of much longer period (70–400 sec.) indicated that the effect of the continents is negligible on waves of such long wave lengths (Ewing and Press, 1954).

In accordance with the findings of previous papers (Ewing and Press, 1952a; Brilliant and Ewing, 1954), there is no evidence of the short-period branch of the dispersion curve, with the exception of an occasional *T* phase.

Love Waves

Beginning with a long-period oscillation, also known as the "G" phase (Fig. 5*A*), this train appears only on the horizontals, and particle motion is transverse. The wave train is much shorter than the Rayleigh-wave train, indicating a much smaller contrast of the elastic properties of layer and substratum than for the Rayleigh waves. This is further confirmation of the theory that the water layer, which has no effect on Love waves, is the primary factor affecting the dispersion of Rayleigh waves. The period range of the train is from 50 seconds to about 12 seconds on the Honolulu instruments. Caution must sometimes be exercised in distinguishing "*G*" from *S*, *SS*, or *SSS*.

Scatter in the data is large, because of the strong effect of any small segment of continental path where the dispersion is much more pronounced. This is a counterpart, in reverse, of the case with Rayleigh waves, in which the dispersion due to the ocean path is by far the stronger. For Rayleigh waves, dispersion under continents can be studied best when some oceanic path has spread out the spectrum (Brilliant and Ewing, 1954). For Love waves the reverse is true. For example, the shock of 21 January, 1952 (*H* 20 55 12, 4°S., 30½°E.), on the Tanganyika border, showed a well-dispersed train at Palisades and would be suitable for precision measurement of Love-wave dispersion across the Atlantic, if records were available from a station on the west coast of Africa where the coast intersects the great-circle path from the epicenter to Palisades.

An additional difficulty is the discrimination against waves of long period by most seismographs and the differences among seismographs in this connection. It is believed that, taken together, these factors can account for the differences in crustal structures deduced by different investigators.

Table 1 includes a column which indicates whether or not each shock made long-period Love or "G" waves at Honolulu. About two thirds of them did not. The well-recorded ones of the remaining third are plotted in Figure 4. Considerable scatter is evident. Seemingly the only reliable information is the shear velocity in the lower layer. Neglecting the quakes from the southeast quadrant, the plot shows that a shear velocity of 4.50 km/sec. with the same layering as Case III fits the data well. This is slightly below the value of 4.68 km/sec. used in the Rayleigh-wave calculations but is near the shear velocity obtained under the assumption that $\sigma = 0.27$ (Gutenberg, 1951), and the compressional velocity is 8.1 km/sec. as in the refraction studies. Since most Rayleigh-wave velocities for periods greater than 20 sec. fall slightly below the theoretical curve for Case III, indicating a shear velocity slightly less than 4.68 km/sec. for the bottom layer, the results from Rayleigh and Love waves may be said to agree within the experimental error.

The low velocity of the long-period Love waves from the southeast substantiates the deductions from the Rayleigh waves that the Easter Island Rise is not typical oceanic crustal structure. On the basis of *PP*/*P* amplitude ratios, Gutenberg deduced that points near and east of the Rise were of continental structure of 20–30 km thickness (Gutenberg, 1951, p. 328). Although some doubt has been cast on the re-

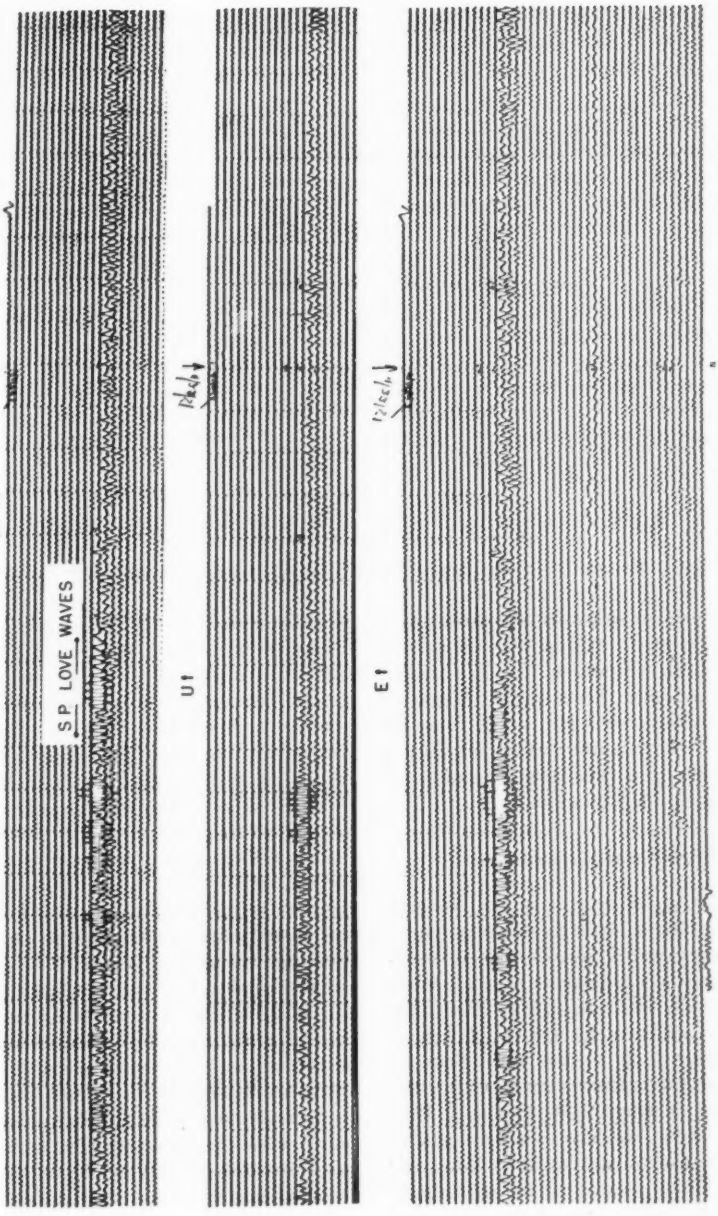

23 April 1951 HAWAIIAN SHOCK RECORDED AT BERKELEY
FIGURE 20.—SHORT-PERIOD SURFACE WAVES, BERKELEY RECORDS (Table 2)

liability of this method (Byerly *et al.*, 1949), the conclusions probably were not wrong. Daly reports findings of typically continental rock on Easter Island and suggests "that the plateau

In this paper the train is broken into tw parts for convenience of description. The firs few cycles of the train are definitely Love wave down to a velocity of about 3.5 km/sec. and

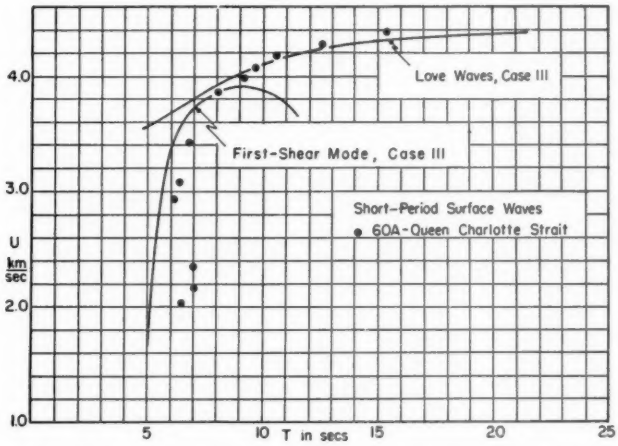

FIGURE 21.—SHORT-PERIOD SURFACE-WAVE DISPERSION (Table 1)

is an extensive but relatively thin slice of rock of continental type" (1951, p. 27). The present findings tend to substantiate this, but are not conclusive evidence. From similar reasoning, the high velocity of Love waves from the Philippines (points marked West in Fig. 4) is unfavorable to a thin layer of continental rocks under the Philippine Sea.

Short-Period Surface Waves

A number of the records of the Honolulu collection exhibit a distinctly different type of surface wave (Fig. 5*B*, 5*E*). The period usually decreases gradually from about 15 sec. to 6 sec., but occasionally starts as high as 20 sec. The velocity ranges from 4.4 km/sec. to an indefinite, lower limit of not more than 2.0 km/sec. These waves have been noted by other investigators (Carder, 1934; Coulomb, 1952; Neumann, 1929) but have not been studied extensively. Ewing and Press (1952a) and Evernden (1952a) pointed out the approximate fit to the dispersion curve of the first shear-mode waves. Coulomb (1952) pointed out their transverse character and suggested that they might be second-mode Love waves.

period of about 7–8 sec. The particle motion i distinctly transverse. There is little or n vertical component, although evidence i meager because of the lack of a vertical in strument at Honolulu during most of the perio covered by this study. The waves are absen on the Berkeley vertical record of Hawaiia shocks (Fig. 20). They are the only coheren part of the train. The dispersion satisfactorily fits the first-mode Love-wave curve calculate for Case III (Fig. 21). Identical trains ar recorded at the Bermuda station for Atlanti and West Indian shocks. This portion of th train consists of Love waves.

The second part of the train, corresponding to velocities from 3.5 to about 2.0 km/sec., i present on all three components. However, th particle motion is incoherent—*i.e.*, no consisten orbital motion can be determined from record to record or from point to point on the same record. With the increasing effect of refraction at continental margins as the wave length become shorter, these short-period surface waves might become less reliable for particle-motion studies. However, the transverse component shows every indication of being a continuation of the short-period train (Fig.

5*B*, 5*C*). Furthermore, the amplitude of the transverse component, where distinguishable, is generally greatest. Shocks due north of Honolulu show Rayleigh waves (long-period) on the longitudinal instrument and the short-period waves on the transverse. One shock, number 71, nearly due east of Hawaii, shows short-period surface waves with almost equal amplitudes on both horizontals.

The previous observations favor a Love-wave hypothesis for the late part of the train. However, the train on the Berkeley and Bermuda verticals with an amplitude of the same order of magnitude as the horizontals weakens this viewpoint. Furthermore, the dispersion only roughly fits the first-shear mode-dispersion curve (Fig. 21); the periods are too large to agree with the water depth derived from Rayleigh mode observations over the same path. There is no known layer of shear velocity low enough to produce a similar dispersion in Love waves. Therefore, at present there is no concrete theoretical explanation for the later part of the short-period surface-wave train.

The similarity of this part of the train to long-period microseisms is inescapable. The conclusions drawn here may be extended with certainty to microseism propagation.

Geographical Factors Relating to Presence or Absence of Various Surface-Wave Types

The Honolulu collection indicated that earthquakes producing the shorter-period surface waves have a peculiar geographical distribution (Fig. 1). Beginning on the Easter Island Rise they can be traced up the west coast of North America, along the Aleutian chain, and down the Kuriles to Japan. Carder (1934) reports two shocks in the Marianas making waves of this period at Berkeley in addition to results that agree with the present study. A few shocks in the Solomons, Fijis, and New Zealand may be added to the list as well as Hawaiian shocks recorded at Berkeley. These scattered examples make it difficult to state that the short-period waves are never generated in any one area. However, the map indicates that they predominate on the Easter Island Rise, the west coast of North America, and the Aleutians. Except for the Aleutian arc, where some intermediate-depth shocks occur the seismicity of these regions is confined to shocks of shallow depth (Gutenberg and Richter, 1941).

Shocks making both Rayleigh waves and short-period surface waves were noted in the Pacific (Fig. 5*C*, 5*D*). To investigate this more thoroughly, Bermuda, Palisades, and Berkeley records in addition to the Honolulu ones were studied with the following results:

(1) Rayleigh waves are present on every shock of normal depth for which the propagation path has an adequate oceanic segment. In many cases the Rayleigh mode cannot be seen on the seismogram owing to masking by the stronger, short-period surface waves. For instance (a) on Mid-Atlantic Ridge shocks whose great-circle path to Palisades passes near Bermuda, Rayleigh waves cannot be seen on the Bermuda long-period Columbia vertical, but can be read on the Palisades long-period Columbia vertical where they show the proper velocities (Fig. 22); (b) a similar situation holds for Hawaiian shocks recorded at Berkeley and Palisades, the former recording short-period waves and the latter Rayleigh waves; (c) Mid-Atlantic Ridge shocks on the Bermuda Milne-Shaws showing only short-period surface waves at the time for R_1 show normal Rayleigh waves at the time for R_2.

(2) In many cases both the Rayleigh waves and the short-period surface waves are present, superposed on one another (Fig. 5*C*).

(3) The short-period surface waves show extreme attenuation upon passing a continental boundary, and similar but less extreme attenuation is suggested for an island arc. However, waves of this period range are propagated efficiently within either oceanic or continental areas. This immediately explains the observations of (1). Because of the differences in character of the continental margins of the Pacific and the Atlantic, Berkeley would be expected to reveal a close approximation to the oceanic train, whereas Palisades is far enough from the continental shelf to record largely continental waves. It likewise explains the fact that Alaskan and west-coast shocks make predominantly short-period waves at Honolulu only if offshore or near the coast.

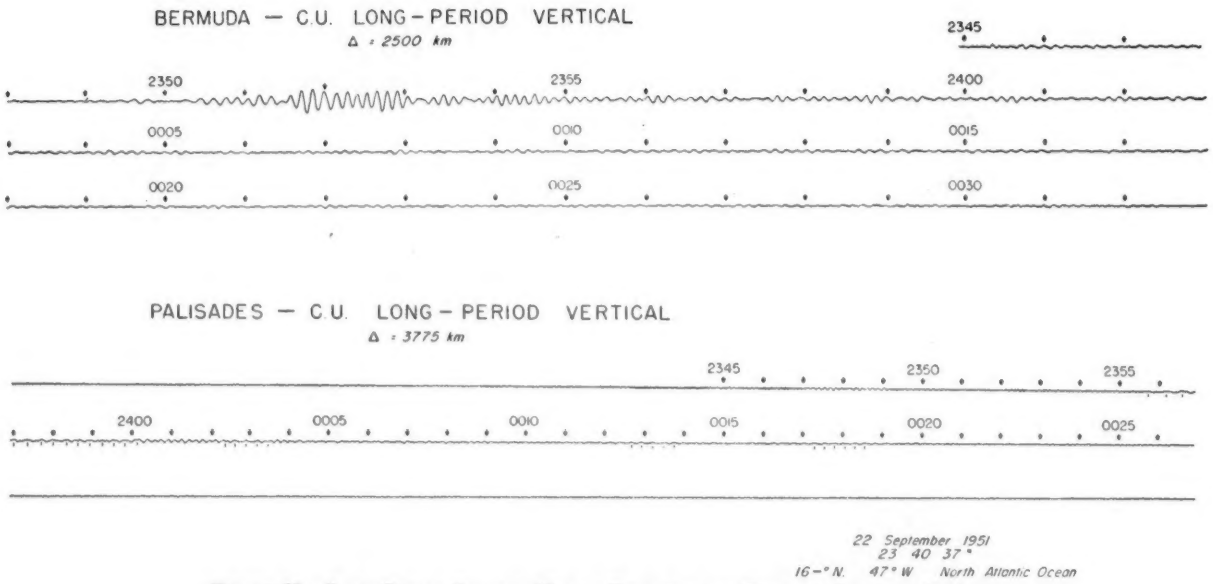

FIGURE 22.—SHORT-PERIOD SURFACE WAVES, PALISADES AND BERMUDA RECORDS (Table 3)

Similar effects for microseisms have been suggested by Donn (1952). These ideas agree with observations on the L_g phase (Press *et al.*, 1952). The L_g phase is a surface-shear wave having periods from ½ to 6 sec. It is confined to continental paths. Earthquakes having epicenters only a few degrees offshore do not make this phase at continental stations. The shorter periods are lost as soon as a small portion of the path is oceanic, whereas the long periods remain until the oceanic segment becomes larger. An assumed value for the phase velocity of these waves and for those of the later part of the short-period train gives a rough value of about 20–35 km for the wave lengths involved. This is also the order of magnitude of the thickness of the continental crust so that the effects noted here are not unreasonable. Theoretical considerations of the problem of surface waves incident on a boundary representative of the ocean-continent one have never been attempted to the writers' knowledge, and, from a cursory inspection, are somewhat involved.

(4) Details at the focus are important factors in determining the excitation ratios for the long- and short-period surface waves. Depth of focus, topography within a few hundred meters, the initial frequency spectrum of the shock, and the geometry of the displacement are relevant.

Greater focal depth clearly discriminates against the shorter waves. In fact, if the usual depths of focus are accepted one must appeal to topographic effects to explain the presence of appreciable energy in the shorter-period surface waves. The principal evidence now available is (a) a few closely neighboring shocks in the Aleutians may produce either long- or short-period surface waves at Honolulu; (b) in Alaska and in the Fiji Islands some shocks farther behind the barrier made only short-period waves at Honolulu, whereas shocks nearer the open water produced both waves; (c) the earthquakes making short-period surface waves tend to group in areas where only normal-depth sources are found.

Conclusions

(1) The theory attributing most of the dispersion of Rayleigh waves over oceanic paths to the effect of the water layer is confirmed in the Pacific at all azimuths from Honolulu, and over parts of the Atlantic.

(2) Love- and Rayleigh-wave disperson in the period range studied agrees with the crustal structure deduced from refraction shooting. This structure consists of a layer of water and sediments about 5.7 km thick overlying a rock layer of similar thickness and with a compressional wave velocity of about 6.5 km/sec. This in turn overlies a thick rock layer with compressional velocity of 8.1 km/sec. Poisson's ratio for the rock is 0.27.

(3) No submerged landmass of continental character and dimensions exists under the Pacific as outlined by the earthquake belt in (Fig. 1) or under parts of the North Atlantic. There is no indication of a submerged Melanesian continent. Limitations of the method, however, prevent the detection of thin layers of continental rock, particularly if they are present over a limited portion of the path.

(4) The Easter Island Rise is an anomalous area. Results of this study agree with the theory that a thin layer of continental rock underlies the Easter Island Rise but are not conclusive evidence.

(5) The average thickness of the sedimentary layer in the Pacific is 0.5–1.0 km. The thicker sediments are in the southwest quadrant. A similar range of thickness is found in the Atlantic.

(6) In addition to Rayleigh waves and Love waves of the "*G*" type, some earthquakes make a surface wave of shorter period. These earthquakes have a peculiar geographical distribution and generally occur in areas where only shallow shocks are known.

(7) The first part of the short-period train consists of Love waves that fit the first-mode Love-wave dispersion curve. Considerable effort was made attempting to find a good theoretical explanation for the later part of the train. Although the first-shear mode gives an approximate fit there are significant difficulties. The problem is further complicated by lateral refraction of the shorter wave lengths. There is no good explanation for the later part of the train.

(8) There are striking similarities between the late short-period waves and long-period

microseisms—*e.g.*, the periods are identical, particle motion is incoherent, and there is a strong vertical component.

(9) The short-period waves are sharply attenuated at a continental margin but travel well through continents and through oceans.

References Cited

Brilliant, R., and Ewing, M., 1954, Dispersion of Rayleigh waves across the U. S.: Seismol. Soc. America Bull., v. 44, p. 149–158.

Bullen, K., 1947, An introduction to the theory of seismology: Cambridge Univ. Press.

Byerly, P., 1930, The dispersion of seismic waves of the Love type and the thickness of the surface layer under the Pacific: Gerlands Beitr. Geophysik, v. 26, p. 27–33.

Byerly, P., Mei, A. I., S.J., and Romney, C., 1949, Dependence on azimuth of the amplitudes of P and PP: Seismol. Soc. America Bull., v. 39, p. 269.

Carder, D. S., 1934, Seismic surface waves and crustal structure of the Pacific region: Seismol. Soc. America Bull., v. 24, p. 231.

Coulomb, J., 1952, Love waves of the Queen Charlotte Islands earthquake of August 27, 1949: Seismol. Soc. America Bull., v. 42, p. 29.

Donn, W. L., 1952, Cyclonic microseisms generated in the western North Atlantic Ocean: Jour. Meteorology, v. 9, p. 61–71.

Evernden, Jack F., 1952a, Direction of approach of Rayleigh waves and related problems (Abstract): Geol. Soc. America Bull., v. 63, p. 1352.

—— 1952b, Love-wave dispersion and the structure of the Pacific basin (Abstract): Geol. Soc. America Bull., v. 63, p. 1352.

Ewing, M. and Press, F., 1950, Crustal structure and surface-wave dispersion, Part I: Seismol. Soc. America Bull., v. 40, p. 271–280.

—— 1952a, Propagation of earthquake waves along oceanic paths: Travaux Sci. n. 18 Bureau Central Seismologique International.

—— 1952b, Crustal structure and surface-wave dispersion, Part II: Seismol. Soc. America Bull., v. 42, p. 315–325.

—— 1954, An investigation of mantle Rayleigh waves: Seismol. Soc. America Bull., v. 44, p. 127–148.

Ewing, M., Press, F., *et al.*, 1950, Seismic refraction measurements in the Atlantic Ocean Basin, Part I: Seismol. Soc. America Bull., v. 40, p. 233–242.

Ewing, M., Sutton, G. H., and Officer, C. B., 1954, Seismic refraction measurements in the Atlantic Ocean, Part VI—typical deep stations, North Atlantic Basin: Seismol. Soc. America Bull., v. 44, p. 21–38.

Gutenberg, B., and Richter, C. F., 1936, On seismic waves (3rd paper): Gerlands Beitr. Geophysik, v. 47, p. 73–131.

—— 1941, Seismicity of the earth: Geol. Soc. America Spec. Paper 34, 131 p.

—— 1951, Internal constitution of the earth: Dover Pub., Inc.

Haskell, N., 1951, The dispersion of surface waves on multi-layered media: Geophysical Research Paper #9, Air Force Cambridge Research Center.

Jardetzky, W. S., and Press, F., 1953, Crustal structure and surface-wave dispersion, Part III: theoretical dispersion curves for sub-oceanic Rayleigh waves: Seismol. Soc. America Bull., v. 43, p. 137–144.

Neumann, F., 1929, The velocity of seismic surface waves over Pacific paths: Seismol. Soc. America Bull., v. 19, p. 63–76.

Officer, C. B., *et al.*, 1952, Seismic refraction measurements in the Atlantic Ocean Basin, Part IV: Geol. Soc. America Bull., v. 63, p. 777–808.

Pekeris, C. L., 1948, Theory of propagation of explosive sound in shallow water *in* Worzel, J. L., Ewing, M., and Pekeris, C. L., Propagation of sound in the ocean: Geol. Soc. America Mem. 27, 116 p.

Press, F., Ewing, M., and Tolstoy, I., 1950, The Airy phase of shallow-focus submarine earthquakes: Seismol. Soc. America Bull., v. 40, p. 111–148.

—— 1952, Two slow surface waves across North America: Seismol. Soc. America Bull., v. 42, p. 219–228.

Raitt, R. W., 1951, Reflection and refraction of explosive waves by the sea bottom: Quart. Prog. Rep., Marine Physical Laboratory, Scripps Inst. Oceanogr. April–June.

Rothe, J. P., 1951, The structure of the bed of the Atlantic Ocean: Am. Geophys. Union Trans., v. 32, p. 457–461.

Sezawa, K., and Kanai, K., 1935, Discontinuity in the dispersion curve of Rayleigh waves: Inst. Tokyo, Bull. Earthquake Research, v. 13, p. 237.

Stoneley, R., 1926, The effect of the ocean on Rayleigh waves: Roy. Astron. Soc. Mon. Notices, Geophys. Supp., v. 1, p. 349–356.

Umbgrove, J. H. F., 1947, The pulse of the earth: The Hague, Martinus Nijhoff, 228 p.

Wilson, J. T., 1941, The Love waves of the South Atlantic earthquake of August 28, 1933: Seismol. Soc. America Bull., v. 30, p. 273–301.

Wilson, J. T. and Baykal, O., 1948, Crustal structure of the North Atlantic as determined from Rayleigh wave dispersion: Seismol. Soc. America Bull., v. 38, p. 41–53.

Lamont Geological Observatory, Columbia University, Palisades, New York.

Lamont Geological Observatory Contribution No. 163.

Air Force Cambridge Research Center, Geophysics Research Division, Contract AF 19 (122) 441.

Manuscript received by the Secretary of the Society October 9, 1953.

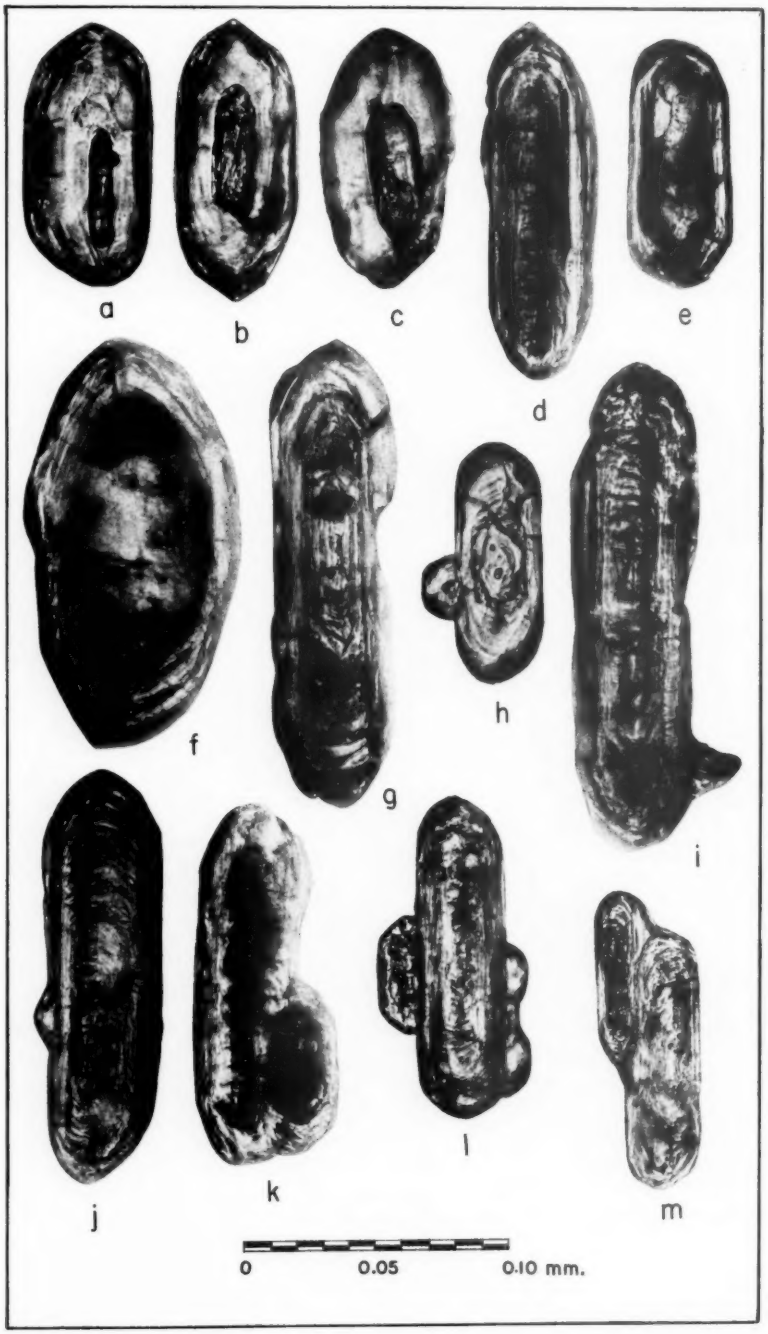

a–g. — Zircons with distinct cores and shells. Note that length of cores may be skew with respect to c axis of shells (b, c); shells fracture independent from cores (e, g).
h–m. — Zircon outgrowths and aggregate crystals.

GROWTH PHENOMENA IN ZIRCONS

BULLETIN OF THE GEOLOGICAL SOCIETY OF AMERICA
VOL. 66, P. 947-948, 1 PL. JULY 1955

Short Notes

GROWTH PHENOMENA IN ZIRCON OF AUTOCHTHONOUS GRANITES

BY ARIE POLDERVAART AND F. DONALD ECKELMANN

Studies in The Union of South Africa (Poldervaart and von Backström, 1950; F. H. S. Vermaas, Ph.D. Thesis, Pretoria Univ., 1949), Bechuanaland Protectorate (Mahalapye granite, Poldervaart and Green, 1954), and the Beartooth Mountains of Montana-Wyoming have yielded field evidence of the transformation of sediments to autochthonous granite (Read, 1951; 1955). In this plutonic process zircons exhibit growth phenomena which bridge the gap between the predominantly rounded zircons of siliceous sediments (Poldervaart, in press) and the predominantly euhedral zircons of intrusive granites. It is emphasized that intrusive granites may contain a few zircons with growth features as shown on Plate 1, but concentrates with high proportions of zircons showing evidence of new growth may be regarded as characteristic of autochthonous granites.

Plate 1 shows 13 zircons from a concentrate obtained from a sample of autochthonous granite gneiss, collected near Highway U. S. 12, on the Montana-Wyoming border in the Beartooth Mountains. Growth features shown are typical of those found in concentrates of other autochthonous granites examined by the writers.

Growth phenomena may be classified as *outgrowths*, *aggregate crystals*, and *overgrowths*. Outgrowths are similar to those described by Smithson (1937) and others in zircon concentrates from coarse-grained arenites. The outgrowths may be pyramidal (*i*, *j*) or hemispherical (*l*). Coalescence of two or more outgrowths, or bonding of two or more grains by new growths may result in aggregate crystals (*k*, *l*, *m*). Overgrowths consist of shells which partly or completely envelope cores of zircon. Generally the cores are brown in this phase of plutonism, while the shells are pale brown, pale purple, or colorless. Shells and cores may also show differences in zoning (cores *d*, *g*; shells *f*) or in cracks (*e*, *g*). With low magnifications, the outlines of shells may appear rounded, but with high magnifications it is evident that terminations of crystals are complex, and crude pyramidal faces are developed which may intersect with rounded edges. If the rock is of sedimentary origin, the cores are rounded or fragmentary, but if the sample is a regenerated intrusive granite the cores are euhedral.

Prevalence of zircons with such growth phenomena in granites formed *in situ* is considered convincing laboratory evidence of the reality of Read's granite series.

REFERENCES CITED

Poldervaart, A., in press, Zircons in rocks. I. Sedimentary rocks: Am. Jour. Sci.

Poldervaart, A., and Backström, J. W. von, 1950, A study of an area at Kakamas (Cape Province): Geol. Soc. South Africa Trans., v. 52, p. 433–495.

Poldervaart, A., and Green, D., 1954, An outline of the geology of the Bechuanaland Protectorate: Internat. Geol. Cong., 19th Sess., Algiers, Assoc. Serv. Géol. Africains, 1e pt., fasc. 20, p. 53–66.

Read, H. H., 1951, Metamorphism and granitization: Geol. Soc. South Africa Trans., v. 54, Annexure, 27 p.

—— 1955, Granite series in mobile belts: Geol. Soc. America Special Paper 62, p. 409–429.

Smithson, F., 1937, Outgrowths on zircon in the Middle Jurassic of Yorkshire: Geol. Mag., 74, p. 281–283.

DEPARTMENT OF GEOLOGY, COLUMBIA UNIVERSITY, NEW YORK 27, N. Y.